UNIVERSIDAD COMPLUTENSE DE MADRID

FACULTAD DE CIENCIAS BIOLÓGICAS

ANÁLISIS ESTRUCTURAL Y FUNCIONAL DE PROTEÍNAS DEL COMPLEMENTO ASOCIADAS CON PATOLOGÍA

MEMORIA PARA OPTAR AL GRADO DE DOCTOR
PRESENTADA POR

Agustín Tortajada Alonso

Bajo la dirección del doctor

Santiago Rodríguez de Córdoba

Madrid, 2012

ANÁLISIS ESTRUCTURAL Y FUNCIONAL DE PROTEÍNAS DEL COMPLEMENTO ASOCIADAS CON PATOLOGÍA

TESIS DOCTORAL

Agustín Tortajada Alonso

UNIVERSIDAD COMPLUTENSE
MADRID

Universidad Complutense de Madrid
Facultad de Ciencias Biológicas

ANÁLISIS ESTRUCTURAL Y FUNCIONAL DE PROTEÍNAS DEL COMPLEMENTO ASOCIADAS CON PATOLOGÍA

AGUSTÍN TORTAJADA ALONSO

T E S I S

PRESENTADA PARA OBTAR AL GRADO DE DOCTOR

DIRIGIDA POR
DR. SANTIAGO RODRÍGUEZ DE CÓRDOBA

MADRID, 2012

SANTIAGO RODRÍGUEZ DE CÓRDOBA, Doctor en Biología, Profesor de Investigación del CSIC en el Centro de Investigaciones Biológicas:

CERTIFICA: Que **AGUSTÍN TORTAJADA ALONSO** ha realizado bajo su dirección el trabajo de Tesis Doctoral que lleva por título:

Análisis estructural y funcional de proteínas del complemento asociadas con patología.

El trabajo que se presenta es original y de relevancia en las áreas de la Genética, Inmunología y Patología Molecular Humana. Los objetivos planteados en esta tesis han sido profundizar en el conocimiento de los mecanismos patogénicos responsables de patologías como el síndrome hemolítico urémico atípico, la enfermedad por depósitos densos y la degeneración macular asociada a la edad mediante la caracterización estructural y funcional de variantes genéticas de proteínas del complemento asociadas a estas patologías. El trabajo de tesis que presenta Agustín Tortajada Alonso ha dado lugar a varias publicaciones en revistas internacionales de alto índice de impacto. Por todo ello considero que el trabajo de tesis presentado por Agustín Tortajada Alonso para optar al grado de Doctor en Biología por la Universidad Complutense de Madrid tiene la debida calidad para su defensa y calificación.

Fdo.: Prof. Santiago Rodríguez de Córdoba

A Carol y a Nora

ÍNDICE

ABREVIATURAS

AMD	*Age-related macular degeneration*
AP	*Alternative pathway*
C1-inh	C1*-inhibitor*
C345c	*Complement* C3*,* C4 *and* C5 *C-terminal*
C3-Nef	C3 *nephritic factor*
C4bp	C4 *binding protein*
CVF	*Cobra venom factor*
CP	*Classical pathway*
CR1 Y 2	*Complement receptor* 1 *and* 2
CUB	*Complement* C1r/C1s, UEGF, BMP1
DAF	*Decay accelerating factor*
DDD	*Dense deposit disease*
HUS	*Hemolytic uremic syndrome*
IC	Inmunocomplejo
ELISA	*Enzime linked immunoadsorvent assay*
KDa	Kilodalton
LP	*Lectin pathway*
MAC	*Membrane attack complex*
MBL	*Manose binding lectin*
MCP	*Membrane cofactor protein*
MG	Macroglobulina
MIDAS	*Metal ion-dependent adhesion site*
MPGN	*Membranoproliferative glomerulonephritis*
OR	*Odds ratio*
RCA	*Regulators of complement activation*
SCR	*Short consensus repeat*
SNP	*Single nucleotide polymorphism*
SP	*Serine protease*
SPR	*Surface plasmon resonance*
TED	*Thioester-containing domain*
UTR	*Untranslated region*
vWA	*Von Willebrand factor type A*

INTRODUCCIÓN

1. El sistema del complemento.

El sistema del complemento es una parte esencial del sistema inmune innato, actuando como una primera línea de defensa frente a infecciones. El complemento es también un modulador importante de la respuesta inmune adaptativa.

Desde su descubrimiento a finales del siglo XIV como un agente del suero termolábil que "complementaba" la acción bactericida y hemolítica de los anticuerpos, el conocimiento sobre los componentes del complemento, su activación y sus implicaciones fisiológicas continúa ampliándose.[1, 2]

Las funciones principales del complemento pueden resumirse de la siguiente manera:[1, 3-5]

Defensa frente a infecciones. La eliminación de patógenos puede realizarse directamente por lisis mediada por el complemento, o mediante mecanismos de opsonización y fagocitosis. La liberación de anafilotoxinas desencadena procesos de quimiotaxis, especialmente sobre leucocitos, y estados pro-inflamatorios en el lugar de la infección.

Función inmunorreguladora. El complemento participa en la modulación la respuesta inmune adaptativa; potenciando la respuesta humoral e incrementando la memoria inmunológica, estimulando la proliferación de linfocitos B y modificando la inmunidad dependiente de linfocitos T.

Eliminación de inmunocomplejos y de los productos del daño inflamatorio. Eliminación de **restos apoptóticos.**

1.1. La activación del complemento.

El sistema del complemento está formado por un conjunto de unas 30 proteínas plasmáticas y de membrana, organizadas en cascadas que se inician frente a señales específicas presentes en los patógenos y las superficies extrañas. Las proteínas del complemento pueden dividirse en componentes, formando parte de las cascadas de activación; o reguladores, ejerciendo un

riguroso control sobre ellas. La activación del complemento tiene lugar de forma secuencial a través de la generación de enzimas activas a partir de zimógenos de serín proteasas. La cascada de activación se irá amplificando, al generarse en cada paso un gran número de moléculas activadoras del paso siguiente.[5, 6]

Dependiendo del elemento que desencadene la activación inicial del complemento, podemos distinguir tres vías: la clásica, la de las lectinas y la alternativa. Todas ellas se encuentran interconectadas y convergen en la formación de unos complejos enzimáticos, denominados convertasas de C3. Estos complejos tienen como sustrato el componente central del complemento, la molécula de C3 (**figura 1**). El C3 es hidrolizado a C3b, que se une a las superficies y actúa de etiqueta, señalizando dónde se va a prolongar la activación del complemento, que terminará en una vía común, la vía lítica. Esta vía terminal da lugar a la formación de un complejo de ataque en las superficies, que causará la destrucción de la célula. Las proteínas reguladoras actúan sobre las enzimas, controlando de manera estricta la activación del complemento, localizándola sobre las superficies extrañas a eliminar, y evitando el daño en el tejido propio.[7]

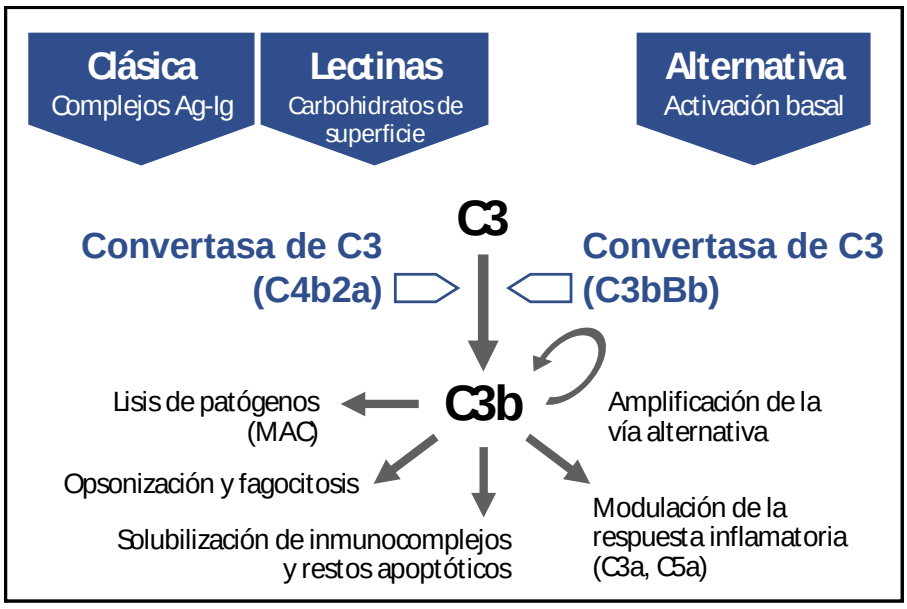

Figura 1. Papel central de la convertasa de C3 en el sistema del complemento. Las tres vías de activación, la clásica, de las lectinas y la alternativa, convergen en la formación de los complejos convertasa de C3 (C4b2a y C3bBb), encargados de hidrolizar el componente C3 a C3b. La generación de C3b conduce a las diferentes funciones del complemento y a la amplificación de la respuesta a través de la vía alternativa.

1.1.1. La vía clásica.

La vía clásica (CP) fue la primera en ser descubierta y se inicia por la formación de inmunocomplejos de IgM y de ciertos isotipos de IgG. Estos inmunocomplejos son reconocidos por el primer componente del complemento, C1, un complejo formado por la proteína globular C1q y las enzimas C1r y C1s, asociadas de manera dependiente de Ca^{2+}. La alta afinidad de C1q por las regiones de la fracción constante de las inmunoglobulinas, da lugar a que las enzimas C1r/C1s se activen.[8, 9]

La proteasa C1s hidroliza consecutivamente los componentes C4 y C2, produciéndose dos fragmentos grandes, C4b y C2a, y dos pequeños, C4a y C2b. El C4b, a través de un grupo tioéster que se expone al ser activada la molécula, se une covalentemente a las superficies celulares y proteínas adyacentes que desencadenan la activación. C4b se une al fragmento C2a, formando la convertasa de C3 de la CP (C4bC2a), siendo esta última molécula el centro activo del complejo.[10, 11] C4bC2a hidroliza numerosas moléculas de C3, originando C3b que, análogamente a C4b, expone un grupo tioéster reactivo que le permite unirse a las superficies. El C3b depositado asegura la amplificación de la activación del complemento hacia la vía lítica (**figura 2**).

1.1.2. La vía de las lectinas.

La lectina de unión a manosa (MBL) y determinadas ficolinas, son proteínas oligoméricas estructuralmente similares a C1q, y tienen afinidad por ciertos carbohidratos presentes en las glicoproteínas y glicolípidos de la superficie de los patógenos. Las MBL y ficolinas circulan en el suero asociadas a proteínas de unión a MBL (MASP1, MASP2, MASP3 y MAP19), que son unas serín proteasas equivalentes a C1r y C1s.[11]

El reconocimiento y la unión a los carbohidratos de los patógenos induce cambios conformacionales en estos complejos permitiendo la activación de las MASP2, que hidrolizan los componentes C4 y C2 de la CP.[5] De igual modo, la activación por la vía de las lectinas (LP) da lugar a la formación de la convertasa C4bC2a. La actividad de este complejo, idéntico al de la CP, desemboca igualmente en la vía lítica (**figura 2**).

1.1.3. La vía alternativa.

La tercera vía del complemento, la vía alternativa (AP), se encuentra constitutivamente activada y la presencia de ciertas moléculas, como carbohidratos, lípidos y proteínas en las superficies extrañas aceleran su activación. El mecanismo que mantiene activa la AP, conocido como *tick over*, asegura una respuesta rápida del sistema del complemento, que constantemente estará preparado para ser activado.[5] El componente C3 es prácticamente inerte en su forma nativa, no tiene apenas ligandos. Sin embargo, una pequeña fracción de estas moléculas se hidrolizan sin necesidad de un corte proteolítico por la convertasa de C3, exponiendo nuevos sitios de unión. Estas moléculas, $C3_{H2O}$, unen de manera dependiente de cationes Mg^{2+} la serín proteasa factor B (fB). fB es posteriormente hidrolizado por otra serín proteasa, factor D (fD) liberándose un fragmento pequeño, Ba, y quedando el de mayor tamaño, Bb, que contiene el centro catalítico, unido a $C3_{H2O}$. Se forma así un complejo, una convertasa inicial ($C3_{H2O}Bb$), que está presente en la fase fluida del plasma en muy baja proporción. $C3_{H2O}Bb$ es capaz de hidrolizar moléculas de C3 y generar C3b. El nivel basal del mecanismo de *tick over* está sujeto a la corta vida media de estos complejos convertasa, que se disocian rápidamente, y también a la actuación de los reguladores del complemento. El $C3_{H2O}$ posee prácticamente las mismas propiedades funcionales que C3b por lo que podrá ser igualmente inactivado.[10, 12]

El fB plasmático puede unirse a las moléculas de C3b generadas por la convertasa inicial, formando la pro-convertasa de C3 (C3bB), y ser activado por fD, dando lugar a la convertasa de C3 de la AP (C3bBb). El producto de la hidrólisis de C3 por esta convertasa genera más C3b, que junto con el producido por las convertasas de la CP y LP, podrá formar a su vez más complejos convertasa. De esta forma, se establece un bucle de retroalimentación que asegura la amplificación de la respuesta, que será muy rápida una vez es activada la AP del complemento.[10, 12]

La alta inestabilidad de los complejos convertasa se ve contrarrestada por la properdina (P), una proteína oligomérica que se asocia a las superficies extrañas y de las células apoptóticas. La P es el activador fisiológico de la AP, se une directamente a C3bB y C3bBb, estabilizando los complejos e impidiendo su rápida disociación. También tiene afinidad por el C3b soluble, sirviendo de base para el ensamblaje de la convertasa. Además juega un papel fundamental en la eliminación de los restos apoptóticos (**figura 2**).[13]

1.2. La convertasa de C5 y la vía terminal.

La convertasa de C3 de la CP y la LP (C4bC2a) y de la AP (C3bBb) realizan un corte proteolítico sobre el C3 circulante en el plasma, liberándose un fragmento pequeño, C3a y originando C3b. El C3b, tras sufrir un cambio conformacional, expone un grupo tioéster que reacciona con las superficies adyacentes, uniéndose de manera covalente a ellas. Este C3b depositado actúa como opsonina, ayuda en la fagocitosis y participa en la amplificación de la activación del complemento. Además, el C3b puede unirse a las convertasas de C3 de las tres vías, dimerizando con el C4b o el propio C3b de los complejos, y dando lugar a las convertasas de C5, C4bC2aC3b y C3bBbC3b. La adición de esta molécula de C3b sobre las convertasas de C3 cambia la especificidad por el sustrato de los centros activos, situados en C2a y Bb, que pasa a ser el componente C5.[14]

El C5, que pertenece a la misma familia de proteínas que C3 y C4 y que comparte una estructura primaria, es hidrolizado por las convertasas de C5 y se corta en los fragmentos C5b y C5a. Este último, junto con el C3a producido por las convertasas de C3, se liberan en el plasma y son potentes anafilotoxinas. La generación de C5b activa un proceso no enzimático de ensamblaje de los componentes finales del complemento, C6 a C9, y que termina en la formación de un complejo multimolecular con capacidad citolítica, o complejo de ataque a membrana (MAC).[15]

En primer lugar se forma un complejo C5b-6, que permanece débilmente unido a C3b y sobre el que se incorpora C7. El complejo trimolecular C5-7 se vuelve anfipático y se trasfiere a la membrana. C5b-7 anclado en la bicapa lipídica une C8 dando lugar a un complejo tetramolecular, C5-8, que funciona como receptor de múltiples moléculas de C9. Todos estos componentes constituyen el MAC, un poro de unos 30 nm que produce lesiones críticas en la membrana celular que alteran su permeabilidad y ocasionan la lisis osmótica de las células (**figura 2**).[16]

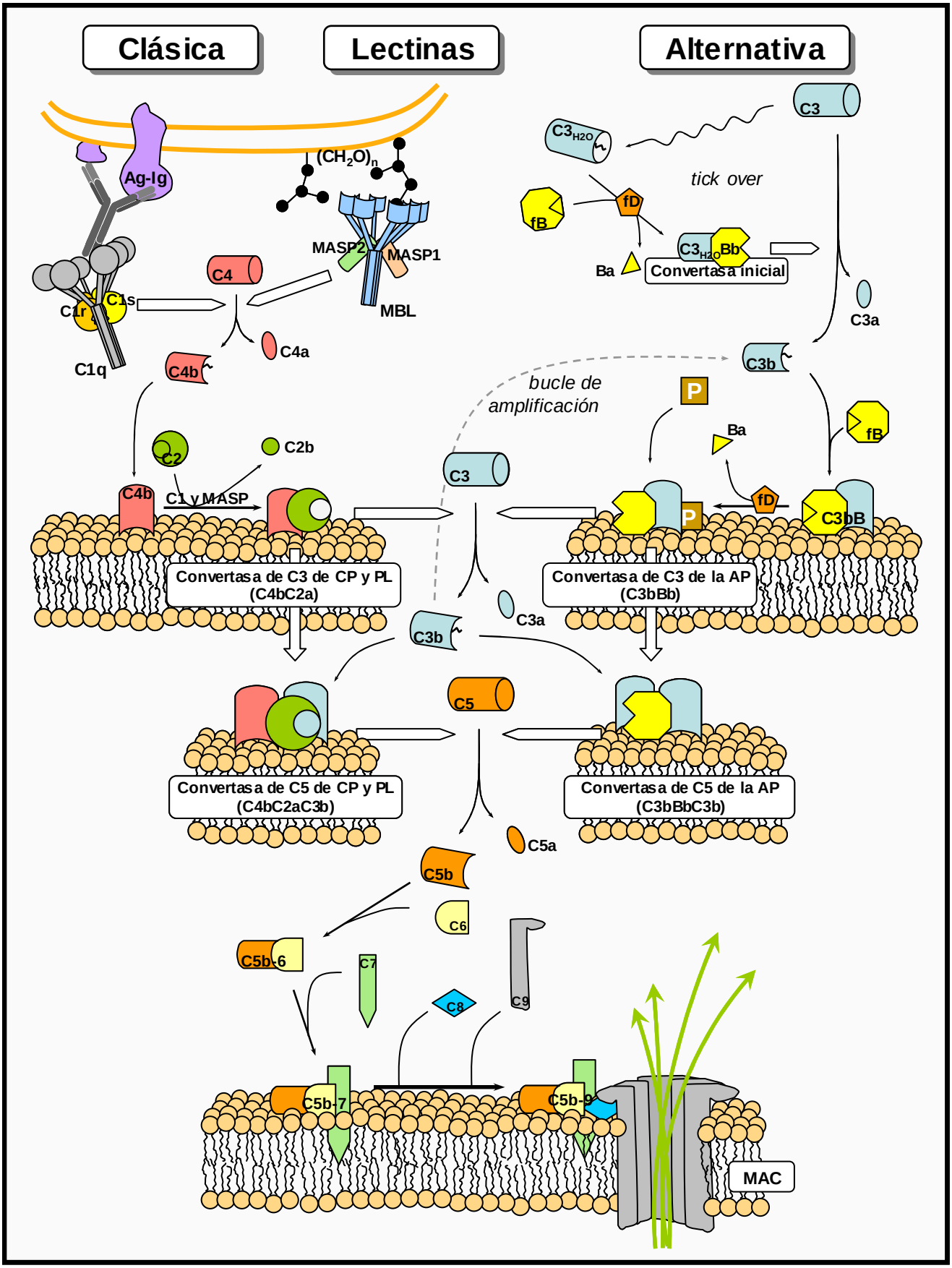

Figura 2. Vías de activación de complemento. La CP se inicia por la presencia de complejos antígeno-anticuerpo (Ag-Ig) y la LP por el reconocimiento de carbohidratos de superficie $(CH_2O)_n$. La AP se encuentra constitutivamente activada gracias al mecanismo

de *tick over*, en el cual se forma una convertasa en fase fluida de manera espontánea. Las tres vías convergen en la hidrólisis del componente C3 por las convertasas de C3 generando C3b, implicado en las diversas funciones del complemento. El propio C3b forma parte de la convertasa de C3 de la AP, dando lugar a un bucle de amplificación de la activación de esta vía. El C3b depositado sobre las convertasas de C3 genera las convertasas de C5. La hidrólisis del componente C5 inicia la vía terminal, que desencadena en la formación del MAC ocasionando la lisis osmótica en el patógeno.

Las anafilotoxinas C3a y C5a actúan en la respuesta inflamatoria, induciendo la degranulación de neutrófilos y mastocitos. Además, junto con otros señalizadores, modulan la respuesta inmune adaptativa. Las células dendríticas y los linfocitos T expresan receptores para C3a y C5a, que participan en la interacción de estas células y en la presentación de antígenos. También juegan un papel importante en la proliferación y supervivencia de linfocitos T.[17]

1.3. La convertasa de C3 de la vía alternativa.

La convertasa de C3 de la AP, C3bBb, es crucial dentro de las cascadas de activación, ya que es el complejo enzimático encargado de amplificar la respuesta una vez es activado el complemento. Para describir el mecanismo de formación de la convertasa C3bBb es preciso comentar algunos aspectos moleculares de sus componentes, C3b y fB.

1.3.1. C3/C3b.

El C3 es el componente más abundante del complemento (700 - 1200 µg/ml). Es una proteína globular de 190 KDa cuya forma secretada está compuesta por dos cadenas, α y β, de 110 y 75 KDa respectivamente, conectadas por un puente disulfuro.[18]

La principal característica de C3 es la presencia de un grupo tioéster interno que se encuentra inaccesible y es incapaz de reaccionar en la molécula nativa. El grupo tioéster, una vez expuesto tras la activación proteolítica de C3 a C3b, es muy reactivo con los grupos nucleofílicos, incluyendo el agua y moléculas que contengan grupos hidroxilo o amino. El resultado es una unión covalente a través de un enlace éster o amida sobre las superficies adyacentes.[19]

Las dos cadenas de C3, α y β, se organizan en 13 dominios perfectamente diferenciados (**figura 3**). Ambas cadenas configuran un núcleo compuesto por 8 dominios macroglobulina (MG 1-8), que forman un anillo. En la región N-terminal de la cadena α, un dominio anafilotoxina (ANA o C3a), liberado tras el corte proteolítico de C3 a C3b; un dominio denominado CUB (*complement* C1r/C1s, VEGF, BMP1) que conecta el anillo de MG con un dominio que contiene el enlace tioéster (TED); y en la región C-terminal de la misma cadena el dominio C345c (*complement* C3, C4 *and* C5 *C-terminal*). La escisión del fragmento C3a, exclusivo de C3, genera el dominio α-NT, que será funcional en C3b.[19]

La estructura a resolución atómica del C3 y del C3b de la especie humana se ha resuelto por medio de cristalografía, lo que ha ayudado a comprender los cambios conformacionales que sufre la molécula de C3 tras su activación a C3b.[20, 21] El dominio ANA (o C3a) se encuentra estabilizando la molécula de C3 en su forma nativa, y su liberación, con la consecuente generación del extremo α-NT, causa una serie de cambios conformacionales característicos de la forma funcionalmente activa, C3b. El cambio más singular, como ya se ha comentado anteriormente, es la exposición del grupo tioéster hacia el medio soluble, que se produce por un desplazamiento del dominio TED hacia afuera de la molécula, alejándose del anillo de MG. Otros cambios se producen a nivel de los dominios MG 7 y 8, C345c, CUB y el α-NT (**figura 3**).[19]

El reordenamiento de los dominios en C3b a de generar también los sitios de unión de fB, imprescindibles para la formación de la convertasa de C3. Los dominios de C3b implicados en la interacción con fB son α-NT, C345c y CUB. Este último dominio parece jugar un papel importante en el mantenimiento de la estructura que permitirá la interacción entre C3b y fB en la pro-convertasa, C3bB. Estos sitios de unión, que sufren importantes cambios conformacionales, no están accesibles en la estructura de la molécula de C3, lo que explica por qué esta no es capaz de formar una convertasa. El dominio TED, cuya orientación y localización sufre un cambio importante, no parece participar en la formación de la convertasa.[19]

La molécula iniciadora del mecanismo de *tick over*, $C3_{H2O}$, posee las mismas propiedades funcionales que C3b, y ha de sufrir cambios conformacionales que la llevan a una configuración similar a la de C3b tras la hidrólisis del grupo tioéster interno. Es por esta razón, que $C3_{H2O}$ pierde la capacidad de unirse a las superficies biológicas.[22]

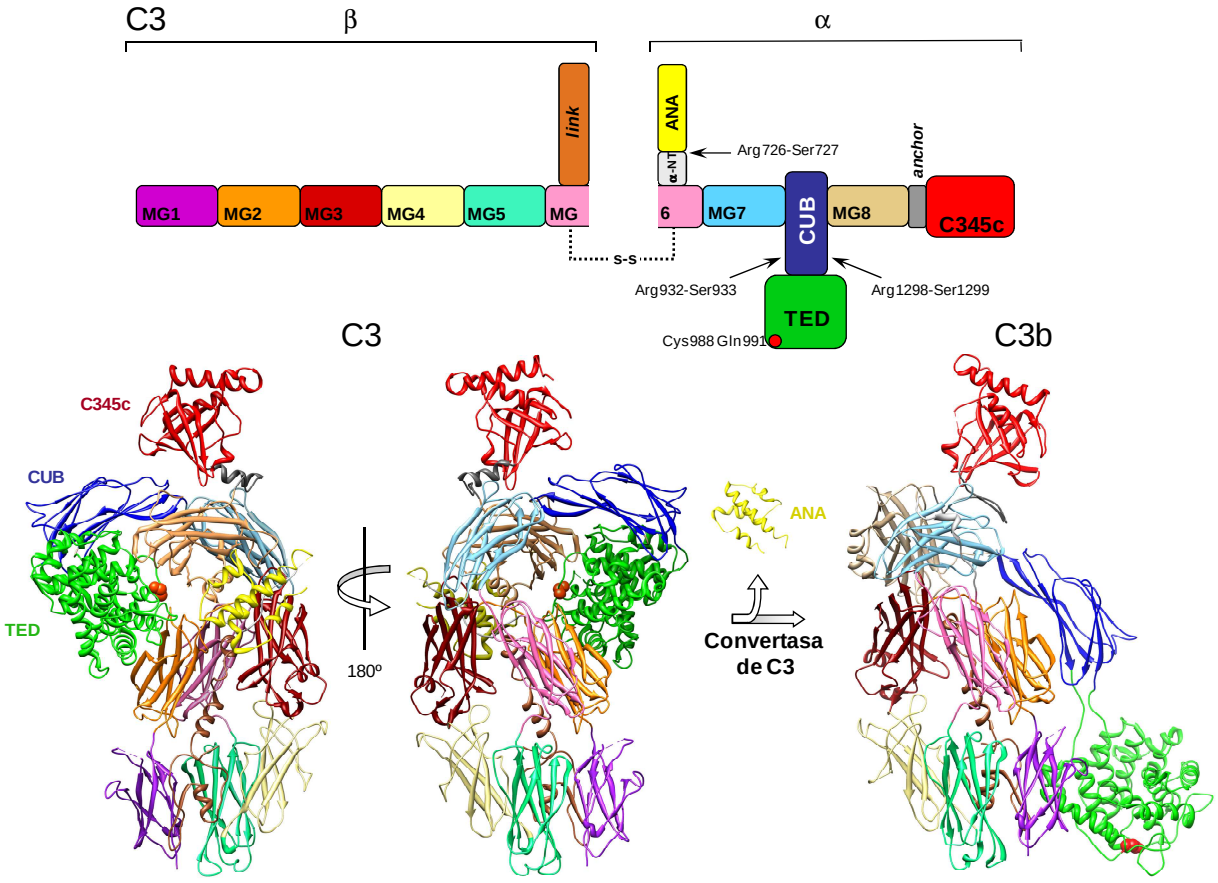

Figura 3. Estructura de C3 y C3b. Se muestra un diagrama representado de forma lineal las cadenas α y β, conteniendo los 13 dominios de la molécula de C3. Debajo, estructura a resolución atómica de C3 (PDB ID 2A73) y C3b (PDB ID 2I07) tras su activación por la convertasa de C3. El cambio estructural más importante se da a nivel del dominio TED, y también en los dominios CUB y C345c. Los sitios de corte de la hidrólisis de C3 a C3b y de la inactivación de C3b (flechas), así como los residuos que configuran el grupo tioéster (círculo rojo) están situados en el diagrama.

1.3.2. Factor B.

El fB es una serín proteasa de 90 KDa que circula en el plasma en forma de zimógeno inactivo, y su concentración en la especie humana es de unos 180 µg/ml.[23] fB cataliza la reacción central en la amplificación de la activación del complemento, la hidrólisis de C3, siendo altamente específica para los sustratos C3 o C5.

El fB está compuesto por 5 dominios estructurales que pueden dividirse en una región N-terminal no catalítica, denominada Ba, que se compone de 3 dominios SCR (*short consensus repeats*), y una región C-terminal catalítica.

Esta última, Bb, está compuesta por un dominio Von Willebrand de tipo A (vWA) y un dominio serín proteasa (SP), que contiene la triada catalítica. Ba y Bb están conectados por una región de unión o *linker* de 45 residuos que contiene un sitio de corte (**figura 4**).[24]

La activación de la serín proteasa fB se realiza en dos pasos. Primero se da una asociación dependiente de Mg^{2+} con su cofactor, C3b, para formar la pro-convertasa C3bB. En este ensamblaje intervienen los SCRs de Ba y un sitio MIDAS (*metal ion-dependent adhesion site*) presente en el dominio vWA de la subunidad Bb.[25, 26] Este motivo hace que la interacción C3b-fB sea dependiente de cationes Mg^{2+}. En un segundo paso se produce la proteólisis y liberación de Ba. La serín proteasa, fD, realiza un corte en el sitio de la región *linker* dejando Bb en el complejo y dando lugar a la convertasa activa C3bBb.[27]

Gracias a la estructura atómica disponible de fB y del fragmento Bb es posible aclarar algunos aspectos moleculares en la activación de fB.[24, 28] La pro-enzima fB sufre una serie de cambios conformacionales al pasar de una forma soluble e inactivak, a otra asociada a C3b que puede ser proteolizada por fD. La región *linker* parece tener un papel clave en este proceso. En primer lugar, el fB soluble presenta los tres SCRs de Ba plegados hacia Bb, de manera que la hélice α de la parte N-terminal de la región *linker* (αL), queda incorporada totalmente en el dominio vWA. La αL desplaza la hélice α7 del dominio vWA de la posición que ocupa en el fragmento Bb, adoptando una conformación bloqueada en la que el sitio MIDAS pierde la capacidad de unir cationes divalentes (**figura 4**). Estas estructuras, α7 y MIDAS, son esenciales en la funcionalidad de los dominios tipo vWA. Por otro lado, el sitio de corte, en la región C-terminal del *linker,* permanece unido entre las hélices αL y α7, quedando inaccesible a fD en el fB soluble.

No se conocen completamente los eventos que han de producirse en la formación de una convertasa C3bBb activa. Sin embrago, el cambio conformacional de la molécula es necesario, y parece ser suficiente para que se produzca la recolocación de las hélices αL y α7, lo que permitirá la configuración del sitio MIDAS para la unión estable dependiente de Mg^{2+} a C3b. Una consecuencia importante es que el sitio corte en la región *linker* quedaría expuesto, siendo susceptible a la acción proteolítica de fD. El dominio catalítico, SP, que contacta con vWA a través de α7 y de αL se reorienta al producirse el corte de Ba (**figura 4**). Esta reorientación no afecta al centro activo, que es muy similar en fB y Bb, y que parece ser activado por la unión con el sustrato.[19]

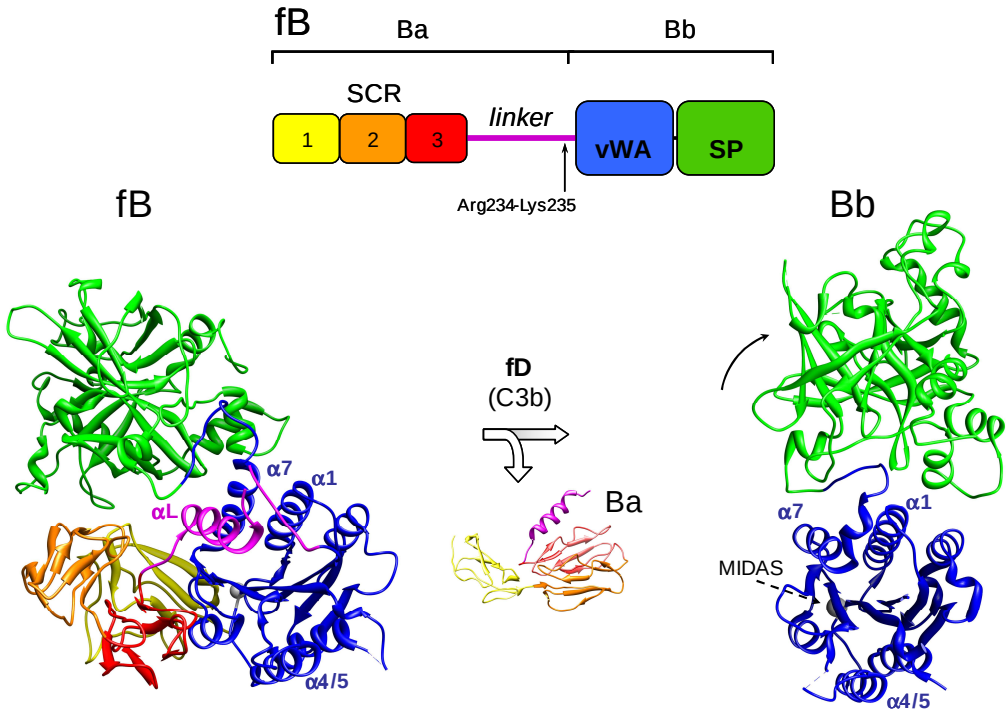

Figura 4. Estructura de factor B y Bb. Se muestra un diagrama representando de manera lineal los 5 dominios de fB, comprendidos en los fragmentos Ba y Bb. Debajo, la estructura atómica de fB (PDB ID 2OK5) y el fragmento Bb (PDB ID 1RRK). Los dominios SCR de Ba están plegados hacia Bb, y la αL de la región *linker* se sitúa dentro del núcleo del dominio vWA, ocupando el sitio de α7. Tras el corte por fD, en complejo con C3b, Ba se libera, y α7 ocupa su lugar en el dominio vWA adoptando la conformación estable para el sitio MIDAS. Puede apreciarse la reorientación del dominio SP respecto a la posición de wWA. En el diagrama se sitúa el sitio de corte por fD.

Estudios de mutagénesis en fB han puesto de manifiesto la importancia del dominio vWA tanto en la formación como en la regulación de la convertasa. El aminoácido Asp279, en la hélice α1, en las proximidades del sitio MIDAS del dominio vWA, es esencial en el reconocimiento inicial por C3. El cambio Asp279Gly aumenta la afinidad por C3b, genera una convertasa más estable y también más resistente a la disociación por los reguladores. En cambio, ls región de las hélices α4/5 del dominio vWA parece estar más implicada en la interacción con los reguladores.[29, 30]

2. El control del sistema del complemento.

Las proteínas reguladoras del complemento son tan importantes como aquellas que permiten su activación. El rápido y potente efecto de la activación del complemento como primera línea de defensa frente a infecciones puede ser también, potencialmente dañino para el propio individuo, conduciendo incluso a estados patológicos. Para evitar el daño y mantener la homeostasis del sistema, un conjunto de proteínas del complemento actúa regulando el sistema, lo que permite que la activación sea además de eficaz, localizada sobre las superficie extrañas.

2.1. Los reguladores del RCA.

La mayoría de los reguladores se encuentran codificados en un agrupamiento génico denominado RCA (*regulators of complement activation*),[31, 32] localizado en el cromosoma 1 en la región 1q32 (**figura 5**). Otros reguladores del complemento no situados en el RCA son el inhibidor de C1 (C1-inh), que actúa en la CP inhibiendo irreversiblemente las serín proteasas C1r, C1s, MASP1 y MASP2 entre otras,[33] y CD59, que se une a C9, bloqueando su polimerización y con ello la formación del MAC.[34] También son reguladores la P, como estabilizador de la AP y la serín proteasa factor I (fI), inhibidor principal de C3b.

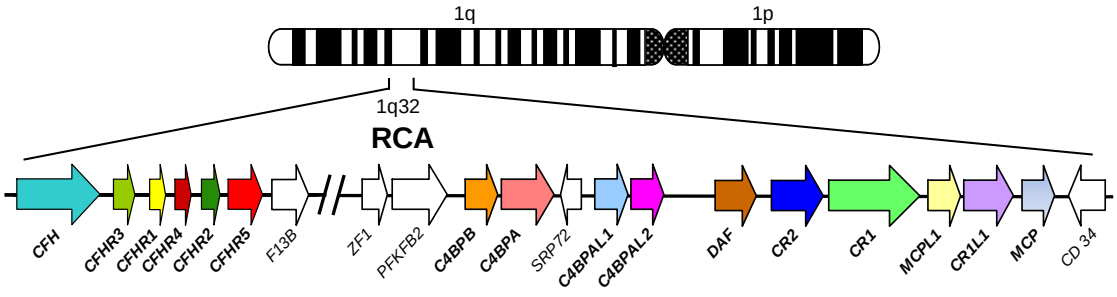

Figura 5. Estructura del agrupamiento génico del RCA en el cromosoma 1 de la especie humana. El agrupamiento del RCA se encuentra localizado en el brazo largo del cromosoma 1, en la región 1q32. Los genes coloreados codifican proteínas ligadas a la regulación del sistema del complemento.

Los reguladores del RCA constituyen una familia de proteínas genética, estructural y funcionalmente relacionada. Están compuestos en su mayor parte de dominios SCR (entre 4 y 30), de unos 60 aminoácidos cada uno. Los SCRs se caracterizan por su alto grado de conservación, incluyendo en su secuencia cuatro cisteínas invariables que establecen puentes disulfuro y ayudan a mantener una estructura globular a estos dominios.[35, 36]

Entre los reguladores que se sitúan en el RCA podemos encontrar los que están asociados a la membrana celular, como DAF (*deacy acceleration factor*), MCP (*membrane cofactor protein*), CR1 y CR2 (*complement receptor* 1 *and* 2) y CD59. Las células humanas están protegidas de la lisis mediada por el complemento ya que poseen estos reguladores. Otros como C4bp (C4 *binding protein*) y factor H (fH) están presentes circulando en el plasma, limitando la activación y el consumo del complemento en fase fluida. fH tiene la capacidad de reconocer las células propias por lo que también es un regulador de superficie.[7]

Otra característica común de estos componentes del RCA es que su función reguladora está estrechamente relacionada. Dado que la hidrólisis de C3 a C3b, proceso en el que convergen las tres vías, es un evento clave en la activación del complemento, el punto de máximo control son las convertasas. Estos reguladores actúan sobre estos complejos de dos formas posibles: acelerando la disociación de las convertasas de C3 y C5; o asistiendo como cofactor de la proteasa fI en la degradación proteolítica de C3b y C4b. El siguiente apartado se centra exclusivamente en la regulación de la convertasa de C3 de la AP.

2.2. Regulación de la convertasa de C3 de la vía alternativa.

2.2.1. Disociación de la convertasa.

Las convertasas son unos complejos multiproteicos muy inestables y una vez formados tienden a decaer espontáneamente. La vida media de la convertasa de C3 de la AP, C3bBb, es de unos 90 segundos (**figura 6.A**).[37, 38] Tras su disociación el componente catalítico Bb no puede reasociar y la actividad enzimática se pierde, mientras que el C3b si puede formar nuevas convertasas (**figura 6.B**). Son varias las proteínas del RCA pueden acelerar la disociación irreversible de los complejos convertasa.

Existen tres reguladores que actúan sobre la convertasa de la AP, C3bBb: DAF, CR1 y fH.[6, 39, 40] La actividad de aceleración de disociación reside en una porción de estas proteínas, siendo solo determinados dominios SCR suficientes para disociar el complejo C3bBb.[41-43] Este mecanismo de regulación no se conoce con exactitud, aunque se postula que depende de interacciones tanto con C3b como con Bb. Además, se sugiere que detrás de los diferentes reguladores se halla un mecanismo de disociación diferente.[29, 44] La disociación de C3bBb se consigue tanto en fase fluida, a través de fH, como sobre las superficies celulares, donde intervienen los tres reguladores.

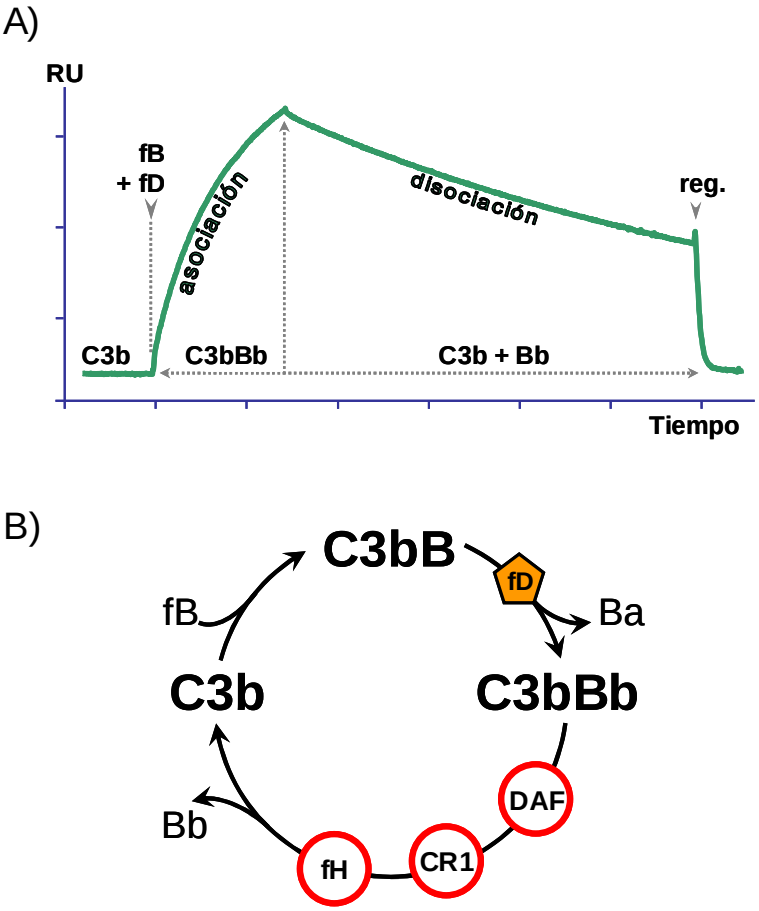

Figura 6. Disociación de la convertasa de C3 de la vía alternativa. A) Ensayo de SPR *(surface plasmon resonance),* de formación de convertasa de C3 de la AP. La adición de fB y fD sobre un chip inmovilizado con C3b genera convertasa C3bBb, y el aumento de masa sobre el chip se traduce en un incremento en la señal de respuesta (RU). Una vez se dejan de aportar estos componentes la señal de respuesta desciende, debido al efecto de la disociación espontánea de C3bBb. La regeneración (reg) de la superficie puede realizarse con proteínas reguladoras. B) Los reguladores fH, CR1 y DAF aceleran la disociación de la convertasa C3bBb. El C3b procedente de la disociación puede volver a formar una convertasa activa.

2.2.2. Proteólisis de C3b.

La degradación proteolítica de C3b es llevada a cabo por fI, una serín proteasa altamente específica, que circula en conformación inactiva en el plasma. Además de C4b, no se conocen otros sustratos naturales y sólo es posible el corte proteolítico en presencia de los cofactores adecuados.[6] El mecanismo por el que se activa fI no se conoce completamente. Aunque se

asume que es necesaria una estrecha interacción entre la enzima, el cofactor y el sustrato en lo que parece un mecanismo de regulación alostérico.[45]

En un primer paso de la hidrólisis de C3b, se producen dos cortes adyacentes en el dominio CUB de la cadena α, generando un C3b inactivo (iC3b) y liberándose un pequeño péptido de 17 aminoácidos (C3f). Este corte lo realiza fI utilizando como cofactores MCP, CR1 y fH. El iC3b es susceptible de otro corte, también en el dominio CUB, generando C3c, que queda soluble en el plasma, y C3dg, que corresponde al dominio TED y queda adherido a la superficie. Este segundo corte sólo se produce cuando CR1 actúa como cofactor(**figura 7**).[19, 46] Ninguno de estos fragmentos puede activar la cascada del complemento. Sin embargo, en condiciones normales, la degradación irreversible de C3b tiene otros efectos además de evitar la formación de convertasa en el tejido propio, y controlar el consumo de C3 en fase fluida. Los productos de hidrólisis como iC3b, C3c y C3dg se unen a determinados receptores del complemento, y median funciones como la eliminación de inmunocomplejos, opsonización, o la estimulación los linfocitos B y la memoria inmunológica.[11, 47]

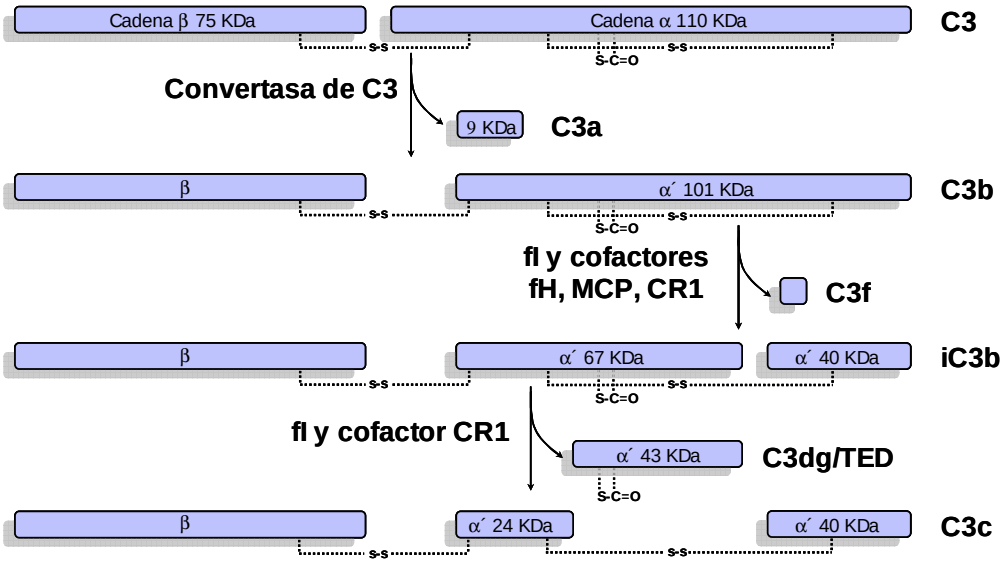

Figura 7. Activación de C3 y proteólisis de C3b. El componente C3 está compuesto por dos cadenas, α y β, unidas por un puente disulfuro. El corte de C3 por la convertasa, que produce las moléculas de C3b y C3a, y los cortes sucesivos sobre C3b ser dan exclusivamente en la cadena α mientras que la cadena β permanece invariable. El fI lleva a cabo la degradación proteolítica de C3b utilizando los cofactores fH, MCP o CR1. El grupo reactivo tioéstrer (S-C=O) está localizado en la cadena α, en el dominio TED.

2.3. Factor H.

El principal regulador de la AP del complemento es el regulador fH, una glicoproteína plasmática de 155 KDa, compuesta por 20 dominios SCR.[48] fH es sintetizado de forma constitutiva por el hígado, aunque puede expresarse localmente en una gran variedad de tejidos incluyendo membranas endoteliales y epiteliales, plaquetas, células madre mesenquimales y el epitelio pigmentario retinal entre otros.[49] La concentración de fH en la especie humana es muy variable (116-562 μg/ml) y está condicionada por factores ambientales, como la edad y el tabaco, pero principalmente por un factor genético. El componente genético que contribuye a la variabilidad de la concentración de fH se ha estimado en un 62%.[50]

fH compite con fB por la unión de C3b, impidiendo la formación del complejo pro-convertasa de la AP, acelera la disociación de la convertasa de C3 y de C5 de la AP, y actúa como cofactor de fI en la degradación proteolítica de C3b.[41, 51-53] La función reguladora de fH, que obedece principalmente a su capacidad de interacción con C3b, se lleva a cabo tanto en la fase fluida del plasma como en las superficies propias donde se haya depositado el C3b. La regulación sobre superficies depende de la capacidad de fH de unirse a polianiones, como son el acido siálico y los glucosaminoglucanos (GAGs) como la heparina. En las superficies propias, la presencia de estos marcadores incrementa la afinidad por el C3b depositado, debido al reconocimiento simultáneo de ambos tipos de moléculas.[54-56] De esta manera, fH actúa de forma selectiva, limitando la progresión de la cascada sobre las superficies de los tejidos propios, y permitiendo la amplificación de la AP solamente sobre las superficies extrañas.

2.3.1. Dominios funcionales de factor H.

Ensayos de interacción y funcionales empleando muestras de fH completo y de fragmentos recombinantes, han permitido establecer un mapa de la proteína caracterizando los sitios de unión a C3b y polianiones.[57-65] Existen dos regiones de unión a C3b, una a cada extremo de la molécula (**figura 8**). En el N-terminal, el sitio de unión que abarca los SCRs 1-4 es el único necesario y suficiente para realizar la función cofactora de fI. También acelera la disociación de las convertasas, aunque para ello deben contribuir otras regiones de fH, ya que la capacidad de disociación de fragmentos fH-SCRs 1-4 es hasta 100 veces

menor que la del fH completo.[60] En C-terminal, la región en los SCRs 19-20 es la de mayor afinidad a C3b, sin embargo, ambos sitios en extremos opuestos deben cooperar en la unión a C3b. Ensayos de interacción mediante SPR demuestran como la afinidad del fH completo es mucho mayor que la de los fragmentos del N y C-terminal por separado.[65] La interacción de fH con polianiones y GAGs se ha localizado en la región central, el SCR 7, con la contribución de los SCRs 6 y 8, y en los SCRs 19-20, siendo este último el principal sitio de unión a heparinas. De esta manera, la región C-terminal de interacción con C3b y polianiones resulta crucial para la capacidad de fH de reconocer y proteger las células del tejido propio.

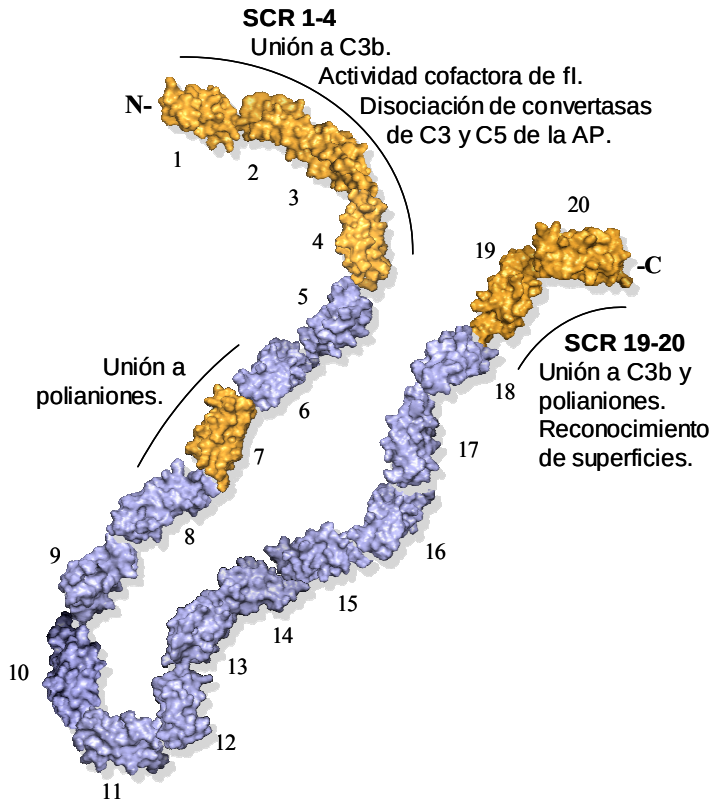

Figura 8. Representación estructural de la molécula de factor H. La figura muestra un modelo teórico de fH, en el que los 20 dominios SCR configuran una molécula cuyas regiones funcionales, SCRs 1-4 y SCRs 19-20 en los extremos N y C-terminal, están acercadas entre sí. Los dominios SCR más relevantes con capacidad de interacción y/o funcional aparecen en naranja. La estructura de los dominios SCR se obtiene de diferentes orientaciones de varios dominios SCR disponibles en www.rcsb.org.

Los 20 dominios SCR que componen fH están conectados por cadenas cortas de tamaño variable (de tres a ocho residuos). La inclinación del unos SCRs respecto a otros configuran una molécula que, contrario a como se pensaba, resulta poco flexible y en la que los extremos N y C-terminal están acercados entre sí (**figura 8**).[66, 67] Esta arquitectura debe resultar funcionalmente relevante al permitir que ambos extremos de fH interaccionen con la misma molécula de C3b. Lo que explicaría como los sitios de unión a C3b, SCRs 1-4 y SCRs 19-20, cooperan y confieren avidez. Morgan HP *et al*

construyen un modelo de fH-C3b, en el que toman la estructura de diferentes segmentos de fH y de los complejos fH_{SCR1-4}-C3b y $fH_{SCR19-20}$-C3d/TED. En este modelo una molécula de fH interacciona con una de C3b en regiones no solapantes a través de sus sitios de unión en los extremos opuestos de fH, y permite además que la región C-terminal de los SCRs 19-20 se una a los polianiones de la superficie.[68]

Todo lo anteriormente indicado, se puede sintetizar en lo siguiente: fH contiene dos regiones funcionales diferenciadas: la región N-terminal de unión a C3b, donde reside la actividad reguladora de fH (cofactora y de aceleración de disociación); y la C-terminal de unión a C3b y polianiones, que aporta la capacidad selectiva en la interacción con superficies. La correcta actividad de fH depende la cooperación de estas dos regiones y otros sitios de interacción.

2.3.2. El gen *CFH*.

El fH está codificado por un único gen (*CFH*), localizado dentro del RCA en la región 1q32.[31, 32] El gen *CFH* contiene 23 exones, siendo el primer exón codificante de las regiones 5'UTR y del péptido señal. Cada uno de los 22 exones restantes codifica uno de los 20 dominios SCR de fH, excepto el SCR 2 que está codificado por los exones 3 y 4 (**figura 9.C**).[69, 70] Existe un transcrito alternativo, fH *like*-1 (fHL-1), que comparte los 9 primeros exones de fH, lo que da lugar a una proteína de 42 KDa que contiene los 7 primeros SCRs de fH más una cola de cuatro aminoácidos (Ser-Phe-Thr-Leu), codificados por el exón 10, que no está presente en el mensajero maduro codificante de fH (**figura 9.A-B**).[71, 72] Ambas proteínas son expresadas mayoritariamente por el hígado, siendo la concentración en plasma de fHL-1 mucho menor (10-50 μg/ml). fHL-1 presenta funciones reguladoras del complemento, como la actividad cofactora de fI y la de disociación de la convertasa C3bBb. fHL-1 también es capaz de unirse a heparinas, diversas proteínas microbianas, y a las superficies celulares, estando implicada en procesos de movilidad celular.[60, 73]

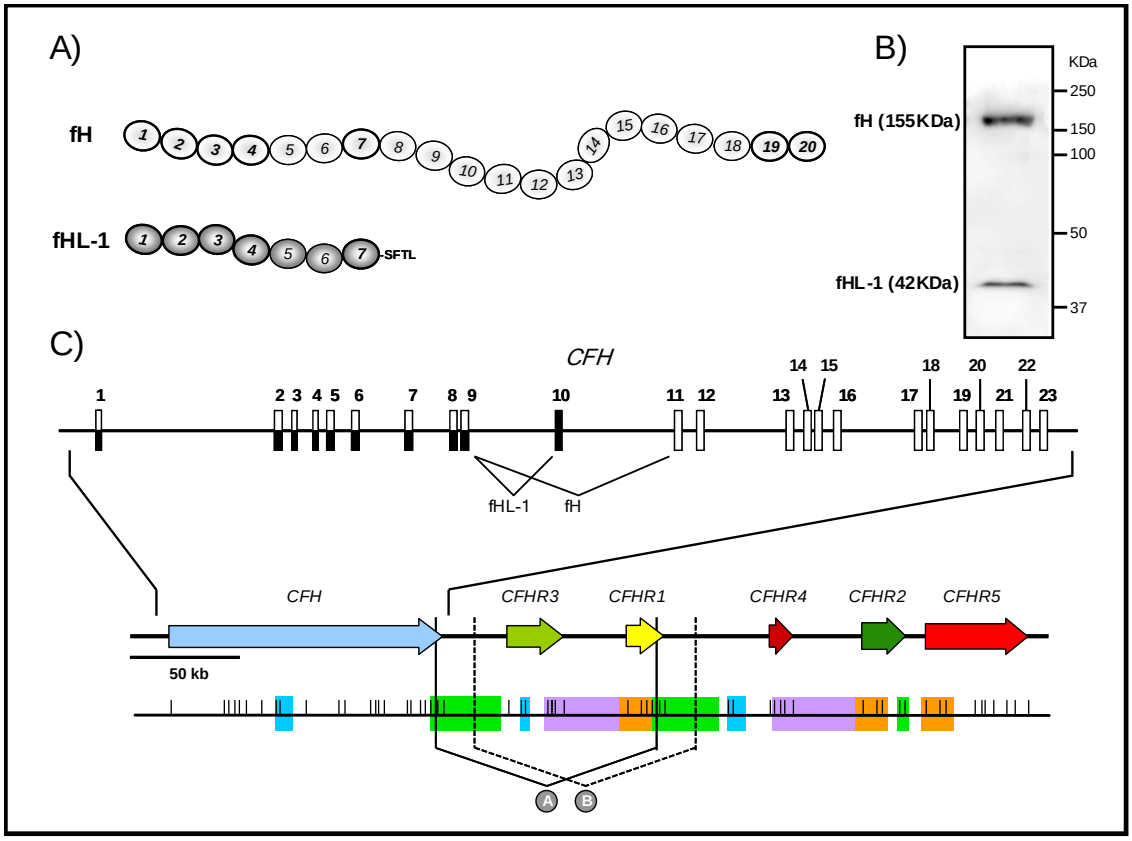

Figura 9. Familia de proteínas relacionadas con factor H. A) Los reguladores fH y fHL-1, codificados por el mismo gen, *CFH*, comparten los siete primeros dominios SCR. Una cola de cuatro aminácidos, codificados por el exón diez, compone la región C-terminal de fHL-1. B) *Western blot* de fH y fHL-1 empleando un anticuerpo específico de la región N-terminal de fH. C) El gen *CFH* esta compuesto por 23 exones. Todos codifican para fH (en blanco), excepto el exón diez, que junto con los nueve primeros codifica para fHL-1 (en negro). Los genes de la familia de fH, *CFH* y *CFHR1-5*, están organizados en tándem. Las zonas conteniendo exones (barras verticales) de igual color representan regiones de alta homología de secuencia. Se muestras dos reordenamientos cromosómicos frecuentes: el gen híbrido, *CFH::CFHR1* (A) y la deleción de los genes *CFHR3* y *CFHR1* (B).

A pesar de compartir las regiones promotoras y de inicio de transcripción, la regulación de la expresión de fH y fHL-1 es diferente dependiendo del tipo celular. El porqué de esta regulación independiente se desconoce, aunque debe obedecer a mecanismos a nivel transcripcional y/o post-transcripcionales diferentes. Esto sugiere que existen funciones específicas para fH y fHL-1, donde tanto el tejido como la concentración local pueden ser muy importantes. Sin embargo, el papel preciso de fHL-1 *in vivo* no está determinado.[70, 74]

2.3.3. Familia de proteínas de factor H.

Además de fHL-1, en la especie humana existen en el plasma otras 5 proteínas relacionadas con fH, denominadas CfHRs 1-5. Todas ellas forman una familia de proteínas de fH, estructural y funcionalmente relacionada, y con correactividad inmunológica. Estas 5 proteínas están codificadas por genes independientes, localizados también en el grupo de ligamiento del RCA junto al gen *CFH,* y se organizan en tándem.[75, 76] La región que comprende esta familia de genes presenta secuencias de alta homología y contiene grandes regiones duplicadas que incluyen diferentes exones de *CFH* y *CFHRs 1-5.* Esta situación favorece que se produzcan fenómenos de reordenamiento cromosómico, como los de conversión génica[77, 78] y otros, relativamente más frecuentes, de recombinación no homóloga que dan como resultado duplicaciones y deleciones de genes (**figura 9.C**). Los reordenamientos en la familia de genes de fH pueden dar lugar, como se verá más adelante, a situaciones de asociación con patología.[70, 79]

Los CfHRs 1-5, al igual que fH, están compuestos exclusivamente de SCRs, conteniendo de 4 a 9 dominios. Presentan dos regiones conservadas, la N-terminal, que corresponde a la región central de fH, SCRs 6-9, y la C-terminal, que es homologa a la región C-terminal de fH, SCRs 18-20. El grado de homología entre los dominios de los CfHRs 1-5 y los respectivos de fH varía entre el 32 y el 100%. Este hecho es consistente con que estas proteínas presenten funciones relacionadas e incluso compartidas. La región conservada C-terminal de los CfHRs 1-5 sugiere que estas proteínas, como fH, puedan unir ligandos de superficie y diferenciar entre tejido propio y no propio. Por el contrario, al carecer de una región reguladora como la de fH (SCRs 1-4, con actividad cofactora y disociación de la convertasa), no poseen una potente capacidad de regulación del complemento.[80] Por otro lado, ciertos cambios en la secuencia de aminoácidos en localizaciones expuestas, y diferencias en las modificaciones de estos confieren unas propiedades únicas de afinidad y de interacción a ligandos. Se ha descrito unión a C3b para los CfHRs 1, 3, 4 y 5.[79] CfHR 3 por su parte, presenta cierta capacidad cofactora,[81] y el CfHR 5, que es el único con una región central de 5 SCRs, posee una débil actividad cofactora y de disociación de la convertasa de C3.[82] El CfHR 1, por el contrario, es capaz de regular la activación del complemento a nivel de la convertasa de C5.[83]

Aunque la función específica de los CfHRs 1-5 se desconoce, la relación funcional entre ellas y con el fH es clara, lo que converge en tres escenarios

posibles para describir el papel biológico de los CfHRs 1-5: cooperación en la regulación de la activación del complemento; competición por ligandos y superficies, lo que se traduciría en una menor regulación; y un último en el que se den las funciones independientes de cada proteína.[80]

3. Asociación con patología.

La activación del complemento y sus mecanismos reguladores se encuentran en equilibrio, de manera que la actividad efectora del complemento se localiza en las superficies extrañas y se limita sobre las propias. Alteraciones en este equilibrio pueden conducir a lesiones en los tejidos, susceptibilidad frente a infecciones, así como a estados patológicos crónicos. Dentro de las enfermedades asociadas al complemento, y concretamente a los componentes de la vía alternativa, cabe destacar: el síndrome hemolítico urémico atípico y la enfermedad por depósitos densos, trastornos que afectan fundamentalmente al riñon y con una localización glomerular predominante (**figura 10**); y la degeneración macular asociada a la edad, trastorno ocular de manifestación tardía que afecta a la visión central.

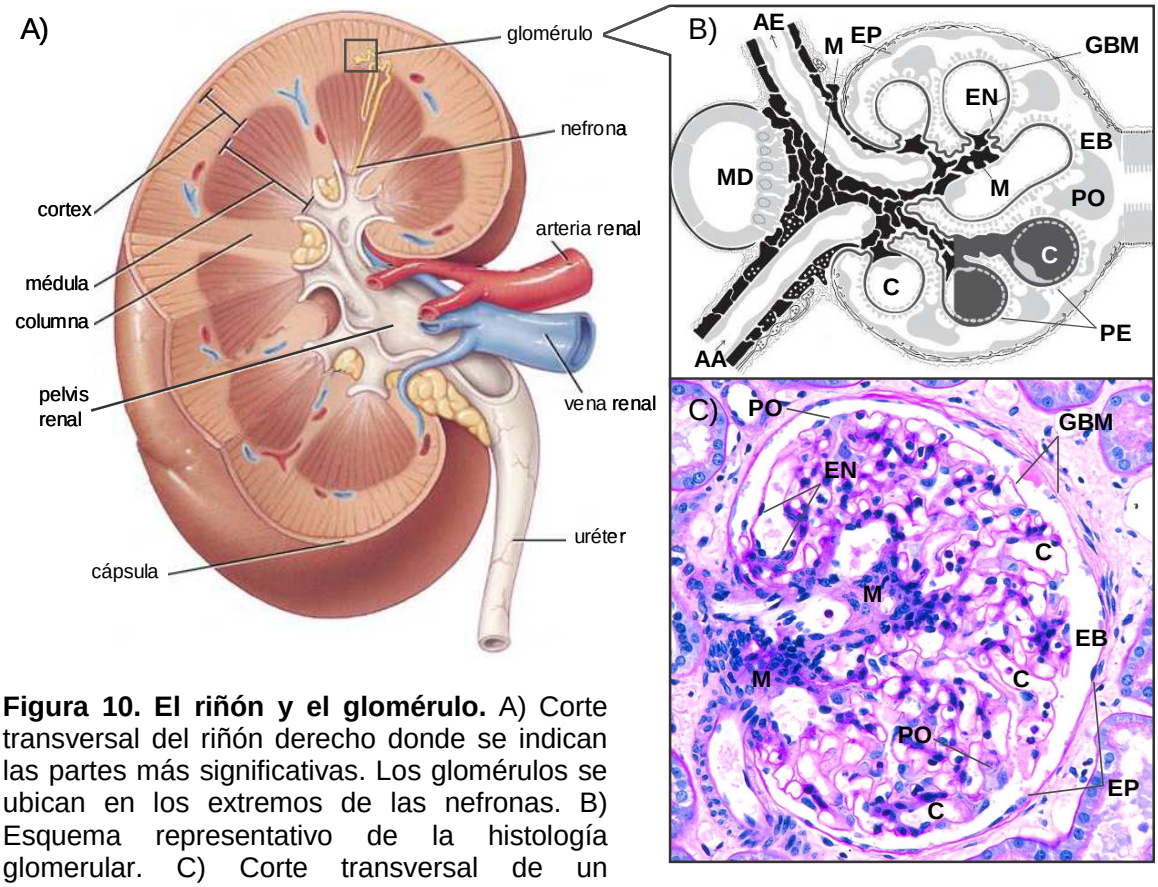

Figura 10. El riñón y el glomérulo. A) Corte transversal del riñón derecho donde se indican las partes más significativas. Los glomérulos se ubican en los extremos de las nefronas. B) Esquema representativo de la histología glomerular. C) Corte transversal de un glomérulo teñido con PAS. MD: mácula densa; AA: arteriola aferente; AE: arteriola eferente; C: capilar glomerular; GBM: membrana basal glomerular; EN: endotelio capilar; EP: epitelio de la cápsula de Bowman; M: células mesangiales; PO: podocito; PE: pedicelos; EB: espacio de Bowman.

3.1. Síndrome hemolítico urémico atípico.

El síndrome hemolítico urémico (HUS) es un trastorno de la microvasculatura que afecta fundamentalmente al riñón, aunque también al sistema nervioso c entral y al gastrointestinal. Está clínicamente definido por anemia hemolítica microangiopática, trombocitopenia y fallo renal agudo. Las lesiones del endotelio en la microvasculatura glomerular tanto por infección u otros daños exógenos, parecen ser el evento que inicia el proceso patogénico. Las lesiones se caracterizan por el engrosamiento de las paredes de arterias y capilares, inflamación del endotelio y su desprendimiento de la membrana basal glomerular (GBM), acumulación subendotelial de proteínas y restos celulares y formación de microtrombos de plaquetas y fibrina que ocluyen los vasos. La generación de esquistocistos (eritrocitos fragmentados) al circular por la microvasculatura renal parcialmente obstruida es otra característica del HUS (**figura 11**).[84]

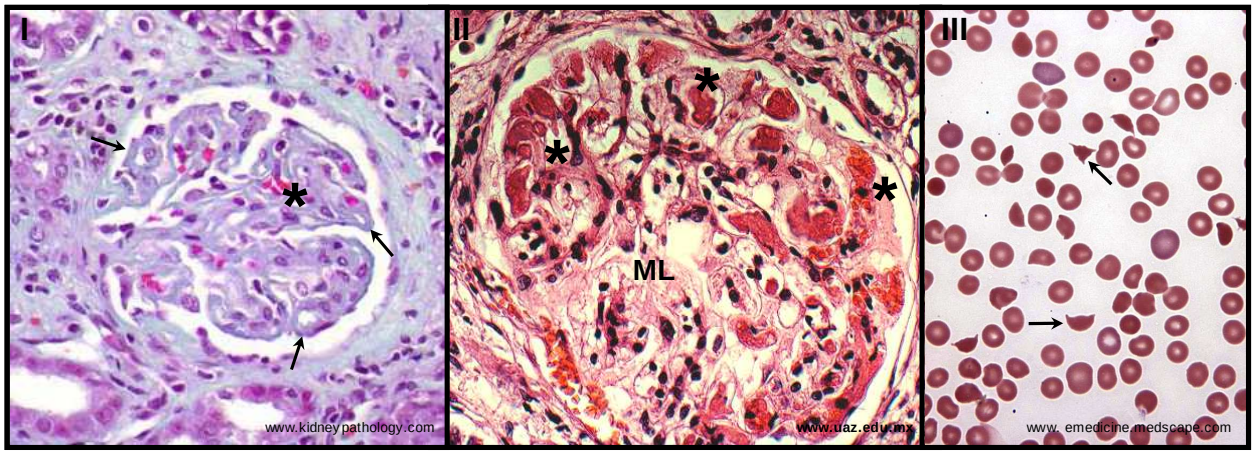

Figura 11. Histopatología del síndrome hemolítico urémico atípico. Las micrografías muestran algunas características patológicas del aHUS. Estas son: engrosamiento de las paredes de los capilares y disminución de la luz capilar (flechas en I, tinción hematoxilina-eosina); microtrombos glomerulares (asteriscos en I y II); mesangiolisis (ML en II, tinción tricrómico de Masson); y esquistocistos (flechas en III).

Tradicionalmente se pueden distinguir dos tipos de HUS. La forma más frecuente (un 90% de los casos), denominada típica, afecta principalmente a niños y tiene una incidencia de unos dos casos al año por cada 100.000 habitantes. El HUS típico está asociado a la infección de una cepa enterohemorrágica de *Escherichia coli* (0157:H), productora de una potente citotoxina tipo Shiga. Aunque el mecanismo por el que actúa esta toxina no se conoce completamente, su implicación como causante de la diarrea

hemorrágica y en desarrollo de la patología es indiscutible. Después de atravesar la barrera intestinal y entrar en la circulación sistémica, las toxinas Shiga se unen a receptores de las superficies endoteliales, provocando lesiones y favoreciendo estados inflamatorios y protrombóticos.[85, 86] La mayor parte de casos de HUS típico evolucionan favorablemente y la función renal se recupera en la mayoría de ellos (75%). El resto pueden desarrollar enfermedades renales crónicas llegando incluso a la muerte (3-5%).[87]

La forma atípica de HUS (aHUS) se manifiesta tanto en niños como en adultos y la asociación a infecciones gastrointestinales por *E. coli* queda excluida en este grupo de pacientes. La incidencia del aHUS corresponde a dos casos anuales por cada 1.000.000 habitantes. En base a los análisis histológicos, las lesiones causadas en aHUS son indistinguibles de las de la forma típica, sin embargo, el aHUS tiene un peor pronóstico. La mayoría de los pacientes presentan recurrencias y la mitad desarrollan insuficiencia renal crónica (IRC). La mortalidad por aHUS es del 25% aproximadamente.[84, 87] No existe una asociación particular para el aHUS pero sí se han identificado una serie de factores de riesgo que predisponen a esta enfermedad. Entre ellos se incluyen tratamientos inmunosupresores o anticancerígenos, anticonceptivos orales, el embarazo y el posparto. Por otro lado, numerosos estudios han encontrado en los casos familiares de aHUS, y menos frecuentemente en los casos esporádicos, un claro componente genético. Mientras que en algunos casos de aHUS se han encontrado mutaciones en proteínas procoagulantes como la trombomodulina (*THBD*),[88] la mayoría de mutaciones en estos pacientes se encuentran sobre genes de la AP del complemento. La implicación del complemento en el HUS se conoce desde 1974, pero ha sido en los últimos años cuando se ha establecido una asociación clara entre el aHUS y las proteínas del complemento. Se han encontrado en numerosas ocasiones mutaciones y polimorfismos asociados a aHUS en proteínas reguladores como fH, MCP o fI;[89] y más recientemente en los componentes fB y C3.[90, 91] En muchas de las mutaciones se ha comprobado una consecuencia funcional y llegan a suponer hasta la mitad de los casos de aHUS, lo que da a entender la gran implicación de la AP del complemento en la patogénesis de esta enfermedad. Sin embargo, en muchos de los casos todavía no se ha detectado una causa, genética o ambiental, que pueda considerarse un desencadenante, lo que indica la existencia de factores adicionales aún por identificar. Entre las mutaciones asociadas, la mayor parte se localizan en el gen *CFH*, que requiere una especial atención en la patogénesis de esta enfermedad.[92] De hecho, un grupo de pacientes aHUS presenta

autoanticuerpos dirigidos contra la región C-terminal de fH y bloquean su función.[93, 94] Además, existe un modelo de aHUS en ratón con una proteína trucada de fH.[95]

3.2. Enfermedad por depósitos densos.

La glomerulonefritis membranoproliferativa (MPGN) hace referencia a un patrón general de lesión glomerular que puede verse en ciertas enfermedades. Se caracteriza por un engrosamiento de las paredes de los capilares glomerulares y una proliferación anormal de las células mesangiales, que difunden también al interior de los capilares. Como consecuencia, el glomérulo se presenta frecuentemente hiperlobulado. Estos cambios pueden detectarse examinando el tejido por microscopía óptica, prestando un diagnóstico del MPGN relativamente sencillo (**figura 12**). De acuerdo a las características patológicas, existen tres tipos de MPGN y todos ellos están asociados con hipocomplementemia, existiendo particularidades en el mecanismo por el que se activa el complemento.[96, 97]

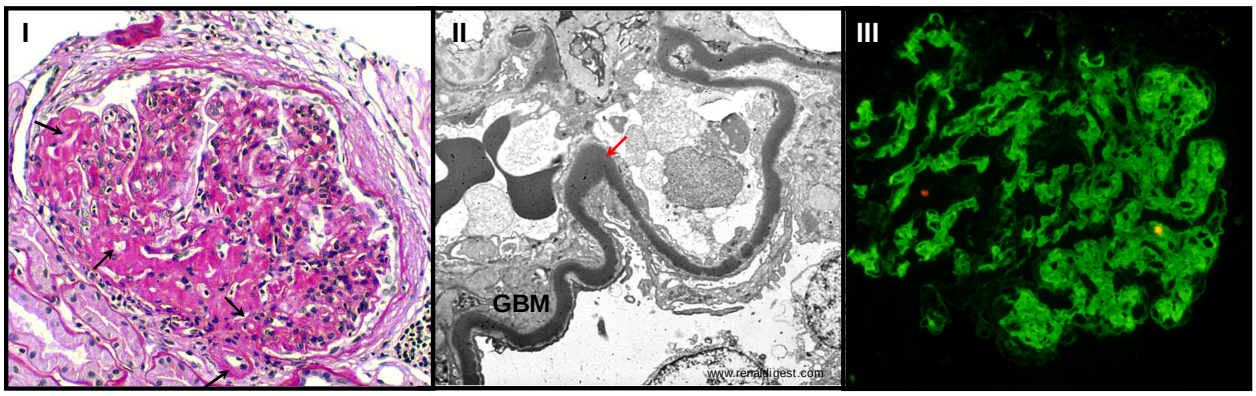

Figura 12. Histopatología de la enfermedad por depósitos densos. Las micrografías muestras algunas de las características patológicas de DDD. Glomérulo hiperlobulado con un importante engrosamiento de las paredes capilares (flechas negras), observándose en ciertas regiones con un doble contorno, debido a los depósitos densos. Es notable la proliferación mesangial en la matriz y la zona endocapilar, y el desprendimiento endotelial (I, tinción PAS). Los depósitos densos se localizan en el en el interior de la GBM que aparece dividida en dos (flecha roja en II, imagen por EM). Inmunofluorescencia demostrando la presencia de C3 a lo largo de la GBM del glomérulo (III).

La DDD corresponde a la MPGN de tipo II, siendo la patología menos común y la de peor prognosis. La mitad progresan a IRC y más del 80% necesitan trasplante. Se caracteriza además por la presencia de depósitos

electrodensos en el interior de la membrana basal glomerular (GBM), que aparece dividida en dos, en observaciones al microscopio electrónico. Estos depósitos pueden encontrarse también en el área mesangial y en la cápsula de Bowman. La composición exacta de los depósitos se desconoce, aunque se ha comprobado la presencia de C3 en la superficie de estos y de componentes de la vía lítica (**figura 12**).[98] Al contrario que en otros tipos de MPGN, el C3 aparece en DDD en ausencia de inmunoglobulinas. Este hecho apoya la idea de que en DDD el complemento es activado en plasma, en lugar de localmente sobre la GBM, lo que excluye la activación por inmunocomplejos a través de la CP del complemento.[96, 97]

La hipótesis más aceptada propone que la activación descontrolada a través de la AP tiene una implicación directa sobre la DDD. La mayoría de los pacientes con DDD (hasta el 80% en algunos estudios) son positivos para el factor nefrítico de C3 (C3-Nef), un autoanticuerpo plasmático contra la convertasa de C3 de la AP. C3-Nef incrementa la vida media de la convertasa y al mismo tiempo la hace más resistente a la acción de los reguladores. También se ha asociado DDD con la deficiencia del regulador fH, como consecuencia de mutaciones, generalmente en homocigosis. Ambas situaciones conllevan una perpetua activación y consumo del C3 circulante. Hecho que es consistente con los niveles bajos de C3 y de actividad hemolítica (CH50) encontrados en estos pacientes.[99] Existen modelos animales de cerdo y ratón deficientes de fH que desarrollan fenotipos similares a DDD.[100, 101] El cruzamiento de estos ratones con otros deficientes para fB rescata el fenotipo, confirmando que la activación por la AP es crítica en la patogénesis de la enfermedad en estos ratones.[101] Otros estudios demuestran que la patología renal puede ser prevenida en estos ratones deficientes para fH, en los que se depleciona también C5, sugiriendo que la vía terminal lítica es igualmente importante.[102] También se ha comprobado la importancia de un fI activo y la presencia de los fragmentos de degradación iC3b, C3c y C3dg en la patogénesis de DDD en ratones deficientes de fH.[103]

3.3. Degeneración macular asociada a la edad.

En los países industrializados, AMD es la principal causa de pérdida de visión en personas mayores. Se trata de una lesión ocular que afecta al área central de la retina, conocida como mácula. El diagnóstico de AMD se basa en los signos que muestran la mácula, independientemente de la agudeza visual.

Aunque existen cambios histológicos apreciables asociados a AMD en la retina, el epitelio pigmentado retinal (RPE) y los capilares coroidales, los síntomas de AMD no se manifiestan antes de los 55 años.[104]

El signo clínico característico de AMD son las drusas, cuyo su origen exacto sigue siendo desconocido. Vistas a través del oftalmoscopio, se presentan como unos puntos situados en la retina que van del blanco al amarillo, a veces con un aspecto cristalino y brillante. Son depósitos extracelulares que se acumulan entre la membrana basal del RPE y la capa colagenosa interna de la membrana de Bruch (**figura 13.B**).[104] Las drusas están presentes en diversas patologías oculares, suponiendo un factor de riesgo muy importante para el desarrollo de AMD. Esta asociación es muy estrecha, pudiendo considerarse las drusas como un signo claro de una etapa temprana de AMD, incluso en ausencia de pérdida de visión. Tanto el tamaño como el número de las drusas están relacionados con la gravedad de AMD. Su composición es inexacta y variable, y se conocen solo algunos de sus componentes. En su interior se han encontrado tanto glicoproteínas como fosfolípidos y en su parte externa se han identificado diversas proteínas: fibronectína, chaperonas, apolipoproteína E, vitronectína, amiloide P o proteínas del complemento como C1q, C4, C5, C3 (y fragmentos los de degradación) y complejos C5b-9. También pueden contener fragmentos celulares del RPE.[105]

Existe una etapa temprana en la AMD si apenas síntomas que se caracteriza por la aparición de drusas y alteraciones leves en la pigmentación del RPE. En la etapa tardía se da una pérdida de visión severa y puede clasificarse como no exudativa "seca" o atrófica y exudativa "húmeda" o neovascular (**figura 13.A**). En la primera se producen zonas hipopigmentadas bien definidas, lo que se conoce como atrofia geográfica, y el síntoma usualmente descrito son vacíos o agujeros en la visión. La etapa más avanzada se define por la presencia de suero o líquido hemorrágico en el espacio extracelular y causa el desprendimiento de la neurorretina o del RPE. Un signo característico es la neovascularización coroidal, que puede extenderse a través de la membrana de Bruch hacia el RPE. Estas alteraciones generan imágenes distorsionadas, lo que es a menudo un primer síntoma de la AMD húmeda. Ambos subtipos de AMD pueden existir en un mismo paciente y transformarse un tipo en el otro. La progresión general es de la seca a la húmeda, desarrollando esta última forma del 10 al 15% de los pacientes de AMD.[106]

El RPE es el elemento de la retina más implicado en la patogénesis de AMD. Las drusas alteran estructural y funcionalmente el RPE, causan un ensanchamiento de la monocapa, desplazándola del aporte vascular inmediato de la región coroidal. Esto supone un impedimento para el suministro normal de metabolitos y la difusión de desechos entre la retina y los capilares coroidales. Las alteraciones en la membrana de Bruch producen, además, una disminución de la adhesión celular y una menor capacidad regeneradora de la neurorretina por las células del RPE. Todo ello, junto con el efecto de la neovascularización, tiene un grave impacto sobre los fotorreceptores, lo que afecta de forma directa a la visión central.[106] Los depósitos extracelulares y ciertos componentes presentes en las drusas como proteínas activadas y reguladoras del complemento, desencadenan por otro lado procesos inflamatorios locales, que están muy implicados en la patogénesis de la AMD.[104] Los cambios en estas estructuras, como el engrosamiento de las paredes y la pérdida de permeabilidad, se producen de forma natural por el envejecimiento. Sin embargo, en el desarrollo de AMD, la influencia del medio ambiente y la genética es muy importante.

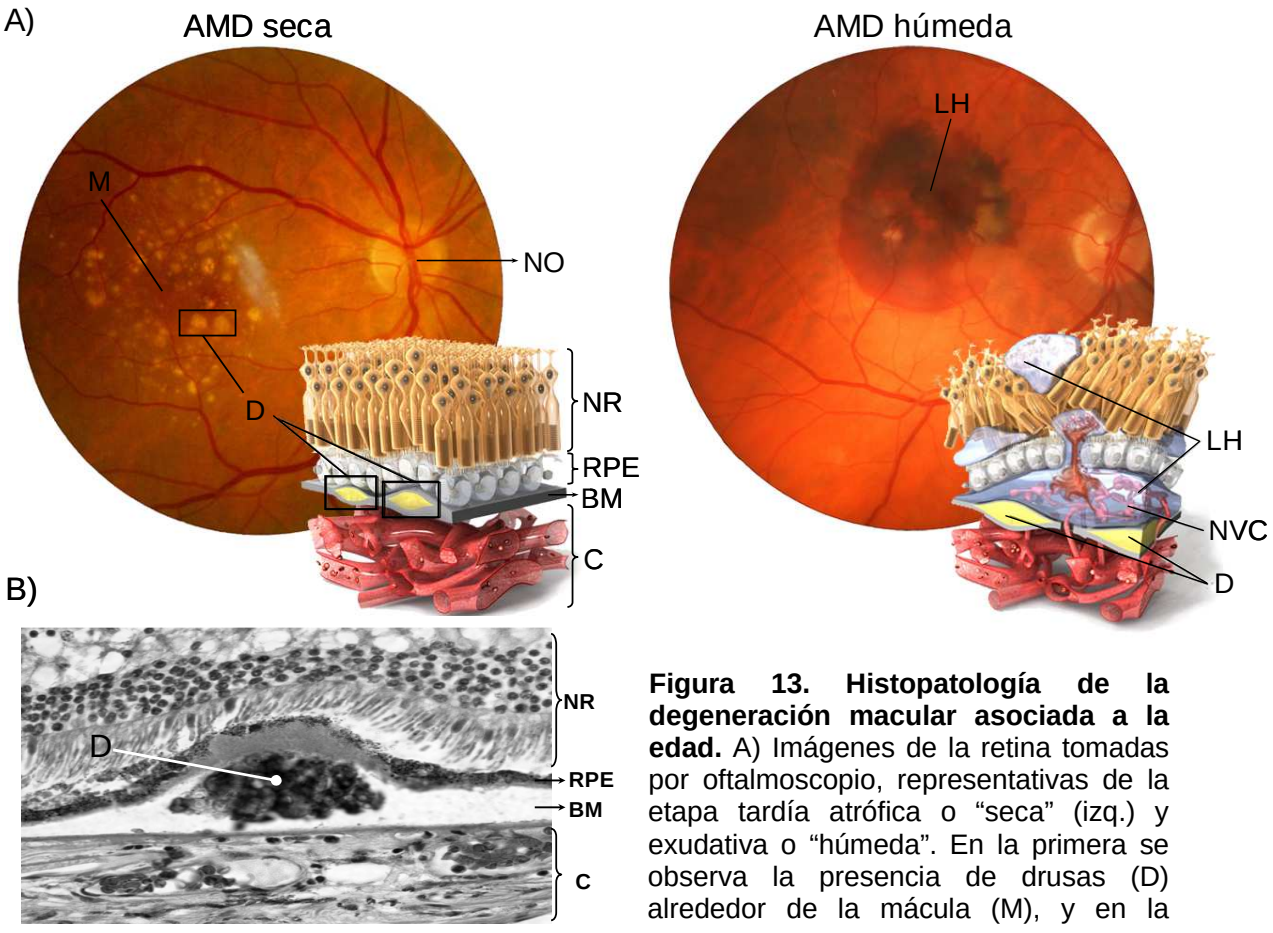

Figura 13. Histopatología de la degeneración macular asociada a la edad. A) Imágenes de la retina tomadas por oftalmoscopio, representativas de la etapa tardía atrófica o "seca" (izq.) y exudativa o "húmeda". En la primera se observa la presencia de drusas (D) alrededor de la mácula (M), y en la

segunda aparece una zona con abundante líquido hemorrágico (LH). Las figuras muestran algunas de las alteraciones de la retina, como el engrosamiento de la membrana de Bruch (BM) por las drusas; o el desprendimiento del epitelio pigmentario retinal (RPE) y la neurorretina (NR), y la presencia de liquido hemorrágico por la neovascularización coroidal (NVC). B) Sección histológica por microscopía óptica de la retina mostrando una drusa entre el epitelio pigmentario retinal y la membrana de Bruch. La región superior corresponde a la neurorretina y la inferior al coroide (C).

AMD es una patología compleja de aparición tardía, causada como otras enfermedades multifactoriales por la convergencia de múltiples factores de riesgo. Los más importantes son la edad, el tabaquismo, un alto índice de masa corporal y especialmente el genético.[104] Existen diversos genes asociados con AMD, entre los que cabe destacar *Fibl5*, *ABCA4*, *ApoE*, *HTRA1*, *ARMS2* y varios genes del complemento: *CFH*, *CFB*, *C2*, *C3* y *CFI*.[107, 108]

Los genes *HTRA1* y *ARMS2* se localizan en el locus 10q26 y están estrechamente asociados con AMD. El primero codifica para una serín proteasa que se encuentra en la retina (entre otros tejidos) y el segundo es un gen hipotético de función desconocida. Se ha descrito un haplotipo de *ARMS2* con un cambio a nivel de en secuencia (Ala69Ser) que eleva el riesgo para AMD hasta 6.3 veces en portadores homocigotos. Sin embargo, no se ha llegado a identificar la existencia esta proteína teórica y su correlación con la patogénesis de la AMD es una incógnita.[107, 108]

La asociación genética con AMD más significativa la encontramos con el locus 1q32, donde se sitúa el gen *CFH*. El polimorfismo Tyr402His de *CFH* representa el factor de riesgo más importante para AMD y la asociación se ha demostrado en diferentes poblaciones con una OR entre 2.45 y 4.6 en individuos heterocigotos (hasta 7.4 en homocigotos).[109-112] La frecuencia del alelo His402 varía entre unas poblaciones y otras lo que explica las diferencias en los grados de incidencia de este polimorfismo para AMD.

3.4. Desregulación de la vía alternativa.

Como se ha visto, existen evidencias tanto genéticas como clínicas que sitúan al complemento entre los factores implicados en el desarrollo de estas enfermedades. La hipótesis más aceptada propone la activación de la AP sobre los tejidos propios y la acumulación de componentes activados, como parte de los desencadenantes en la patogénesis. La activación anormal del complemento se produce por una desregulación en esta vía, que viene a ser

una característica patológica común para estas enfermedades. La desregulación se produce a su vez, por la pérdida del equilibrio que se mantiene entre los componentes y los reguladores de esta vía, que puede ser consecuencia de un defecto funcional de la regulación o un aumento en la activación. Ambas situaciones tienen consecuencias similares, y se han encontrado en pacientes con aHUS y DDD (**figura 14**).

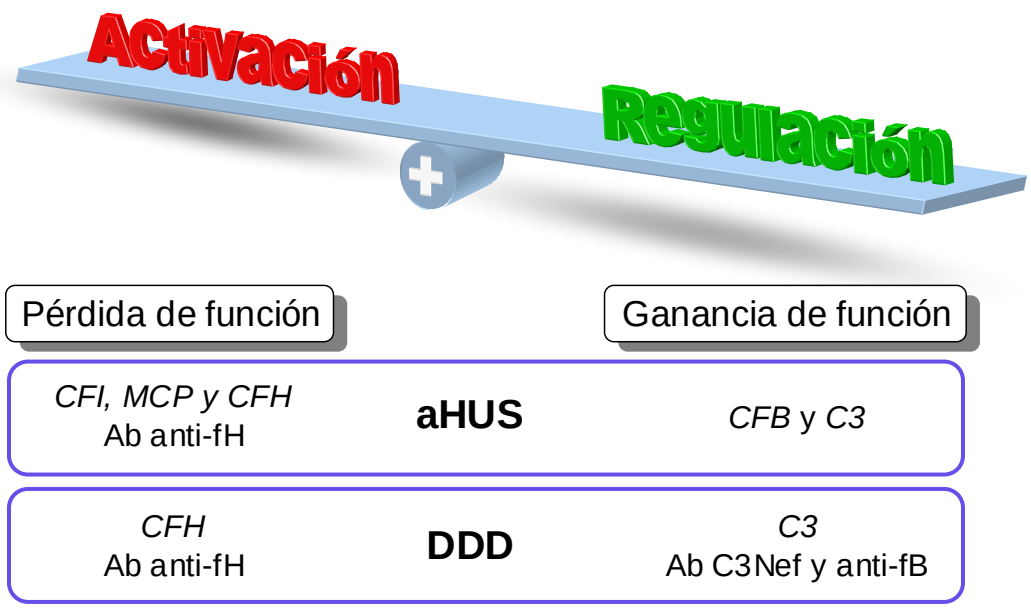

Figura 14. Desregulación de la vía alternativa. El correcto funcionamiento del sistema del complemento se consigue gracias al equilibrio entre la activación y la regulación del sistema. La desregulación que lleva a una mayor activación es una característica patológica de enfermedades como aHUS, DDD y AMD. Se muestran diversos factores de riesgo asociados con aHUS y DDD (genes portadores de mutaciones y presencia de autoanticuerpos), que causan desregulación por ganancia o pérdida de función. En la patología por AMD existe asociación con ciertos factores de riesgo, aunque las consecuencias funcionales no se conocen y no es posible afirmar si causan desregulación. Parte de los resultados presentados en esta tesis aportan información sobre esta cuestión.

En aHUS, se ha comprobado que las mutaciones en fH, MCP y fI causan una alteración y perdida de función reguladora.[92] Mientras que las mutaciones encontradas en fB y C3 son de ganancia de funcion.[90, 91, 113] En el componente fB potencian la formación de la convertasa C3bBb o confieren resistencia a su disociación por los reguladores.[90] Ensayos funcionales con C3 mutados muestran una disminución de la unión con reguladores como MCP.[91] En DDD, las mutaciones más frecuentes son en *CFH*, produciendo deficiencias de la proteína y la consecuente desregulación de la AP. También se ha descrito un caso de mutación en el componente C3. Se trata de una deleción de dos

aminoácidos que da como resultado un C3 que no puede ser activado a C3b, es decir, que no funciona como sustrato para la convertasa de C3. Por otro lado, impide la regulación por fH tanto en la inactivación por fI como en la disociación de la convertasa.[114]

Además de las mutaciones en genes del complemento, se dan otros factores como la presencia de autoanticuerpos, también asociados a estas enfermedades y con consecuencias similares a la desregulación de la AP. El factor nefrítico C3-Nef, presente en muchos de los casos con DDD, actúa estabilizando la convertasa de C3 y manteniéndola funcionalmente activa. Recientemente se ha descrito un caso de DDD con autoanticuerpos contra fB que igualmente estabilizan la convertasa.[115] Autoanticuerpos contra fH que bloquean su función se han descrito tanto en DDD como en aHUS. [93, 116] En aHUS son más frecuentes, hallándose en entre el 6 y el 10% de los casos (**figura 14**).

Menos evidencias se han encontrado en relación a AMD, sin embargo, existen muchos datos clínicos que implican al complemento en la patogénesis, y la asociación genética con el complemento, y en especial con el gen *CFH* es muy significativa. Además, muchos de los casos de DDD presentan también depósitos oculares (drusas) como los encontrados en pacientes con AMD, lo que reafirma la relación de la AMD con la activación descontrolada de la AP.[99, 117] En realidad, AMD y DDD, que son ambas enfermedades por depósitos densos, comparten cierta asociación genética y algunas características patológicas, como la acumulación de productos activados del complemento en la RPE o la GBM. Mientras que aHUS se caracteriza por un daño en el endotelio renal y trombosis. Esto ya nos da una idea de que la relación causal existente entre la desregulación de la AP y estas patologías tiene ciertas particularidades como veremos más adelante. Algo que habrá que tener en cuenta a la hora de entender los mecanismos patomoleculares de estas enfermedades.

3.5. Mutaciones en factor H.

El regulador principal de la AP en fase fluida y superficie, fH, es un nexo común para aHUS, DDD y AMD. Existen considerables evidencias que establecen la asociación de mutaciones y polimorfismos en el gen *CFH* con estas tres patologías. También se ha ilustrado como esta asociación tiene una

marcada correlación genotipo-fenotipo en la que determinadas alteraciones genéticas predisponen específicamente para una u otra enfermedadad.[118]

En DDD, las mutaciones encontradas en *CFH* se hallan en su mayoría en homocigosis y suelen conducir a la deficiencia de fH. Muchas resultan en proteínas truncadas o sustituciones de aminoácidos que afectan a la estructura de la proteína y a su correcto plegamiento, impidiendo la secreción del fH en la circulación.[119-121] La mutación ΔLys224 supone una excepción entre las asociadas con DDD. La deleción de esta lisina en el SCR 4, región clave en la función reguladora de fH, afecta a la unión a C3b, viéndose reducida la actividad cofactora y la de aceleración de la disociación de la convertasa. El paciente porta la mutación en homocigosis por lo que la función de fH está ausente (**figura 15**).[122]

La deficiencia de fH desestabiliza la regulación de la AP, y la presencia de C3-Nef, tan frecuente entre estos pacientes, exacerba la situación crónica de activación del complemento y consumo de C3. Esto conduce a la acumulación de componentes activados en la GBM y a las lesiones anteriormente comentadas. Además, la hipocomplementemia en plasma, característica de estos pacientes, tendrá efectos en el riesgo por determinadas infecciones.[123]

En la patología por aHUS nos encontramos con un escenario claramente distinto ya que las mutaciones encontradas raramente resultan en hipocomplementemia. Las alteraciones genéticas en el gen *CFH* suponen alrededor del 30% de las encontradas, y se encuentran en un 15% de los pacientes. En la mayoría de los casos se trata de mutaciones en heterocigosis, predominando las de cambio de aminoácido, y se agrupan en la región C-terminal de la proteína de fH, en los SCRs 19-20 (**figura 15**).[92] aHUS también se ha asociado con eventos de conversión génica entre el exón 23 de *CFH* y el exón 6 de *CFHR1* o un reordenamiento geonómico que da lugar a un gen híbrido *CFH::CFHR1.* Estos fenómenos afectan igualmente a la región C-terminal de fH,[77, 78, 124] que como se ha comentado anteriormente, tiene un papel esencial en el reconocimiento de las superficies celulares del tejido propio.[64, 125] Los ensayos funcionales con proteínas de fH portando estas alteraciones y mutaciones, han permitido comprobar en muchos casos, tanto una expresión como una actividad reguladora en plasma normales. Mientras que la unión a superficies celulares y la protección de la activación del complemento por la AP se ve limitada.[77, 126, 127] De igual forma, los a la región C-terminal y afectan a la regulación sobre las superficies celulares.[94]

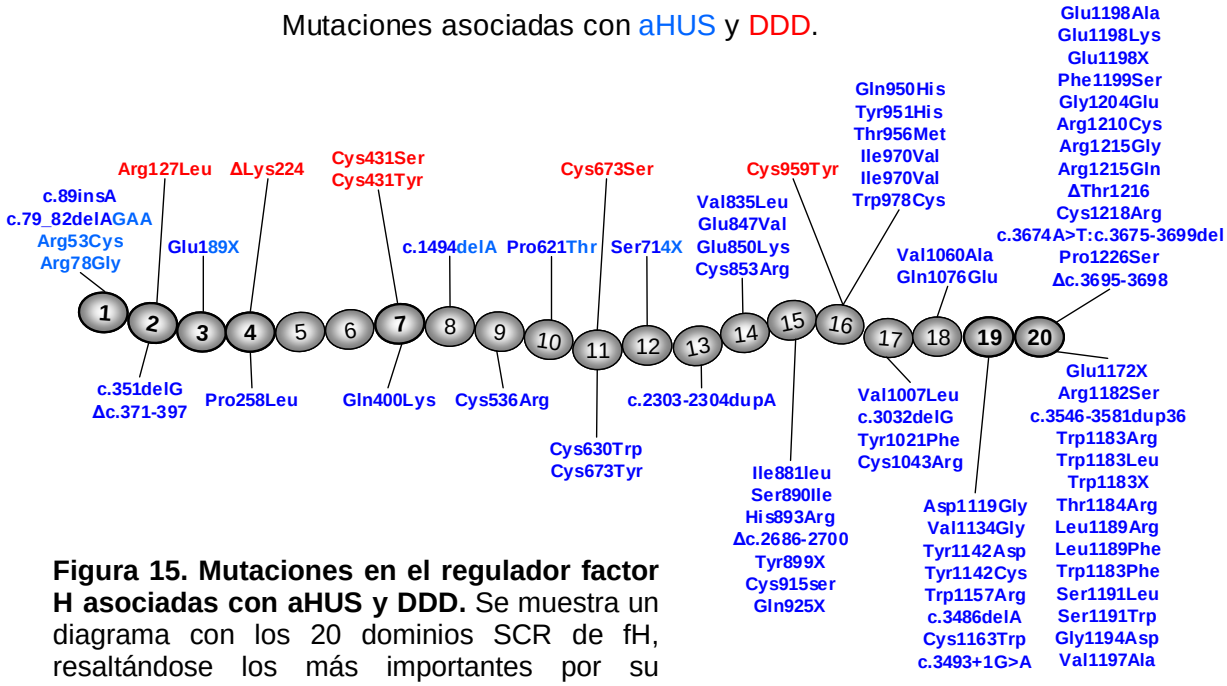

Figura 15. Mutaciones en el regulador factor H asociadas con aHUS y DDD. Se muestra un diagrama con los 20 dominios SCR de fH, resaltándose los más importantes por su implicación funcional. La mayor parte de las mutaciones de pacientes aHUS son de cambio de aminoácido, y una gran parte se agrupan en la región C-terminal de fH afectando a la función reguladora y reconocimiento de las superficies propias. También se dan mutaciones en cisternas que afectan a la expresión. En la DDD no hay una localización predominante, y todas las mutaciones afectan a la expresión de fH, salvo ΔLys224, que compromete la función reguladora.[94]

En algunos casos de aHUS también se han descrito deficiencias parciales de la proteína fH en plasma. Las causas suelen ser mutaciones nulas que dan codones *stop* prematuros y cambios de aminoácido que afectan a la estructura de la proteína. Estas mutaciones suelen estar también en heterocigosis y raramente resultan en deficiencias totales como las encontradas en los casos de DDD.[121] En cualquier caso, los bajos niveles de fH son un factor de riesgo a tener en cuenta para esta enfermedad ya que menguan la capacidad reguladora de fH en fase fluida y sobre las superficies, teniendo efecto sobre la regulación de la AP y la activación del complemento. Cabe recordar aquí, el amplio rango de los niveles de fH encontrados en plasma y que esta variabilidad tiene un componente genético muy alto.[50]

El concepto de que la deficiencia del regulador fH está asociada con DDD; y que la unión defectuosa de fH a tejidos propios junto con una actividad reguladora de la AP en plasma normal se correlaciona con aHUS; están apoyados por modelos animales. Existe una raza de cerdos noruegos con una deficiencia espontánea de fH y una línea de ratón generado por ingeniería

genética al que se le ha deplecionado este gen. Ambos modelos desarrollan una MPGN similar a la enfermedad en humanos por depósitos densos.[100, 101] En otro modelo, el ratón deficiente de fH se cruzó con uno transgénico portador un gen *CFH* truncado ($fH_{\Delta SCR16-20}$), simulando las mutaciones de fH en C-terminal. El cruzamiento no solo rescata los niveles bajos de C3 y la actividad del complemento en plasma; los ratones transgénicos $fH_{\Delta SCR16-20}$ desarrollan espontáneamente una microangiopática trombótica con las mismas características que el HUS.[95]

Todo ello, indica que aHUS no es el resultado de una deficiencia clásica de ausencia de C3 y perdida de actividad del complemento, sino de un fenómeno de autolesión producido por un complemento activo combinado con una desregulación sobre las superficies celulares.

Siguiendo en el contexto de estas dos enfermedades, aHUS y DDD, encontramos que la penetrancia es incompleta, más baja en el caso de aHUS que es del 50%. En DDD tampoco hay una asociación completa con C3-Nef, ya que está presente en individuos sanos y se asocia también con otras patologías.[122, 128] En los casos familiares de aHUS que presentan mutaciones en algún gen del complemento, es frecuente que la mutación no segregue con la enfermedad y sólo algunos individuos portadores estén afectados. Además, en los que lo hace, existe una heterogeneidad en la presentación de la enfermedad. Todo ello, junto con el hecho de que a aproximadamente la mitad de los pacientes de aHUS no se les ha detectado ninguna alteración genética, indica la influencia de factores de riesgo adicionales (ambientales y genéticos) en el desarrollo de estas enfermedades. En la identificación de estos factores de riesgo, los estudios con los polimorfismos están aportando una muy valiosa información.

3.6. Polimorfismos en genes del complemento asociados con aHUS, DDD y AMD.

La búsqueda de polimorfismos en genes del complemento ha permitido identificar variantes frecuentes en población normal que muestran una fuerte asociación con estas enfermedades. Es en este tipo de asociación, junto datos clínicos como la presencia de componentes del complemento en las drusas, donde encontramos el vínculo más sólido entre AMD y complemento. Hasta el

momento no se han documentado mutaciones en genes del complemento exclusivas de AMD, pero la asociación con ciertos polimorfismos, especialmente con *CFH,* es muy significativa.

Se prevé que estas variaciones genéticas tienen consecuencias funcionales pequeñas que modulan la efectividad del complemento. Esto, que puede no tener consecuencias en la mayor parte de la población, puede ser crucial en aquellos individuos con una predisposición genética, como lo son los que portan mutaciones en genes del complemento, u otros factores que afectan a la activación del complemento como los autoanticuerpos. Así, estudios en casos familiares de aHUS, han comprobado que ciertos polimorfismos contribuyen al desarrollo de la enfermedad, y la confluencia de factores, como pueden ser una mutación y un polimorfismo de riesgo, puede ser decisiva en manifestación de la enfermedad.[129-131]

Se han identificado polimorfismos que aumentan o disminuyen el riesgo para aHUS, DDD y AMD en genes como *CFH, CFB, C3, MCP* o la familia de proteínas de fH. La caracterización funcional de todos estos polimorfismos asociados a enfermedades (y otros no incluidos aquí) es esencial no sólo para entender la propia asociación genética; también al aportar información valiosa sobre los mecanismos fisiopatológicos que desencadenan estas enfermedades.

3.6.1. Haplotipo MCP_{ggaac}.

Entre un 10 y un 15% de los pacientes aHUS presenta mutaciones en el regulador de la AP, *MCP*, muchas de ellas causando deficiencias en la expresioin.[89, 132] El haplotipo MCP_{ggaac} está asociado con una menor expresión del regulador en la superficie celular y está considerado como un polimorfismo común, con una frecuencia alélica del 23% en población sana. Sin embargo, este haplotipo es un alelo de riesgo en pacientes aHUS, especialmente en aquellos que presentan mutaciones en otros genes, donde puede ser determinante para la manifestación de la enfermedad. En aHUS, la frecuencia alélica es del 44% (**tabla 1**).[130]

3.6.2. Polimorfismos en factor H.

La secuenciación completa del gen *CFH* en la búsqueda de marcadores genéticos y variantes asociadas a enfermedades ha llevado a establecer una serie de haplotipos de *CFH*. Las frecuencias y el riesgo relativo para cada uno de estos haplotipos se han calculado en poblaciones control y de pacientes aHUS, DDD y AMD, encontrándose asociaciones de riesgo y de protección.[95, 109] Consistente con la correlación genotipo-fenotipo descrita anteriormente no hay un solapamiento entre los haplotipos de riesgo para aHUS y los que lo son para DDD y AMD, lo que da una idea de los distintos mecanismos patogénicos.[92] Por el contrario, sí hay una coincidencia en el caso del haplotipo protector de fH.

Estos haplotipos están representados por una serie de polimorfismos de un solo nucleótido, o SNPs, a lo largo de todo el gen *CFH*. A continuación se describe más en detalle dos de estos SNPs más relevantes por su asociación con estas enfermedades.

- **Tyr402His.**

El polimorfismo Tyr402His está asociado con un alto riesgo para DDD y AMD (**tabla 1**).[95, 133] Se localiza en el SCR 7 de fH, dentro de una región importante en la unión de polianiones. También está presente en el fHL-1, que solamente contiene este sitio de unión. Además de GAGs como heparinas, se han identificado otros ligandos como la proteína C-reactiva (CRP) y la proteína M. El análisis estructural sitúa a este residuo de manera expuesta haciendo factible su capacidad de interacción con ligandos, pero por otro lado, no revelan cambios estructurales importantes entre las dos variantes Tyr402 e His402. Existen datos funcionales comparativos utilizando tanto fragmentos recombinantes como proteína nativa de las dos variantes de fH. Sin embargo, las discrepancias en los resultados no han hecho posible determinar una alteración en la función de fH como consecuencia de este polimorfismo. Experimentos de unión a GAGs y heparinas con el SCR 7 o SCRs 6-8 muestran diferencias en la interacción entre las formas fH_{Tyr402} e fH_{His402}, pero se comportan de manera idéntica cuando se comparan las variantes del fH completo.[66] Se ha visto en ensayos de unión a superficies celulares que la variante de riesgo se une ligeramente peor en cultivos de RPE, lo que se traduce en una menor capacidad reguladora, aunque la actividad cofactora en

fase fluida es la misma para el fH y el fHL-1. Por otro lado, la interacción con C3b tampoco se ve modificada.[134]

El estudio de interacción entre el fH y CRP es de interés. El CRP está aumentado en los casos de AMD y además está presente en las drusas. El reconocimiento de fH al CRP en las superficies de células apoptóticas asegura su correcta eliminación evitando estados pro-inflamatorios. Aunque es posible detectar complejos fH-CRP y se ha observado en diferentes ocasiones una unión disminuida por la variante de riesgo fH_{His402}; la relevancia de la asociación de estas dos proteínas está puesta en duda debido principalmente a las condiciones desnaturalizantes en las que se da esta interacción.[66]

- **Val62Ile.**

Uno de los haplotipos descritos de fH está asociado con un menor riesgo para AMD (OR= 0.39), DDD (OR=0.42) y aHUS (OR=0.38) (**tabla 1**).[95, 109] Este haplotipo contiene el SNP Val62Ile, situado en el SCR 1, dentro de la región funcional de fH más importante (SCRs 1-4), esencial en la actividad cofactora y de aceleración de la disociación de la convertasa de C3. La cadena lateral de este aminoácido se encuentra en el núcleo hidrofóbico del primer dominio de fH y la sustitución Val62Ile no altera su correcto plegamiento. Sí se han observado algunos desplazamientos en las cadenas de los residuos adyacentes y un pequeño incremento en la termoestabilidad de la variante fH_{Ile62}.[135] Independientemente del conocimiento estructural y de si este residuo participa directamente o no en la función de fH, la variante fH_{Ile62} puede incrementar la capacidad en la capacidad reguladora de fH,[136] confiriendo de este modo protección para estas enfermedades al reducir la activación de la AP del complemento.

- **Reordenamientos de la familia de factor H.**

Como se ha comentado anteriormente, la región del RCA donde se encuentra la familia de genes de fH es de muy alta homología, favoreciendo que se produzcan fenómenos de reordenamiento cromosómico. Los eventos de conversión génica o el gen híbrido *CFH:CFHR1* generan una proteína con dos cambios adicionales en la región C-terminal (SCR 18 y 20). Esto tiene unas consecuencias funcionales significativas: la unión a C3b y la protección sobre

superficies celulares se ven drásticamente reducidas. La aparición de estos reordenamientos es rara y su asociación de es exclusiva de aHUS.[78, 124]

Por el contrario, la deleción de los genes *CFHR1* y *CFHR3* (Δ*CFHR1-3*) es un fenómeno muy común. Este reordenamiento se ha fijado en la población con una frecuencia alélica del 25%[137] y forma parte de uno de los haplotipos descritos de *CFH*.[138] La Δ*CFHR1-3* en homocigosis se ha asociado tanto con la protección para AMD como con un mayor riesgo en la predisposición a aHUS.[138-140] En el caso de aHUS, la Δ*CFHR1-3* también está relacionada con el desarrollo de autoanticuerpos contra fH. Aunque el mecanismo de esta correlación se desconoce, y por lo tanto no es posible aclarar si ambos factores de riesgo para aHUS son independientes.[140, 141] En el caso de AMD, cómo la ausencia de estas proteínas protege contra la enfermedad es todavía una incógnita. Asimismo, se han descrito otros reordenamientos de la región *CFHR1-5*, con la consecuente deficiencia de proteínas, asociados a aHUS y DDD.[137]

3.6.3. Polimorfismos en factor B y C3.

En 2006 se dieron a conocer variantes alélicas en otros dos componentes de complemento, fB y C2, asociadas a un menor riesgo para AMD (**tabla 1**).[142, 143] En fB, el aminoácido que ocupa la posición 32 (7 en la proteína madura) tiene tres variantes polimórficas: fB_{Arg32}, fB_{Trp32} y fB_{Gln32},[144] habiéndose asociado con un mayor o menor riesgo también para diferentes patologías.[145-147] La variante de fB protectora para AMD, fB_{Gln32} (OR= 0.32), ya había sido relacionada con una menor actividad hemolítica comparada con la variante más frecuente, fB_{Arg32}. Se postuló que la sustitución de este residuo afectaba de algún modo a la formación de la convertasa, y por lo tanto, a la actividad de la AP.[148] El polimorfismo está situado en el extremo N-terminal del dominio Ba de fB, que se ha visto implicado en la formación de los complejos convertasa.[25, 149] Es por esto que la asociación del polimorfismo Arg32Gln con AMD puede estar mediada por una alteración de la proteína a nivel de funcional.

Poco después, otro estudio demostró la asociación de AMD con un polimorfismo frecuente del componente C3 (**tabla 1**). Dicha asociación, supone un factor de riesgo independiente y tiene una OR de 1.7 según un estudio sobre diferentes poblaciones.[150] El polimorfismo, inicialmente descrito como C3S y C3F por su movilidad electroforética, supone una sustitución

Arg102Gly.[151] La variante de predisposición para AMD, $C3_{Gly102}$, ya había sido asociada con otras patologías como la nefropatía IgA[152] o a la presencia del C3-Nef en pacientes DDD.[153] Más recientemente, este polimorfismo se ha encontrado formando parte de un haplotipo de riesgo para DDD.[133] El residuo está situado en la cadena β, cerca del dominio TED y dentro de una región de interacción con los reguladores de la AP.[154, 155]

	aHUS	**DDD**	**AMD**
MCPggaac	**2.68 (1.43-5.05)** [130] (5.25 en pacientes con mutaciones adicionales)	- - -	- - -
CFH Tyr402His	- - -	1.92 (1.04-3.54) [133] **2.27 (1.06-4.88)** [95]	2.46 (1.95-3.11) [109] 2.7 (1.9-3.9) [110] 4.6 (2.0-11) [111] **2.27 (1.71-3.0)** [178]
CFH Val62Ile	**0.38 (0.23-0.64)** [95]	0.67 (0.3-1.22) [133]	0.39 (0.23-0.67) [95] **0.48 (0.34-0.67)** [178]
CFB Arg32Gln	- - -	- - -	0.32 (0.21-0.48) [142] 0.5 (0.3-0.8) [150] **0.66 (0.48-0.90)** [178]
C3 R102G	---	2.42 (1.35-4.33) [133]	1.7 (1.3-2.1) [150] **1.32 (0.95-1.82)** [178]

Tabla 1. Riesgo para aHUS, DDD y AMD de los polimorfismos más destacados de *MCP, CFH, CFB* y *C3*. El riesgo en cada caso viene dado por el parámetro OR (CI 95%) en portadores de al menos un alelo con la variante de riesgo o protectora. Los valores resaltados en negrita provienen de estudios realizados con las poblaciones españolas de pacientes.

OBJETIVOS

1. Purificación y caracterización estructural de complejos convertasa de C3 de la vía alternativa.

-Mecanismo de activación de la convertasa C3bBb e implicaciones en patología.

Para este objetivo hemos contado con la colaboración del grupo de microscopía electrónica dirigido por el Dr. Oscar Llorca Blanco (Dept. Biología Físico-Química, CIB, CSIC)

2. Identificación de alelos de riesgo y variantes cuantitativas en el gen de fH.

-Polimorfismo común Tyr402His de *CFH* en AMD.

-Variantes cuantitativas de fH asociadas a aHUS.

Estos objetivos se realizaron conjuntamente con el grupo de investigación de los Drs. Claire Harris y Paul Morgan (*Dept. of Medical Biochemistry and Immunology, Cardiff University School of Medicine*).

3. Caracterización funcional de polimorfismos en genes de fH y fB asociados con patología

-Polimorfismo Arg32Trp/Gln del gen de *CFB*.

-Polimorfismo Val62Ile y variantes raras Ser890Ile Val1007Leu del gen de *CFH*.

Para la caracterización de los polimorfismos de de *CFB* y *CFH* hemos trabajado en colaboración con los Drs. Claire Harris y Paul Morgan. En el estudio de las variantes de *CFH* han contribuido considerablemente las Dras. Pilar Sánchez Corral y Margarita López Trascasa del Servicio de Nefrología del Hospital Universitario La Paz.

MATERIALES Y MÉTODOS

RESULTADOS

Los materiales y métodos empleados en esta tesis y los resultados obtenidos, están comprendidos en los siguientes artículos publicados en revistas científicas. Cada uno de estos artículos se puede consultar en el **ANEXO**.

3D structure of the C3bB complex provides insights into the activation and regulation of the complement alternative pathway convertase. Torreira E*, **Tortajada A***, Montes T*, Rodríguez de Córdoba S, Llorca O. Proc Natl Acad Sci USA. 2009 Jan 20;106(3):882-7.
http://www.ncbi.nlm.nih.gov/pubmed/19136636

Coexistence of closed and open conformations of complement factor B in the alternative pathway C3bB(Mg^{2+}) proconvertase. Torreira E*, **Tortajada A***, Montes T*, Rodríguez de Córdoba S, Llorca O. J Immunol. 2009 Dec 1;183(11):7347-51.
http://www.ncbi.nlm.nih.gov/pubmed/19890040

* Autoría compartida.

Resumen:

La convertasa de C3 de la AP es un complejo bimolecular inestable compuesto por los componentes C3b y fB, y juega un papel crucial en las cascadas de activación del complemento al amplificar la activación inicial. Tanto la formación del complejo como la estabilidad están estrictamente reguladas para asegurar una correcta función efectora que eliminará las superficies extrañas, evitando al mismo tiempo la activación inespecífica y el daño en el tejido propio. De hecho, las alteraciones que afectan a la formación o estabilidad de la convertasa resultan en una desregulación de la AP, predisponiendo para ciertas enfermedades. Conocer los mecanismos de ensamblaje de la convertasa de C3 y de regulación es, por tanto, fundamental.

Partiendo de proteínas purificadas de C3b y fB hemos generado y aislado complejos pro-convertasa y convertasa de C3 de la AP, y elaborado un modelo tridimensional. El modelo de la pro-convertasa (C3bB) pone de manifiesto el cambio conformacional que sufre fB al interaccionar con C3b. Este cambio conformacional supone la apertura de la molécula, lo que permitirá que se den

una serie de eventos necesarios, como son la exposición de un sitio de corte y la liberación del fragmento Ba por la proteasa fD, para generar una convertasa de C3 activa (C3bBb) y funcional. Por otro lado, el modelo de pro-convertasa de C3, revela la existencia de dos configuraciones coexistiendo en equilibrio. Una de ellas representa el estado de reconocimiento inicial entre fB y C3b, en la que el fB se presenta en una conformación cerrada, y en la otra, el fB presenta la conformación abierta y puede ser activado. El modelo propuesto de convertasa de C3 (C3bBb) ilustra la importancia del dominio wWA del fragmento Bb en estabilidad del complejo, y ciertos aspectos que pueden afectar al la funcionamiento del dominio catalítico SP. Asimismo, los modelos propuestos aportan información sobre los mecanismos de regulación de los complejos convertasa, por parte de reguladores como DAF, y probablemente de otros como fH y CR1. Además, proporcionan un marco estructural para el estudio de residuos relevantes y con implicación en patologías asociadas a la desregulación de la AP del complemento.

Measurement of factor H variants in plasma using variant-specific monoclonal antibodies: application to assessing risk of age-related macular degeneration. Hakobyan S, Harris CL, **Tortajada A**, Goicochea de Jorge E, García-Layana A, Fernández-Robredo P, Rodríguez de Córdoba S, Morgan BP. Invest Ophthalmol Vis Sci. 2008 May;49(5):1983-90.
http://www.ncbi.nlm.nih.gov/pubmed/18436830

Variant-specific quantification of factor H in plasma identifies null alleles associated with atypical hemolytic uremic syndrome. Hakobyan S*, **Tortajada A***, Harris CL, de Córdoba SR, Morgan BP. Kidney Int. 2010 Oct;78(8):782-8.
http://www.ncbi.nlm.nih.gov/pubmed/20703214

* Autoría compartida.

Resumen:

aHUS y AMD son dos enfermedades asociadas a la desregulación de la AP del complemento. Se han descrito numerosos factores que predisponen para estas enfermedades, entre ellos mutaciones y polimorfismos que afectan a fH, el regulador principal de la AP. Nuestro propósito ha sido la identificación de algunos de estos factores de riesgo en pacientes aHUS y AMD.

Para abordar esta cuestión hemos generado anticuerpos monoclonales dirigidos específicamente contra el polimorfismo Tyr402His de fH, factor de riesgo que supone la asociación genética más importante para AMD. Hemos diseñado un ensayo de ELISA que nos permite detectar el portadores de este polimorfismo, y determinar el genotipo, lo que puede aportar una información importante, sobre todo en aquellos pacientes portadores, donde va a permitir evaluar más de forma más precisa el riesgo para la enfermedad e influir en las estrategias terapéuticas.

En aHUS, las deficiencias parciales de fH generan situaciones de predisposición a la enfermedad, y, aunque no exista una asociación particular entre el polimorfismo Tyr402His, el anticuerpo ha resultado ser una herramienta muy útil en la cuantificación alelo-específica de fH, y en la identificación de alelos de baja expresión de fH entre los pacientes. La identificación de estos alelos ha contribuido a explicar situaciones patológicas en diversos casos de pacientes aHUS, portadores de mutaciones en *CFH* u otros factores de riesgo.

The disease-protective complement factor H allotypic variant Ile62 shows increased binding affinity for C3b and enhanced cofactor activity. **Tortajada A**, Montes T, Martínez-Barricarte R, Morgan BP, Harris CL, de Córdoba SR. Hum Mol Genet. 2009 Sep 15;18(18):3452-61.
http://www.ncbi.nlm.nih.gov/pubmed/19549636

Functional basis of protection against age-related macular degeneration conferred by a common polymorphism in complement factor B. Montes T, **Tortajada A**, Morgan BP, Rodríguez de Córdoba S, Harris CL. Proc Natl Acad Sci U S A. 2009 Mar 17;106(11):4366-71.
http://www.ncbi.nlm.nih.gov/pubmed/19255449

Complement factor H variants I890 and L1007 while commonly associated with atypical hemolytic uremic syndrome are polymorphisms with no functional significance. **Tortajada A**, Pinto S, Martínez-Ara J, López-Trascasa M, Sánchez-Corral P, de Córdoba SR. Kidney Int. 2012 Jan;81(1):56-63. doi: 10.1038/ki.2011.291. Epub 2011 Aug 31.
http://www.ncbi.nlm.nih.gov/pubmed/21881555

Resumen:

Mutaciones y polimorfismos en genes del complemento están asociados con enfermedades raras como aHUS y DDD u otras más frecuentes como la AMD, implicando la desregulación del complemento en la patogénesis. Partiendo de proteínas purificadas, y empleando diversas aproximaciones experimentales como ensayos de interacción, funcionales y hemolíticos, hemos llevado a cabo la caracterización funcional de algunas de estas variantes. Por un lado, los polimorfismos comunes de *CFB* Arg32Trp/Gln y *CFH* Val62Ile, asociados con un menor riesgo para AMD, o aHUS, DDD y AMD, respectivamente. Por otro lado, las variantes raras de *CFH* Ser890Ile / Val1007Leu, asociadas en repetidas ocasiones con aHUS, DDD y AMD.

Los datos obtenidos han demostrado que las variantes fB_{Gln32} y fH_{Ile62} son protectoras porque reducen la activación de la AP, modulando la actividad global del complemento. Ambas variantes protectoras afectan a la afinidad con C3b, pero de manera opuesta. El fB_{Gln32} tiene menos afinidad por C3b lo que afecta a la formación de convertasa, mientras que el fH_{Ile62} presenta más afinidad por C3b, lo que resulta en una mayor capacidad reguladora. Estos resultados explican las bases moleculares de la asociación protectora con las enfermedades, aportando información sobre los mecanismos patogénicos. Además, hemos comprobado que las consecuencias funcionales de estas y otras variantes son aditivas, influyendo de manera drástica en la actividad del complemento, y en la susceptibilidad frente a diversas patologías. En el estudio de las variantes Ser890Ile / Val1007Leu de fH, los ensayos realizados demuestran que estos cambios no tienen consecuencias funcionales que afectan a la capacidad reguladora de fH. Además, los datos genéticos y clínicos sugieren que estos cambios deben ser considerados como polimorfismos, y sin una asociación particular con patología.

El conocimiento de las consecuencias funcionales de todas estas variantes, puede resultar útil tanto en la predicción del riesgo, como en las estrategias terapéuticas frente a las enfermedades causadas por la desregulación del complemento.

DISCUSIÓN

1. Purificación y caracterización estructural de complejos convertasa de C3 de la vía alternativa.

Las convertasas de C3 son los elementos más importantes en las cascadas de activación del complemento. Son complejos bimoleculares de naturaleza muy inestable que catalizan la hidrólisis del componente C3 a C3b, que actúa como señalizador permitiendo la activación del complemento sobre las superficies extrañas. C3b actúa también como cofactor para la serín proteasa fB, cuyo complejo constituye la convertasa de C3 de la AP. Esta convertasa, al generar más C3b, resulta crucial al amplificar la activación y por tanto, la respuesta efectora del complemento. La formación de la pro-convertasa de C3 de la AP, C3bB, y su conversión a convertasa activa, C3bBb, requiere de una secuencia de pasos en la que se dan interacciones proteína-proteína y la activación proteolítica por la serín proteasa fD. Además, resulta necesario que se dé un cambio conformacional sobre fB para su correcta proteólisis y activación.[19]

Dada la importancia de este complejo en la respuesta del complemento, su actividad está estrictamente regulada. El regulador P estabiliza los complejos, promoviendo la activación del complemento sobre superficies de patógenos y células apoptóticas.[13] Los reguladores DAF, fH, CR1 y MCP aceleran su disociación y/o participan en la proteólisis de C3b, evitando, de este modo la activación inespecífica y el daño sobre los tejidos propios. Las alteraciones que afectan a la formación y estabilidad de la convertasa, y que conducen a la excesiva o insuficiente activación de la AP del complemento, pueden conducir a situaciones de predisposición con patología.[11] Entender cómo se forman estos complejos y cómo están regulados es, por tanto, esencial. Para abordar este objetivo hemos establecido una colaboración con el grupo del Dr. Oscar Llorca, expertos en técnicas de microscopía electrónica (ME) y procesamiento de digital de imágenes.

Partiendo de proteínas purificadas, bien sea de plasma (C3b) o recombinantes (fB) hemos reconstituido *in vitro* complejos pro-convertasa, C3bB, y convertasa de C3, C3bBb. La interacción de los componentes se realizó en condiciones que favorecen la estabilidad de los complejos, y en todos los casos con un exceso de fB. Posteriormente, las muestras se repurificaron mediante columnas de exclusión por tamaño, lo que nos permitió

eliminar el exceso de fB. Las fracciones conteniendo los complejos fueron identificadas con anticuerpos monoclonales específicos mediante *western blot*. Además, seleccionamos aquellas fracciones con una movilidad correspondiente a un mayor tamaño y más enriquecidas en complejos convertasa. Las muestras fueron depositadas sobre rejillas de carbón, tratadas para la correcta adsorción de la muestra, y posteriormente observadas por ME, tras el protocolo de tinción negativa. Las imágenes individuales de los complejos aislados se clasificaron por distintos métodos de procesamiento digital de imagen. Estos métodos permiten separar grupos de imágenes idénticas correspondientes a la misma vista de la molécula, y el promedio de este subgrupo homogéneo de imágenes permite obtener unas medias, cuya relación señal/ruido es mucho mayor que en las partículas individuales. Con las diferentes medias, que representan las diferentes orientaciones de una misma molécula sobre la rejilla, se reconstruyen modelos tridimensionales. Estos modelos nos sirven para obtener información estructural a nivel macromolecular, pero también es posible integrar los mapas a resolución atómica para identificar interacciones entre los dominios de los componentes.

1.1. Análisis de los modelos propuestos de C3bB y C3bBb.

La formación de C3bB requiere el catión Mg^{2+} en condiciones fisiológicas, resultando un complejo inestable con una rápida disociación espontánea. El empleo del catión Ni^{2+} permite aumentar la estabilidad de C3bB hasta 10 veces sin que con ello se pierda actividad.[37] Gracias a esto, el rendimiento en la purificación de complejos C3bB(Ni^{2+}) estables fue lo suficientemente alto como para obtener una gran cantidad de imágenes de partículas individuales. La reconstrucción del modelo tridimensional se calculó mediante metodologías de refinamiento angular con los datos de estas imágenes.

La integración de las estructuras resueltas a resolución atómica de fB y C3b en el modelo a media resolución del complejo C3bB estabilizado con Ni^{2+}, muestra aspectos claves en la formación de la convertasa. La estructura de C3b encaja inequívocamente en el modelo tridimensional, permitiéndonos identificar cada dominio de C3b. Sin embargo, el volumen adicional observado en los complejos C3bB(Ni^{2+}), correspondiente al fB, presenta una forma muy distinta a como lo hace fB en solución, observado a una resolución similar. La estructura compacta y cerrada del fB libre es claramente incompatible con la estructura de fB en el complejo, sugiriéndonos que la molécula se abre en el

complejo pro-convertasa C3bB, e implicando que el fB sufre un cambio conformacional al unirse a C3b, como ya se había sugerido.[37] Dada la limitada resolución de mapa obtenido por ME, no es posible definir la estructura a alta resolución del fB en la conformación abierta. Para intentar modelar esta estructura en el complejo, asumimos que los fragmentos de fB se podían encajar por separado, tal como se dividen en condiciones fisiológicas en el proceso de formación de la convertasa, es decir, como Bb y Ba. Empleando un *software* y estableciendo criterios que respetaban la estructura primaria de la proteína, modelamos la orientación de los dominios de fB en el volumen. Sin embargo, a la vista de la estructura a resolución atómica de la pro-convertasa, en presencia de Ni^{2+}, resuelta por cristalografía en 2010, el modelo propuesto inicialmente no fue el correcto. El dominio desplazado en el cambio conformacional de fB es SP y no Ba habíamos deducido, mientras que los dominios vWA y los tres SCRs de Ba apenas varían su posición respecto a la configuración soluble y cerrada.[156] La estructura de la pro-convertasa ha sido fundamental para complementar la información en nuestro modelo. Por otro lado, el modelo de pro-convertasa por ME es totalmente compatible con la de cristalografía, apoyando la evidencia del cambio conformacional observado en fB (**figura 17.A**).

En cuanto a la interacción entre los componentes fB y C3b, comprobamos en el modelo de convertasa que el dominio vWA de fB contacta con el dominio C345c de C3b, dejando el sitio MIDAS orientado hacia C3b. El otro punto de contacto importante se vio entre el dominio de fB desplazado y C3b a nivel de α-NT y CUB. Los dominios de C3b, C345c, α-NT y CUB ya se habían propuesto como las regiones de unión a fB.[19] El modelo de C3bB(Ni^{2+}) propuesto, no sólo confirma estas interacciones, representa una demostración física de la hipótesis de la necesidad de un cambio en la estructura de fB para formar una convertasa activa, aportando por primera vez una evidencia experimental de ese cambio conformacional.

El paso de una conformación globular cerrada del fB soluble, a otra abierta, tal como la encontramos en el modelo de C3bB(Ni^{2+}), debería ser suficiente para generar los cambios en los dominios de fB implicados en la activación de la enzima. La región *linker* de unión de los dominios vWA y Ba debe recolocarse favoreciendo que se den, al menos, dos eventos esenciales. Primero, el sitio de corte, situado en la región que conecta vWA y el SCR 3 de Ba, ha de colocarse de manera expuesta y accesible para fD. Segundo, el desplazamiento de la hélice αL, perteneciente también al *linker*, fuera del

dominio vWA, permitiendo que vWA adopte una configuración funcional. Todo ello, hará posible la formación de una convertasa activa.

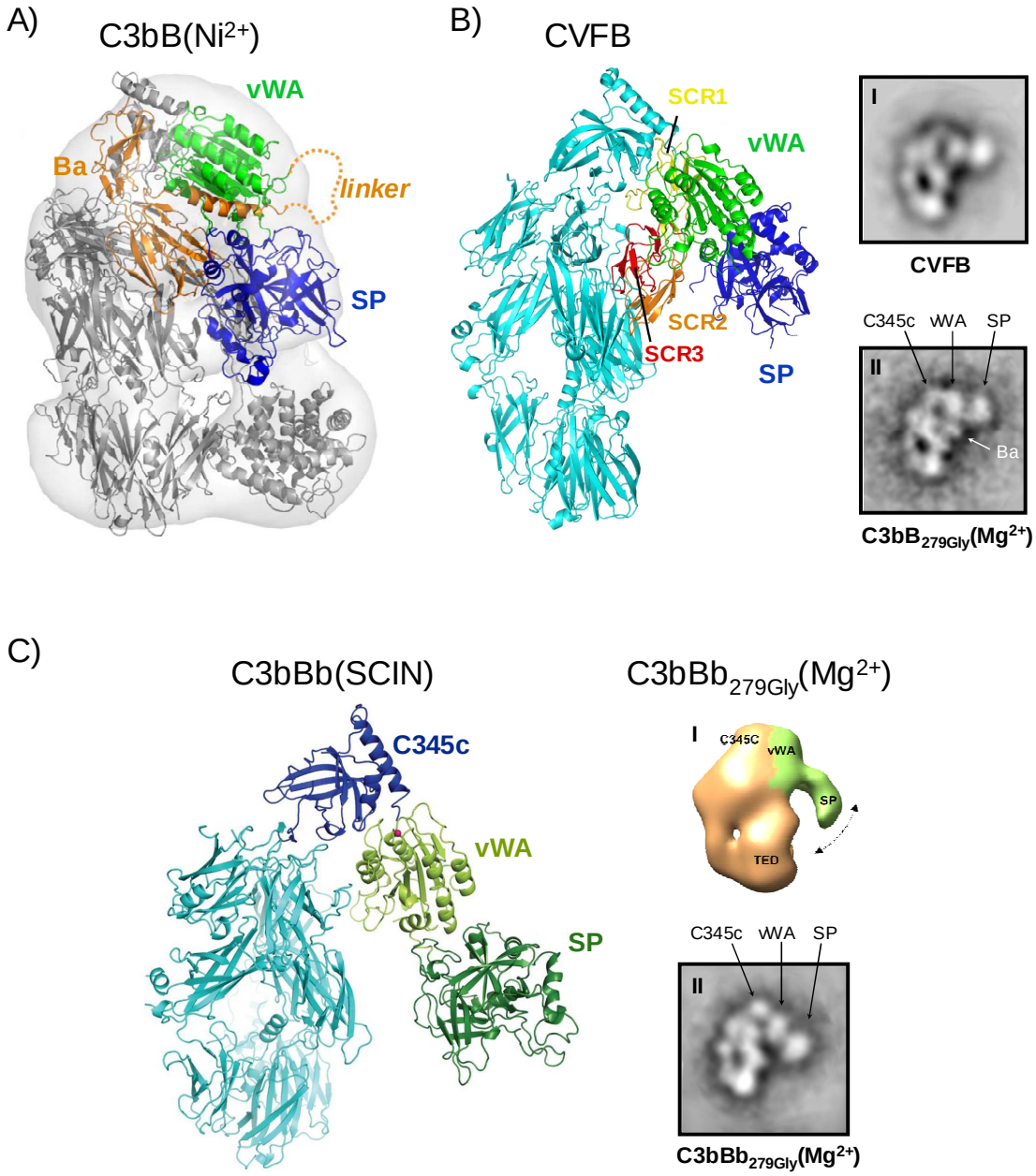

Figura 17. Complejos convertasa de C3 de la AP. A) Composición de la pro-convertasa de C3 de la AP entre los datos del modelo de ME y de cristalografía (PDB ID 2XWB). La molécula de fB en conformación abierta, con el dominio SP desplazado, encaja muy bien en el modelo tridimensional (coeficiente de correlación de 0.87).[156] B) Estructura a resolución atómica de CVFB en el que el fB se encuentra en conformación cerrada (PDB ID 3HRZ).[157] Este complejo resulta muy similar al observado por ME (II). I y II son imágenes medias de partículas únicas de los complejos CFVB (I) y $C3bB_{279Gly}(Mg^{2+})$ (II). En este último es posible reconocer todos los dominios de fB. C) Estructura atómica de la convertasa de C3, C3bBb, estabilizada con SCIN (PDB ID 2WIN).[159] Estos datos son totalmente compatibles con los resultados obtenidos por ME de $C3bB_{279Gly}(Mg^{2+})$. Se muestra una vista del modelo tridimensional (I) y una imagen media seleccionada (II).

Con el fin de confirmar estos resultados y aproximarnos más a las condiciones fisiológicas aislamos y resolvimos la estructura de complejos C3bB en presencia de Mg^{2+}. Para ello, utilizamos el mutante de fB Asp279Gly, diseñado por mutagénesis, que alarga la vida media del complejo y es activado correctamente por fD.[30] Con este diseño, observamos una mayor cantidad de moléculas de C3b aisladas, pero la forma característica y la orientación predominante de esta molécula permitió eliminar este grupo de imágenes en la clasificación inicial. Esto nos dejó una galería de imágenes cuya reclasificación y cálculo de medias mostró la existencia de dos configuraciones diferentes para el complejo $C3bB_{279Gly}$ en presencia de Mg^{2+}.

En la configuración predominante (65%), el fB se presenta en una conformación abierta, de manera idéntica a como aparece en el modelo para C3bB(Ni^{2+}), y está próximo a C3b. En la minoritaria (35%) el fB tiene una conformación cerrada y la estructura es similar a la del fB nativo en solución. En esta configuración, el fB queda proyectado hacia fuera, con el dominio SP alejado del complejo. El fragmento Ba, que fue posible identificarlo en algunas de las medias obtenidas, se localiza plegado hacia los dominios vWA y SP de fB, pero contactando también con C3b. En esta configuración de la pro-convertasa, Ba parece interaccionar con los dominios α-NT, MG 2, MG 7 y CUB. Se había propuesto que la interacción entre C3b y fB se realiza mediante dos puntos discretos de unión en fB. Uno en el dominio vWA del fragmento Bb y otro en los SCRs de Ba.[25, 30] La existencia de esta configuración es una prueba más de estas afirmaciones.

Coincidiendo con el desarrollo y publicación de este trabajo, otros autores dieron a conocer la estructura atómica del fB estabilizado con CVF.[157] CVF (*cobra venom factor*) es un componente del veneno de cobra, homólogo a C3b, que forma complejos convertasa solubles muy estables en presencia del catión Mg^{2+}.[158] La estructura de CVFB resulta muy similar a la de $C3bB_{279Gly}(Mg^{2+})$ con el fB en conformación cerrada (**figura 17.B**). En CVFB se dan interacciones específicas entre Bb y el dominio C345c, mientras que Ba contacta con diferentes dominios de CVF (α-NT, MG 2, MG 6, MG 7 y CUB), de igual forma a lo descrito en nuestro modelo de pro-convertasa. Sin embargo, el fB se encuentra en conformación cerrada, y es incompatible con el corte proteolítico por fD para formar C3bBb. Probablemente esta sea la razón de la baja tasa de activación encontrada en el complejo CVFB en comparación con el complejo C3bB. Para explicar estos resultados, los autores sugieren la existencia de dos estados funcionales diferentes de la pro-convertasa en un

equilibrio dinámico. CVFB representa un estado de asociación de la pro-enzima anterior al de una enzima activada. El modelo obtenido de ensamblaje de la $C3bB_{279Gly}(Mg^{2+})$, se ajusta perfectamente a esta hipótesis.

El fB se une a C3b en un complejo que tiene dos configuraciones, o estados coexistentes. Uno en el que fB está abierto y puede ser activado (el empleo de Ni^{2+} favorece este estado) y otro en el que fB está cerrado, que se mantiene por las interacciones entre los dominios vWA y Ba con C3b, y con el dominio SP proyectado hacia afuera. Esta configuración ha de representar un estado de reconocimiento inicial entre fB y C3b. La coexistencia de las dos conformaciones de fB en el complejo $C3bB_{279Gly}(Mg^{2+})$ implica que el cambio conformacional no es necesario para la correcta unión estable dominio vWA a través del sitio MIDAS al dominio C345c, y que esta puede ser inducida tras el primer contacto entre fB y C3b. Después de la unión a C3b, las dos conformaciones de fB coexisten en un equilibrio o transita de la cerrada a la abierta para ser activado por fD y formar la convertasa activa.

La purificación y resolución de la estructura de complejos convertasa C3bBb por ME, nos sirve para ampliar estos resultados y tener una visión más global del mecanismo de formación y activación de la convertasa de C3 de la AP. Para ello, reconstituimos complejos convertasa en presencia de Mg^{2+} empleando de nuevo, el mutante estable fB_{279Gly}. Las imágenes revelaron que el fragmento Bb se mantiene unido al dominio C345c de C3b por el dominio vWA, quedando el dominio SP proyectado fuera del complejo. Esta configuración resulta similar a la que encontramos en el complejo $C3bB_{279Gly}(Mg^{2+})$, en el estado de asociación o de reconocimiento inicial, con el fB en conformación cerrada. La ausencia del fragmento Ba, tanto en los *western blot* de las fracciones en la repurificación como en la reconstrucción tridimensional posterior, descarta la posibilidad de una contaminación de complejos pro-convertasa, e indica que esta configuración es exclusiva de la convertasa activa.

En el modelo $C3bBb_{279Gly}(Mg^{2})$ identificamos inequívocamente los dominios C345c, vWA y SP, que aparecen como tres puntos de densidad situados en tándem. Observamos cómo la densidad correspondiente al dominio SP adopta varias posiciones al proyectarse del complejo (como consecuencia, la masa de esta densidad y el volumen se ven reducidos). Según este modelo, sugerimos que el fragmento Bb, unido a C3b, es flexible, probablemente debido a la ausencia otros sitios de unión, aportados por Ba y SP en las conformaciónes

de la pro-convertasa. El dominio SP en el modelo $C3bBb_{279Gly}(Mg^2)$, no contacta con C3b, dejando el sitio catalítico accesible para acomodar el sustrato C3. Tras la publicación de estos resultados se resolvió la estructura a resolución atómica de la convertasa C3bBb estabilizada con SCIN.[159] SCIN *(Staphylococcal complement inhibitor*) es una proteína bacteriana dirigida contra las convertasas de C3. Se une a convertasas activas, C3bBb y C4b2a, depositadas en la superficie de la bacteria previniendo la opsonización y la fagocitosis. Para ello, SCIN secuestra los complejos convertasa y los estabiliza.[160] La estructura a resolución atómica de C3bBb estabilizado con SCIN es totalmente compatible a la de la convertasa que proponemos en nuestro modelo (**figura 17.C**). En ambos, el complejo convertasa se mantiene únicamente por la unión de vWA de Bb al dominio C345c de C3b. Con el sitio MIDAS en estado de alta afinidad interaccionando con C3b. Y en el otro extremo de fB, el dominio catalítico SP, se coloca alejado del complejo sin contacto alguno con C3b.

Por otro lado, los autores sostienen que las variaciones de posición en el dominio C345c se deben a la propia flexibilidad de la molécula en esta región.[159] Este hecho contribuye muy probablemente al efecto observado en las imágenes medias del complejo $C3bBb_{279Gly}(Mg^2)$ y que nosotros atribuimos a la flexibilidad del fragmento Bb. Esta libertad de posicionamiento podría aportar a Bb el movimiento necesario para que el centro catalítico en el dominio SP, que se mantiene alejado del complejo, pueda aproximarse al sitio de corte en C3.

1.2. Mecanismo de activación de la convertasa de C3 de la vía alternativa.

Gracias a la combinación de la alta resolución por cristaloografía de rayos X y los estudios a media resolución por ME, ha sido posible reinterpretar algunos de nuestros datos iniciales, y hemos podido extraer varias conclusiones importantes. El siguiente apartado tratará de describir el mecanismo de ensamblaje y activación de la convertasa de C3 de la AP.

En un primer contacto entre los dos componentes de la convertasa de C3 de la AP, fB se une a C3b a través del dominio vWA y los 3 SCRs de Ba. El sitio MIDAS de vWA interacciona con el dominio C345c de C3b adoptado un estado de alta afinidad, que será importante también para la actividad de la convertasa. El fragmento Ba se une en sitios específicos de C3b como α-NT,

MG 7 y CUB, que se reorganizan tras la activación de C3. Lo que es muy importante para la especificidad de la unión. Sólo C3b puede formar convertasa y no C3. Aunque Ba no forma parte de la convertasa activa, es esencial en la formación y regulación del complejo. La pro-convertasa, C3bB, en este estado de reconocimiento inicial en el que el sitio de corte por fD está inaccesible (fB en conformación cerrada), transita a un estado en el que la pro-convertasa puede ser activada (fB en conformación abierta). El equilibrio entre estas dos configuraciones tiende al estado de activación de la pro-convertasa y supone un cambio conformacional en fB (**figura 18**).

El dominio vWA y los SCRs 1-3 de Ba se mantienen interaccionando con C3b en el mismo sitio mientras que el dominio SP rota casi 90° abriendo la molécula de fB. El reordenamiento del dominio SP, genera los cambios en la región que conecta los dominios vWA y SP que desbloquean el sitio de corte de fD, que estaba enterrado en el dominio vWA, interaccionando con las hélices αL y α7 del *linker* y vWA respectivamente. El sitio de corte queda de este modo expuesto. fD interacciona únicamente con el fB en conformación abierta, uniéndose a los nuevos sitios generados tras el cambio conformacional. El fragmento Ba que está muy próximo al dominio vWA, se libera tras el corte proteolítico, llevándose también la hélice αL de la región *linker,* incorporada en el núcleo de vWA. Con esto, la hélice α7 de vWA se posiciona correctamente lo que afecta a la colocación del dominio SP. Este dominio vuelve a reorientarse a la posición donde lo encontramos en la convertasa C3bBb, sin contactar con C3b (**figura 18**). El reordenamiento de SP y la flexibilidad que confiere el dominio C345c de C3b al fragmento Bb, le permite acomodar y cortar el sustrato C3.

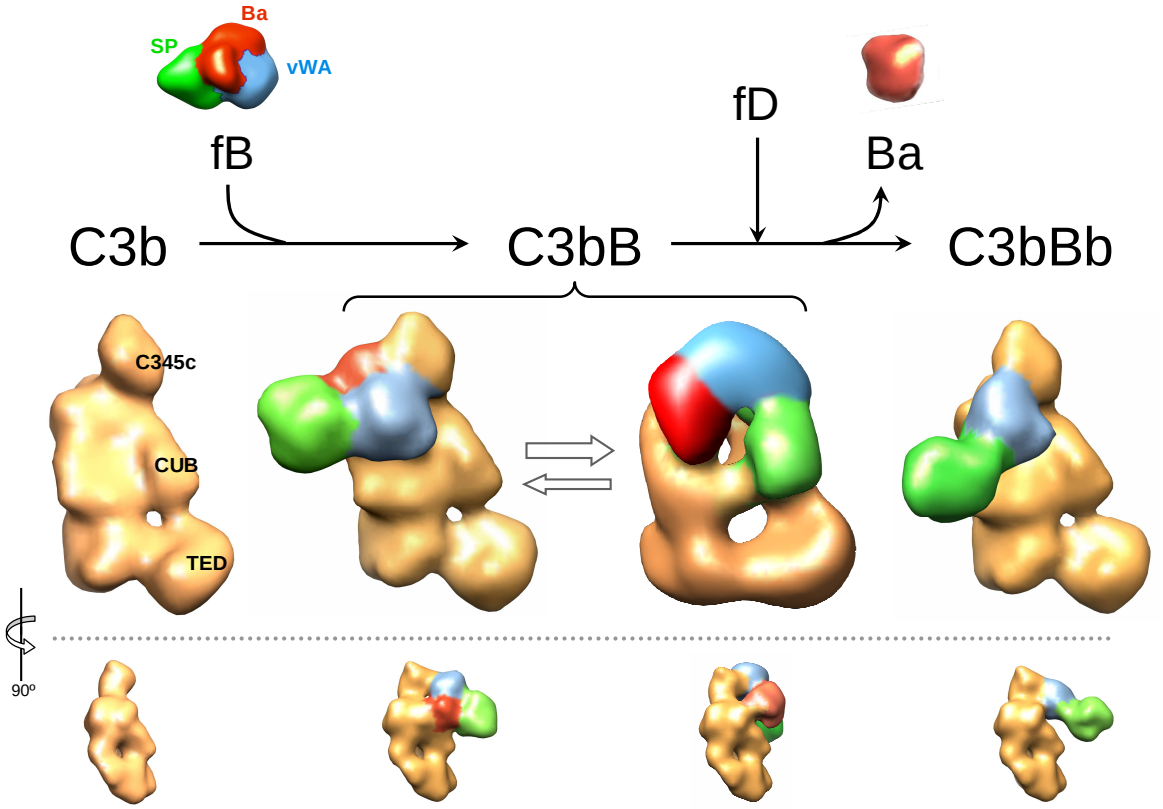

Figura 18. Ensamblaje y activación de la convertasa de C3 de la vía alternativa. La figura describe la secuencia de eventos que tienen lugar desde la interacción de los componentes C3b y fB hasta la formación del complejo C3bBb. fB inicialmente se une a C3b en conformación cerrada a través de lod dominios Ba y vWA. Posteriormente ocurre un cambio conformacional en el que la molécula de fB se abre, y el dominio SP contacta a nivel del dominio CUB de C3b. Elll cambio conformacional permitirá que se exponga el sitio de corte de fD, entre los dominios SCR 3 y vWA. El corte por fD libera el fragmento Ba para generar la convertasa activa C3bBb. El dominio SP se reorienta quedando alejado del complejo que se mantiene por la interacción entre los dominios vWA de fB y C345c de C3b. Los modelos de fB, C3b, de la pro-convertasa en conformación cerrada y de la convertasa, se han obtenido a partir de las estructuras atómicas filtradas a 30 Å de resolución. El modelo para la pro-convertasa en conformación cerrada se construye posicionando el fB libre en la estructura de la convertasa.[21, 24, 159] El modelo para la pro-convertasa con el fB en conformación abierta se obtiene de la reconstrucción tridimensional de las imágenes por ME. Los dominios de fB para este complejo se han modelado según los datos estructurales de Forneris et al.[157]

1.3. Modelo de estudio para reguladores, residuos asociados con patología y diseño de terapias.

La estructura de los complejos convertasa puede aportar también aspectos fundamentales de los mecanismos de regulación, además, ofrece una base sobre la que estudiar las consecuencias funcionales de residuos importantes y de mutaciones asociadas con patología.

El modelo propuesto encaja con la situación de ciertos residuos, cuyo estudio por mutagénesis y ensayos de interacción y funcionales muestran su implicación en la formación, estabilidad o regulación de la convertasa. Las mutaciones ganancia de función de fB Asp279Gly, Phe286Leu y Lys350Asn, están asociadas con la patología aHUS ya que aumentan la formación de complejos convertasa y por lo tanto la activación del complemento. Asp279Gly y Lys350Asn generan además convertasas mucho más estables.[90, 161] Estos residuos están localizados cerca del sitio MIDAS, en la región de interacción vWA-C345c lo que correlaciona con las consecuencias funcionales de estas sustituciones y respalda el importante papel del sitio MIDAS en el mantenimiento de la estructura de la convertasa.

Por el contrario, residuos alejados del sitio MIDAS, situados en las hélices α4/5 de vWA, influyen de algún modo en la unión con reguladores (principalmente DAF y CR1).[29] Según el modelo, esta región no interacciona con C3b y está orientada al exterior del complejo. La mutación ganancia de función asociada a aHUS, Lys323Glu, cerca de esta región y también expuesta al medio, no afecta a la formación de pro-convertasa o la estabilidad de la convertasa. Sin embargo, sí la hace más resistente a la disociación por DAF y fH.[90] Todo ello, sugiere que esta región de fB interacciona exclusivamente con los reguladores y es crítica en la función de aceleración de disociación de la convertasa.

Por otro lado, existen evidencias de que DAF, para ejercer su función, se une en dos sitios diferentes del complejo convertasa al interaccionar con Bb (en el dominio vWA) y con C3b. Además, solo actúa disociando la convertasa, no la pro-convertasa.[44] El modelo apoya el concepto de los dos sitios de unión de DAF. Uno en la superficie expuesta de vWA, respaldado por los estudios de mutagenesis[29] y los datos estructurales, y otro en C3b, probablemente en la región que ocupa el dominio SP en la pro-convertasa una vez abierto fB, es

decir, en el dominio CUB. Este dato explicaría la necesidad del corte de Ba, que induce la recolocación de SP, para que DAF pueda unirse a C3b y ejercer su función.

Hemos visto que otros dominios de C3b como α-NT y CUB intervienen y tienen un papel importante en el mecanismo activación de la convertasa. α-NT participa en el reconocimiento inicial por Ba, lo que correlaciona con estudios de mutagénesis que muestran como la sustitución de ciertos residuos en α-NT afecta negativamente a la formación de la pro-convertasa.[162] Del mismo modo, el polimorfismo de fB Arg32Trp/Gln situado en Ba, tiene consecuencias que afectan a la formación del complejo y explican aspectos de su asociación con las patologías. Los detalles de las bases de esta asociación se explican más adelante en la caracterización funcional de este polimorfismo. El dominio CUB de C3b interacciona con el fragmento Ba y el dominio SP de fB durante la formación y estabilización de la pro-convertasa. El sitio de corte que inactiva C3b a iC3b está localizado en el dominio CUB, además, tras la inactivación este sufre una gran reorientación junto con el dominio TED, lo que explica por qué fB no puede formar un convertasa con la molécula inactivada, iC3b.[163]

Desde el punto de vista de la patología, los modelos estructurales pueden aportar una información muy útil a la hora de explorar estrategias terapéuticas. No debemos olvidar los distintos mecanismos patogénicos en los que interviene el complemento, que se dan en las enfermedades asociadas: en aHUS, la inadecuada regulación en superficies celulares propias, lleva a la autolesión del endotelio glomerular mediada por la vía lítica; en DDD, la hipocomplementemia persistente y el depósito de fragmentos activados en la GMB; y en AMD, la acumulación de proteínas activadas en el RPE junto con un ambiente pro-inflamatorio parecen ser fenómenos de gran importancia en la patogénesis. Sin embargo, el evento desencadenante común a todos ellos es la activación del complemento. De ahí, que las nuevas estrategias terapéuticas tengan como objetivo prevenir la formación de elementos claves de las cascadas proteolíticas, evitando la activación del complemento, la progresión hacia la vía lítica y la liberación de anafilotoxinas. Estas terapias deben tener en cuenta, por otro lado, el balance entre la supresión de la desregulación asociada a la patología, y comprometer la defensa y la inmunidad mediada por el complemento.[164]

Aunque existen muchos inhibidores que actúan específicamente sobre el complemento y se están llevando a cabo numerosos estudios clínicos, solo

unos pocos se han llegado a comercializar. Eculizumab (Soliris®), un anticuerpo monoclonal humanizado dirigido contra el componente C5, es uno de los más significativos. Eculizumab impide la activación de C5 a C5b y C5a, y la formación del complejo lítico MAC y representa el único tratamiento aprobado frente a la hemoglobinuria paroxística nocturna, una anemia hemolítica mediada por la acción del complemento.[165] En la actualidad se están llevando a cabo estudios clínicos con eculizumab en una variedad de condiciones, entre ellas aHUS, DDD y AMD. (www.clinicaltrials.gov) y muy recientemente se ha aprobado el uso de eculizumab, tanto en Estados Unidos como en Europa, para el tratamiento del aHUS.[166] El tratamiento con eculizumab está resultando muy eficaz en estos pacientes, donde parece recuperar el recuento plaquetario, mejorar la función renal durante la recurrencia antes y después del trasplante y previene los estados pro-trombóticos.[165] En DDD el uso de este medicamento debe ser considerado cuidadosamente, ya que el papel de la activación de C5 en la patogénesis no está tan claro, aunque si se ha comprobado una reducción de la inflamación en ensayos con ratones.[165] Un inhibidor del complemento con muy buenas perspectivas de aplicación clínica es compstatin, un péptido que impide el corte proteolítico de C3 a C3b, previniendo cualquier activación del complemento y reduciendo también el efecto pro-inflamatorio. Análisis funcionales y de interacción, combinado con un enfoque estructural y de modelado computacional han permitido diseñar análogos de compstatin mucho más potentes (hasta una capacidad de inhibición de más de 250 veces mayor que el compuesto original), que actualmente se están ensayando en el tratamiento de la AMD (POT-4®).[167]

Las nuevas terapias como el eculizumab han cambiado el modo de actuar frente a las enfermedades asociadas al complemento. La realidad es que están salvando vidas, por lo que su valor es indiscutible, y en poco tiempo se prevé la aprobación de nuevos tratamientos para estas enfermedades. Sin embargo, debido a su mecanismo de acción, la eficacia del sistema del complemento en la respuesta frente a infecciones se ve comprometida. La susceptibilidad frente a determinadas infecciones aumenta, en particular por *Neisseria meningitidis* y los pacientes deben vacunarse antes de empezar el tratamiento.[164] El diseño terapias más selectivas y más efectivas se beneficia enormemente del conocimiento de los mecanismos moleculares implicados en la activación y la desregulación mediada del complemento. En este sentido explorar la formación del complejo convertasa de C3 de la AP como diana terapéutica puede ser interesante. El desafío radica en encontrar el equilibrio para lograr una inhibición del complemento y prevenir el daño sin menoscabar las funciones de

protección; y al mismo tiempo, en dirigir la terapia de forma localizada sin inhibir de forma sistémica el complemento. Ya existen varios proyectos en desarrollo que bloquean específicamente la vía alternativa.[168, 169] Nuestro grupo, trabajando conjuntamente con el de la Dra. Mercedes Domínguez del Instituto de Salud Carlos III, ha desarrollado un anticuerpo monoclonal contra epítopos del fragmento Ba de fB. El anticuerpo es capaz de inhibir específicamente la formación de la convertasa de C3 de la AP, y actualmente estamos llevando a cabo una caracterización en profundidad de este anticuerpo, evaluando la capacidad de modular la activación el complemento, para valorar su interés terapéutico.

Partiendo de los modelos estructurales de la convertasa de C3 de la AP, se han planteado otros estudios con una aplicación clínica potencial, como son los complejos con P, C3-Nef y el propio C3b en la convertasa de C5.

2. Identificación de variantes de riesgo en el gen *CFH* asociadas con patología.

2.1. El polimorfismo Tyr402His de *CFH* en AMD.

AMD es la principal causa de ceguera en los países industrializados y supone un impacto personal y socio económico inmenso. Los estudios epidemiológicos muestran que los factores de riesgo más fuertes son la edad, el tabaquismo y el componente genético.[170]

Diferentes estudios apuntan a la desregulación del sistema del complemento como factor importante en el desarrollo de la AMD. Existen evidencias clínicas como la presencia de componentes activados del complemento en las drusas.[105, 171] En las genéticas encontramos una asociación con componentes del complemento como *CFH*, *CFB*, *C2*, *C3* y la deleción de *CFHR1* y *CFHR3*.[107, 139] Por otra parte, esta idea está apoyada por el hecho de que AMD comparte cierta asociación genética y algunas características clínicas con DDD, cuyo mecanismo patogénico está basado en la desregulación de la AP del complemento.[170]

El gen *CFH*, y concretamente el polimorfismo Tyr402His, representa el factor de riesgo genético más importante de predisposición a AMD. En portadores homocigotos His402, el riesgo aumenta hasta más de 7 veces según diferentes estudios casos-controles, mientras que individuos heterocigotos tienen un riesgo intermedio para la enfermedad.[110-112] A pesar de la asociación genética, cómo contribuye este polimorfismo en la patología de AMD se desconoce. Además de este, y de un polimorfismo protector, se han identificado otras variantes asociados a AMD en regiones no codificantes de *CFH*, que probablemente estén afectando a los niveles de expresión de fH.[172]

Nuestro propósito ha sido la caracterización del polimorfismo de riesgo Tyr402His de *CFH* en el contexto de AMD, su identificación en portadores y su influencia en la expresión de fH. Para abordar esta cuestión, hemos contado con la colaboración de los Dres. Claire Harris y Paul Morgan de la universidad de Cardiff. Se ha generado un anticuerpo monoclonal (MBI-7), reactivo contra fH y fHL-1 y dirigido específicamente contra las variantes His402. Este anticuerpo, en combinación con otro no especifico que reconoce el fH total, nos

permite cuantificar la contribución de cada alelo de fH, Tyr402 e His402, en individuos heterocigotos. Además, hace posible detectar el estatus del polimorfismo Tyr402His en cada individuo.

Según los resultados obtenidos, no existen diferencias en los niveles de fH respecto a una población control que puedan influir en la patología AMD. En cambio, si ponen de manifiesto el efecto que tiene la edad al aumentar los niveles de fH en plasma, y la alta variabilidad en la expresión de esta proteína, confirmando estudios previos.[50] Por otra parte, el polimorfismo Tyr402His no parece influir a la expresión de *CFH*. Aunque en individuos heterocigotos Tyr402His los niveles de fH son mayores entre pacientes AMD, no encontramos una expresión diferencial específica para cada alelo Tyr402 e His402. En este grupo de pacientes AMD, ambos alelos se expresan más que en el grupo sano, hecho que consideramos irrelevante pues estos mayores niveles entre pacientes no se encuentran cuando se comparan los otros dos grupos, homocigotos Tyr402 y homocigotos His402. Este dato, aunque no parece tener más importancia necesitaría ser explorado en otras poblaciones y en contexto con otros factores que afectan a los niveles de fH, como el tabaco.

El uso de MBI-7 nos ha permitido identificar portadores del alelo His402 de *CFH* de predisposición a AMD, y si está presente en una o dos copias. El análisis genético confirmó en todos los casos el fenotipo obtenido mediante el uso del anticuerpo MBI-7. El conocimiento del estatus polimórfico Tyr402His, supone una información valiosa para el paciente. Aporta una evaluación más precisa del riesgo y puede ayudar en la prevención de otros factores de predisposición a AMD. El tabaquismo, por ejemplo, un factor fácilmente modificable, es la causa ambiental con mayor contribución en AMD y tiene un efecto dosis-respuesta.[173] Además, se ha visto una interacción genotipo-fenotipo con la variante His402 de *CFH*, que eleva el riesgo para AMD.[174, 175] El estudio AREDS (*Age-related eye macular disease study*) ha demostrado una interacción genotipo-tratamiento que afecta directamente a este polimorfismo. El tratamiento de pacientes de AMD con concentrados nutricionales de antioxidantes suplementados con zinc reduce significativamente el desarrollo de la enfermedad a estadios avanzados. En comparación con el placebo, la progresión a AMD se reduce en un 68% en individuos homocigotos Tyr402, mientras que en pacientes homocigotos para el alelo de riesgo, la progresión se reduce solamente en un 11% de los casos.[176]

El diseño de mejores terapias de prevención y de tratamiento en el ámbito de la AMD está avanzando día a día. Por lo tanto, el contar modelos predictivos fiables de evaluación del riesgo, y las herramientas necesarias para el diagnóstico tiene un gran valor potencial. Más aun cuando se trata de enfermedades tan extendidas como AMD, donde impacto socioeconómico es altísimo. En un estudio en los Estados Unidos el coste socio-económico causado por la AMD seca y húmeda es de unos 30 mil millones de dólares anuales. A esto hay que añadirle que el número de casos aumenta cada año, debido principalmente al envejecimiento de la población. Actualmente una de cada tres personas mayores de 75 años padecerá AMD, y en una de cada diez progresará a estadios tardíos y neovasculares.[177] Frenar el avance de la enfermedad en la población, aunque solo sea en un mínimo porcentaje, supone un beneficio a nivel personal y económico enorme. En este sentido, nuestro laboratorio sigue ampliando el conocimiento respecto a la asociación del polimorfismo Tyr402His con AMD. Recientemente, hemos demostrado que la variante de riesgo His402 está en desequilibrio de ligamiento con un alelo de del gen *CFHR1* y forman parte de un haplotipo que se extiende desde *CFH* e incluye los genes *CFHR3* y *CFHR1*. Los diferentes haplotipos descritos de *CFH* correlacionan con los tres alelos descritos de *CFHR1*, existiendo uno protector (que incluye la deleción ∆*CFHR1-3*), uno de riesgo (que incluye el SNP Tyr402His) y otro neutro para AMD (pero de riesgo para aHUS, confirmando una vez más la relación genotipo-fenotipo). Con estos datos se ha desarrollado un modelo de predicción de riesgo para AMD, basado en los polimorfismos de *CFB* y *ARMS2* y las variantes alélicas de *CFHR1*, con una sensibilidad aproximada del 70%.[178]

2.2. Variantes cuantitativas de fH asociadas a aHUS.

Dada la alta frecuencia alélica de la variante His402 de *CFH* en la población occidental (entre el 30 y el 40% según la base de datos del *National Center of Biotechnology Information*), podemos aplicar el anticuerpo MBI-7 en campos en los que el fH tiene especial interés, aunque no exista una asociación con el polimorfismo Tyr402His.

La desregulación de la AP es probablemente la principal causa en la patología aHUS, y más de la mitad de los pacientes presentan alteraciones que afectan de una u otra manera a esta vía del complemento. La penetrancia incompleta del aHUS indica que las alteraciones en las proteínas del

complemento confieren una predisposición a la enfermedad, y que la confluencia con otros factores genéticos o ambientales es determinante en el desarrollo del aHUS.[84]

Aproximadamente un 30% de las alteraciones son mutaciones en el gen *CFH*.[84] De estas, la mayoría son mutaciones puntuales en los dominios de C-terminal que afectan a la capacidad de fH de unirse a las superficies celulares de los tejidos propios, mientras que otras influyen en los niveles de fH en el plasma, produciendo deficiencias parciales y disminuyendo la capacidad reguladora sobre la AP.[92] No es fácil establecer un criterio en cuanto al nivel de fH que nos indique la existencia de una deficiencia. El rango en la expresión de esta proteína es muy amplio, como ya hemos visto, lo que puede enmascarar deficiencias de fH en heterocigosis.

Para determinar el impacto de estas variantes cuantitativas de fH en predisposición a aHUS, diseñamos un ensayo en el que empleamos anticuerpos específicos de las variantes Tyr402 (MBI-6) e His402 (MBI-7) de fH. Este ensayo nos ha permitido identificar alelos nulos y de baja expresión en el gen *CFH*. Puesto que solamente nos podemos centrar en los individuos heterocigotos Tyr402His, es razonable pensar que en individuos homocigotos haya también alelos de baja expresión. Pero que permanecen ocultos por su estatus homocigótico y por amplio rango de variación en los niveles de fH.

Estudiando los individuos heterocigotos Tyr402His, no detectamos alelos nulos o de baja expresión entre una población de individuos sanos, pero sí en el grupo de pacientes aHUS. Es interesante señalar que, en todos los casos, el alelo de baja expresión identificado es el de la variante His402 de *CFH*. Aunque este polimorfismo no tiene una asociación particular con aHUS, no siendo así para AMD y DDD donde supone un factor de riesgo importante,[133] no podemos obviar este hecho, y es algo que tenemos en cuenta para futuras investigaciones.

En dos de los casos, H90 y H169, la baja expresión del alelo de fH se confirma con la presencia de mutaciones segregando con los bajos niveles de fH. Las mutaciones Cys853Arg y Cys1218Arg en los pacientes H90 y H169 respectivamente, no descritas con anterioridad, afectan a cisteínas conservadas y son responsables de la ausencia de fH en plasma. Sin embargo, estos cambios no afectan a la expresión de fHL-1, lo que explica las trazas siempre detectables en la cuantificación alelo-especifica. Hecho que se

confirmó al observar el patrón de expresión de fH y fHL-1 mediante *western blot* con el anticuerpo MBI-7 en el que detectamos únicamente la proteína fHL-1. Como consecuencia de esta deficiencia parcial, estos pacientes presentan niveles bajos de fH, en el rango bajo de variación de los niveles de fH total, lo que ha de generar unas condiciones de susceptibilidad para el desarrollo de aHUS.[121, 179] Las mutaciones identificadas segregan en la familia de los pacientes con la deficiencia parcial de fH en plasma, y son el único factor de riesgo encontrado, aunque no descartamos la existencia de otros factores adicionales.

El caso del paciente H29 es de especial interés. Este individuo es portador de una mutación en un alelo de *CFH*, y en el otro, un alelo de baja expresión cuya causa está aún por identificar. El patrón de expresión de fH y fHL-1 por *western blot* muestra que la baja expresión solo afecta a fH, que no llega a ser total, pero no a la isoforma fHL-1 que incluso se ve aumentada. La proteínas fH y fHL-1 comparten un mismo origen de replicación y región promotora en *CFH*, y están traducidas a partir de transcritos maduros diferentes.[71] Una posibilidad que explique este patrón de expresión es que la mutación responsable esté alterando regiones reguladoras del *splicing* alternativo (probablemente adyacentes al exón 10), pero el análisis genético en regiones intrónicas no ha mostrado ninguna variación de secuencia. Por otro, lado, el hecho de que la expresión de ambas proteínas esté regulada de manera diferente,[74] complica la situación y hace más difícil encontrar una causa para este patrón anómalo de expresión de fH y fHL-1. El paciente H29, es portador además de una mutación en *CFH*, Arg1210Cys, que se ha visto asociada con aHUS en varias ocasiones y que reduce la capacidad reguladora de fH sobre superficies, pero no en fase fluida.[126, 127, 180-182] Gracias al estudio familiar, hemos comprobado que la segregación de la mutación Arg1210Cys está ligada al alelo Tyr402 de *CFH*. El caso índice hereda este alelo mutado por vía paterna, y por vía materna, el alelo de baja expresión en la variante His402 de *CFH*. La hermana, también heterocigoto Tyr402His, hereda la mutación Arg1210Cys pero un alelo His402 de expresión normal, y está sana. Este hecho ilustra cómo el alelo de baja expresión es determinante para el desarrollo de la enfermedad en portadores de la mutación Arg1210Cys.

Desde la publicación de estos resultados se han incluido otros pacientes aHUS en este ensayo, y se ha podido detectar una deficiencia parcial del alelo His402 de fH en más casos (**figura 19**). El paciente H143 es portador de una mutación nula (c.89insA) que produce un cambio en el marco de lectura y

genera una proteína truncada, por lo que la deficiencia de fH y fHL-1, ambas variantes His402, es total. El paciente H196 porta una mutación de cambio de aminoácido (Glu847Val), aunque aún no ha sido posible determinar si este cambio se encuentra en el alelo Tyr402 o His402 de *CFH* y establecer una asociación con la baja expresión. Ambos casos, H143 y H196, tienen niveles bajos de fH y son portadores además, del polimorfismo de riesgo MCP_{ggaac}, que está asociado a aHUS e influye en la severidad cuando hay otros factores, como es la deficiencia parcial en estos casos.[130]

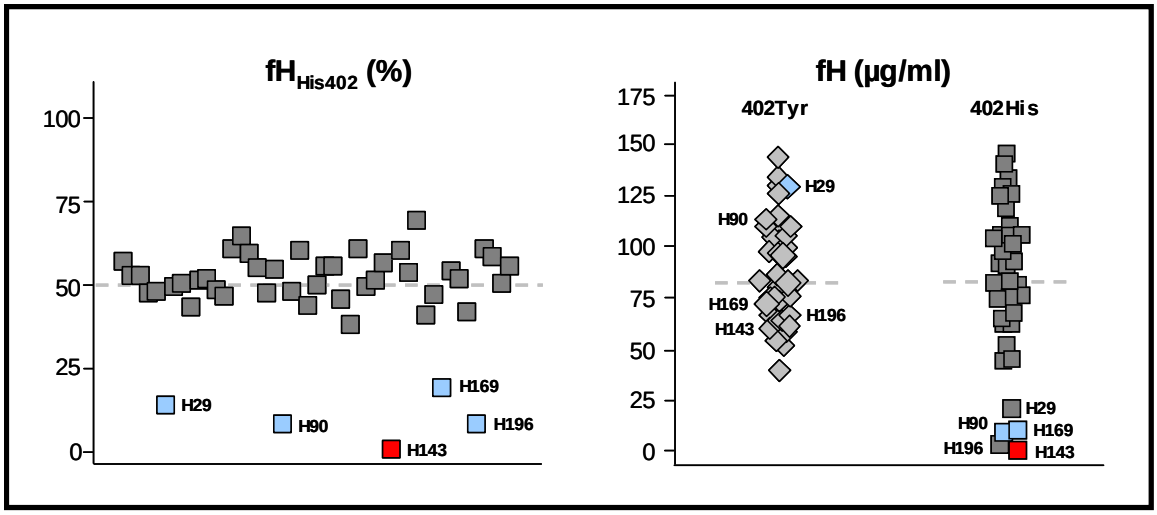

Figura 19. Cuantificación alelo-específica de pacientes aHUS Tyr402His. El empleo del anticuerpo MBI-7, específico de la variante His402 de fH, en combinación con otro que reconoce el fH total, nos permite detectar aquellos individuos con deficiencias parciales de fH. En todos los casos la deficiencia afecta al la variante His402 de fH (y a las variantes His402 de fH y fHL-1 en el caso del paciente H143). En los cinco pacientes se han identificado mutaciones en el gen *CFH*. Mutaciones cambio de aminoácido (azul) en H29 (Arg1210Cys), H90 (Cys853Arg), H169 (Cys1218Arg) y H196 (Glu847Val); y una mutación nula (rojo) en H143 (c.89insA). En H90, H143 y H169, las mutaciones explican la baja o nula expresión de la proteína, pero en el caso de H29 no se ha encontrado una causa genética. En el paciente H196 no se a determinado en qué alelo de fH se encuentra la mutación Glu847Val, y por lo tanto si causa o no la deficiencia de fH.

El anticuerpo MBI-7, y la técnica para identificar alelos de baja expresión aquí descrita, está siendo de gran utilidad para estudios similares. Johnson *et al* asocian una mutación de *CFH* (Tyr899Asp) a los bajos niveles de fH detectados en estos portadores. Algo únicamente posible mediante cuantificaciones alelo-específicas. Heterocigotos compuestos portadores de esta y otra mutación que afecta a la capacidad reguladora sobre superficies, son los únicos enfermos de aHUS.[183] Este estudio, como el caso descrito previamente de H29, resalta una vez más la importancia de la presencia de

varios factores de riesgo, incluidas las deficiencias parciales de fH, en un mismo individuo para el desarrollo de aHUS.

Las deficiencias de fH no siempre se deben a mutaciones en cisteínas conservadas o a proteínas truncadas de fH, y suponen una característica patológica que necesita ser puesta en evidencia. Herramientas como el anticuerpo MBI-7 proporcionan una nueva vía desde la que se pueden hallar respuestas para el aHUS. Una aplicación clínica del uso de este anticuerpo es la identificación de alelos de baja expresión de fH, ya que se trata de factores de riesgo cuantificables que debemos añadir a la lista de factores de predisposición a aHUS. Lista, que por otro lado sigue incompleta, ya que en muchos de los casos no se ha detectado una causa que justifique el desequilibrio de la AP característico de esta enfermedad. La identificación de nuevos factores aporta una información que puede complementar la información genética existente, y viceversa. Actualmente usamos esta técnica para detectar estos alelos en pacientes aHUS, previo genotipado del polimorfismo Tyr402His, y adelantarnos así, en la búsqueda de las posibles mutaciones responsables.

3. Caracterización funcional de polimorfismos en genes de *CFB* y *CFH* asociados con patología.

3.1. Polimorfismos Arg32Trp/Gln *CFB* y Val62Ile de *CFH*.

La desregulación del complemento es un desencadenante muy importante en el desarrollo ciertas patologías. La activación excesiva y no específica produce el daño tisular, y la liberación de anafilotoxinas genera estados inflamatorios. Existen numerosos factores, genéticos y no genéticos, que pueden causar una perdida de función en los reguladores, o bien, una ganancia de función en los componentes, lo que conduce a la desregulación del complemento.[184, 185] Partiendo de esta idea de mecanismo patológico, el escenario que resulta de invertir estas alteraciones, es decir, una ganancia de función reguladora o una perdida funcional en componentes, debe conducir a una sobrerregulación y una menor activación del sistema del complemento. Se genera así, una situación que puede ser también potencialmente dañina en determinadas circunstancias; por ejemplo, en caso de infección si el complemento no se llega a activar. Sin embargo, este estado donde la capacidad efectora del complemento queda mermada, puede resultar beneficioso, y tener un carácter protector, en un contexto donde la activación descontrolada es la característica patológica, tal y como se asume que sucede en aHUS, DDD y AMD.[184, 185] Existen polimorfismos comunes en el componente del complemento fB y en el regulador fH que confieren protección para estas enfermedades, y estudios previos han sugerido que actúan de este modo.[136, 148] Esta idea, ha sido en realidad, nuestra hipótesis de trabajo para investigar la caracterización funcional de los polimorfismos Arg32Trp/Gln de *CFB* y Val62Ile de *CFH*. Para ello, hemos trabajado conjuntamente con los grupos del los Dres. Claire Harris y Paul Morgan.

La variante fB-Gln32 está fuertemente asociada con un menor riesgo para AMD,[142, 143] mientras que la variante fH-Ile62 lo está para aHUS, DDD y AMD.[95, 109] Ambos polimorfismos se localizan en regiones esenciales para su actividad funcional. Arg32Trp/Gln se sitúa en el dominio Ba de fB, cuyo papel en el ensamblaje de la pro-convertasa y en el reconocimiento inicial de C3b resulta crucial, como ya ha quedado patente con anterioridad. En el caso de fH, el polimorfismo Val62Ile se localiza en el domino SCR 1, en un sitio de unión a C3b, y en una región que abarca las funciones reguladoras de actividad

cofactora de fI y de aceleración de la disociación de la convertasa (SCRs 1-4).[58, 60]

Partiendo de proteínas purificadas de cada una de las variantes de los polimorfismos Arg32Trp/Gln de *CFB* y Val62Ile de *CFH*, diseñamos una serie de experimentos con el fin de describir las diferencias funcionales de estas variantes comunes, y comprender su asociación con las distintas enfermedades.

3.1.1. Caracterización funcional del polimorfismo Arg32Trp/Gln de *CFB.*

La variante protectora para AMD, fB_{Gln32}, se comporta en un ensayo hemolítico disminuyendo la lisis, al compararla con la variante más común, fB_{Arg32}. Los ensayos de interacción muestran que la variante fB_{Gln32} une C3b con menos afinidad, y como consecuencia, forma menos complejos pro-convertasa y genera menos actividad hemolítica. La variante B_{Trp32}, presenta una interacción y una actividad intermedias. Estas diferencias pudieron observarse también con proteínas recombinantes y fragmentos aislados de Ba. La tasa de disociación espontánea del complejo C3bB es, por el contrario, la misma para los distintos residuos del polimorfismo.

El mecanismo subyacente del efecto protector de la variante fB_{Gln32} en AMD, se debe a una pérdida de función de uno de los componentes claves de la AP. La alteración no influye directamente en la actividad enzimática de la convertasa, sino en la capacidad de formar pro-convertasa, lo que reduce cuantitativamente la función de las convertasas, y por lo tanto, la amplificación de la cascada del complemento. De acuerdo con estos resultados, un estudio de asociación ha mostrado que el cambio Trp32 de *CFB* confiere protección para AMD (OR=0,64).[186] El menor riesgo asociado a este cambio del polimorfismo, se ajusta perfectamente a la pérdida funcional, intermedia entre fB_{Arg32} y fB_{Gln32}, que se ha caracterizado para esta variante, fB_{Trp32}.

El mapa estructural de fB sitúa el aminoácido Arg32 (séptima posición en la proteína madura) en un fragmento desestructurado del extremo N-terminal del dominio Ba.[24] Las diferencias funcionales observadas atribuyen un papel importante a este residuo en el reconocimiento inicial de C3b, cuya región de interacción puede ser deducida gracias a los conocimientos estructurales del complejo C3bB.

3.1.2. Caracterización funcional del polimorfismo Val62Ile de *CFH*.

El diseño experimental para la caracterización del polimorfismo Val62Ile se llevó a cabo en base a las diferentes funciones de fH: actividad cofactora de fI y aceleración de la disociación de la convertasa de C3, mediadas en gran medida por la capacidad de fH de unión a C3b. De la interacción entre fH y C3b, también depende la competición con fB por el ligando, C3b, para controlar la formación de la pro-convertasa de C3.

La sustitución Val62Ile en el SCR 1 de fH incrementa la afinidad por C3b lo que se traduce en una ganancia de función reguladora. fH_{Ile62} actúa como cofactor de fI más eficientemente que fH_{Val62}, lo que genera una mayor inactivación de C3b a iC3b. fH_{Ile62} impide la formación de pro-convertasa en mayor medida que Val62, gracias a una mayor competición con fB. Los efectos se observaron de forma similar, en diseños experimentales en fase fluida o sobre superficies celulares, tanto con proteínas purificadas como en ensayos hemolíticos. Por el contrario, la función de aceleración de la disociación de la convertasa no se ve afectada y ambas variantes son comparables.

Cada uno de los cuatro dominios SCR de la región N-terminal de fH está implicado en la actividad reguladora.[58, 72] Estos resultados indican que las regiones que participan en la actividad cofactora de fI y de aceleración de la disociación, son probablemente diferentes, y al mismo tiempo solapantes. El sitio de interacción del dominio SCR 1 de fH con C3b, que se ve afectado por el polimorfismo Val62Ile, no influye directamente en la disociación del complejo C3bBb. Desde un punto de vista estructural (se ha cristalizado el complejo C3b-fH_{SCR1-4}), el residuo Val62 no está localizado en la zona de interacción entre fH y C3b, sino en el núcleo hidrofóbico del dominio SCR 1, y podría influir en su estabilizacion.[155] Los estudios de resonancia magnética de esta región demuestran, de hecho, pequeñas perturbaciones en la termoestabilidad, así como la pérdida de puentes de Hidrógeno con residuos adyacentes en la sustitución Val62Ile.[135] En este sentido, las pequeñas perturbaciones estructurales se ajustan a las modificaciones observadas de la actividad funcional de fH. Como se verá más adelante, estas variaciones influyen en la cascada de activación y pueden verse amplificadas por la suma de otras variaciones como las del polimorfismo de fB.

3.1.3. Influencia de los polimorfismos en el complemento e implicaciones patológicas.

Arg32Trp/Gln de *CFB* y Val62Ile de *CFH* son polimorfismos comunes por lo que es relativamente frecuente encontrar individuos con las distintas combinaciones de estas proteínas, a las que denominamos complotipos. Ensayos funcionales con proteínas purificadas han mostrado cómo los complotipos de las variantes de fH y fB se comportan de manera aditiva, como se predice de su actividad individual. Si las variantes funcionan en el mismo sentido, como en este caso, reduciendo la actividad del complemento, el efecto en la actividad global se ve amplificado. El complotipo protector, fB_{Gln32} fH_{Ile62}, es hemolíticamente mucho menos activo, el parámetro EC50 aumenta en más del doble comparado con el complotipo más común, y más activo, fB_{Arg32} fH_{Val62}.

Recientemente, se ha caracterizado a nivel funcional el polimorfismo de C3, Arg102Gly, cuya variante Gly102 confiere predisposición a DDD y AMD.[133, 150] Este polimorfismo influye sobre la eficiencia reguladora de fH, como cofactor de fI. $C3_{Gly102}$ une fH con menos afinidad, disminuyendo la inactivación a iC3b e incrementando el nivel de activación del complemento. Cuando se combina este polimorfismo de C3 con los aquí descritos de fB y fH, el resultado es una modificación drástica de la capacidad de activación de la AP del complemento. La actividad hemolítica del complotipo menos activo, fB_{Gln32} fH_{Ile62} $C3_{Arg102}$, que incluye las variantes protectoras de fB y fH, es mucho más baja. El parámetro EC50 es casi seis veces mayor que el del complotipo más activo, fB_{Arg32} fH_{Val62} $C3_{Gly102}$, que incluye la variante de riesgo de C3 (**figura 20**).[187]

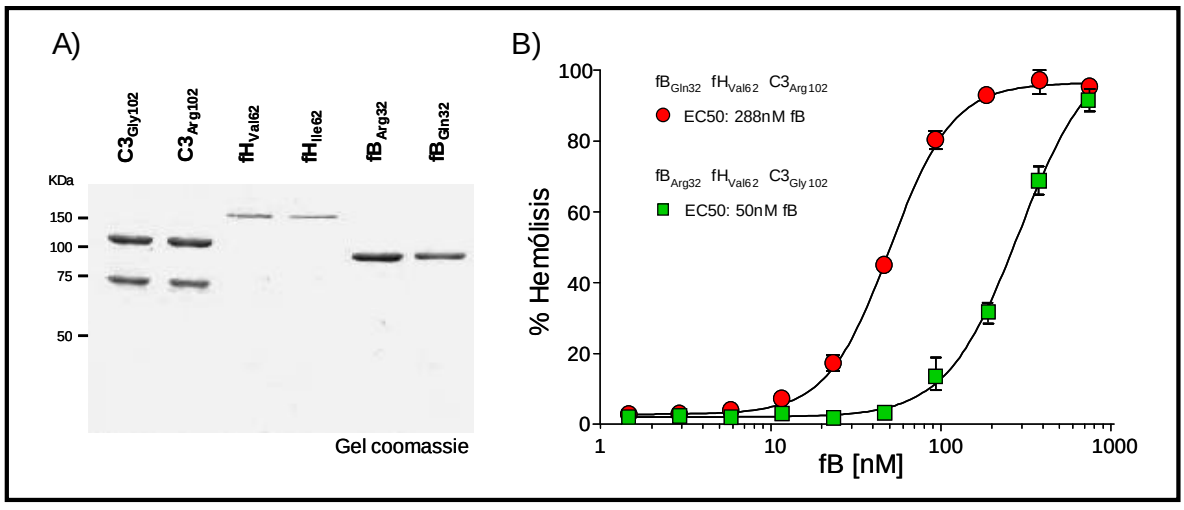

Figura 20. Efecto de las variantes polimórficas de C3, fB y fH en la actividad hemolítica de la AP.[187] A) Muestras purificadas de ambas variantes de $fB_{Arg32Gln}$ $fH_{Val62Ile}$ $C3_{Arg102Gly}$ empleadas en el ensayo hemolítico. B) Ensayo hemolítico en el que se comparan las variantes de mayor actividad: fB_{Arg32} fH_{Val62} $C3_{Gly102}$, con las de menor actividad de la AP: fB_{Gln32} fH_{Ile62} $C3_{Arg102}$. Partiendo de muestras purificas y suero deplecionado de C3, fB y fH, se preparan eritrocitos recubiertos de ambas variantes de C3b. Sobre estos eritrocitos se realiza un ensayo de actividad cofactora de fI con las dos variantes de fH, con el fin de inactivar el C3b depositado sobre los eritrocitos. Posteriormente se forma una convertasa empleando ambas variantes de fB, a diferentes concentraciones, y fD. La lisis de los eritrocitos es dependiente de la AP, y resulta proporcional tanto al efecto de la actividad cofactora como a la cantidad de convertasa formada. El parámetro EC50 representa la concentración efectiva para obtener un 50% de lisis. En este ensayo se comparan las combinaciones de variantes, o complotipos, con actividades más extremas, el resto de combinaciones dan lugar a actividades hemolíticas intermedias.

Los polimorfismos Arg32Trp/Gln de *CFB* y Val62Ile de *CFH*, frecuentes en población, tienen consecuencias funcionales al modular ligeramente la AP del complemento, haciéndola menos activa. En enfermedades como aHUS, DDD y AMD, donde la activación del complemento es una característica patológica, esto supone una ventaja, de ahí que portadores de estos cambios tengan menos riesgo a desarrollar las enfermedades. La variante Ile62 de *CFH* tiene un papel protector en aHUS, DDD y AMD porque es mejor regulador del complemento que la variante Val62. La clara correlación genotipo-fenotipo existente entre *CFH* y estas patologías podría contrastar con la asociación protectora de Val62Ile. Sin embargo, la ganancia de función reguladora, a nivel de la actividad cofactora y de competición con fB observada en fase fluida y superficies, explica el efecto protector en patologías asociadas tanto a una deficiencia de fH e hipocomplementemia (DDD), como a una desregulación restringida en las superficies celulares (aHUS).

En el caso del polimorfismo Arg32Gln de *CFB*, la variación funcional afecta a la formación del complejo central de la activación del complemento en plasma, la convertasa de C3 de la AP. Sin embargo, no está claro porqué la asociación protectora parece ser específica de AMD y no influir en otras enfermedades relacionadas con la desregulación del complemento, como aHUS y DDD. Los mayores niveles plasmáticos de productos activados del complemento (C3a, C3d, Ba y C5b-9) encontrados entre pacientes AMD, indican una desregulación sistémica del complemento. A pesar de este componente sistémico, la retina parece especialmente sensible a los efectos de la activación y el daño tisular se manifiesta localmente y de forma tardía.[188] No debemos olvidar aquellos procesos patogénicos en los que el complemento se ve implicado. La composición de las drusas, cuya aparición, por otra parte aún desconocida, está muy ligada al desarrollo y la gravedad de la AMD, implica procesos locales

de inflamación y particularmente de activación del complemento por la AP en la retina.[105] Cabe recordar aquí otros factores de riesgo muy asociados a AMD, como el polimorfismo de *CFH* Tyr402His, cuya implicación en la patología podría aportar claves en relación a los mecanismos patogénicos de la AMD. Según investigaciones recientes la variante His402 de fH ve muy reducida su interacción con ligandos pro-inflamatorios, como las proteínas modificadas por malondialdehidos (MDA), generados en diversas patologías incluyendo la AMD de manera local en el coroide, membrana de Bruch y las drusas. En las superficies modificadas con MDA el fH resulta anti-inflamatorio, y por tanto, portadores de la variante His402 de *CFH* ven reducida esta capacidad contribuyendo a la patogénesis de la enfermedad.[189] Teniendo en cuenta procesos como estos, las diferencias funcionales a nivel sistémico podrían tener un efecto significativo a nivel local en la retina, explicando también la especificidad de las asociaciones.

En el desarrollo de patologías como aHUS, DDD y AMD el papel del complemento es cada vez más evidente, y su implicación está determinada por el equilibrio entre la activación y la regulación. La suma de diferentes factores, como el efecto de las mutaciones y los polimorfismos, la presencia de autoanticuerpos, los niveles de proteína y la influencia de factores ambientales entre otros, inclina el balance global hacia la activación. Desde el punto de vista patogénico, cada uno de ellos es importante y debe ser tenido en cuenta, especialmente en enfermedades multifactoriales como aHUS, DDD y AMD. Los resultados aquí descritos, tratan de mostrar cómo los polimorfismos comunes de fB y fH son funcionales, y modulan este equilibrio hacia una menor activación y una mayor regulación. Aunque las diferencias en la actividad son sutiles, la propia naturaleza del complemento se encargará de amplificar estos efectos. Y lo que es más importante, las variaciones funcionales en reguladores y componentes son aditivas, tal como se ha comprobado en las combinaciones de los polimorfismos de fB, fH y C3. El complotipo aquí descrito está representado por variantes comunes en tres proteínas del complemento, pudiendo extenderse a polimorfismos en otras proteínas y a otras variables como los niveles de expresión, pudiendo amplificar aún más el impacto funcional. Un determinado complotipo puede cambiar drásticamente las características de las cascadas de activación del complemento, y establecer un nivel de actividad sistémica que determine en el individuo portador, un mayor o menor riesgo frente a las enfermedades asociadas al complemento. Del mismo modo, los complotipos pueden explicar la penetrancia incompleta observada en patologías como aHUS y DDD, e incluso, influir en la severidad con que se

presentan. Además, estas diferencias funcionales van a tener influencia en otros contextos. Heredar un polimorfismo o complotipo menos activo (fB_{Gln32} fH_{Ile62} $C3_{Arg102}$) puede resultar beneficioso en enfermedades crónicas inflamatorias, pero al mismo tiempo conferir predisposición frente a infecciones al reducir el grado de opsonización y lisis por la vía terminal.

Gracias a la caracterización funcional de los polimorfismos protectores Arg32Trp/Gln de *CFB* y Val62Ile de *CFH* es posible entender la base molecular de la asociación genética con aHUS, DDD y AMD. Estos datos aportan información sobre los mecanismos patogénicos de estas enfermedades, que no se comprenden completamente, y pueden tener aplicaciones clínicas concretas. La identificación de portadores de estos polimorfismos y complotipos va a ser de gran importancia en la predicción del riesgo y en la mejora del diagnóstico en aquellos desordenes en los que el complemento está implicado.

Los datos funcionales también pueden contribuir en el diseño de terapias dirigidas más eficaces, que tienen como objetivo restablecer el equilibrio de la actividad del complemento. La fuente de proteínas del complemento con uso terapéutico está limitada a la plasmaféresis o a la infusión de plasma. Es por esto que los reguladores naturales del complemento, se han considerado como estrategia terapéutica desde los primeros pasos en las terapias de inhibición del complemento. Existen formas solubles de C1-Inh (comercializado para el tratamiento del angioedema hereditario como Cinryze®), CR1 (que se ha llegado a probar en humanos), MCP, DAF, CD59 y fH.[164] El tratamiento con concentrados de fH purificado es una terapia, actualmente en desarrollo, con una aplicación potencial en aHUS y DDD,[190] y en 2007 fue designado como medicamento huérfano por la Agencia Europea del Medicamento.[191] Paul N. Barlow y colaboradores han logrado producir fH recombinante en células de *Pichia pastoris* con completa actividad funcional. Estos mismos autores proponen su uso terapéutico, así como el diseño y la producción de variantes con mayor capacidad reguladora.[192] La variante Ile62 de fH, siendo un regulador más efectivo que la variante Val62, debería resultar más beneficiosa al suplementarla de forma externa en pacientes que presenten factores que conducen a la desregulación de la AP.

3.2. Caracterización de las variantes Ser890Ile y Val1007Leu de *CFH* e implicaciones en patología.

Hoy en día, la búsqueda de mutaciones y polimorfismos en *CFH* y otros genes del complemento en pacientes de aHUS, DDD y AMD, se ha convertido en una práctica habitual. Los clínicos reclaman cada vez más la información proveniente de los estudios genéticos. En muchos de los casos, la identificación de las mutaciones condiciona no solo la prognosis, también las decisiones clínicas en el tratamiento y el consejo genético ofrecido al paciente y a sus familiares. De ahí, la importancia del diagnóstico genético, sin embargo, existe la necesidad de obtener información adicional que apoye la relación causal entre la alteración y las enfermedades asociadas.

En colaboración con las Dras. Pilar Sánchez Corral y Margarita López Trascasa se ha caracterizado a nivel genético y funcional las variantes de fH Ser890Ile y Val1007Leu, que se han encontrado repetidamente en el registro español de pacientes de aHUS y DDD. Estas variantes se habían asociado a aHUS en otras poblaciones caucásicas y se habían descrito como polimorfismos raros asociados a AMD.[89, 111, 193, 194] La particular correlación genotipo-fenotipo entre determinadas variaciones genéticas de *CFH* y las distintas enfermedades asociadas contrasta con la situación de los cambios Ser890Ile y Val1007Leu, lo que hacía interesante su investigación. Los resultados que se discuten a continuación, indican que estos cambios son en realidad variantes polimórficas que no influyen en la capacidad reguladora de la proteína fH.

En primer lugar, el estudio familiar de segregación seguido en dos de los casos de aHUS, muestra que Ser890Ile y Val1007Leu no son alteraciones aisladas, sino cambios que segregan en el mismo alelo, formando parte de un mismo haplotipo de *CFH*. El haplotipo en el que están presentes estos cambios contiene la variante His402, que es más frecuente en pacientes con DDD y AMD. Por otra parte, está descrita una alta frecuencia alélica de las variantes Ile890 (rs515299) y Leu1007 (rs534399) de *CFH* en poblaciones subsahariana (0,267; 0,317) y afroamericana (0,455; 0,591). Esto sugiere que el haplotipo de *CFH* que incluye estas variaciones tiene un origen evolutivo común, probablemente en el continente africano, y que se está introduciendo en la población caucásica. El hecho de encontrar en uno de los pacientes una

combinación de este y otro haplotipo, indica que se trata además, de cambios genéticos ancestrales.

El haplotipo en el que se localizan los cambios Ile890 Leu1007 incluye el polimorfismo de riesgo His402, lo que nos permitió comprobar, en aquellos pacientes heterocigotos Tyr402His, una expresión normal del alelo. Empleando columnas inmovilizadas con el anticuerpo MBI-7, fuimos capaces de separar y purificar la variante de fH Ile890 Leu1007 para realizar el estudio funcional. Ninguno de los ensayos mostró alteraciones funcionales en la actividad reguladora de la variante de fH Ile890 Leu1007. La interacción con C3b depositado en superficie, la actividad cofactora de fI en fase fluida y actividad reguladora global, probada en un ensayo hemolítico, resultaron normales y equivalentes a las de la variante Ser890 Val1007. La localización de estos cambios, SCR 15 y 17 respectivamente, concuerda con la ausencia de alteraciones funcionales ya que no se trata de regiones funcionalmente relevantes, como pueden ser los SCRs 1-4 o los SCRs 19-20.[68]

Por último, si observamos la historia clínica de los pacientes portadores de los cambios Ile890 Leu1007, encontramos factores adicionales que están relacionados con las enfermedades. Todos ellos están bien caracterizados, y se trata de factores de riesgo asociados a las enfermedades y pueden ayudar a explicar el desarrollo de la patología en cada caso. Los pacientes H54 y H97 portan en homocigosis el alelo de riesgo para aHUS, MCP_{ggaac}, que reduce los niveles de este regulador en la superficie celular.[130] H97 presenta, además, una mutación en fI, Cys86Tyr, que produce una deficiencia parcial de esta enzima en el plasma. El paciente H142 es portador, en el mismo alelo que la variante Ile890 Leu1007, del reordenamiento que da lugar al gen híbrido *CFH::CFHR1*. Esta alteración reduce la capacidad reguladora de la AP sobre las superficies celulares, tal como se ha mostrado también en los ensayos funcionales, y confiere susceptibilidad para aHUS.[78] El paciente de DDD, GN3, es positivo para C3-Nef, que resulta crucial en el desarrollo de esta enfermedad. Además, el haplotipo en el que están incluidos los cambios Ile890 Leu1007 está, de hecho, incrementado en pacientes DDD y AMD ya que contiene el polimorfismo de riesgo His402, muy asociado a estas enfermedades.[95, 133] En el paciente aHUS, H244, no se han detectado otros factores de riesgo. Este individuo es de origen subsahariano, lo que apoya la conclusión del origen evolutivo del haplotipo y el hecho de que sea portador. A todo ello, debemos añadir que ambos cambios también fueron encontrados juntos, tanto en familiares sanos de los pacientes, como en individuos sanos de una población control.

Del análisis genético, de los resultados funcionales y de los datos clínicos extraídos en esta investigación, concluimos que los cambios Ser890Ile y Val1007Leu encontrados en *CFH* pueden ser considerados polimorfismos sin consecuencias funcionales, y sin una asociación particular con las patologías aHUS, DDD y AMD. La caracterización de los cambios Ile890 Leu1007 en fH, explica además la situación que los relacionaba con enfermedades causadas por mecanismos patológicos diferentes, cuya correlación fenotipo-genotipo, destaca especialmente en las mutaciones sobre *CFH*. En este caso, los cambios Ile890 Leu1007 en *CFH* no implican una correlación con el fenotipo de los portadores.

Desde el punto de vista clínico, la identificación de los factores de riesgo que predisponen a las patologías, ya sean mutaciones, polimorfismos, autoanticuerpos u otras alteraciones, va a simplificar la elección y la justificación del tratamiento, y también va a ayudar a definir el pronóstico del mismo. El genotipado de varios genes es por tanto fundamental, y la caracterización funcional de los cambios genéticos aporta una información adicional igualmente importante. Como sucede con Ser890Ile y Val1007Leu en *CFH*, que no tienen consecuencias funcionales, resulta crucial distinguir las mutaciones patológicamente relevantes de las que no lo son. Esta información afecta de manera directa a los pacientes portadores y a sus familiares, ya que va a permitir una evaluación más precisa de su enfermedad, centrando la atención en otros factores de riesgo, y plantear estrategias terapéuticas que estarán condicionadas por los datos genéticos y funcionales.

aHUS, DDD y AMD son enfermedades multifactoriales por lo que el fenotipo en cada individuo puede ser muy variable. En la mayoría de los casos de aHUS y DDD la enfermedad aparece a una edad temprana y aunque muchos progresan hacia IRC, otros se recuperan totalmente.[84, 195] La presencia de mutaciones, el tipo y el gen en que están localizadas, o la existencia de autoanticuerpos ayudan a definir la estrategia terapéutica, que va determinar el desarrollo de la enfermedad. En aHUS, se ha comprobado una correlación entre la mutación y la severidad; así, las mutaciones en *CFH* se asocian con una presentación más agresiva, mientras que los pacientes con mutaciones en *MCP* son los que tienden a evolucionar mejor.[84] La infusión de plasma o la plasmaféresis son estrategias de primera línea para aHUS, donde ha conseguido reducir la mortalidad a la mitad, y también para el tratamiento de DDD. En general, pacientes aHUS con mutaciones en *CFH*, o autoanticuerpos

contra fH responden bien a esta terapia, pero no está tan claro que funcione en aquellos con mutaciones en *MCP*, ya que se trata de una proteína transmembrana.[196] La eliminación de los autoanticuerpos o la proteína mutada, y el aporte de proteína funcional en el plasma, recupera la homeostasis del sistema y reduce el riesgo de remisión. Por la misma razón, en pacientes DDD que presentan deficiencia de fH o C3-Nef, la terapia con plasma está recomendada. Sin embargo, en ambas enfermedades la eficacia depende de la duración y la frecuencia del tratamiento, y los pacientes pueden terminar siendo plasma-dependientes.[96, 196]

A pesar de los tratamientos, aproximadamente la mitad de los casos aHUS y DDD evolucionan a IRC, lo que los convierte en candidatos para el trasplante renal. El inconveniente es que la elevada recurrencia tiene un efecto perjudicial en la supervivencia del órgano tras el trasplante, que se pierde en la mayoría de los casos, hasta en más del 80% en ambos tipos de pacientes.[96, 196] El trasplante de órgano de donante vivo conlleva un gran riesgo para el paciente, considerando la elevada recurrencia, pero también para el donante, especialmente en el caso de existir parentesco.[191] Evaluar la presencia de mutaciones o polimorfismos que ayuden a predecir este riesgo, justifica la importancia que tiene el genotipado del complemento también en el donante, pudiendo aportar información relevante para el desarrollo del tratamiento. En aHUS, de nuevo, se ha comprobado una correlación con el genotipo y los pacientes con mutaciones en *MCP* tienen menos recurrencias tras el trasplante renal, lo que puede deberse a que esta proteína se expresa mayoritariamente en riñón. En portadores de mutaciones en *CFH* el porcentaje de recurrencias y de rechazo es el más elevado y está contraindicado.[197] El hígado es el principal órgano productor de fH por lo que el trasplante renal en estos casos no evita la presencia de la proteína mutada en el plasma. Por este motivo, los trasplantes simultáneos de hígado-riñón persiguen por un lado restaurar la función renal, y por otro prevenir las recurrencias por la presencia de la proteína mutada. Los resultados están siendo muy prometedores y mejoran aún más cuando se combina con plasmaféresis pre-operatoria, infusiones de plasma durante la operación e inmunosupresores.[198] La llegada de nuevas terapias más selectivas como los inhibidores del complemento (eculizumab o compstatin, entre otros que están en desarrollo), han planteado alternativas a los tratamientos tradicionales. Los excelentes resultados que hoy en día está generando el empleo del eculizumab, lo han convertido en el tratamiento de elección en aHUS.[164, 195, 197]

CONCLUSIONES

- El análisis estructural de la convertasa de C3 de la AP aporta una información esencial para comprender los aspectos fundamentales del mecanismo de ensamblaje y activación de estos complejos.

- El modelo de pro-convertasa (C3bB) revela la existencia de dos configuraciones de complejos pro-convertasa coexistiendo en equilibrio. Uno de ellos representa un estado de reconocimiento inicial de los componentes fB y C3b, en el que fB permanece en conformación cerrada. En el otro, el fB sufre un cambio conformacional, necesario para la activación de la molécula y la formación de una convertasa de C3 de la AP activa.

- En el modelo de convertasa (C3bBb), el fragmento Bb permanece unido al complejo, a través del dominio vWA, contactando con el dominio C345c de C3b. El dominio SP queda proyectado fuera del complejo y adopta varias posiciones, lo que le permitirá acomodar el sustrato, C3.

- Los modelos propuestos sirven como marco estructural en el estudio de residuos relevantes y con implicación en patología, que pueden afectar a la afectan a la formación y estabilidad de los complejos. Asimismo, estos modelos revelan aspectos importantes sobre el mecanismo de regulación de los complejos por DAF, pudiendo aplicarse también a otros reguladores.

- Los niveles plasmáticos de fH no influyen en la predisposición a AMD, y el polimorfismo de *CFH* Tyr402His no parece afectar la expresión de esta proteína. Los resultados cuantitativos si ponen de manifiesto el amplio rango de variación de fH y la influencia de la edad en el aumento de la concentración plasmática de fH.

- El anticuerpo MBI-7 permite identificar portadores del polimorfismo de riesgo para AMD Tyr402His en *CFH,* y determinar el genotipo. Además, resulta útil en la cuantificación alelo-específica de fH en individuos heterocigotos Tyr402His.

- El empleo de anticuerpos específicos del polimorfismo Tyr402His ha permitido detectar pacientes aHUS portadores de alelos nulos y de baja expresión, causados, aunque no en todos los casos, por mutaciones en el gen *CFH*.

- Las variantes cuantitativas del gen *CFH* encontradas en pacientes aHUS, son factores de riesgo cuantificables adicionales para aHUS, y pueden determinar el desarrollo de la enfermedad.

- La variante protectora fB_{Gln32} tiene una menor actividad hemolítica, ya que presenta una menor afinidad por C3b en la formación de pro-convertasa y convertasa de C3, en comparación con la variante más común fB_{Arg32}. La variante fB_{Trp32} presenta una actividad intermedia.

- La pérdida de función activadora en fB confiere protección para AMD debido a la menor capacidad de amplificación de la AP del complemento.

- La variante de protección fH_{Ile62} tiene mayor afinidad por C3b que la variante fH_{Val62}, confiriéndola una mejor competición con fB en la formación de la pro-convertasa, y actuando más eficientemente como cofactor de fI en la inactivación de C3b.

- Como mejor regulador de la AP en fase fluida y sobre superficies, la variante fH_{Ile62} juega un papel protector en enfermedades asociadas a la desregulación de la AP (aHUS, DDD y AMD).

- fB Arg32Trp/Gln y fH Val62Ile son polimorfismos funcionales cuyos efectos son aditivos, pudiendo modificar drásticamente la capacidad de activación de la AP y del sistema del complemento.

- Los cambios Ser890Ile / Val1007Leu segregan juntos en un mismo haplotipo de *CFH*, sugiriendo un origen evolutivo común.

- Las variantes Ile890 Leu1007 son polimorfismos sin consecuencias funcionales para la capacidad reguladora de fH, y sin una asociación particular con patología.

BIBLIOGRAFÍA

1. Walport MJ. Complement. First of two parts. *N Engl J Med* 2001; **344:** 1058-1066.

2. Lachmann P. Complement before molecular biology. *Mol Immunol* 2006; **43:** 496-508.

3. Walport MJ. Complement. Second of two parts. *N Engl J Med* 2001; **344:** 1140-1144.

4. Thurman JM, Holers VM. The central role of the alternative complement pathway in human disease. *J Immunol* 2006; **176:** 1305-1310.

5. Sarma JV, Ward PA. The complement system. *Cell Tissue Res* 2011; **343:** 227-235.

6. Law SK, Reid KB. *Complement*, 2 edn. Oxford, IRL Press, 1995.

7. Trouw LA, Daha MR. Role of complement in innate immunity and host defense. *Immunol Lett* 2011; **138:** 35-37.

8. Arlaud GJ, Gaboriaud C, Thielens NM*, et al.* Structural biology of the C1 complex of complement unveils the mechanisms of its activation and proteolytic activity. *Mol Immunol* 2002; **39:** 383-394.

9. Gaboriaud C, Teillet F, Gregory LA*, et al.* Assembly of C1 and the MBL- and ficolin-MASP complexes: structural insights. *Immunobiology* 2007; **212:** 279-288.

10. Muller-Eberhard HJ. Molecular organization and function of the complement system. *Annu Rev Biochem* 1988; **57:** 321-347.

11. Ricklin D, Hajishengallis G, Yang K*, et al.* Complement: a key system for immune surveillance and homeostasis. *Nat Immunol* 2010; **11:** 785-797.

12. Lachmann PJ. The amplification loop of the complement pathways. *Adv Immunol* 2009; **104:** 115-149.

13. Kemper C, Atkinson JP, Hourcade DE. Properdin: emerging roles of a pattern-recognition molecule. *Annu Rev Immunol* 2010; **28:** 131-155.

14. Rawal N, Pangburn MK. Structure/function of C5 convertases of complement. *Int Immunopharmacol* 2001; **1:** 415-422.

15. Hong K, Kinoshita T, Pramoonjago P*, et al.* Reconstitution of C5 convertase of the alternative complement pathway with isolated C3b dimer and factors B and D. *J Immunol* 1991; **146:** 1868-1873.

16. Muller-Eberhard HJ. The killer molecule of complement. *J Invest Dermatol* 1985; **85:** 47s-52s.

17. Ehrnthaller C, Ignatius A, Gebhard F*, et al.* New insights of an old defense system: structure, function, and clinical relevance of the complement system. *Mol Med* 2011; **17:** 317-329.

18. Sahu A, Lambris JD. Structure and biology of complement protein C3, a connecting link between innate and acquired immunity. *Immunol Rev* 2001; **180:** 35-48.

19. Gros P, Milder FJ, Janssen BJ. Complement driven by conformational changes. *Nat Rev Immunol* 2008; **8:** 48-58.

20. Janssen BJ, Huizinga EG, Raaijmakers HC*, et al.* Structures of complement component C3 provide insights into the function and evolution of immunity. *Nature* 2005; **437:** 505-511.

21. Janssen BJ, Christodoulidou A, McCarthy A*, et al.* Structure of C3b reveals conformational changes that underlie complement activity. *Nature* 2006; **444:** 213-216.

22. Pangburn MK, Schreiber RD, Muller-Eberhard HJ. Formation of the initial C3 convertase of the alternative complement pathway. Acquisition of C3b-like activities by spontaneous hydrolysis of the putative thioester in native C3. *J Exp Med* 1981; **154:** 856-867.

23. Oglesby TJ, Ueda A, Volanakis JE. Radioassays for quantitation of intact complement proteins C2 and B in human serum. *J Immunol Methods* 1988; **110:** 55-62.

24. Milder FJ, Gomes L, Schouten A*, et al.* Factor B structure provides insights into activation of the central protease of the complement system. *Nat Struct Mol Biol* 2007; **14:** 224-228.

25. Pryzdial EL, Isenman DE. Alternative complement pathway activation fragment Ba binds to C3b. Evidence that formation of the factor B-C3b complex involves two discrete points of contact. *J Biol Chem* 1987; **262:** 1519-1525.

26. Tuckwell DS, Xu Y, Newham P*, et al.* Surface loops adjacent to the cation-binding site of the complement factor B von Willebrand factor type A module determine C3b binding specificity. *Biochemistry* 1997; **36:** 6605-6613.

27. Pangburn MK, Muller-Eberhard HJ. The C3 convertase of the alternative pathway of human complement. Enzymic properties of the bimolecular proteinase. *Biochem J* 1986; **235:** 723-730.

28. Ponnuraj K, Xu Y, Macon K*, et al.* Structural analysis of engineered Bb fragment of complement factor B: insights into the activation mechanism of the alternative pathway C3-convertase. *Mol Cell* 2004; **14:** 17-28.

29. Hourcade DE, Mitchell L, Kuttner-Kondo LA*, et al.* Decay-accelerating factor (DAF), complement receptor 1 (CR1), and factor H dissociate the complement

AP C3 convertase (C3bBb) via sites on the type A domain of Bb. *J Biol Chem* 2002; **277:** 1107-1112.

30. Hourcade DE, Mitchell LM, Oglesby TJ. Mutations of the type A domain of complement factor B that promote high-affinity C3b-binding. *J Immunol* 1999; **162:** 2906-2911.

31. Rodriguez de Cordoba S, Diaz-Guillen MA, Heine-Suner D. An integrated map of the human regulator of complement activation (RCA) gene cluster on 1q32. *Mol Immunol* 1999; **36:** 803-808.

32. Rodriguez de Cordoba S, Lublin DM, Rubinstein P*, et al.* Human genes for three complement components that regulate the activation of C3 are tightly linked. *J Exp Med* 1985; **161:** 1189-1195.

33. Davis AE, 3rd, Lu F, Mejia P. C1 inhibitor, a multi-functional serine protease inhibitor. *Thromb Haemost* 2010; **104:** 886-893.

34. Lachmann PJ. The control of homologous lysis. *Immunol Today* 1991; **12:** 312-315.

35. Barlow PN, Baron M, Norman DG*, et al.* Secondary structure of a complement control protein module by two-dimensional 1H NMR. *Biochemistry* 1991; **30:** 997-1004.

36. Campbell RD, Law SK, Reid KB*, et al.* Structure, organization, and regulation of the complement genes. *Annu Rev Immunol* 1988; **6:** 161-195.

37. Fishelson Z, Pangburn MK, Muller-Eberhard HJ. Characterization of the initial C3 convertase of the alternative pathway of human complement. *J Immunol* 1984; **132:** 1430-1434.

38. Kerr MA. The human complement system: assembly of the classical pathway C3 convertase. *Biochem J* 1980; **189:** 173-181.

39. Lublin DM, Atkinson JP. Decay-accelerating factor: biochemistry, molecular biology, and function. *Annu Rev Immunol* 1989; **7:** 35-58.

40. Ahearn JM, Fearon DT. Structure and function of the complement receptors, CR1 (CD35) and CR2 (CD21). *Adv Immunol* 1989; **46:** 183-219.

41. Weiler JM, Daha MR, Austen KF*, et al.* Control of the amplification convertase of complement by the plasma protein beta1H. *Proc Natl Acad Sci U S A* 1976; **73:** 3268-3272.

42. Kirkitadze MD, Krych M, Uhrin D*, et al.* Independently melting modules and highly structured intermodular junctions within complement receptor type 1. *Biochemistry* 1999; **38:** 7019-7031.

43. Brodbeck WG, Liu D, Sperry J*, et al.* Localization of classical and alternative pathway regulatory activity within the decay-accelerating factor. *J Immunol* 1996; **156:** 2528-2533.

44. Harris CL, Abbott RJ, Smith RA*, et al.* Molecular dissection of interactions between components of the alternative pathway of complement and decay accelerating factor (CD55). *J Biol Chem* 2005; **280:** 2569-2578.

45. Roversi P, Johnson S, Caesar JJ*, et al.* Structural basis for complement factor I control and its disease-associated sequence polymorphisms. *Proc Natl Acad Sci U S A* 2011; **108:** 12839-12844.

46. Nilsson SC, Sim RB, Lea SM*, et al.* Complement factor I in health and disease. *Mol Immunol* 2011; **48:** 1611-1620.

47. Wagner E, Frank MM. Therapeutic potential of complement modulation. *Nat Rev Drug Discov* 2010; **9:** 43-56.

48. Ripoche J, Day AJ, Harris TJ*, et al.* The complete amino acid sequence of human complement factor H. *Biochem J* 1988; **249:** 593-602.

49. Ferreira VP, Pangburn MK, Cortes C. Complement control protein factor H: the good, the bad, and the inadequate. *Mol Immunol* 2010; **47:** 2187-2197.

50. Esparza-Gordillo J, Soria JM, Buil A*, et al.* Genetic and environmental factors influencing the human factor H plasma levels. *Immunogenetics* 2004; **56:** 77-82.

51. Whaley K, Ruddy S. Modulation of C3b hemolytic activity by a plasma protein distinct from C3b inactivator. *Science* 1976; **193:** 1011-1013.

52. Pangburn MK, Schreiber RD, Muller-Eberhard HJ. Human complement C3b inactivator: isolation, characterization, and demonstration of an absolute requirement for the serum protein beta1H for cleavage of C3b and C4b in solution. *J Exp Med* 1977; **146:** 257-270.

53. Pangburn MK, Muller-Eberhard HJ. Complement C3 convertase: cell surface restriction of beta1H control and generation of restriction on neuraminidase-treated cells. *Proc Natl Acad Sci U S A* 1978; **75:** 2416-2420.

54. Fearon DT. Regulation by membrane sialic acid of beta1H-dependent decay-dissociation of amplification C3 convertase of the alternative complement pathway. *Proc Natl Acad Sci U S A* 1978; **75:** 1971-1975.

55. Kazatchkine MD, Fearon DT, Austen KF. Human alternative complement pathway: membrane-associated sialic acid regulates the competition between B and beta1 H for cell-bound C3b. *J Immunol* 1979; **122:** 75-81.

56. Pangburn MK, Schreiber RD, Muller-Eberhard HJ. C3b deposition during activation of the alternative complement pathway and the effect of deposition on the activating surface. *J Immunol* 1983; **131:** 1930-1935.

57. Pangburn MK, Atkinson MA, Meri S. Localization of the heparin-binding site on complement factor H. *J Biol Chem* 1991; **266:** 16847-16853.

58. Gordon DL, Kaufman RM, Blackmore TK*, et al.* Identification of complement regulatory domains in human factor H. *J Immunol* 1995; **155:** 348-356.

59. Blackmore TK, Sadlon TA, Ward HM*, et al.* Identification of a heparin binding domain in the seventh short consensus repeat of complement factor H. *J Immunol* 1996; **157:** 5422-5427.

60. Kuhn S, Zipfel PF. Mapping of the domains required for decay acceleration activity of the human factor H-like protein 1 and factor H. *Eur J Immunol* 1996; **26:** 2383-2387.

61. Sharma AK, Pangburn MK. Identification of three physically and functionally distinct binding sites for C3b in human complement factor H by deletion mutagenesis. *Proc Natl Acad Sci U S A* 1996; **93:** 10996-11001.

62. Blackmore TK, Hellwage J, Sadlon TA*, et al.* Identification of the second heparin-binding domain in human complement factor H. *J Immunol* 1998; **160:** 3342-3348.

63. Jokiranta TS, Hellwage J, Koistinen V*, et al.* Each of the three binding sites on complement factor H interacts with a distinct site on C3b. *J Biol Chem* 2000; **275:** 27657-27662.

64. Ferreira VP, Herbert AP, Hocking HG*, et al.* Critical role of the C-terminal domains of factor H in regulating complement activation at cell surfaces. *J Immunol* 2006; **177:** 6308-6316.

65. Schmidt CQ, Herbert AP, Kavanagh D*, et al.* A new map of glycosaminoglycan and C3b binding sites on factor H. *J Immunol* 2008; **181:** 2610-2619.

66. Schmidt CQ, Herbert AP, Hocking HG*, et al.* Translational mini-review series on complement factor H: structural and functional correlations for factor H. *Clin Exp Immunol* 2008; **151:** 14-24.

67. Schmidt CQ, Herbert AP, Mertens HD*, et al.* The central portion of factor H (modules 10-15) is compact and contains a structurally deviant CCP module. *J Mol Biol* 2010; **395:** 105-122.

68. Morgan HP, Schmidt CQ, Guariento M*, et al.* Structural basis for engagement by complement factor H of C3b on a self surface. *Nat Struct Mol Biol* 2011; **18:** 463-470.

69. Male DA, Ormsby RJ, Ranganathan S*, et al.* Complement factor H: sequence analysis of 221 kb of human genomic DNA containing the entire fH, fHR-1 and fHR-3 genes. *Mol Immunol* 2000; **37:** 41-52.

70. Rodriguez de Cordoba S, Esparza-Gordillo J, Goicoechea de Jorge E*, et al.* The human complement factor H: functional roles, genetic variations and disease associations. *Mol Immunol* 2004; **41:** 355-367.

71. Estaller C, Schwaeble W, Dierich M*, et al.* Human complement factor H: two factor H proteins are derived from alternatively spliced transcripts. *Eur J Immunol* 1991; **21:** 799-802.

72. Kuhn S, Skerka C, Zipfel PF. Mapping of the complement regulatory domains in the human factor H-like protein 1 and in factor H1. *J Immunol* 1995; **155:** 5663-5670.

73. Zipfel PF, Skerka C. FHL-1/reconectin: a human complement and immune regulator with cell-adhesive function. *Immunol Today* 1999; **20:** 135-140.

74. Friese MA, Hellwage J, Jokiranta TS*, et al.* FHL-1/reconectin and factor H: two human complement regulators which are encoded by the same gene are differently expressed and regulated. *Mol Immunol* 1999; **36:** 809-818.

75. Zipfel PF, Skerka C. Complement factor H and related proteins: an expanding family of complement-regulatory proteins? *Immunol Today* 1994; **15:** 121-126.

76. Zipfel PF, Jokiranta TS, Hellwage J*, et al.* The factor H protein family. *Immunopharmacology* 1999; **42:** 53-60.

77. Perez-Caballero D, Gonzalez-Rubio C, Gallardo ME*, et al.* Clustering of missense mutations in the C-terminal region of factor H in atypical hemolytic uremic syndrome. *Am J Hum Genet* 2001; **68:** 478-484.

78. Heinen S, Sanchez-Corral P, Jackson MS*, et al.* De novo gene conversion in the RCA gene cluster (1q32) causes mutations in complement factor H associated with atypical hemolytic uremic syndrome. *Hum Mutat* 2006; **27:** 292-293.

79. Skerka C, Zipfel PF. Complement factor H related proteins in immune diseases. *Vaccine* 2008; **26 Suppl 8:** I9-14.

80. Jozsi M, Zipfel PF. Factor H family proteins and human diseases. *Trends Immunol* 2008; **29:** 380-387.

81. Fritsche LG, Lauer N, Hartmann A*, et al.* An imbalance of human complement regulatory proteins CFHR1, CFHR3 and factor H influences risk for age-related macular degeneration (AMD). *Hum Mol Genet* 2010; **19:** 4694-4704.

82. McRae JL, Duthy TG, Griggs KM*, et al.* Human factor H-related protein 5 has cofactor activity, inhibits C3 convertase activity, binds heparin and C-reactive protein, and associates with lipoprotein. *J Immunol* 2005; **174:** 6250-6256.

83. Heinen S, Hartmann A, Lauer N*, et al.* Factor H-related protein 1 (CFHR-1) inhibits complement C5 convertase activity and terminal complex formation. *Blood* 2009; **114:** 2439-2447.

84. Noris M, Remuzzi G. Atypical hemolytic-uremic syndrome. *N Engl J Med* 2009; **361:** 1676-1687.

85. Ruggenenti P, Noris M, Remuzzi G. Thrombotic microangiopathy, hemolytic uremic syndrome, and thrombotic thrombocytopenic purpura. *Kidney Int* 2001; **60:** 831-846.

86. Moxley RA. Escherichia coli 0157:H7: an update on intestinal colonization and virulence mechanisms. *Anim Health Res Rev* 2004; **5:** 15-33.

87. Noris M, Remuzzi G. Hemolytic uremic syndrome. *J Am Soc Nephrol* 2005; **16:** 1035-1050.

88. Delvaeye M, Noris M, De Vriese A*, et al.* Thrombomodulin mutations in atypical hemolytic-uremic syndrome. *N Engl J Med* 2009; **361:** 345-357.

89. Caprioli J, Noris M, Brioschi S*, et al.* Genetics of HUS: the impact of MCP, CFH, and IF mutations on clinical presentation, response to treatment, and outcome. *Blood* 2006; **108:** 1267-1279.

90. Goicoechea de Jorge E, Harris CL, Esparza-Gordillo J*, et al.* Gain-of-function mutations in complement factor B are associated with atypical hemolytic uremic syndrome. *Proc Natl Acad Sci U S A* 2007; **104:** 240-245.

91. Fremeaux-Bacchi V, Miller EC, Liszewski MK*, et al.* Mutations in complement C3 predispose to development of atypical hemolytic uremic syndrome. *Blood* 2008; **112:** 4948-4952.

92. de Cordoba SR, de Jorge EG. Translational mini-review series on complement factor H: genetics and disease associations of human complement factor H. *Clin Exp Immunol* 2008; **151:** 1-13.

93. Dragon-Durey MA, Loirat C, Cloarec S*, et al.* Anti-Factor H autoantibodies associated with atypical hemolytic uremic syndrome. *J Am Soc Nephrol* 2005; **16:** 555-563.

94. Jozsi M, Strobel S, Dahse HM*, et al.* Anti factor H autoantibodies block C-terminal recognition function of factor H in hemolytic uremic syndrome. *Blood* 2007; **110:** 1516-1518.

95. Pickering MC, de Jorge EG, Martinez-Barricarte R*, et al.* Spontaneous hemolytic uremic syndrome triggered by complement factor H lacking surface recognition domains. *J Exp Med* 2007; **204:** 1249-1256.

96. Alchi B, Jayne D. Membranoproliferative glomerulonephritis. *Pediatr Nephrol* 2010; **25:** 1409-1418.

97. Fakhouri F, Fremeaux-Bacchi V, Noel LH*, et al.* C3 glomerulopathy: a new classification. *Nat Rev Nephrol* 2010; **6:** 494-499.

98. Sethi S, Gamez JD, Vrana JA*, et al.* Glomeruli of Dense Deposit Disease contain components of the alternative and terminal complement pathway. *Kidney Int* 2009; **75:** 952-960.

99. Appel GB, Cook HT, Hageman G*, et al.* Membranoproliferative glomerulonephritis type II (dense deposit disease): an update. *J Am Soc Nephrol* 2005; **16:** 1392-1403.

100. Hogasen K, Jansen JH, Mollnes TE*, et al.* Hereditary porcine membranoproliferative glomerulonephritis type II is caused by factor H deficiency. *J Clin Invest* 1995; **95:** 1054-1061.

101. Pickering MC, Cook HT, Warren J*, et al.* Uncontrolled C3 activation causes membranoproliferative glomerulonephritis in mice deficient in complement factor H. *Nat Genet* 2002; **31:** 424-428.

102. Pickering MC, Warren J, Rose KL*, et al.* Prevention of C5 activation ameliorates spontaneous and experimental glomerulonephritis in factor H-deficient mice. *Proc Natl Acad Sci U S A* 2006; **103:** 9649-9654.

103. Rose KL, Paixao-Cavalcante D, Fish J*, et al.* Factor I is required for the development of membranoproliferative glomerulonephritis in factor H-deficient mice. *J Clin Invest* 2008; **118:** 608-618.

104. Hageman GS, Gehrs K, Johnson LV*, et al.* Age-Related Macular Degeneration (AMD). 1995.

105. Hageman GS, Mullins RF. Molecular composition of drusen as related to substructural phenotype. *Mol Vis* 1999; **5:** 28.

106. de Jong PT. Age-related macular degeneration. *N Engl J Med* 2006; **355:** 1474-1485.

107. Scholl HP, Fleckenstein M, Charbel Issa P*, et al.* An update on the genetics of age-related macular degeneration. *Mol Vis* 2007; **13:** 196-205.

108. Francis PJ, Klein ML. Update on the role of genetics in the onset of age-related macular degeneration. *Clin Ophthalmol* 2011; **5:** 1127-1133.

109. Hageman GS, Anderson DH, Johnson LV*, et al.* A common haplotype in the complement regulatory gene factor H (HF1/CFH) predisposes individuals to age-related macular degeneration. *Proc Natl Acad Sci U S A* 2005; **102:** 7227-7232.

110. Edwards AO, Ritter R, 3rd, Abel KJ*, et al.* Complement factor H polymorphism and age-related macular degeneration. *Science* 2005; **308:** 421-424.

111. Klein RJ, Zeiss C, Chew EY*, et al.* Complement factor H polymorphism in age-related macular degeneration. *Science* 2005; **308:** 385-389.

112. Haines JL, Hauser MA, Schmidt S*, et al.* Complement factor H variant increases the risk of age-related macular degeneration. *Science* 2005; **308:** 419-421.

113. Lhotta K, Janecke AR, Scheiring J*, et al.* A large family with a gain-of-function mutation of complement C3 predisposing to atypical hemolytic uremic syndrome, microhematuria, hypertension and chronic renal failure. *Clin J Am Soc Nephrol* 2009; **4:** 1356-1362.

114. Martinez-Barricarte R, Heurich M, Valdes-Canedo F*, et al.* Human C3 mutation reveals a mechanism of dense deposit disease pathogenesis and provides insights into complement activation and regulation. *J Clin Invest* 2010; **120:** 3702-3712.

115. Strobel S, Zimmering M, Papp K*, et al.* Anti-factor B autoantibody in dense deposit disease. *Mol Immunol* 2010; **47:** 1476-1483.

116. Meri S, Koistinen V, Miettinen A*, et al.* Activation of the alternative pathway of complement by monoclonal lambda light chains in membranoproliferative glomerulonephritis. *J Exp Med* 1992; **175:** 939-950.

117. Montes T, Goicoechea de Jorge E, Ramos R*, et al.* Genetic deficiency of complement factor H in a patient with age-related macular degeneration and membranoproliferative glomerulonephritis. *Mol Immunol* 2008; **45:** 2897-2904.

118. Goodship TH. Factor H genotype-phenotype correlations: lessons from aHUS, MPGN II, and AMD. *Kidney Int* 2006; **70:** 12-13.

119. Ault BH, Schmidt BZ, Fowler NL*, et al.* Human factor H deficiency. Mutations in framework cysteine residues and block in H protein secretion and intracellular catabolism. *J Biol Chem* 1997; **272:** 25168-25175.

120. Schmidt BZ, Fowler NL, Hidvegi T*, et al.* Disruption of disulfide bonds is responsible for impaired secretion in human complement factor H deficiency. *J Biol Chem* 1999; **274:** 11782-11788.

121. Dragon-Durey MA, Fremeaux-Bacchi V, Loirat C*, et al.* Heterozygous and homozygous factor h deficiencies associated with hemolytic uremic syndrome or membranoproliferative glomerulonephritis: report and genetic analysis of 16 cases. *J Am Soc Nephrol* 2004; **15:** 787-795.

122. Licht C, Heinen S, Jozsi M*, et al.* Deletion of Lys224 in regulatory domain 4 of Factor H reveals a novel pathomechanism for dense deposit disease (MPGN II). *Kidney Int* 2006; **70:** 42-50.

123. Lopez Trascasa M. Deficiencias del complemento. Diagnóstico de laboratorio. Presentación del Registro Español de deficiencias del complemento. *Inmunología* 2000; **19:** 41-48.

124. Venables JP, Strain L, Routledge D*, et al.* Atypical haemolytic uraemic syndrome associated with a hybrid complement gene. *PLoS Med* 2006; **3:** e431.

125. Jokiranta TS, Cheng ZZ, Seeberger H*, et al.* Binding of complement factor H to endothelial cells is mediated by the carboxy-terminal glycosaminoglycan binding site. *Am J Pathol* 2005; **167:** 1173-1181.

126. Sanchez-Corral P, Perez-Caballero D, Huarte O*, et al.* Structural and functional characterization of factor H mutations associated with atypical hemolytic uremic syndrome. *Am J Hum Genet* 2002; **71:** 1285-1295.

127. Manuelian T, Hellwage J, Meri S*, et al.* Mutations in factor H reduce binding affinity to C3b and heparin and surface attachment to endothelial cells in hemolytic uremic syndrome. *J Clin Invest* 2003; **111:** 1181-1190.

128. Jelezarova E, Schlumberger M, Sadallah S*, et al.* A C3 convertase assay for nephritic factor functional activity. *J Immunol Methods* 2001; **251:** 45-52.

129. Caprioli J, Castelletti F, Bucchioni S*, et al.* Complement factor H mutations and gene polymorphisms in haemolytic uraemic syndrome: the C-257T, the A2089G and the G2881T polymorphisms are strongly associated with the disease. *Hum Mol Genet* 2003; **12:** 3385-3395.

130. Esparza-Gordillo J, Goicoechea de Jorge E, Buil A*, et al.* Predisposition to atypical hemolytic uremic syndrome involves the concurrence of different susceptibility alleles in the regulators of complement activation gene cluster in 1q32. *Hum Mol Genet* 2005; **14:** 703-712.

131. Esparza-Gordillo J, Jorge EG, Garrido CA*, et al.* Insights into hemolytic uremic syndrome: segregation of three independent predisposition factors in a large, multiple affected pedigree. *Mol Immunol* 2006; **43:** 1769-1775.

132. Provaznikova D, Rittich S, Malina M*, et al.* Manifestation of atypical hemolytic uremic syndrome caused by novel mutations in MCP. *Pediatr Nephrol* 2012; **27:** 73-81.

133. Abrera-Abeleda MA, Nishimura C, Frees K*, et al.* Allelic variants of complement genes associated with dense deposit disease. *J Am Soc Nephrol* 2011; **22:** 1551-1559.

134. Skerka C, Lauer N, Weinberger AA*, et al.* Defective complement control of factor H (Y402H) and FHL-1 in age-related macular degeneration. *Mol Immunol* 2007; **44:** 3398-3406.

135. Hocking HG, Herbert AP, Kavanagh D*, et al.* Structure of the N-terminal region of complement factor H and conformational implications of disease-linked sequence variations. *J Biol Chem* 2008; **283:** 9475-9487.

136. Kuttner-Kondo L MN, Crabb JW, Hollyfield JG, Medof ME. Effects on factor H function of polymorphisms linked to age-related macular degeneration. *Mol Immunol* 2007; **44:** 201.

137. Abarrategui-Garrido C, Martinez-Barricarte R, Lopez-Trascasa M*, et al.* Characterization of complement factor H-related (CFHR) proteins in plasma reveals novel genetic variations of CFHR1 associated with atypical hemolytic uremic syndrome. *Blood* 2009; **114:** 4261-4271.

138. Hughes AE, Orr N, Esfandiary H*, et al.* A common CFH haplotype, with deletion of CFHR1 and CFHR3, is associated with lower risk of age-related macular degeneration. *Nat Genet* 2006; **38:** 1173-1177.

139. Hageman GS, Hancox LS, Taiber AJ*, et al.* Extended haplotypes in the complement factor H (CFH) and CFH-related (CFHR) family of genes protect against age-related macular degeneration: characterization, ethnic distribution and evolutionary implications. *Ann Med* 2006; **38:** 592-604.

140. Zipfel PF, Edey M, Heinen S*, et al.* Deletion of complement factor H-related genes CFHR1 and CFHR3 is associated with atypical hemolytic uremic syndrome. *PLoS Genet* 2007; **3:** e41.

141. Jozsi M, Licht C, Strobel S*, et al.* Factor H autoantibodies in atypical hemolytic uremic syndrome correlate with CFHR1/CFHR3 deficiency. *Blood* 2008; **111:** 1512-1514.

142. Gold B, Merriam JE, Zernant J*, et al.* Variation in factor B (BF) and complement component 2 (C2) genes is associated with age-related macular degeneration. *Nat Genet* 2006; **38:** 458-462.

143. Spencer KL, Hauser MA, Olson LM*, et al.* Protective effect of complement factor B and complement component 2 variants in age-related macular degeneration. *Hum Mol Genet* 2007; **16:** 1986-1992.

144. Davrinche C, Abbal M, Clerc A. Molecular characterization of human complement factor B subtypes. *Immunogenetics* 1990; **32:** 309-312.

145. Hagglof B, Holmgren G, Holmlund G*, et al.* Studies of HLA, factor B (Bf), complement C2 and C4 haplotypes in type 1 diabetic and control families from northern Sweden. *Hum Hered* 1986; **36:** 201-212.

146. Papiha SS, Duggan-Keen M, Roberts DF. Factor B (BF) allotypes and multiple sclerosis in north-east England. *Hum Hered* 1991; **41:** 397-402.

147. Messias-Reason IJ, Urbanetz L, Pereira da Cunha C. Complement C3 F and BF S allotypes are risk factors for Chagas disease cardiomyopathy. *Tissue Antigens* 2003; **62:** 308-312.

148. Lokki ML, Koskimies SA. Allelic differences in hemolytic activity and protein concentration of BF molecules are found in association with particular HLA haplotypes. *Immunogenetics* 1991; **34:** 242-246.

149. Hourcade DE, Wagner LM, Oglesby TJ. Analysis of the short consensus repeats of human complement factor B by site-directed mutagenesis. *J Biol Chem* 1995; **270:** 19716-19722.

150. Yates JR, Sepp T, Matharu BK*, et al.* Complement C3 variant and the risk of age-related macular degeneration. *N Engl J Med* 2007; **357:** 553-561.

151. Botto M, Fong KY, So AK*, et al.* Molecular basis of polymorphisms of human complement component C3. *J Exp Med* 1990; **172:** 1011-1017.

152. Rambausek M, van den Wall Bake AW, Schumacher-Ach R*, et al.* Genetic polymorphism of C3 and Bf in IgA nephropathy. *Nephrol Dial Transplant* 1987; **2:** 208-211.

153. Finn JE, Mathieson PW. Molecular analysis of C3 allotypes in patients with nephritic factor. *Clin Exp Immunol* 1993; **91:** 410-414.

154. Abdul Ajees A, Gunasekaran K, Volanakis JE*, et al.* The structure of complement C3b provides insights into complement activation and regulation. *Nature* 2006; **444:** 221-225.

155. Wu J, Wu YQ, Ricklin D*, et al.* Structure of complement fragment C3b-factor H and implications for host protection by complement regulators. *Nat Immunol* 2009; **10:** 728-733.

156. Forneris F, Ricklin D, Wu J*, et al.* Structures of C3b in complex with factors B and D give insight into complement convertase formation. *Science* 2010; **330:** 1816-1820.

157. Janssen BJ, Gomes L, Koning RI*, et al.* Insights into complement convertase formation based on the structure of the factor B-cobra venom factor complex. *EMBO J* 2009; **28:** 2469-2478.

158. Vogel CW, Muller-Eberhard HJ. The cobra venom factor-dependent C3 convertase of human complement. A kinetic and thermodynamic analysis of a protease acting on its natural high molecular weight substrate. *J Biol Chem* 1982; **257:** 8292-8299.

159. Rooijakkers SH, Wu J, Ruyken M*, et al.* Structural and functional implications of the alternative complement pathway C3 convertase stabilized by a staphylococcal inhibitor. *Nat Immunol* 2009; **10:** 721-727.

160. Rooijakkers SH, Ruyken M, Roos A*, et al.* Immune evasion by a staphylococcal complement inhibitor that acts on C3 convertases. *Nat Immunol* 2005; **6:** 920-927.

161. Roumenina LT, Jablonski M, Hue C*, et al.* Hyperfunctional C3 convertase leads to complement deposition on endothelial cells and contributes to atypical hemolytic uremic syndrome. *Blood* 2009; **114:** 2837-2845.

162. Taniguchi-Sidle A, Isenman DE. Interactions of human complement component C3 with factor B and with complement receptors type 1 (CR1, CD35) and type 3 (CR3, CD11b/CD18) involve an acidic sequence at the N-terminus of C3 alpha'-chain. *J Immunol* 1994; **153:** 5285-5302.

163. Alcorlo M, Martinez-Barricarte R, Fernandez FJ*, et al.* Unique structure of iC3b resolved at a resolution of 24 A by 3D-electron microscopy. *Proc Natl Acad Sci U S A* 2011; **108:** 13236-13240.

164. Ricklin D, Lambris JD. Complement-targeted therapeutics. *Nat Biotechnol* 2007; **25:** 1265-1275.

165. Schrezenmeier H, Hochsmann B. Drugs that inhibit complement. *Transfus Apher Sci* 2012; **46:** 87-92.

166. Alexion. http://www.alxn.com/SolirisAndPNH/AboutSoliris/Default.aspx.

167. Ricklin D, Lambris JD. Compstatin: a complement inhibitor on its way to clinical application. *Adv Exp Med Biol* 2008; **632:** 273-292.

168. Fridkis-Hareli M, Storek M, Mazsaroff I*, et al.* Design and development of TT30, a novel C3d-targeted C3/C5 convertase inhibitor for treatment of human complement alternative pathway-mediated diseases. *Blood* 2011; **118:** 4705-4713.

169. Katschke KJ, Wu P, Ganesan R*, et al.* Inhibiting alternative pathway complement activation by targeting the exosite of factor D. *J Biol Chem* 2012.

170. Rattner A, Nathans J. Macular degeneration: recent advances and therapeutic opportunities. *Nat Rev Neurosci* 2006; **7:** 860-872.

171. Mullins RF, Aptsiauri N, Hageman GS. Structure and composition of drusen associated with glomerulonephritis: implications for the role of complement activation in drusen biogenesis. *Eye (Lond)* 2001; **15:** 390-395.

172. Francis PJ, Schultz DW, Hamon S*, et al.* Haplotypes in the complement factor H (CFH) gene: associations with drusen and advanced age-related macular degeneration. *PLoS One* 2007; **2:** e1197.

173. Thornton J, Edwards R, Mitchell P*, et al.* Smoking and age-related macular degeneration: a review of association. *Eye (Lond)* 2005; **19:** 935-944.

174. Schmidt S, Hauser MA, Scott WK*, et al.* Cigarette smoking strongly modifies the association of LOC387715 and age-related macular degeneration. *Am J Hum Genet* 2006; **78:** 852-864.

175. Delcourt C, Delyfer MN, Rougier MB*, et al.* Associations of complement factor H and smoking with early age-related macular degeneration: the ALIENOR study. *Invest Ophthalmol Vis Sci* 2011; **52:** 5955-5962.

176. Klein ML, Francis PJ, Rosner B*, et al.* CFH and LOC387715/ARMS2 genotypes and treatment with antioxidants and zinc for age-related macular degeneration. *Ophthalmology* 2008; **115:** 1019-1025.

177. Brown MM, Brown GC, Sharma S*, et al.* The burden of age-related macular degeneration: a value-based analysis. *Curr Opin Ophthalmol* 2006; **17:** 257-266.

178. Martinez-Barricarte R, Recalde S, Fernandez-Robredo P*, et al.* Relevance of Complement Factor H-Related 1 (CFHR1) Genotypes in Age-Related Macular Degeneration. *Invest Ophthalmol Vis Sci* 2012; **53:** 1087-1094.

179. Ault BH. Factor H and the pathogenesis of renal diseases. *Pediatr Nephrol* 2000; **14:** 1045-1053.

180. Caprioli J, Bettinaglio P, Zipfel PF*, et al.* The molecular basis of familial hemolytic uremic syndrome: mutation analysis of factor H gene reveals a hot spot in short consensus repeat 20. *J Am Soc Nephrol* 2001; **12:** 297-307.

181. Neumann HP, Salzmann M, Bohnert-Iwan B*, et al.* Haemolytic uraemic syndrome and mutations of the factor H gene: a registry-based study of German speaking countries. *J Med Genet* 2003; **40:** 676-681.

182. Martinez-Barricarte R, Pianetti G, Gautard R*, et al.* The complement factor H R1210C mutation is associated with atypical hemolytic uremic syndrome. *J Am Soc Nephrol* 2008; **19:** 639-646.

183. Johnson SA, Williams JM, Hakobyan S*, et al.* Impact of compound heterozygous complement factor H mutations on development of atypical hemolytic uremic syndrome-A pedigree revisited. *Mol Immunol* 2010; **47:** 1585-1591.

184. Zipfel PF, Heinen S, Jozsi M*, et al.* Complement and diseases: defective alternative pathway control results in kidney and eye diseases. *Mol Immunol* 2006; **43:** 97-106.

185. Holers VM. The spectrum of complement alternative pathway-mediated diseases. *Immunol Rev* 2008; **223:** 300-316.

186. Hughes AE, Mullan GM, Bradley DT. Complement factor B polymorphism 32W protects against age-related macular degeneration. *Mol Vis* 2011; **17:** 983-988.

187. Heurich M, Martinez-Barricarte R, Francis NJ*, et al.* Common polymorphisms in C3, factor B, and factor H collaborate to determine systemic complement activity and disease risk. *Proc Natl Acad Sci U S A* 2011; **108:** 8761-8766.

188. Scholl HP, Charbel Issa P, Walier M*, et al.* Systemic complement activation in age-related macular degeneration. *PLoS One* 2008; **3:** e2593.

189. Weismann D, Hartvigsen K, Lauer N, *et al.* Complement factor H binds malondialdehyde epitopes and protects from oxidative stress. *Nature* 2011; **478:** 76-81.

190. Fakhouri F, de Jorge EG, Brune F, *et al.* Treatment with human complement factor H rapidly reverses renal complement deposition in factor H-deficient mice. *Kidney Int* 2010; **78:** 279-286.

191. European Medicines Agency. http://www.ema.europa.eu/ema/index.jsp?curl=pages/medicines/human/orphans/2009/11/human_orphan_000075.jsp&mid=WC0b01ac058001d12b&jsenabled=true.

192. Schmidt CQ, Slingsby FC, Richards A, *et al.* Production of biologically active complement factor H in therapeutically useful quantities. *Protein Expr Purif* 2011; **76:** 254-263.

193. Noris M, Bucchioni S, Galbusera M, *et al.* Complement factor H mutation in familial thrombotic thrombocytopenic purpura with ADAMTS13 deficiency and renal involvement. *J Am Soc Nephrol* 2005; **16:** 1177-1183.

194. Maga TK, Nishimura CJ, Weaver AE, *et al.* Mutations in alternative pathway complement proteins in American patients with atypical hemolytic uremic syndrome. *Hum Mutat* 2010; **31:** E1445-1460.

195. Smith RJ, Harris CL, Pickering MC. Dense deposit disease. *Mol Immunol* 2011; **48:** 1604-1610.

196. Noris M, Remuzzi G. Translational mini-review series on complement factor H: therapies of renal diseases associated with complement factor H abnormalities: atypical haemolytic uraemic syndrome and membranoproliferative glomerulonephritis. *Clin Exp Immunol* 2008; **151:** 199-209.

197. Loirat C, Fremeaux-Bacchi V. Atypical hemolytic uremic syndrome. *Orphanet J Rare Dis* 2011; **6:** 60.

198. Saland JM, Ruggenenti P, Remuzzi G. Liver-kidney transplantation to cure atypical hemolytic uremic syndrome. *J Am Soc Nephrol* 2009; **20:** 940-949.

ANEXO

3D structure of the C3bB complex provides insights into the activation and regulation of the complement alternative pathway convertase

Eva Torreira[a,1], Agustín Tortajada[a,b,1], Tamara Montes[a,b,1], Santiago Rodríguez de Córdoba[a,b,2,3], and Oscar Llorca[a,2,3]

[a]Centro de Investigaciones Biológicas, Consejo Superior de Investigaciones Científicas; and [b]Centro de Investigación Biomédica en Enfermedades Raras and Instituto Reina Sofía de Investigaciones Nefrológicas, Ramiro de Maeztu 9, 28040 Madrid, Spain

Edited by Douglas T. Fearon, University of Cambridge, Cambridge, United Kingdom, and approved December 4, 2008 (received for review October 31, 2008)

Generation of the alternative pathway C3-convertase, the central amplification enzyme of the complement cascade, initiates by the binding of factor B (fB) to C3b to form the proconvertase, C3bB. C3bB is subsequently cleaved by factor D (fD) at a single site in fB, producing Ba and Bb fragments. Ba dissociates from the complex, while Bb remains bound to C3b, forming the active alternative pathway convertase, C3bBb. Using single-particle electron microscopy we have determined the 3-dimensional structures of the C3bB and the C3bBb complexes at ≈27Å resolution. The C3bB structure shows that fB undergoes a dramatic conformational change upon binding to C3b. However, the C3b-bound fB structure was easily interpreted after independently fitting the atomic structures of the isolated Bb and Ba fragments. Interestingly, the divalent cation-binding site in the von Willebrand type A domain in Bb faces the C345C domain of C3b, whereas the serine-protease domain of Bb points outwards. The structure also shows that the Ba fragment interacts with C3b separately from Bb at the level of the α′NT and CUB domains. Within this conformation, the long and flexible linker between Bb and Ba is likely exposed and accessible for cleavage by fD to form the active convertase, C3bBb. The architecture of the C3bB and C3bBb complexes reveals that C3b could promote cleavage and activation of fB by actively displacing the Ba domain from the von Willebrand type A domain in free fB. These structures provide a structural basis to understand fundamental aspects of the activation and regulation of the alternative pathway C3-convertase.

C3 convertase | electron microscopy | factor B

Complement is a major component of innate immunity, with crucial roles in microbial killing, apoptotic cell clearance, and immune complex handling. Complement activation can be initiated by three different pathways: the classical pathway (CP), the alternative pathway (AP), or the lectin pathway (LP). Common to each initiation pathway is the formation of unstable bimolecular complexes, named C3-convertases (AP, C3bBb; CP/LP, C4b2a), which cleave C3 to generate C3b. The AP C3-convertase, C3bBb, is crucial within the complement cascade, as it provides exponential amplification to the initial activating trigger. C3b molecules generated by either the CP/LP or the AP C3-convertases bind factor B (fB), thus forming more AP C3-convertases and providing rapid amplification (1).

To generate the AP C3-convertase, fB first associates with C3b in a Mg^{2+}-dependent manner, to form the proconvertase C3bB. In the presence of the serum protease factor D (fD), fB is cleaved and the N-terminal Ba fragment is released from the C3bB complex, creating the active AP C3-convertase (2).

Interaction sites in both C3b and fB have been delineated using different approaches. The α′NT and C345C domains in C3b include putative binding sites for fB required for C3 convertase formation (3–5). Both the α′NT and C345C domains are located in a part of the C3 molecule that undergoes large rearrangements upon activation of C3 into C3b, which explains why C3 does not interact with fB (6). Similarly, structural analyses have suggested that formation of the AP C3-convertase probably depends on the structure and orientation of the CUB domain of C3b and that the interaction between C3b and fB is independent of the TED domain (7).

Factor B is composed of 5 structural domains. Three short consensus repeats (SCRs) at the N terminus comprise the Ba fragment, whereas the large Bb fragment at the C terminus is comprised of a von Willebrand type A (vWA) domain followed by a serine-protease (SP) domain. Mutagenesis analyses of fB and functional characterization of rare mutations and common polymorphims associated with diseases involving complement dysregulation have suggested regions in the fB molecule that are crucial for the interaction with C3b (8–11). Thus, a number of fB residues near the Mg^{2+}-dependent metal ion-dependent adhesion site (MIDAS), including D279 (all amino acids are numbered to include the 25-aa long signal peptide), in the vWA domain have been shown to influence the initial recognition of C3b by fB and the stability of the AP C3-convertase C3bBb (8–11). Mutagenesis studies have shown that the fB vWA α1 helix also contributes to the C3b-binding region of the fB vWA domain, while the fB vWA α4/5 helix region is somewhat removed from the C3b-binding region and more likely is involved in the binding site recognized by the complement regulators decay accelerating factor (DAF) and complement receptor 1 (CR1) in C3bBb (12).

Formation of the C3bB complex also involves contact with the Ba domain (13). Using mutagenesis, antibody blocking and surface plasmon resonance methods, it has been shown that both the triad of SCR domains (14–16) and an 8-aa long unstructured fragment at the amino terminus of the Ba fragment (17) provide important binding sites for C3b.

The crystal structure of human fB, recently resolved at 2.3Å resolution, demonstrated that the Ba domain was not extended but folded back onto the Bb domain. SCR2 and SCR3 of Ba were packed tightly into an antiparallel dimer capped by SCR1 (6). These structural data also indicate that SCR1 probably hinders access of the ligand C3b to the MIDAS of the vWA domain, and that the triad of SCR domains is probably only weakly associated

Author contributions: E.T., A.T., T.M., S.R.d.C., and O.L. designed research; E.T., A.T., T.M., S.R.d.C., and O.L. performed research; E.T., A.T., T.M., S.R.d.C., and O.L. analyzed data; and S.R.d.C. and O.L. wrote the paper.

The authors declare no conflict of interest.

This article is a PNAS Direct Submission.

Data deposition: The EM map of the C3bB(Ni^{2+}) complex has been deposited in the 3D EM database, www.ebi.ac.uk/msd (accession code EMD-1583).

[1]E.T., A.T., and T.M. contributed equally to this work.

[2]S.R.d.C. and O.L. contributed equally to this work.

[3]To whom correspondence may be addressed. E-mail: ollorca@cib.csic.es or srdecordoba@cib.csic.es.

This article contains supporting information online at www.pnas.org/cgi/content/full/0810860106/DCSupplemental.

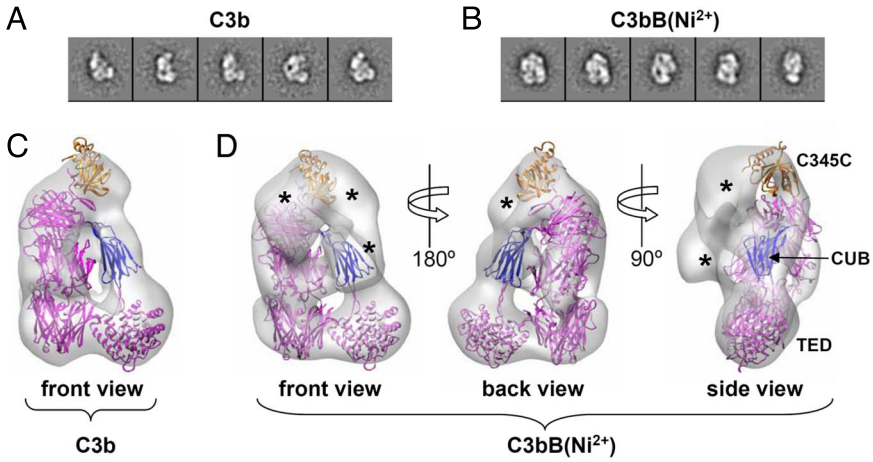

Fig. 1. Electron microscopy and 3D reconstruction of C3b and C3bB(Ni^{2+}). (*A*) Reference-free 2D averages obtained for the data set containing images of single molecules of C3b. These averages reveal a characteristic ''L'' shape evocative of the C3b crystal structure. (*B*) Reference-free 2D averages of C3bB(Ni^{2+}) display a bulky appearance compatible with fB binding to C3b. (*C*) Front view of the 3D structure of C3b derived from the EM data at a resolution of 28 Å (*gray density*). The atomic structure of C3b (PDB file 2i07) has been fitted within the EM map and displayed in purple with the C345C and CUB domains highlighted in orange and blue, respectively. (*D*) Several views of the 3D structure of C3bB(Ni^{2+}) at 27 Å resolution (*gray density*). Fitting of the atomic structure of C3b (PDB file 2i07) allows the assignment of specific regions of the EM map to specific C3b domains. Some densities of the 3D reconstruction cannot be accounted by C3b (*asterisks*) and correspond to C3b-bound fB.

with the vWA and SP domains. Most interestingly, comparison of the fB proenzyme (18) and the Bb fragment (19) structures suggests that fB undergoes conformational changes upon binding to C3b, displacing the helix αL from its binding groove in the vWA domain and exposing the long linker domain between the SCR3 and the vWA domains of fB that contains the scissile bond cleaved by fD (7, 18, 19).

Here, we sought to elucidate the structure of AP proconvertase C3bB. To this end we have generated stable C3bB complexes in the presence of Ni^{2+}, purified them, and determined their three-dimensional (3D) structure at ≈27 Å resolution using electron microscopy (EM). We also report structural analysis of the AP convertase C3bBb using the fB mutant D279G. These studies have revealed the architecture of the C3bB and C3bBb complexes, providing key insights into the initial stages of the AP C3-convertase formation, its activation by fD, and fundamental aspects of its regulation.

Results and Discussion

Electron Microscopy of C3b and C3bB(Ni^{2+}) Complexes Reveals that fB Binds Near the C345C Domain in C3b. The Ni^{2+} cation was used instead of Mg^{2+} to promote a stable C3bB(Ni^{2+}) complex that is otherwise undistinguishable from the physiological C3bB(Mg^{2+}) proconvertase (8, 20, 21). Briefly, purified C3b and fB were mixed at 1:2 molar excess of fB in the presence of 5-mM $NiCl_2$. Subsequently, the C3bB(Ni^{2+}) complex was purified by gel-filtration chromatography [supporting information (SI) Fig. S1; SI *Materials and Methods*] and fresh fractions containing C3bB(Ni^{2+}) were applied to carbon-coated EM grids and observed by EM after staining. Images from individual molecules were clearly detected in the EM fields (Fig. S2); these were extracted and reference-free two-dimensional (2D) averages were obtained using EMAN (22) and maximum likelihood analysis (23). Averages of C3b were clearly evocative of the typical structure of C3b (Fig. 1*A*), whereas those of the complex were clearly larger, indicating the presence of an additional component bound to C3b (Fig. 1*B*). C3bB(Ni^{2+}) averages revealed views of the complex with an abundance of distinct shapes (see Fig. 1*B*), indicating that it has likely bound to the support film in many different orientations, representing rotations along its longitudinal axis. This assumption was confirmed later when performing the 3D reconstruction of the complex (see below). By contrast, single C3b molecule averages complied with a predominant orientation, probably because of the flat nature of its structure (24, 25).

Images from single C3b molecules and the C3bB(Ni^{2+}) complex were processed using angular refinement methods to reconstruct their 3D structures. For each sample, we performed 2 independent experiments, using as initial template for refinement either a very low-resolution (> 60 Å) density map obtained after filtering the atomic structure of C3b, or a featureless Gaussian blob after adding noise. In both refinements, identical 3D solutions were obtained, compatible with the reference-free averages, indicating the absence of a significant bias from the initial reference (Fig. S3). During refinement, we detected that the data set for the C3bB(Ni^{2+}) complex covered views of the complex in many different orientations, whereas a more limited range of views was obtained for the free C3b molecule. Therefore, we collected additional data for C3b after tilting the specimen holder to complete the range of views (see *Methods* for details).

The 3D structure of C3b obtained by EM at a resolution of ≈28 Å is, within the limits of this resolution, virtually identical to the published crystal structures (24, 25) (Fig. 1*C*). These atomic coordinates can be unambiguously fitted using unbiased computational methods into our EM density, allowing a straightforward assignment of the different domains of the EM structure to specific domains of C3b. On the other hand, the C3bB(Ni^{2+}) complex at a similar resolution reveals significant additional mass located in the proximities of the C345C domain but contacting a broad area of C3b (Figs. 1*D* and 2*A*). The atomic structure of C3b was fitted within the EM structure of the C3bB(Ni^{2+}) complex by an exhaustive six-dimensional search looking for all its possible orientations with the EM map. C3b was readily located within the complex, given its very characteristic shape (see Fig. 1*D*).

Overall, these findings indicate that the C3bB(Ni^{2+}) complex presents a more globular shape than the single C3b molecule, which allows the complex to adopt different poses on the carbon-coated support film. Furthermore, the comparison between the 2D averages and the 3D structures of C3b and C3bB(Ni^{2+}) revealed that the 2 data sets were clearly distinct (see Fig. 1 *A* and *B*), confirming the homogeneity of both

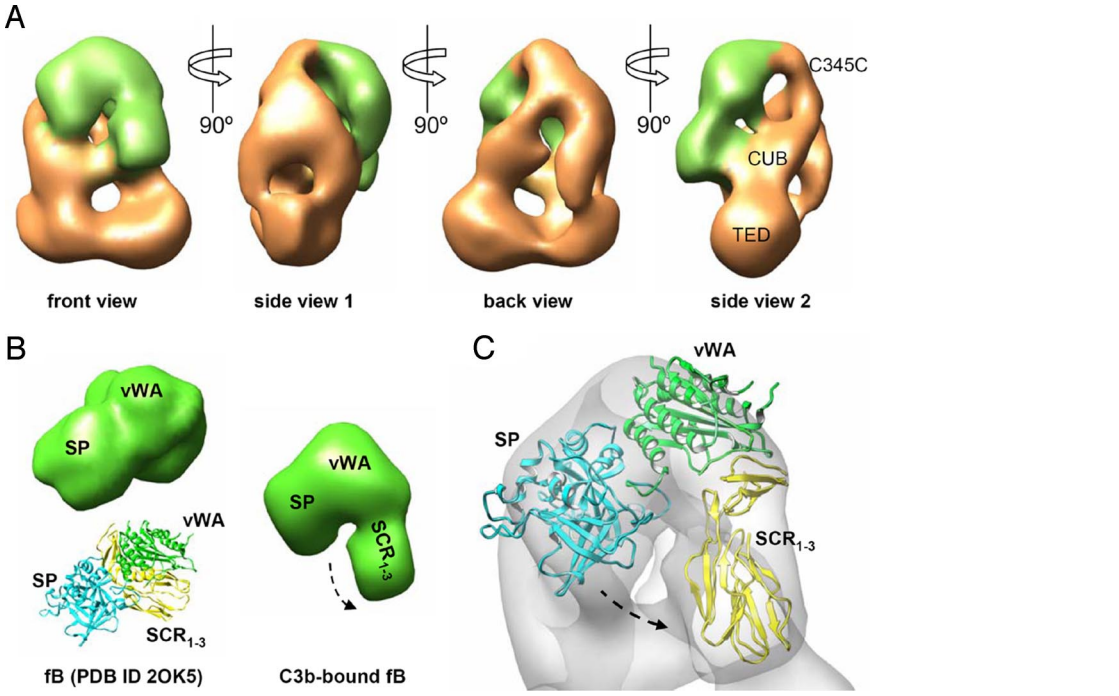

Fig. 2. Open conformation of fB within the C3bB(Ni^{2+}) complex.(*A*) Views of the 3D reconstruction of C3bB(Ni^{2+}). C3b in the complex has been colored in orange whereas fB is shown in green. (*B*) The structure of inactive fB (PDB file 2OK5) shows a compact conformation (*Left*). This structure was filtered to ≈25 Å resolution and was compared with the EM reconstruction (*Top Left*). C3b-bound fB was extracted by calculating the difference map between the EM density for C3bB(Ni^{2+}) and the fitted atomic structure of C3b (*Right*), and was found to display a more open conformation. SP, vWA, and SCR1–3 domains have been colored in pale blue, green, and yellow, respectively. (*C*) Fitting of the atomic structure of fB into the structure of C3bB(Ni^{2+}) complex. Factor B structure was divided in 2 segments corresponding to Bb and Ba fragments, and fitted separately within the density assigned to fB in the complex.

preparations and pinpointing the location of fB in the C3bB(Ni^{2+}) complex.

Open Conformation of fB Within the C3bB(Ni^{2+}) Complex. We comprehensively analyzed the conformation of fB after binding to C3b. The density of the fitted C3b was subtracted from that of the C3bB(Ni^{2+}) complex to determine the region of the map that accounts for fB (Fig. 2*A* and *B*). Factor B in complex with C3b revealed a well-defined V-shape density divided into a large and a small domain, notably distinct from the compact globular shape that represents the crystallized isolated fB when observed at a similar resolution (see Fig. 2*B*). Such differences indicate that fB undergoes substantial conformational changes when binding to C3b, as previously suggested (18).

To analyze further the conformation of fB within the C3bB(Ni^{2+}) complex, we performed several fitting experiments within the density assigned to fB. Because the crystal structure of full-length fB, recently solved at 2.3Å resolution (PDB file 2OK5), could not account for the observed density, we divided the fB structure into two halves, one containing the three SCRs (amino acid 26–220) and the other including the vWA and the SP domains (amino acid 253–764). The linker between SCR3 and vWA, including the αL helix, was removed from the analysis, as its conformation in our structure should be considerably different to that in the lock conformation of fB and we cannot model these changes at the resolution of our EM maps. When the atomic structure of the vWA-SP half was fitted within the whole density of fB in the C3bB(Ni^{2+}) complex using computational methods, vWA-SP was unambiguously located at the larger EM domain (cross-correlation coefficient 0.76) (Fig. 2*C*). In fact, this is the only region of the EM map with sufficient size to accommodate Bb and, as a consequence, the remaining small domain of the fB EM density must comprise the Ba fragment containing the N-terminal SCR1–3 domains (see Fig. 2*C*). Given the flat shape of the vWA-SP region in the C3bB(Ni^{2+}) complex, these 2 domains were found to fit the EM structure in only two possible orientations, placing the SP and vWA domains at either end of the large EM domain, respectively (Fig. S4). One of these two solutions was discarded because it placed the SCR1–3 domains in a location where connection to the vWA domain could not be achieved with the length of the linker between them. The atomic structure corresponding to this region of fB (Ba fragment) could only be fitted manually, placing its C terminus in the proximity of the vWA N terminus, to best accommodate to the EM density (see Fig. 2*C*). Therefore, the proposed orientation of the SCR1–3 triad represents an informed approximation.

Mechanistic Insights into the Assembly of the C3bB Proconvertase. The proposed arrangement for the C3bB(Ni^{2+}) complex illustrates key events during formation of the C3bB proenzyme. First, consistent with early biochemical data (13), the arrangement shows that the Ba and Bb fragments both interact with C3b (Figs. 2 and 3). Moreover, it reveals that the vWA domain interacts with C345C with the MIDAS facing toward C3b (see Fig. 3*A*), which is also in agreement with previous data, demonstrating that a number of fB residues near the MIDAS influence the initial recognition of C3b by fB and the stability of the AP C3-convertase (8–11). The putative C3b- and DAF-interacting sites in the vWA are also located within the C3bB structure as expected. Thus, the fB vWA α1 helix, shown by mutagenesis to contribute to the C3b-binding region of the fB vWA domain (12), faces the interface with C3b, whereas the vWA α4/5 helix, not implicated in the interaction and more likely involved in the binding site recognized by the complement regulators DAF and CR1, faces away from the complex (see Fig. 3*A*).

Most important is the distortion in conformation of fB bound to C3b in the C3bB(Ni^{2+}) complex, compared to that recently

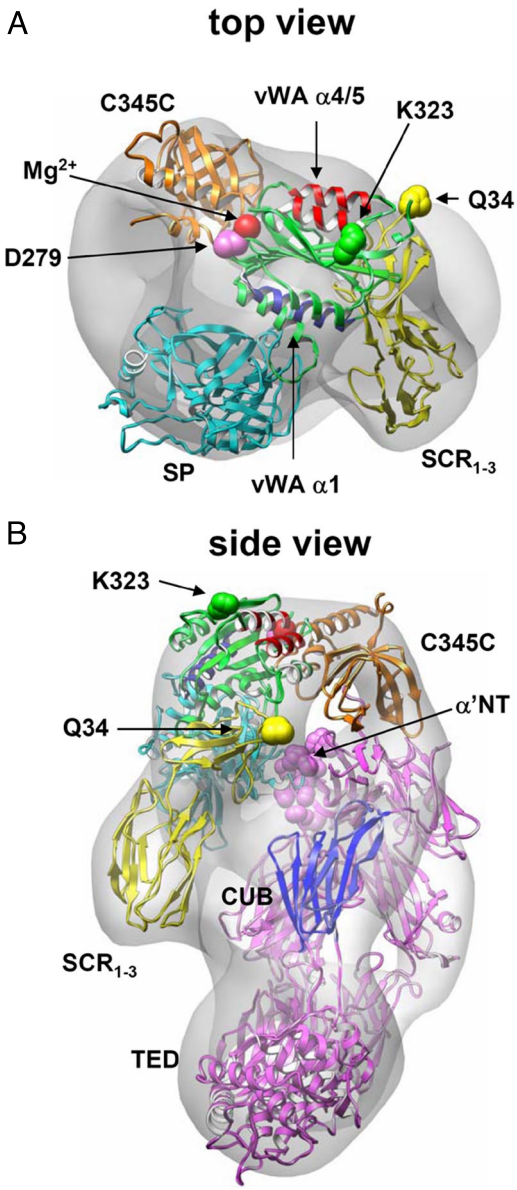

Fig. 3. Structural insights in the assembling of the proconvertase. (*A*) Representation of an atomic model for fB within the C3bB(Ni^{2+}) complex. For clarity only the C345C domain of C3b is represented. Color codes for domains as in Fig. 2. Specific residues have been highlighted, representing them as space-filled amino acids. These include D279 (known to affect proenzyme formation), K323 (known to affect regulation by DAF), and Q34 (to label the N terminus of the Ba fragment). The vWA α1 helix (contributing to the C3b-binding region) and vWA α4/5 helix (implicated in the DAF/CR1 binding site) are highlighted in blue and red ribbons, respectively. The N terminus of the C3b α' chain (α'NT) is depicted with space-filled amino acids. (*B*) A side view of the structural model of the C3bB(Ni^{2+}) complex where the atomic structure of C3b (PDB file 2i07) is also represented in purple color. Color codes as in Figs. 1 and 2.

reported for isolated fB (18). In the C3b-bound fB, the vWA-SP tandem is maintained as a unit, whereas the SCR1–3 region is displaced, likely interacting with the α'NT and CUB domains of C3b (see Fig. 3*B*). This C3b-bound fB conformation supports the proposed model for the activation of fB, which suggests that upon binding to C3b, the 3 SCRs of fB dislocate from the vWA and SP domains to allow access of the vWA domain to C3b (7, 18). The data also demonstrate contact points between the N-terminal region of Ba and the α'NT domain of C3b and between the Ba SCR2/3 and the CUB domain, in agreement with early mutagenesis, antibody blocking, and surface plasmon resonance experiments (14–17).

The proposed C3bB structure validates the hypothesis that the large conformational rearrangements of fB upon interaction with C3b expose the flexible linker between the vWA and SCR3 domains that contains the site cleaved by fD. This conformational change implies a major displacement of the SCR1–3 triad. Such a movement is certainly possible, given the long and flexible linker (residues 221–252) connecting SCR3 with the vWA domain, only some of which is evident in the electron density of the published atomic structure of factor B (18). This linker must be cleaved between residues 259 and 260 by fD to release the Ba fragment (26–259) to form the active convertase. Our model would place this cleavage point in the region connecting the 2 sides of the open conformation of fB in the C3bB complex. It is, therefore, quite exposed and potentially accessible to fD.

It has been hypothesized that dislocation of the SCRs from the vWA and SP domains may be coupled, through the short SCR3-αL connecting loop, to the displacement of helix αL from its binding groove in the vWA domain. This, in turn, may induce the vWA and SP domains to adopt a conformation more closely resembling that of the active Bb fragment (18). Therefore, we tested whether the atomic structure of the active Bb fragment, where the vWA domain is rotated with respect to the SP domain (18), fitted better into the fB EM density in our structure of the C3bB complex. However, while the atomic structure of the activated Bb fragment also adequately fitted the EM structure, the differences in cross-correlation coefficients between the two "Bb" fits were not sufficient to allow a computational discrimination between the models (data not shown).

Three-dimensional Structure of the Active C3bBb Complex. To support our model for the C3bB(Ni^{2+}) complex, we generated a stable, active C3bBb convertase. We used, in this case, the fB-D279G mutant because Ni^{2+} does not stabilize the active enzyme to the same extent as the proenzyme. The fB-D279G mutant promotes high-affinity C3b-binding and is correctly cleaved by fD in the C3bB proenzyme to generate a very stable, functionally-active, AP convertase C3bBb (8, 11, 12) (*SI Materials and Methods*). The $C3bBb_{279G}$ complex was purified by gel filtration (Fig. S5) and analyzed by EM in a similar way to the C3bB(Ni^{2+}) complex. Intriguingly, some 2D averages of C3bBb revealed lobes of density projecting out from the C3b structure; we later ascribed these to the C345C, vWA, and SP domains (Fig. 4*A*). Some of these 2D averages are very similar to the EM images of a AP convertase generated with fB-WT reported earlier by Smith *et al.* (26), suggesting that the SP domain projects out from the convertase.

Three-dimensional reconstruction analyses showed that the active convertase lacked the small domain of fB in the C3bB complex that we had ascribed to the Ba fragment (Fig. 4*B*), fully supporting our structural model. Interestingly, during the 3D refinement we observed that the density accounting for the SP domain was spread out along a range of possible conformations, reducing its average density in the 3D reconstruction (see Fig. 4*B*). Reference-free 2D averages of the EM data revealed that, whereas some averages show a defined 3-dot pattern (Fig. 4*C*, *i*), most side views of C3bBb demonstrated a well-defined C3b molecule with an indistinct density for the projecting Bb region (see Fig. 4*C*, *ii*). Such blurring suggests that the conformation of the vWA-SP domains is flexible, likely because of the absence of additional interaction points provided by the Ba SCR triad. In addition, the C3bBb structure shows that the SP domain of fB projects from the structure without contacting C3b and makes the catalytic site accessible to its substrate. Whether this difference between C3bB and C3bBb regarding the position of the SP

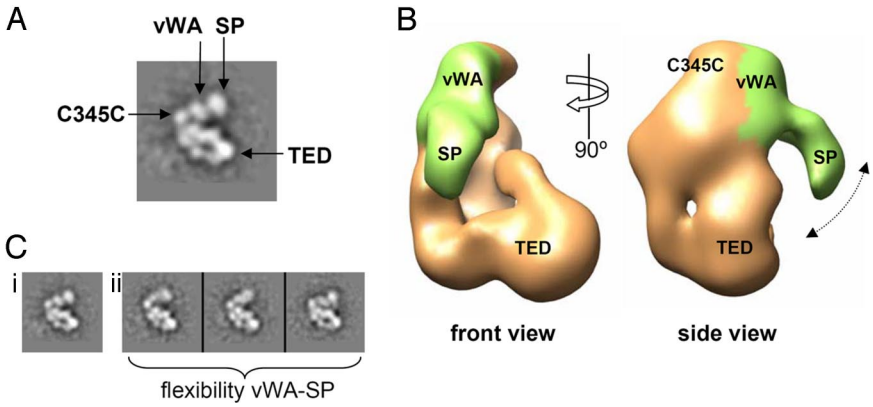

Fig. 4. Three-dimensional structure of the C3bBb convertase. (*A*) A reference-free 2D average corresponding to a side view of the C3bBb complex, where the vWA and SP domains appear projecting from the C3b structure. (*B*) Two views of the C3bBb complex revealing that the density assigned to the SCR1–3 domains in the structure of C3bB(Ni^{2+}) is missing. This reconstruction represents a 3D average, where the density of the SP domain is blurred because of conformational flexibility. (*C*) The flexibility of the vWA-SP cassette projecting from the C3bBb complex is reflected in the 2D reference-free averages of the data. Whereas some averages show a good definition of 3 dots of density corresponding to the C345C, vWA and SP domains (*i*), others reveal some blurring of this area (*ii*), while maintaining the definition of the C3b molecule.

domain is a consequence of conformational changes within the Bb fragment after the release of the Ba fragment cannot be solved at the resolution provide by our studies.

Functional Implications of the 3D Structures of C3bB(Ni^{2+}) and C3bBb Regarding Decay Acceleration Mediated by DAF, CR1, and fH. The AP C3 convertase plays a central role in the amplification of complement cascade, and for this reason its activity is strictly regulated. This regulation is achieved by modulating the stability of the AP C3 convertase, which localize complement amplification to the surface of the pathogens and prevents unspecific damage to self-tissues. Complement regulatory proteins either stabilize the C3bBb complex (Properdin) or accelerate its decay (factor H or fH, DAF, or CR1). The C3bB and C3bBb EM structures described here shed new light on the mechanisms underlying the decay acceleration mediated by DAF, CR1 and fH.

In DAF, the functional activity is located within four SCR domains at the N terminus. Using surface plasmon resonance, it has been shown that DAF mediates decay of the C3bBb convertase, but not of the proenzyme, C3bB, and the major site of interaction is within the Bb fragment (27). Using truncated recombinant DAF molecules, it has been demonstrated that DAF-SCR2 interacts with Bb, whereas DAF-SCR4 interacts with C3b. These data suggest that DAF interacts with C3bBb through major sites in SCR2 and SCR4. It has been suggested that the high affinity of binding to Bb via SCR2 (compared to little or no binding to fB), concentrates DAF on the active convertase, whereas the weaker interactions through SCR4 with C3b directly mediate decay acceleration (28).

We have already discussed that the fB vWA α4/5 helix region is exposed in our structure (see Fig. 3), and that mutagenesis data highlight this helix region as a binding site recognized by DAF and CR1 (12). We recently described a unique fB mutation, K323E, in a patient with atypical hemolytic uremic syndrome that makes the C3bBb convertase resistant to decay by DAF and fH (11). This mutation, located in close proximity to the α4/5 helix region of the vWA domain (see Fig. 3), is remarkable because it modifies neither the formation rate of the C3bB and C3bBb complexes nor their spontaneous decay, suggesting that the mutation specifically affects the binding site in the vWA domain for the complement regulators DAF and fH (11).

The C3bB and C3bBb EM structures described here support the concept of 2 binding sites for DAF in the C3bBb complex, one located on the surface of the vWA domain in Bb, away from the interaction surface with C3b (DAF-SCR2), and the other in C3b in the region that is occupied by the Ba fragment in the C3bB proconvertase (DAF-SCR4). This readily explains the requirement for Ba removal from the C3bB complex in order that DAF can bind and mediate efficient decay acceleration.

Concluding Remarks. The AP C3-convertase is an unstable bimolecular complex formed by C3b and fB that plays a crucial role within the complement cascade, as it provides the exponential amplification to the initial activating trigger. Assembly and regulation of the AP C3 convertase is exquisitely modulated to make possible the elimination of foreign agents by effector cells, while at the same time protecting self-tissues from complement-mediated destruction. In fact, alterations in its formation rate, its stability, or its regulation result in AP complement dysregulation, leading to infectious diseases or tissue damage (29). Understanding how the AP convertase is assembled and regulated is, therefore, essential. Here we present in 3D the conformational transitions of fB following binding to C3b and formation of the AP proenzyme. Importantly, we demonstrate that binding to C3b promotes an opening of the fB conformation by displacing the SCR1–3 region (Ba fragment) from the SP-vWA tandem (Bb fragment). This open conformation of fB exposes the linker connecting the Bb and Ba fragments, permitting its cleavage by fD. Interestingly, the conformation of Bb in the active convertase reveals some degree of flexibility, with the SP domain adopting various conformations with respect to C3b. Our model also reveals important aspects of the regulation of the AP C3 convertase by DAF and perhaps other complement regulators, such as fH and CR1. These data will aid to explore the potential of the AP C3 convertase as a therapeutic target in the development of inhibitors to prevent or reduce tissue damage caused by dysregulated complement activation. Most importantly, our model provides a structural framework onto which other proteins of considerable interest in the pathophysiology of the AP convertase, such as properdin or C3Nef, can be easily modeled. The methodology used in this work, single-particle EM in combination with crystallography, offers a powerful tool to dissect protein interactions underlying the activity and regulation of this remarkable protein complex, the AP C3 convertase.

Materials and Methods

EM and 3D Reconstruction. Purified C3b, C3bB(Ni^{2+}) or C3bBb complexes in 25-mM Tris·HCl pH 8.0, 50-mM NaCl were applied to carbon-coated grids and negatively stained with 1% uranyl formate. The molecular weight of these

complexes (≈200 kDa) did not allow their detection without staining. Observations were performed in a JEOL 1230 electron microscope operated at 100kV and micrographs were recorded at a nominal magnification of 50,000 under low-dose conditions. Micrographs were digitized and averaged to 4.2 Å/pixel and the contrast transfer function estimated using CTFFIND3 (30) and corrected by flipping phases. Around 6,000 images of molecules for each specimen were extracted and refined using EMAN (22). Reference-free averages were obtained using EMAN and maximum likelihood (23). We used 2 different starting 3D templates for refinement in 2 independent experiments. Identical results were obtained with either initial reference (see Fig. S3), substantiating the final reconstruction and the absence of bias during the refinement. One reference was built by low-pass filtering the atomic structure of C3b (PDB file 2i07) to very low resolution (> 60 Å), whereas a second template was a featureless noisy Gaussian blob (see Fig. S3). Images collected for the C3bB(Ni^{2+}) and C3bBb complexes revealed adequate Euler angles coverage. On the other hand, images of C3b mostly corresponded to tilting angles around an abundant front view, consistent with the flat appearance of C3b. To increase this angular coverage, micrographs were also taken after tilting the specimen holder at 20 and 35°, and the images were added to the data set collected without tilting. The resolution of the maps was estimated to be ≈28 Å, ≈27 Å, and ≈28 Å for C3b, C3bB(Ni^{2+}), and C3bBb, respectively, by Fourier Shell Correlation, using the criteria of a correlation coefficient of 0.5. The absolute handedness of the reconstruction was defined by comparison with the atomic structure of C3b.

Fitting of the Atomic Atructures into the EM Maps. We performed a rigid-body fit of C3b (PDB file 2i07) into the EM reconstruction of C3b and the C3bB(Ni^{2+}) complex using ADP_EM (31). C3b was unambiguously located in the C3bB(Ni^{2+}) complex, and a difference map between this fitted C3b and the full map was used to extract the density in the complex assigned to fB. The vWA and SP domains of fB (PDB file 2OK5) (18) were fitted as a rigid-body into this difference map using ADP_EM without any a priori assumption. Only one solution was compatible with the polypeptide backbone linking SCR3 to the vWA domain; this solution was then selected. The Ba fragment corresponding to the SCR1–3 trimer was manually fitted in the remaining density.

ACKNOWLEDGMENTS. We thank B. P. Morgan and C. Harris for their long-term collaborative support of our work and their comments on the manuscript. We also thank Elena Goicoechea de Jorge and Ernesto Arias-Palomo for their help. This work has been supported by projects SAF2005–00775 (to O.L.), SAF2008–00451 (to O.L.), SAF2005–0913 and SAF2008–00226 (to S.R.d.C.) from the Spanish Ministry of Science, CAM S-BIO-0214–2006 (to O.L.) from the Autonomous Region of Madrid, and RD06/0020/1001 (to O.L.) of the Red Temática Investigación Cooperativa en Cáncer from the Instituto Carlos III. O.L.'s group is additionally supported by the Human Frontiers Science Program (RGP39/2008). S.R.d.C.'s group is additionally supported by Centro de Investigación Biomédica en Red de Enfermedades Raras (INTRA/08/738.2) and the Fundacion Renal Iñigo Alvarez de Toledo.

1. Volanakis JE (1998) *The Human Complement System in Health and Disease* (Marcel Dekker, Inc., New York) 10th Ed. pp 9–32.
2. Pangburn MK, Muller-Eberhard HJ (1986) The C3 convertase of the alternative pathway of human complement. Enzymic properties of the bimolecular proteinase. *Biochem J* 235(3):723–730.
3. Taniguchi-Sidle A, Isenman DE (1994) Interactions of human complement component C3 with factor B and with complement receptors type 1 (CR1, CD35) and type 3 (CR3, CD11b/CD18) involve an acidic sequence at the N-terminus of C3 α-chain. *J Immunol* 153(11):5285–5302.
4. Kölln J, Bredehorst R, Spillner E (2005) Engineering of human complement component C3 for catalytic inhibition of complement. *Immunol Lett* 98(1):49–56.
5. Kölln J, Spillner E, Andra J, Klensang K, Bredehorst R (2004) Complement inactivation by recombinant human C3 derivatives. *J Immunol* 173(9):5540–5545.
6. Janssen BJC, Gros P (2007) Structural insights into the central complement component C3. *Mol Immunol* 44(1–3):3–10.
7. Gros P, Milder FJ, Janssen BJC (2008) Complement driven by conformational changes. *Nat Rev Immunol* 8(1):48–58.
8. Hourcade DE, Mitchell LM, Oglesby TJ (1999) Mutations of the type A domain of complement factor B that promote high- affinity C3b-binding. *J Immunol* 162(5):2906–2911.
9. Tuckwell DS, Xu Y, Newham P, Humphries MJ, Volanakis JE (1997) Surface loops adjacent to the cation-binding site of the complement factor B von Willebrand factor type A module determine C3b binding specificity. *Biochemistry* 36(22):6605–6613.
10. Hinshelwood J, Spencer DIR, Edwards YJK, Perkins SJ (1999) Identification of the C3b binding site in a recombinant vWF-A domain of complement factor B by surface-enhanced laser desorption-ionisation affinity mass spectrometry and homology modelling: Implications for the activity of factor B. *J Mol Biol* 294(2):587–599.
11. Goicoechea De Jorge E, *et al.* (2007) Gain-of-function mutations in complement factor B are associated with atypical hemolytic uremic syndrome. *Proc Natl Acad Sci USA* 104(1):240–245.
12. Hourcade DE, Mitchell L, Kuttner-Kondo LA, Atkinson JP, Edward Medof M (2002) Decay-accelerating factor (DAF), complement receptor 1 (CR1), and factor H dissociate the complement AP C3 convertase (C3bBb) via sites on the type A domain of Bb. *J Biol Chem* 277(2):1107–1112.
13. Pryzdial ELG, Isenman DE (1987) Alternative complement pathway activation fragment Ba binds to C3b. *J Biol Chem* 262(4):1519–1525.
14. Hourcade DE, Wagner LM, Oglesby TJ (1995) Analysis of the short consensus repeats of human complement factor B by site-directed mutagenesis. *J Biol Chem* 270(34):19716–19722.
15. Xu Y, Volanakis JE (1997) Contribution of the complement control protein modules of C2 in C4b binding assessed by analysis of C2/factor B chimeras. *J Immunol* 158(12):5958–5965.
16. Thurman JM, *et al.* (2005) A novel inhibitor of the alternative complement pathway prevents antiphospholipid antibody-induced pregnancy loss in mice. *Mol Immunol* 42(1):87–97.
17. Montes T, *et al.* (2008) Functional differences between common factor B polymorphic variants: An explanation for association with AMD. *Mol Immunol* 45:4098.
18. Milder FJ, *et al.* (2007) Factor B structure provides insights into activation of the central protease of the complement system. *Nat Struct Mol Biol* 14(3):224–228.
19. Ponnuraj K, *et al.* (2004) Structural analysis of engineered Bb fragment of complement factor B: Insights into the activation mechanism of the alternative pathway C3-convertase. *Mol Cell* 14(1):17–28.
20. Hourcade DE, Mitchell LM, Oglesby TJ (1998) A conserved element in the serine protease domain of complement factor B. *J Biol Chem* 273(40):25996–26000.
21. Fishelson Z, Muller-Eberhard HJ (1984) Residual hemolytic and proteolytic activity expressed by Bb after decay-dissociation of C3b, Bb. *J Immunol* 132(3):1425–1429.
22. Ludtke SJ, Baldwin PR, Chiu W (1999) EMAN: Semiautomated software for high-resolution single-particle reconstructions. *J Struct Biol* 128(1):82–97.
23. Scheres SHW, Valle M, Carazo JM (2005) Fast maximum-likelihood refinement of electron microscopy images. *Bioinformatics* 21(SUPPL. 2):ii243–ii244.
24. Janssen BJC, *et al.* (2005) Structures of complement component C3 provide insights into the function and evolution of immunity. *Nature* 437(7058):505–511.
25. Wiesmann C, *et al.* (2006) Structure of C3b in complex with CRIg gives insights into regulation of complement activation. *Nature* 444(7116):217–220.
26. Smith CA, Vogel CW, Muller Eberhard HJ (1984) MHC class III products: An electron microscopic study of the C3 convertases of human complement. *J Exp Med* 159(1):324–329.
27. Harris CL, Abbott RJM, Smith RA, Morgan BP, Lea SM (2005) Molecular dissection of interactions between components of the alternative pathway of complement and decay accelerating factor (CD55). *J Biol Chem* 280(4):2569–2578.
28. Harris CL, Pettigrew DM, Lea SM, Morgan BP (2007) Decay-accelerating factor must bind both components of the complement alternative pathway C3 convertase to mediate efficient decay. *J Immunol* 178(1):352–359.
29. Holers VM (2008) The spectrum of complement alternative pathway-mediated diseases. *Immunol Rev* 223(1):300–316.
30. Mindell JA, Grigorieff N (2003) Accurate determination of local defocus and specimen tilt in electron microscopy. *J Struct Biol* 142(3):334–347.
31. Garzón JI, Kovacs J, Abagyan R, Chacón P (2007) ADP_EM: Fast exhaustive multi-resolution docking for high-throughput coverage. *Bioinformatics* 23(4):427–433.

Supporting Information

Torreira *et al.* 10.1073/pnas.0810860106

SI Materials and Methods

Preparation of the Complement C3b Fragment. C3 was prepared from pooled normal human plasma. Plasma was subjected to a 4 to 12% cut with PEG4000, the pellet was solubilized in 10-mM Na/K phosphate pH7.6, 5-mM NaCl, and applied to a DEAE-Sepharose anion exchange column attached to an Akta Prime system (GE Healthcare). Protein was fractionated using a gradient to 0.5M NaCl, C3-containing fractions were identified by SDS/PAGE, dialyzed against 20-mM Na/K phosphate pH6, 60-mM NaCl and applied to a Source S cation exchange column (GE Healthcare). Protein was eluted with a gradient to 0.5M NaCl. C3-containing fractions were pooled and concentrated. C3b was generated by limited digestion with trypsin as previously described (1) and repurified by gel filtration on a SuperoseTM 6 10/300 column (GE Healthcare). C3b was obtained without any detectable contaminants or aggregates [supporting information (SI) Fig. S1*A*].

Production and Purification of Recombinant fB. The D279G amino acid substitution was introduced in the fB cDNA by using QuikChange site-directed mutagenesis kit (Stratagene) and appropriate primers. Both cDNAs encoding full length fB-WT and fB-D279G were introduced in the eukaryote expression vector pCI-Neo (Promega) and the resulting clones entirely sequenced to confirm a correct DNA sequence. CHO cells were maintained in Ham-F12 medium (GIBCO-BRL) supplemented with 10% FCS, L-glutamine (2 mM final concentration), penicillin and streptomycin (10 U/ml and 100 μg/ml). The neomycin analogue, G418 sulfate (Geneticin; GIBCO-BRL), at 500 μg/ml, was used for selection of transfected cells. Factor B-cDNA transfections were performed using Lipofectine (Invitrogen), as recommended by the manufacturer. Cells were plated in p60 plates 1 day before transfection at 5 $\times$ 105 cells per well. Transfections were carried out with 10 μg of the pCI-Neo constructs and 24 μl of Lipofectine in a total volume of 1 ml of medium per well. Stable transfected CHO cells were cloned by limiting dilution and clones producing the highest levels of fB (fB-WT 20 μg/ml; fB-D279G 2 μg/ml) were expanded for production. Factor B concentration was quantified by ELISA as previously described (2). The recombinant fBs were purified from tissue culture supernatant by affinity chromatography using the JC1 monoclonal antibody (anti-human Bb, a gift from Prof. B.P. Morgan, Cardiff, U.K.) coupled to a HiTrap NHS-activated column according to the manufacturer's instructions (GE Healthcare). Bound fB was eluted with 0.1M Glycine/HCl pH 2.5, immediately neutralized with 2M Tris pH 8.6, and re-purified by gel filtration on a SuperoseTM 6 10/300 column (GE Healthcare). Both fB-WT and fB-D279G were obtained without any detectable contaminants or aggregates (see Fig. S1*A*).

Generation and Purification of C3bB Complexes. The Ni^{2+} cation was used instead of Mg^{2+} to promote a stable C3bB(Ni^{2+}) complex that is otherwise undistinguishable from the physiological C3bB(Mg^{2+}) proconvertase. Purified C3b and fB were mixed in a (1:2) molar excess of fB in 20-mM Tris, pH = 7.6 buffer containing 50-mM NaCl and either 20-mM EDTA or in 5-mM $NiCl_2$, and allowed to interact for 15 at room temperature. Subsequently, both preparations were size-fractionated by gel-filtration chromatography on a calibrated SuperoseTM 6 10/300 column (GE Healthcare) (Fig. S1*B*). In the absence of divalent cations (EDTA-sample), fB does not interact with C3b and both proteins elute separately from the Superose column as illustrated by the SDS/PAGE analysis of the corresponding fractions (Fig. S1*C*). In the presence of Ni^{2+} and a 1:2 molar excess of fB, C3b readily interacts with fB to form C3bB(Ni^{2+}) complexes. SDS/PAGE characterization of the elution fractions from the Superose column illustrates the presence of the C3bB(Ni^{2+}) complex, which elutes from the column in a single peak that precedes and partially overlaps the peak containing the single C3b molecules (see Fig. S1 *B* and *C*). To avoid a potential contamination of single C3b molecules in the fractions corresponding to the C3bB(Ni^{2+}) complex, samples for the EM analysis were collected exclusively from the initial elution fractions of the peak containing the C3bB(Ni^{2+}) complex.

Generation and Purification of C3bBb Complexes. We have used the fB-D279G mutant instead of the fB-WT protein to promote a relatively stable active C3bBb convertase. For the generation of the C3bB complex, purified C3b and fB-D279G were mixed in a (1:2) molar excess of fB in 20-mM Tris, pH = 7.6 buffer containing 50-mM NaCl and 5-mM MgCl2 and were incubated for 15 min at room temperature. Subsequently, we added fD (Comptech. Inc.,) at a 1:500 molar ratio to fB, incubated for 1 min at 37 °C and size-fractionated the mix by gel-filtration chromatography on a calibrated SuperoseTM 6 10/300 column (GE Healthcare) (Fig. S4*A*). The presence of C3bBb complexes was demonstrated by SDS/PAGE analysis, illustrating that, as expected, most of the Bb fragment eluted in the fractions containing the C3b molecule (Fig. S4*B*). The C3bBb complex eluted from the column in a single peak that significantly overlapped the peak containing the single C3b molecules (see Fig. S4 *A* and *B*). To minimize the contamination of single C3b molecules in the fractions corresponding to the C3bBb complex, samples for the EM analysis were collected exclusively from the initial elution fractions of the peak containing the C3bBb complex.

1. Sánchez-Corral P, *et al.* (1989) Separation of active and inactive forms of the third component of human complement, C3, by fast protein liquid chromatography (FPLC). *J Immunol Methods* 122 (1):105–113.

2. Goicoechea De Jorge E, *et al.* (2007) Gain-of-function mutations in complement factor B are associated with atypical hemolytic uremic syndrome. *Proc Natl Acad Sci USA* 104(1):240–245.

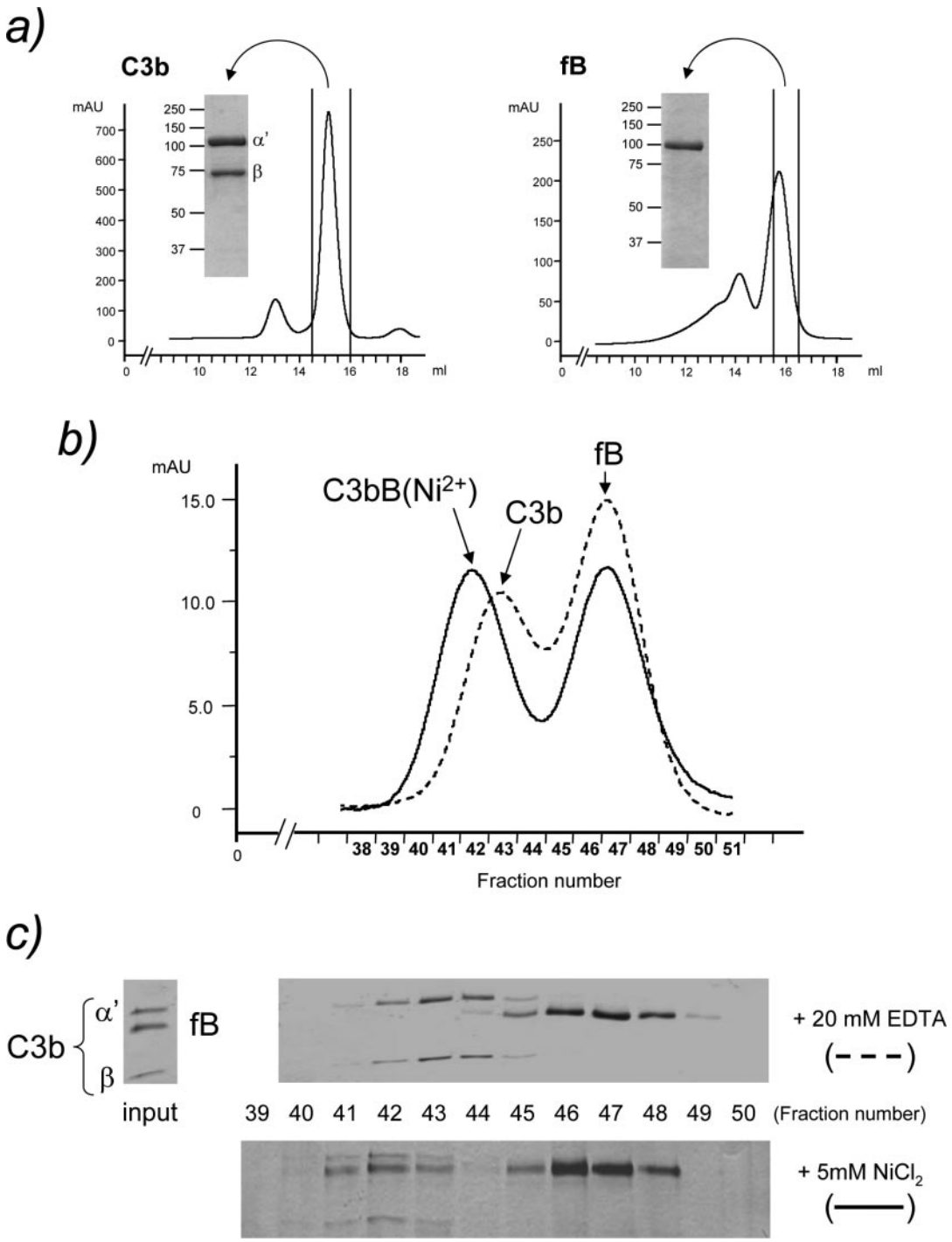

Fig. S1. Purification of C3b, fB and the C3bB(Ni^{2+}) complex. (*a*) Purification of C3b and fB. Chromatograms from the final step of C3b and fB-WT purification on a Superose 6 10/300 gel-filtration column. The *y* axis (milliabsorbance units, mAU) plots absorbance at 280 nm, the *x* axis plots retention time in ml. Vertical lines indicate the fractions that were pooled for generating the C3bB(Ni^{2+}) complex and for the EM experiments. The Coomassie-stained gel illustrates purity of the final C3b and fB preparations. (*b*) Purification of the C3bB(Ni^{2+}) complexes. Elution profiles of the C3b-fB mix in the presence of 20-mM EDTA (no complex formed; *dotted line*) or 5-mM $NiCl_2$ (complex formed; *solid line*) from the Superose 6 10/300 gel-filtration column. The *y* axis (mAU) plots absorbance at 280 nm, the *x* axis plots number of fraction collected. Elution position for fB, C3b and the C3bB(Ni^{2+}) complex are indicated. (*c*) Characterization of C3bB(Ni^{2+}) and complexes by SDS/PAGE. Fractions of the gel-filtration chromatography experiments shown in (*b*) were analyzed by SDS/PAGE silver-stained gels. The presence of the C3bB(Ni^{2+}) complex was clearly demonstrated in the presence of 5-mM $NiCl_2$, as illustrated by the advanced elution position of fB (fractions 40–43), compared to that of the single fB molecules (fractions 45–48). Note that for the EM analysis of the C3bB(Ni^{2+}) complex, only fractions 40 and 41 were used.

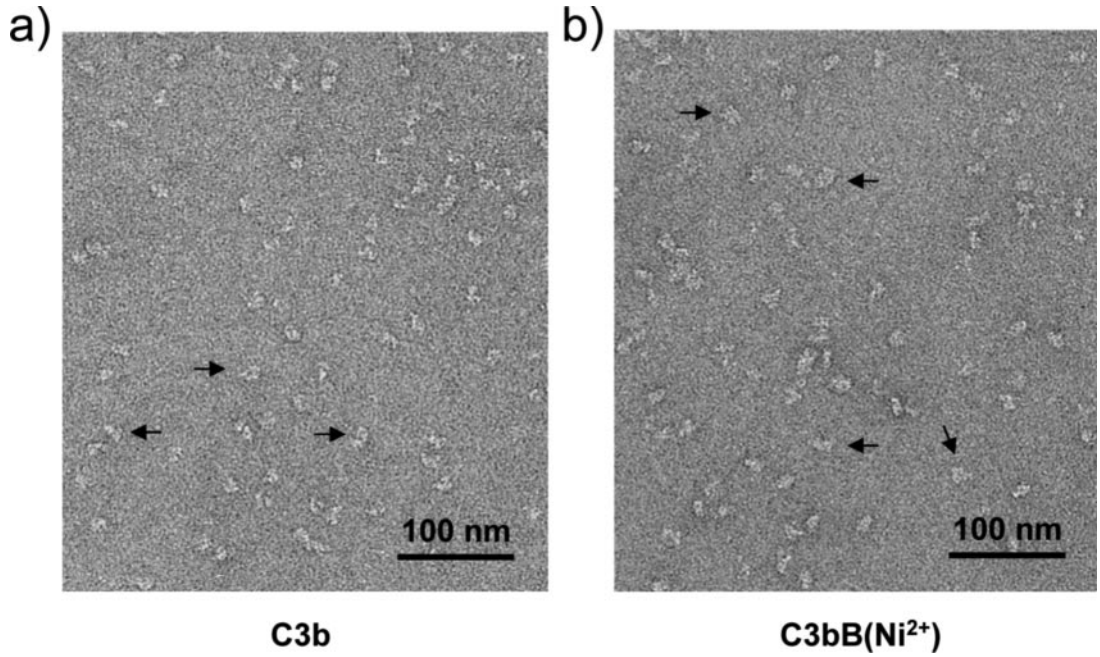

Fig. S2. Electron micrographs of C3b and C3bB(Ni^{2+}). Selected field of an electron micrograph of C3b (*a*) and C3bB(Ni^{2+}) complex (*b*). (Scale bar, 100 nm.) Some representative images of individual molecules are indicated using arrows.

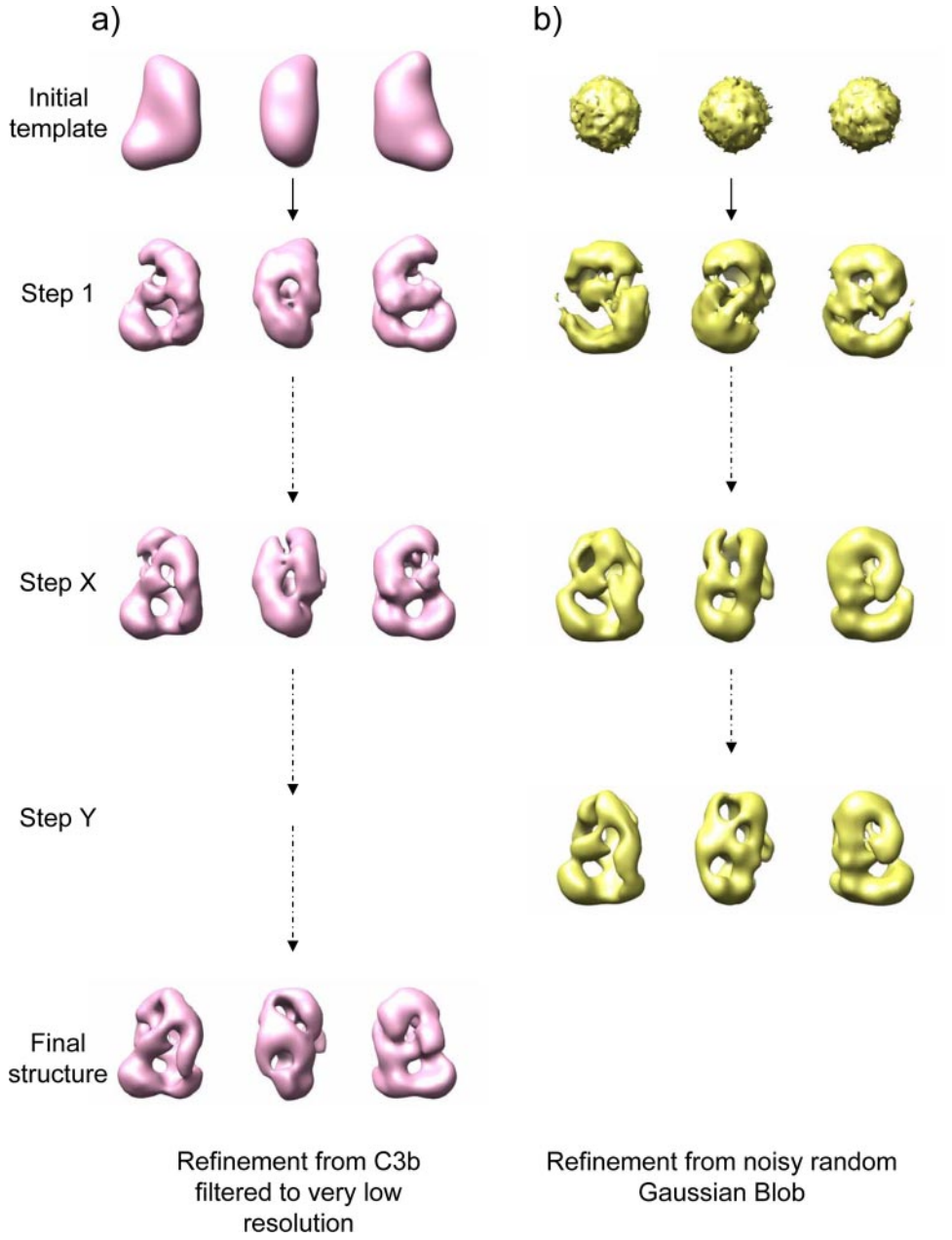

Fig. S3. Image processing of C3bB(Ni^{2+}) using angular refinement methods. Angular refinement was performed in 2 independent experiments from 2 different volumes, either a low-pass filtered version of the atomic structure of C3b (*a*) or a random noisy Gaussian blob (*b*). Three views of the initial template in each case and of several output volumes along the progression of the refinement are shown. It can be noted that two very distantly related initial references converge into a similar 3D structure, indicating the absence of bias of the initial template during the refinement and the accuracy of the final reconstruction.

a)

Solution #	Correlation	Orientation (OK or flip)
1	0.780	flip
2	0.776	flip
3	**0.757**	**OK**
4	**0.757**	**OK**
5	0.755	flip
6	**0.755**	**OK**
7	**0.753**	**OK**
8	0.744	flip
9	0.743	flip
10	0.743	flip
11	**0.743**	**OK**
:	:	:
:	:	:
20	0.648	----
21	0.648	----

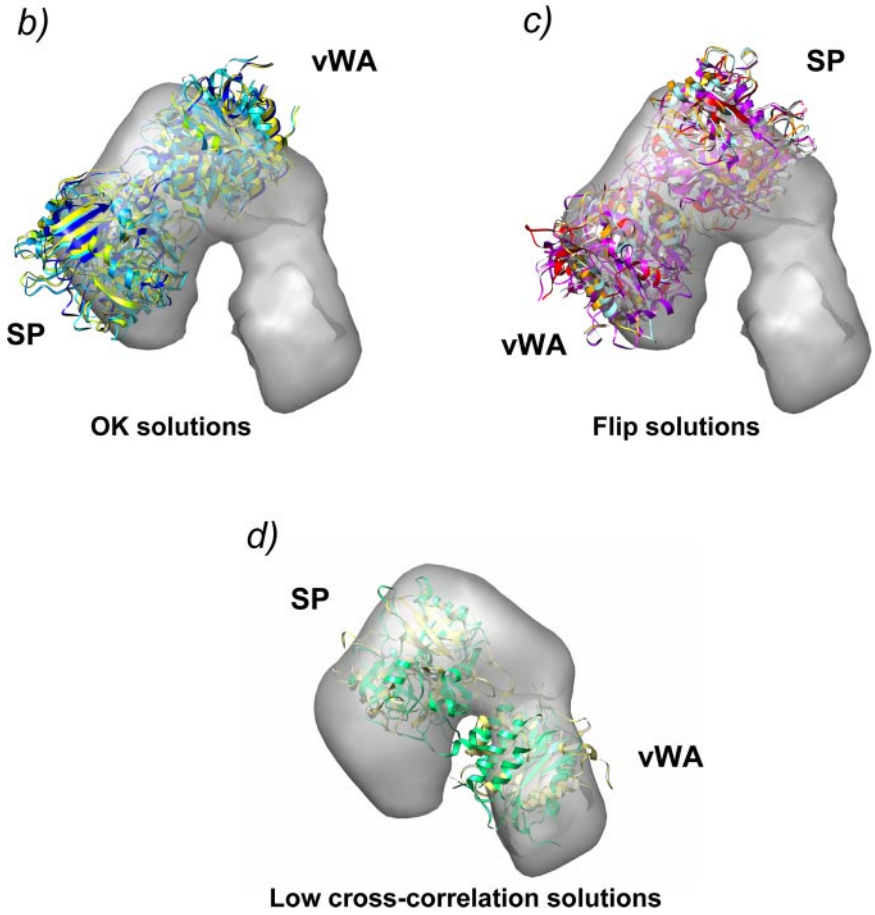

Fig. S4. Output solutions after fitting the atomic structure of the vWA and the SP domains of fB (amino acids 253 to 764) into the EM density for fB extracted from the 3D structure of C3bB(Ni2+).(*a*) List of the top 11 solutions automatically obtained in the fitting experiment using computational methods with their corresponding cross-correlation values for the comparison between the EM density and the atomic structures. The table includes an indication of whether the vWA-SP orientation was interpreted as compatible with the continuity of the polypeptide chain (labeled ''OK'') or incompatible with this continuity (labeled ''flip''). The figure also shows the correlation values for the first 2 fitting outputs (20 and 21) that are significantly different from the top 11 outputs. (*b*) All of the output solutions considered to be correct in the above list are practically identical and represented just slight variations around a similar common output. These solutions are depicted as ribbons using a different color for each solution. (*c*) Likewise, all ''flipped'' solutions were very similar and are also represented as ribbons using different colors. (*d*) The two outputs with low cross-correlation values are also color-coded.

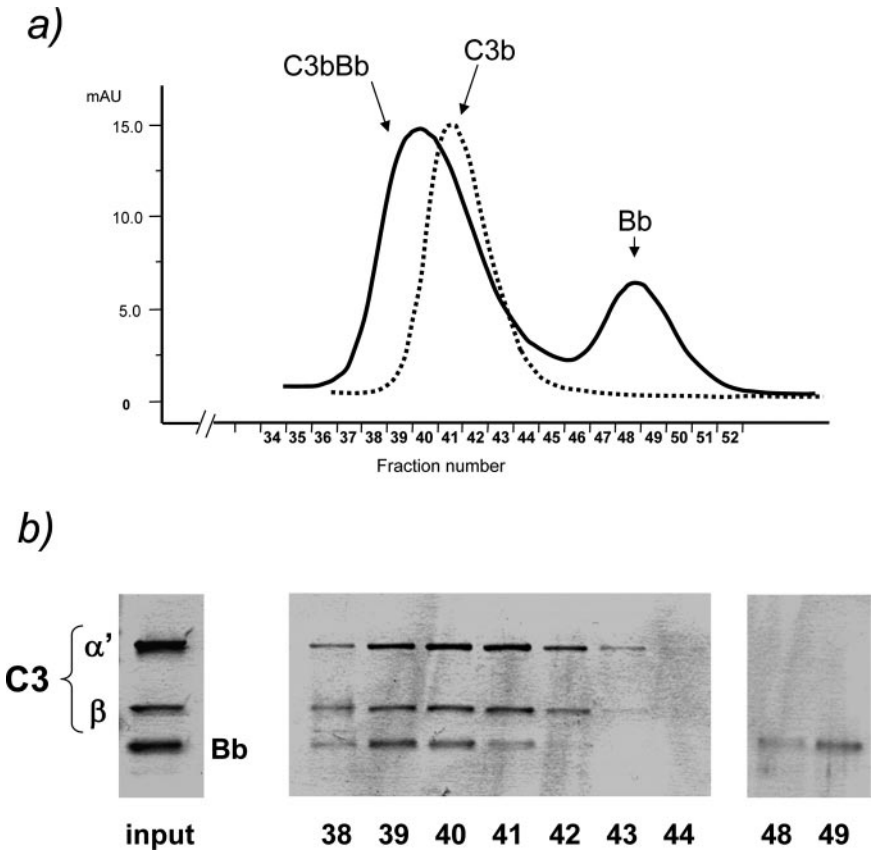

Fig. S5. Purification of the C3bBb complex. (*a*) Purification of the C3bBb complexes. Elution profiles of the C3b/fB-D279G mix in the presence of 5-mM $MgCl_2$ and fD (active convertase formed; *solid line*) and isolated C3b (*dotted line*) from the Superose 6 10/300 gel-filtration column. The *y* axis (mAU) plots absorbance at 280 nm, the *x* axis plots number of fraction collected. Elution position for the Bb fragment, C3b and the C3bBb complex are indicated. (*b*) Characterization of C3bBb complexes by SDS/PAGE. Fractions of the gel-filtration chromatography experiments shown in (*a*) were analyzed by SDS/PAGE silver-stained gels. The presence of the C3bBb complex was clearly demonstrated by the earlier elution of the Bb fragment (fractions 37–41), compared to that of the single Bb molecules (fractions 47–50). Only the initial fractions (38 and 39) of the C3bBb peak from gel-filtration chromatography were used in the EM experiments to minimize the presence of single C3b molecules in the C3bBb preparations.

Coexistence of Closed and Open Conformations of Complement Factor B in the Alternative Pathway C3bB(Mg^{2+}) Proconvertase[1,2]

Eva Torreira,* Agustín Tortajada,*† Tamara Montes,*† Santiago Rodríguez de Córdoba,[3]*† and Oscar Llorca[3]*

Complement factor B (fB) circulates in plasma as a proenzyme that, upon binding to C3b in the presence of Mg^{2+}, is cleaved by factor D to produce Ba and Bb fragments. Activated Bb remains bound to C3b organizing the alternative pathway C3 convertase (C3bBb). Recently, we have visualized the stable C3bB(Ni^{2+}) proconvertase using electron microscopy, revealing a large conformational change of the C3b-bound fB likely exposing the fD-cleavage site. In contrast, the crystal structure of the proconvertase formed by human fB and the cobra venom factor reveals fB in the closed conformation of the proenzyme. In this study, we have used single-particle electron microscopy and image processing to examine the C3bB(Mg^{2+}) proconvertase. We describe two C3bB(Mg^{2+}) conformations, one resembling cobra venom factor, likely representing the loading state of fB to C3b, and another identical with C3bB(Ni^{2+}). These data illustrate the coexistence of C3b-bound fB in closed and open conformations that either exist in equilibrium or represent structural transitions during the assembly of the C3bB proconvertase. ***The Journal of Immunology,*** **2009, 183: 7347–7351.**

Complement plays crucial roles in microbial killing, apoptotic cell clearance, and immune complex handling. Activation of complement by foreign surfaces (alternative pathway, AP),[4] Ab (classical pathway, CP), or mannan (lectin pathway) causes target opsonization, leukocyte recruitment, and cell lysis. A critical step in complement activation is the formation of unstable bimolecular complexes, named C3-convertases (AP, C3bBb; CP/lectin pathway, C2aC4b), that cleave C3 to generate C3b. The AP C3-convertase is fundamental to provide exponential amplification to the initial activation, because C3b generated by either the CP or the AP C3-convertases can form more AP C3-convertase. The generation of the AP C3-convertase initiates in vivo with the interaction between C3b and factor B (fB), in a Mg^{2+}-dependent manner, to form the proconvertase C3bB. In the presence of factor D (fD), fB is cleaved and the N-terminal Ba fragment is released from the C3bB complex, resulting in the active AP C3-convertase, C3bBb (1).

fB is composed of five domains, three short consensus repeats (SCRs), also known as complement control protein repeats, followed by a von Willebrand type A (vWA) and a serine-protease (SP) domain (2). The vWA and SP domains comprise the Bb fragment and the fD cleavage site locates between the SCRs and the vWA domain. The atomic structure of full-length fB reveals that this fD cleavage site is not accessible in the proenzyme, suggesting that it is exposed as a consequence of Mg^{2+}-dependent binding to C3b (2, 3). Our recent three-dimensional structure of the C3bB complex stabilized with nickel ions has revealed the structural basis for the specific activation of fB upon binding to C3b (4). The structure reveals that fB undergoes a dramatic conformational change when in complex with C3b so that the Ba region is displaced and the link between the Bb and Ba fragments is likely exposed. In this structure, the vWA domain recognizes the C345C domain of C3b whereas some of the SCRs seem to be facing the CUB domain, although a specific interaction between Ba and CUB is not confirmed by the structure. In the structure of C3bB(Ni^{2+}), both Bb and Ba segments are found in close proximity to C3b and the Bb does not project outwards from the complex. This deeply contrasts the configuration found in the active C3bBb convertase (see below).

More recently, the atomic structure of the complex formed between the human fB and the cobra venom factor (CVF), a homologue of C3b, has been solved (5). CVF forms soluble convertases that are significantly more stable than C3-convertases. Specific interactions between several regions of the Ba and Bb segments of fB and five domains of CVF hold the complex. The Ba segment contacts αNT, CUB, MG2, MG6, and MG7 of CVF whereas the vWA domain on the Bb segment interacts with the C345C domain, similarly to what is found in the electron microscopy (EM) structure of C3bBb(Mg^{2+}) (4). Quite unexpectedly, the conformation of CVF-bound fB reveals a compact conformation closely similar to that found in the free proenzyme. This conformation is incompatible with the activation of the convertase because the scissile

*Centro de Investigaciones Biológicas, Consejo Superior de Investigaciones Científicas and †Centro de Investigación Biomédica en Red de Enfermedades Raras and Instituto Reina Sofía de Investigaciones Nefrológicas. Ramiro de Maeztu 9, Madrid, Spain

Received for publication July 16, 2009. Accepted for publication September 24, 2009.

The costs of publication of this article were defrayed in part by the payment of page charges. This article must therefore be hereby marked *advertisement* in accordance with 18 U.S.C. Section 1734 solely to indicate this fact.

[1] This work has been supported by projects SAF2008-00451 (to O.L.) and SAF2008-00226 (to S.R.C.) from the Spanish Ministry of Science, and the "Red Temática de Investigación Cooperativa en Cáncer (RTICC), RD06/0020/1001" from the "Instituto de Salud Carlos III" (to O.L.). O.L. group is additionally supported by the Human Frontiers Science Program (RGP39/2008) and the Autonomous Region of Madrid (CAM S-BIO-0214-2006). SRC group is additionally supported by CIBERER (INTRA/08/738.2) and the Instituto Reina Sofía de Investigaciones Nefrológicas.

[2] All authors contributed equally to this work.

[3] Address correspondence and reprint requests to Dr. Santiago Rodríguez de Córdoba or Dr. Oscar Llorca, Centro de Investigaciones Biológicas, Ramiro de Maeztu 9, 28040 Madrid, Spain. E-mail addresses: srdecordoba@cib.csic.es or ollorca@cib.csic.es

[4] Abbreviations used in this paper: AP, alternative pathway; CP, classical pathway; fB, factor B; fD, factor D; SCR, short consensus repeat; vWA, von Willebrand type A; SP, serine-protease; CVF, cobra venom factor; SCIN, staphylococcal complement inhibitor.

www.jimmunol.org/cgi/doi/10.4049/jimmunol.0902310

site is completely inaccessible to fD (2, 5). The authors proposed that the structure of the CVFB could represent the "loading" state of the proconvertase in an equilibrium with an "activation" state described by the EM structure of C3bB(Ni^{2+}) (5).

fD-mediated cleavage of fB in the C3bB complex generates the active C3 convertase, whose three-dimensional architecture has been recently described by EM and x-ray structures. The atomic structure of the C3bBb convertase was obtained after stabilization using the staphylococcal complement inhibitor (SCIN) (6), whereas the EM structure was stabilized using a fB-D279G mutant (4). The fB-D279G mutation is also referred to as fB-D254G depending on the criteria used for the amino acid numbering (4, 7, 8) (see *Materials and Methods* for further details). Both x-ray crystallography and EM showed that the complex between Bb and C3b is maintained by interactions between the C345C and vWA domains. The Bb fragment projects outwards of the complex so that the SP domain is far from contacting C3b. Additionally, the EM structure of the C3 convertase suggests that some conformational flexibility of the C345C-vWA-SP cassette could permit the accommodation of the C3 convertase to the substrate so that the SP domain can reach and cleave C3 (4).

The structural characterization of the protein complexes of the alternative pathway of complement activation is challenged by their large size, conformational flexibility, and low stability. As a result, many of the structures solved have made use of different approaches to chemically stabilize the complexes. Alternatively, the interactions have been formed with selected isolated domains rather than full-length molecules. In this study, we have characterized the structure and conformations of the C3bB complex formed between the fB-D279G mutant and C3b in the presence of the natural divalent ion Mg^{2+}. This C3bB complex is significantly less stable that the C3bB(Ni^{2+}) proconvertase but still suitable for single particle electron microscopy analysis. Our results revealed a complex mixture containing free C3b and C3bB complexes. We have taken advantage of visualizing single molecules with the microscope to computational classify and "in silico" purify the conformational complexity of the sample. Unexpectedly, this analysis revealed that the C3bB complex displays at least two distinct conformations that provide a first glimpse at the conformation transitions of fB leading to the formation of an active AP C3 convertase. The implications of these transitions in assembly and activation of the AP C3 convertase are discussed.

Materials and Methods

Purification of C3b, fB, and assembly of the C3bB(Mg^{2+}) complex

C3 was prepared from pooled normal human plasma whereas recombinant fB-D279G mutant (4, 7, 8) was expressed in CHO cells. This mutation in fB is named D279G when using the numbering that is recommended by the Human Genome Variation Society for residues in secreted proteins and includes numbering of amino acids in signal peptides (4, 7) or D254G when using the first amino acid of the mature serum protein (8). This later case is found in the original description of this mutation (8) and in most of the high-resolution structural works (5).

Expression and purification of both proteins was performed as described (4). Purified C3b and fB-D279G were mixed in a molar excess of fB-D279G in buffer containing 5 mM $MgCl_2$ for 15 min at room temperature. The mixture was loaded to a SuperoseTM 6 10/300 gel filtration chromatography (GE Healthcare). Only in the presence of divalent ions fB-D279G comigrates with C3b to form C3bB(Mg^{2+}) complexes. The fractions were analyzed by SDS electrophoresis and Western blotting using rabbit polyclonal Abs against human C3b (in house) and human fB (a gift of Dr. Claire Harris, University of Cardiff, U.K.). Both Abs recognize well in Western blot the C3b and fB full-length proteins, the α- and β-chains of C3b, and both Ba and Bb fragments of fB.

Electron microscopy and three-dimensional reconstruction

A fraction from the gel filtration chromatography containing the C3bB(Mg^{2+}) complexes was applied to carbon-coated grids and negatively stained with 1% uranyl formate. Preparations were observed in a JEOL 1230 electron microscope and micrographs recorded using a low dose mode at a nominal magnification of 50,000. Micrographs were digitized and averaged to 4.2 Å/pixel, the contrast transfer function estimated using CTFFIND3 (9) and corrected by flipping phases with BSOFT (10). In brief, 9728 images for the reaction mixture of C3b and fB in the presence of Mg^{2+} were extracted using EMAN (11). Initial classification and averaging were performed using methods in EMAN. Particles belonging to the new conformation were split and their classification improved using maximum likelihood (12) and further classification of each subgroup by self-organizing maps using XMIPP (13). To verify that each final subclass contained a homogeneous subset of the data, the images for each subgroup were aligned and averaged independently using reference-free methods. In a different set of experiments, the incubation between C3b and wild-type fB in the presence of Ni^{2+} was performed as described before (4). The C3bB(Ni^{2+}) complexes were purified by gel filtration and the fractions observed in the electron microscope. In brief, 10929 images of individual molecules were extracted from the micrographs, classified, and averaged using similar methods to those described above for the complexes formed using magnesium.

To explore how many distinct conformations were found in the dataset obtained in the presence of Mg^{2+}, three-dimensional reconstructions by angular refinement were performed allowing for several output solutions using the *multirefine* command in EMAN (11) and three-dimensional maximum likelihood classification. After all these analyses, it became apparent that, once the images corresponding to C3b were discarded, the images of the C3bB(Mg^{2+}) complex corresponded to two distinct structures, with the novel averages belonging to the less abundant conformation within our dataset. As an additional test, when all the images for C3bB(Mg^{2+}) complexes were process together, the images corresponding to the novel conformation were automatically discarded of the reconstruction because they showed a low correlation with the three-dimensional average, confirming that these images do not match the most abundant conformation of the complex.

The final three-dimensional reconstructions were performed with a dataset cleaned from the images of C3b. These were easily identified because the flat shape of the molecule induces preferential binding to the grid to produce the typical L-shape observed in the electron microscope (4). Images were then refined using angular refinement methods and the *multirefine* command (11). As starting templates for refinement, two phantoms based on the reference-free averages were built. The resolution of the C3bB(Mg^{2+}) reconstructions were ~32.5 and ~27.0 Å for the closed and open conformation, respectively, estimated by Fourier Shell Correlation using a correlation coefficient of 0.5. The absolute handedness of the reconstruction was defined by comparison with the atomic structure of C3b.

Results

Electron microscopy of C3b incubated with fB in the presence of Mg^{2+} reveals a mixture of complexes

The complex formed between C3b and fB in the absence of properdin is extremely unstable (3, 8). For this reason, previous structural studies have made used of Ni^{2+} (4), the bacterial inhibitor SCIN (6), or CVF to generate relatively stable conformations of the complex (5). To approach conditions more similar to the physiological unstable C3bB proconvertase, we have generated moderately stable C3bB complexes between C3b and the fB-D279G mutant (4, 7, 8) in the presence of $MgCl_2$ and used EM to visualize the structural complexity of this preparation. The fB-D279G mutant promotes high-affinity C3b-binding and generates a C3bB complex with a half live of ~30 min that it is correctly cleaved by factor D to generate a functionally active, AP convertase C3bBb (7, 8, 14). Purified C3b and fB-D279G proteins were mixed with a molar excess of fB-D279G and unbound fB-D279G was removed by gel filtration chromatography (Fig. 1*A*). The first fraction of the main peak eluting from the column, enriched of C3bB complexes, was immediately adsorbed to carbon-coated grids and observed by EM. A total of 9728 images of individual molecules were extracted from the micrographs and subjected to reference-free classification methods searching for similar images. These

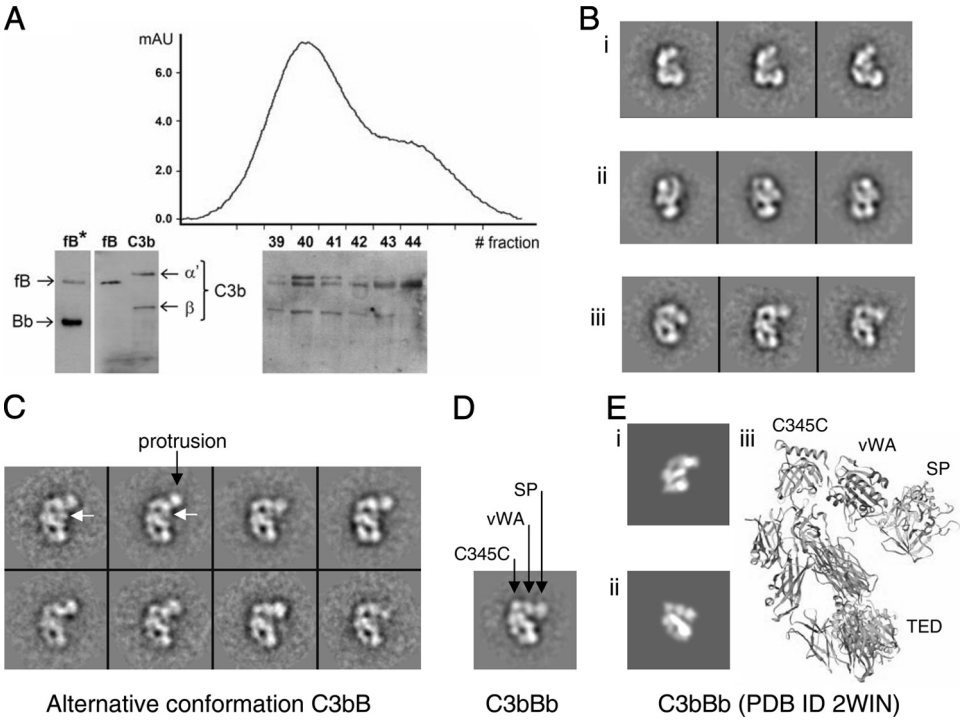

FIGURE 1. Purification and electron microscopy of C3bB(Mg^{2+}) complexes. *A*, Gel filtration chromatography of purified C3b incubated with an excess of fB. Fractions were analyzed by SDS-PAGE and Western blotting using Abs against C3b and fB. Fraction no.39 containing full-length fB and C3b was used for the EM experiments. A representative Western blot is shown in the left side to illustrate the identity of the different protein bands, including the position of the Bb fragment in a sample of fB activated with fD (fB*). *B*, Reference-free two-dimensional averages obtained for the whole data set. Averages were found to correspond to projections of C3b with its characteristic "L" shape (*i*), a conformation of C3bB(Mg^{2+}) similar to that described for C3bB(Ni^{2+}) (4) (*ii*), and a novel conformation (*iii*). *C*, Selected reference-free averages of the new conformation of C3bB(Mg^{2+}) obtained after systematic re-classification of the images assigned to the classes shown in *B*, *iii*. The location of the protrusion in the averages is indicated and the putative location of the Ba fragment is labeled with white arrows. *D*, EM image for the C3bBb convertase (4) showing three dots protruding from the structure and corresponding to the C345C domain in C3b and vWA and SP from fB. *E*, Atomic structure of the C3bBb convertase resolved by Rooijakkers et al. (6). Computational projections of this structure after low-pass filtering to a resolution of 22 Å (*i* and *ii*). One view of the atomic model (PDB ID 2WIN) (*iii*).

were then averaged to increase the signal to noise ratio so that significant structural information could be recovered. Inspection of these averages revealed three main groups of class averages (Fig. 1*B*). One group contained 5610 images and comprised the distinctive projections of the C3b molecule (4, 15, 16) (Fig. 1*Bi*). C3b showed a preferred view when binding to the EM support film and this group of images corresponded to C3b molecules that were not bound to fB under our experimental conditions. A second group, comprising 3530 particles, contained averages very similar to those of the C3bB proconvertase assembled in the presence of Ni^{2+}, where an open conformation of fB has been described (4) (Fig. 1*Bii*). Unexpectedly, a third set of averages revealed a novel structure for the AP C3 proconvertase that was incompatible with the structure of C3bB(Ni^{2+}) (Fig. 1*Biii*) but which resembled some of the structural features of the fully active C3 convertase (C3bBb) obtained after fD cleavage (4) (Fig. 1*D*). As expected, because fD was not present in the incubation, all fB in this sample is intact, in the proenzyme form, as revealed by a Western blotting using a polyclonal Ab that recognizes both full length fB and the Bb fragment (Fig. 1*A*). 588 images were classified into this third group corresponding to ~6% of the total number of images and ~15% of all C3bB proconvertase molecules (Fig. 1*Biii*).

An alternative conformation of C3bB(Mg^{2+}) resembles the structure of the C3bBb convertase and the CVFB complex

The consistency of the new conformation was evaluated by a thorough analysis where the subset of particles initially classified into this group (Fig. 1*Biii*) were further reclassified using a combination of tools such as maximum-likelihood and neural networks (see *Materials and Methods* for details). The improved classification permitted to isolate subsets of very homogeneous particles and the images within each new subgroup were then aligned by reference-free methods to discard any bias. The averages obtained preserved the structural features initially observed, and their improved quality confirmed the existence of the new conformation (Fig. 1*C*). The distinctive feature of these averages was the presence of a strong density projecting from the core of the top of the complex, a feature that is never found in the projections from the C3bB(Ni^{2+}) complex (4). Remarkably, these images were similar though not identical to the EM images obtained for the fully active C3 convertase (C3bBb) (Fig. 1*D*) (4) and the EM images and computational projections of the complex between human fB and CVF (5). Three dots of density at the top right corner of the EM images of C3bBb were interpreted as the projections of the C345C, vWA, and SP domains of the convertase, an assignment now confirmed by the atomic structure of the C3 convertase stabilized by SCIN (6). In this atomic structure of the C3 convertase the SP domain projects outwards from the complex (Fig. 1*Eiii*), and computational projections of a low resolution version of this structure resembled some of the features of the new images obtained now for the C3 proconvertase (Fig. 1*E*, *i* and *ii*). Importantly, the SP domain also appears as a protruding density in the structure of CVFB, where fB was found in a closed conformation similar to the proenzyme (5). In contrast, the averages of the novel conformation (Fig. 1*C*) revealed structural features not found in the EM images of the

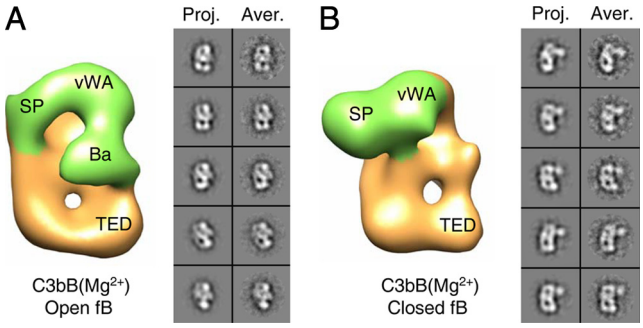

FIGURE 2. The C3bB(Mg^{2+}) complex assembles in two distinct conformations. *A*, One view of the 3D structure of C3bB(Mg^{2+}) with an open conformation of fB. The components and domains of the structure have been mapped by comparing with the structure of C3bB(Ni^{2+}) previously described (4). The C3b molecule is shown in orange color whereas fB is shown in green. Selected computational projections (Proj.) and averages (Aver.) after three-dimensional refinement are shown as an *inset*. *B*, As in *A* but showing the conformation of the C3bB(Mg^{2+}) complex where fB is found in an closed conformation.

C3-convertase (Fig. 1*D*) such as a density that might be related with the presence of the Ba fragment (Fig. 1*C*, white arrows).

In conclusion, the density protruding from the C3 proconvertase in the novel conformation of C3bB(Mg^{2+}) that we have discovered cannot be explained by the open conformation of fB found in the C3bB(Ni^{2+}) complex. The new structure can only be modeled as a conformation where the SP domain projects outwards likely resembling the conformation found in the CVFB complex (5).

Coexistence of two conformations of fB in the C3bB proconvertase

We tested two alternative hypotheses, either that the whole data set (after discarding free C3b) represented projections of a unique conformation for C3bB(Mg^{2+}) or that we had a mixture of at least two conformations, one resembling the previously described structure of C3bB(Ni^{2+}) and another one more closely related to C3bBb and the CVFB complex. A systematic image processing of the data to cover many distinct possibilities clearly indicated that the new averages represented a unique conformation separate from the majority of the data (see *Materials and Methods* for details).

We then used a supervised classification and three-dimensional refinement methods where each particle image was assigned to one of two possible output solutions during each round of refinement. This approach produced two subsets of the data enriched in images belonging to each of the conformations (Fig. 2), and three-dimensional reconstructions for each subgroup were generated. The projections of these two reconstructions and the averages obtained during the three-dimensional refinement nicely matched the structural features of C3bB(Ni^{2+}) or the novel conformation respectively (Fig. 2, *A* and *B*, *insets*), confirming that the procedures used have been capable of assigning most images to their correct conformation. Nevertheless, the resolution of the two structures was limited and we suspect that some images could still be misclassified, distorting the final reconstructions. After convergence of the refinement, roughly 65% of the particles corresponded to a C3bB(Mg^{2+}) complex, solved at 27 Å resolution, with a similar conformation to C3bB(Ni^{2+}) where fB has undergone large conformational changes that promote the access of fD to the cleavage site between the Ba and Bb fragments (4) (Fig. 2*A*). A second conformation accounting for ~35% of the molecules was resolved at 32.5 Å resolution showing fB projecting outwards from the structure as in the CVFB complexes (Fig. 2*B*). In this conformation, the large displacement of the Ba fragment was not detected suggesting that the conformation of fB in this complex could be reminiscent of that in the proenzyme. Whereas the particles assigned to the new conformation in the previous two-dimensional analysis (Fig. 1*B*) contained only those views with a protruding density, additional views were classified and incorporated into the new conformation during three-dimensional refinement, increasing the estimated percentage of molecules corresponding to the novel conformation from 15 to 35%.

Discussion

In this study, we took advantage of observing individual molecules of a complex mixture of protein complexes to computational isolate the major components of the association reaction between C3b and fB in the presence of the physiological cation Mg^{2+}. Our findings indicate that under these conditions, fB binds to C3b to assemble a C3bB complex presenting at least two coexisting structures. One structure depicts an open conformation of fB where the Ba fragment has been displaced and the scissile site is likely exposed for cleavage by fD. This conformation is strongly favored when nickel is used instead of magnesium (4). The other structure shows fB in a closed conformation, projecting from the core of the complex in a way similar though not identical with that observed in the C3bBb convertase (4, 6) and it is compatible with the atomic structure recently solved for the CVFB complex (5). This conformation probably represents an initial recognition complex between the fB and C3b at the stage when the two molecules first interact. This conclusion is in agreement with Janssen et al.'s (5) proposition that their CVFB structure captures the "loading state" of fB to C3b. Importantly, the coexistence of these two conformations of the C3bB proconvertase indicates that the dislocation of the Ba region is not necessarily concomitant to fB loading, but it could be induced after the initial binding to C3b. After fB binding to C3b, the two conformations of the C3bB(Mg^{2+}) proconvertase could either coexist in equilibrium or inevitably transit from the closed to the open conformation.

We built a model using the atomic structure of C3bBb (6) where Bb was substituted by full-length fB after alignment of the vWA domains (Fig. 3). This model closely matched the atomic structure of the CVFB complex and, at the level of resolution of these EM studies, also fitted the novel conformation of the C3bB proconvertase that we have solved in this report. In our model, fB, in the form of the proenzyme, is loaded to C3b through interactions involving both the vWA and the SCR domains. The vWA domain binds C345C whereas residues located in the Ba fragment will contact the αNT region, the MG2, MG7, and CUB domains (5). These interactions are likely sufficient to maintain the complex between a proenzyme-like fB and C3b, whereas the SP domain projects outwards without contacting C3b. After this initial loading, a large conformational change displaces the Ba fragment to generate an "activated" conformation of fB where the scissile site is made accessible to fD.

fB in the open conformation does not project outwards from the structure of the C3bB proconvertase suggesting the existence of extensive contacts between the two proteins (4) (Fig. 2) and that the open conformation of fB, probably unstable, is stabilized on the surface of C3b. As a result of this increased interaction between fB and C3b, the C3bB proconvertase with the open conformation of fB is likely more stable than the C3bB structure with fB in a closed conformation. Previous analysis using surface plasmon resonance have reported that the dissociation rate of the C3bB complex is dependent on the time of incubation of C3b with fB (17). These data, interpreted then to suggest that a time-dependent conformational transition stabilized the interaction between C3b

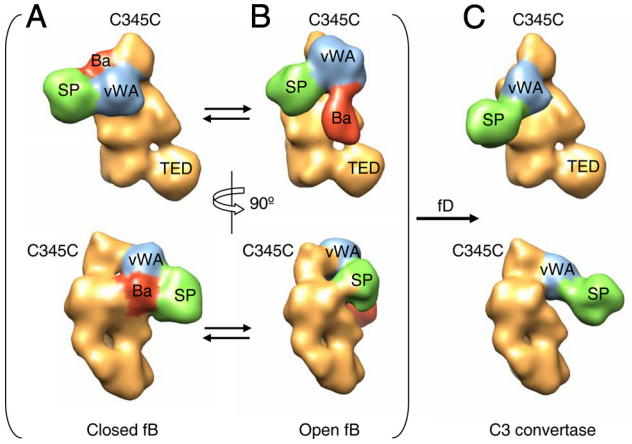

FIGURE 3. Conformational transitions during assembly of the C3 proconvertase. *A*, A model for the new conformation of C3bB described in this work was built by positioning full-length fB within the atomic structure of the C3 convertase (PDB ID 2WIN) (6) so that the vWA domains from both structures were aligned. The model was then filtered to 22 Å. C3b is shown in orange color. The SP and vWA domains and the Ba fragment are shown in green, blue, and red colors respectively. *B*, Three-dimensional model for the open conformation of the C3 proconvertase. This model was generated by filtering to 22 Å the atomic modeling proposed for the C3bB(Ni^{2+}) complex (4). *C*, Low resolution model of the C3 convertase obtained after filtering the atomic structure resolved by Rooijakkers et al. (6) after removing the inhibitor SCIN.

and fB, can now be explained by the transition of fB from a closed to a open conformations during the C3bB proconvertase assembly.

We report in this study that in the case of C3bB(Mg^{2+}), 65% of the complexes corresponded to the open conformation vs 35% of the closed conformation. Interestingly, when we now collected a new dataset of C3b incubated with fB in the presence of Ni^{2+} comprising 10929 images, analyzed in a similar way, the open conformation represented 98% of the C3bB complexes while the closed conformation was only a 2%. Thus, conditions that increase the strength of the interaction between the vWA and the C345C domain and the affinity between C3b and fB, like the presence of Ni^{2+}, seem to favor the open conformation of fB.

The crystal structure of the CVFB complex suggests that in CVF the transition toward the open conformation of fB cannot be completed and C3bB remains in the closed conformation (5). CVF is 49% identical in sequence to C3 (18). One possibility is that the sequences in C3b that stabilize fB in the open conformation are not conserved in CVF and thus, in CVF, the equilibrium strongly favors the closed conformation (5). Although the open conformation should be the optimal state for cleavage by fD, fB in the CVFB complex is also cleaved by fD though with less efficiency (5, 17), perhaps suggesting that fD could cleave the available CVFB complexes in the open conformation displacing the equilibrium. Alternatively, fD could have an active role in the reaction by actively favoring the structural transition toward the open conformation of fB.

In summary, in this work we have demonstrated that fB bound to C3b coexists in at least two conformations, one representing the initial binding of fB to C3b and another one displaying a large conformational opening of fB. The structures that we describe in this study provide further insights into the structural mechanisms implicated in the assembly and activation of the AP C3 proconvertase. Further research should delineate if fD and perhaps also properdin have a role in promoting these structural transitions so that under physiological conditions the structural changes in the C3bB proconvertase toward the open conformation of fB is a favored and essentially irreversible process.

Disclosures

The authors have no financial conflict of interest.

References

1. Walport, M. J. 2001. Complement: first of two parts. *N. Engl. J. Med.* 344: 1058–1066.
2. Milder, F. J., L. Gomes, A. Schouten, B. J. Janssen, E. G. Huizinga, R. A. Romijn, W. Hemrika, A. Roos, M. R. Daha, and P. Gros. 2007. Factor B structure provides insights into activation of the central protease of the complement system. *Nat. Struct. Mol. Biol.* 14: 224–228.
3. Gros, P., F. J. Milder, and B. J. Janssen. 2008. Complement driven by conformational changes. *Nat. Rev. Immunol.* 8: 48–58.
4. Torreira, E., A. Tortajada, T. Montes, S. Rodriguez de Cordoba, and O. Llorca. 2009. 3D structure of the C3bB complex provides insights into the activation and regulation of the complement alternative pathway convertase. *Proc. Natl. Acad. Sci. USA* 106: 882–887.
5. Janssen, B. J., L. Gomes, R. I. Koning, D. I. Svergun, A. J. Koster, D. C. Fritzinger, C. W. Vogel, and P. Gros. 2009. Insights into complement convertase formation based on the structure of the factor B-cobra venom factor complex. *EMBO J.* 28: 2469–2478.
6. Rooijakkers, S. H., J. Wu, M. Ruyken, R. van Domselaar, K. L. Planken, A. Tzekou, D. Ricklin, J. D. Lambris, B. J. Janssen, J. A. van Strijp, and P. Gros. 2009. Structural and functional implications of the alternative complement pathway C3 convertase stabilized by a staphylococcal inhibitor. *Nat. Immunol.* 10: 721–727.
7. Goicoechea de Jorge, E., C. L. Harris, J. Esparza-Gordillo, L. Carreras, E. A. Arranz, C. A. Garrido, M. Lopez-Trascasa, P. Sanchez-Corral, B. P. Morgan, and S. Rodriguez de Cordoba. 2007. Gain-of-function mutations in complement factor B are associated with atypical hemolytic uremic syndrome. *Proc. Natl. Acad. Sci. USA* 104: 240–245.
8. Hourcade, D. E., L. M. Mitchell, and T. J. Oglesby. 1999. Mutations of the type A domain of complement factor B that promote high-affinity C3b-binding. *J. Immunol.* 162: 2906–2911.
9. Mindell, J. A., and N. Grigorieff. 2003. Accurate determination of local defocus and specimen tilt in electron microscopy. *J. Struct. Biol.* 142: 334–347.
10. Heymann, J. B., and D. M. Belnap. 2007. Bsoft: image processing and molecular modeling for electron microscopy. *J. Struct. Biol.* 157: 3–18.
11. Ludtke, S. J., P. R. Baldwin, and W. Chiu. 1999. EMAN: semiautomated software for high-resolution single-particle reconstructions. *J. Struct. Biol.* 128: 82–97.
12. Scheres, S. H., M. Valle, R. Nunez, C. O. Sorzano, R. Marabini, G. T. Herman, and J. M. Carazo. 2005. Maximum-likelihood multi-reference refinement for electron microscopy images. *J. Mol. Biol.* 348: 139–149.
13. Scheres, S. H., R. Nunez-Ramirez, C. O. Sorzano, J. M. Carazo, and R. Marabini. 2008. Image processing for electron microscopy single-particle analysis using XMIPP. *Nat. Protoc.* 3: 977–990.
14. Hourcade, D. E., L. Mitchell, L. A. Kuttner-Kondo, J. P. Atkinson, and M. E. Medof. 2002. Decay-accelerating factor (DAF), complement receptor 1 (CR1), and factor H dissociate the complement AP C3 convertase (C3bBb) via sites on the type A domain of Bb. *J. Biol. Chem.* 277: 1107–1112.
15. Janssen, B. J., A. Christodoulidou, A. McCarthy, J. D. Lambris, and P. Gros. 2006. Structure of C3b reveals conformational changes that underlie complement activity. *Nature* 444: 213–216.
16. Wiesmann, C., K. J. Katschke, J. Yin, K. Y. Helmy, M. Steffek, W. J. Fairbrother, S. A. McCallum, L. Embuscado, L. DeForge, P. E. Hass, and M. van Lookeren Campagne. 2006. Structure of C3b in complex with CRIg gives insights into regulation of complement activation. *Nature* 444: 217–220.
17. Harris, C. L., R. J. Abbott, R. A. Smith, B. P. Morgan, and S. M. Lea. 2005. Molecular dissection of interactions between components of the alternative pathway of complement and decay accelerating factor (CD55). *J. Biol. Chem.* 280: 2569–2578.
18. Fritzinger, D. C., R. Bredehorst, and C. W. Vogel. 1994. Molecular cloning and derived primary structure of cobra venom factor. *Proc. Natl. Acad. Sci. USA* 91: 12775–12779.

Measurement of Factor H Variants in Plasma Using Variant-Specific Monoclonal Antibodies: Application to Assessing Risk of Age-Related Macular Degeneration

Svetlana Hakobyan,[1] *Claire L. Harris,*[1] *Agustín Tortajada,*[2] *Elena Goicochea de Jorge,*[2] *Alfredo García-Layana,*[3] *Patricia Fernández-Robredo,*[3] *Santiago Rodríguez de Córdoba,*[2] *and B. Paul Morgan*[1]

Purpose. The Y402H polymorphism in the complement regulator factor H (fH) is strongly associated with age-related macular degeneration (AMD) across diverse populations. Persons homozygous for histidine at this position have up to 12-fold greater risk for AMD than those homozygous for tyrosine. Knowledge of fH-Y402H status is, therefore, valuable in predicting risk and focusing preventive measures in the elderly. This knowledge requires genetic analysis, which is unavailable in most laboratories and which provides no information about the levels of fH protein, a putative linked determinant of disease risk.

Methods. The authors describe novel monoclonal antibodies that distinguish the two fH allelic variants in plasma. ELISA with these antibodies not only reliably identifies the fH-Y402H status, confirmed by genotyping, but also quantifies the concentration of total fH and the fH-Y402 and fH-H402 variants.

Results. In young adult control subjects, mean fH concentration was 233 mg/L. In elderly control subjects, mean fH concentration was 269 mg/L, whereas in a matching AMD cohort, mean fH concentration was 288 mg/L. Total fH concentration was similar in each subgroup of young and elderly control subjects; however, in the AMD group, fH concentration was significantly higher in the heterozygous subgroup. Measurement of the two variants in this subgroup showed that both were elevated to a similar degree.

Conclusions. The novel monoclonal antibody MBI-7 was used to develop a robust assay for measurement of fH and the variants in plasma. The simplicity of the assay means that it may be used by any clinical laboratory to identify polymorphic status and to quantify plasma levels in persons at risk for AMD. (*Invest Ophthalmol Vis Sci.* 2008;49:1983–1990) DOI: 10.1167/iovs.07-1523

Complement factor H (fH) is the major fluid-phase regulator of the alternative pathway of complement and plays a key role in controlling complement activation in vivo. fH is produced mainly in the liver and is reported to be present in plasma at a concentration of approximately 500 mg/L.[1] The molecule is made up entirely of a string of 20 folded globular domains known as short consensus repeats (SCRs).[2]

The relevance of fH to homeostasis is apparent in patients with fH deficiency; uncontrolled complement activation consumes the components, rendering the patient secondarily deficient in C3 and, hence, susceptible to pyogenic infections.[3,4] Importantly, persons deficient in fH are susceptible to a specific pathologic renal condition, type II membranoproliferative glomerulonephritis (MPGN II), not seen in association with primary C3 deficiency, implying a unique and undefined role for fH in protecting the kidney from injury. In addition, common polymorphisms and rare mutations in fH have been described and shown to be associated with other diseases, including atypical hemolytic uremic syndrome (aHUS) and age-related macular degeneration (AMD).[5]

AMD is the leading cause of vision loss in the elderly in Western societies, with the severe, vision-threatening complications of geographic atrophy (GA) and choroidal neovascularization (CNV) accounting for nearly 50% of all blindness in the Western world.[6] Two major AMD susceptibility loci (1q31, *CFH*, and 10q26, LOC387715/HTRA1) that independently contribute to risk for AMD have been identified recently by candidate region linkage studies and whole genome association analyses.[7–12] At the *CFH* locus, the Y402H polymorphism, which represents a tyrosine (Y) to histidine (H) change at position 402 within SCR 7 of fH, is strongly associated with the disease and has been suggested as a global marker for AMD.[13] Persons homozygous for the H402 isoform of fH (fH-H402; 10% of Caucasians) were at increased risk for AMD compared with those homozygous for the fH-Y402 variant, which ranged between 3-fold and 12-fold in the published cohorts. No increased risk was found in Japanese or Chinese cohorts; however, the H402 variant is rare in these populations.[14–16]

Identification of H402-homozygous persons at high risk for disease would enable clinicians to provide an accurate risk assessment and initiate strategies to reduce extrinsic risk factors or even to implement prophylactic therapy. Current methods for identifying the fH-Y402H status of a patient require extraction of DNA followed by tedious and expensive sequencing analysis that can only be provided within specialized diagnostic laboratories. A serum assay that differentiates the relevant fH variants would simplify diagnosis and enable the screening of relevant at-risk populations. Additionally, it would provide information on the serum levels of fH that may be relevant to disease risk. Although the variants differ by only a

From the [1]Department of Medical Biochemistry and Immunology, School of Medicine, Cardiff University, Cardiff, United Kingdom; the [2]Department of Molecular and Cellular Physiopathology, Centro de Investigaciones Biologicas and Centro de Investigación Biomedica en Red de Enfermedades Raras, Madrid, Spain; and the [3]Department of Ophthalmology, University Clinic of Navarra University, Pamplona, Spain.

Supported by Wellcome Trust Programme Grant 068590 (BPM), Wellcome Trust University Award 068823 (CLH), Spanish Ministerio de Educación y Cultura Grant SAF2005–00913 (SRdC), and Ministerio de Sanidad y Consumo, Tecnologias Sanitarias Grant 06/90133 (AG-L).

Submitted for publication November 27, 2007; revised December 18, 2007 and January 2, 2008; accepted March 3, 2008.

Disclosure: **S. Hakobyan,** None; **C.L. Harris,** None; **A. Tortajada,** None; **E. Goicochea de Jorge,** None; **A. García-Layana,** None; **P. Fernández-Robredo,** None; **S. Rodríguez de Córdoba,** None; **B.P. Morgan**, None

The publication costs of this article were defrayed in part by page charge payment. This article must therefore be marked "*advertisement*" in accordance with 18 U.S.C. §1734 solely to indicate this fact.

Corresponding author: B. Paul Morgan, Department of Medical Biochemistry and Immunology, Henry Wellcome Building, School of Medicine, Cardiff University, Heath Park Way, Cardiff CF14 4XN, UK; morganbp@cardiff.ac.uk.

single amino acid, we reasoned that monoclonal antibodies (mAbs) might be generated that would differentiate between the two, permitting the development of an assay to reveal risk for AMD from routine serum samples.

We here describe the production, characterization, and use of such reagents in the development of a variant-specific, direct sandwich enzyme-linked immunosorbent assay (ELISA) for the quantification of total fH and the fH-Y402 and fH-H402 variants in serum or plasma. The assays have been validated against the gold standard of DNA genotyping and show 100% accuracy in identifying the fH-Y402H status in healthy persons and AMD patients. In addition, the assays provide valuable information regarding the concentration of fH variants in plasma that we anticipate will help explain the association of the fH-H402 protein with AMD.

Materials and Methods

Generation of fH-Immunoglobulin Fusion Proteins as Immunogen

Immunoglobulin fusion proteins comprising SCR6–8 of human fH and the Fc portion of human IgG4 (fH-Fc) were prepared using published methods.[17,18] Briefly, cDNA encoding SCR6–8 of fH with H at amino acid position 402 in SCR7 was amplified by RT-PCR from RNA prepared from peripheral blood mononuclear cells (PBMCs). DNA was ligated in frame with the CD33 signal sequence (SigpIg; R&D Systems, Minneapolis, MN), as previously described,[19] and then subcloned into the expression vector pDR2ΔEF1α (gift from Ignacio Anegon, INSERM U437, Nantes, France). DNA was cloned upstream of and in-frame with that encoding the hinge and Fc domains of human IgG4, as previously described.[19] Using this vector as template, a second expression vector was prepared that encoded SCR6–8 of fH-Y402. Two-stage join-up PCR was used to introduce a mutation in the H402 codon such that it was replaced with Y. DNA was cloned into pDR2ΔEF1α in-frame with DNA encoding IgG4 Fc, as described. Sequencing confirmed that no errors had been introduced by PCR. Chinese hamster ovary (CHO) cells were transfected with these plasmids using lipofectamine (Invitrogen, Carlsbad, CA) according to the manufacturer's instructions. Stable lines were selected with 400 mg/L hygromycin B (Invitrogen) in RPMI-1640 (Gibco, Invitrogen) medium supplemented with 10% heat-inactivated fetal bovine serum (FBS; Gibco, Invitrogen) and maintained in hygromycin B (100 mg/L) in 5% FBS-RPMI-1640. The fH-Fc constructs were purified from the culture supernatant by protein-A affinity chromatography (HiTrap Protein A; GE Healthcare, Chalfont, St. Giles, UK), as described.[17]

Identification of Subjects Homozygous for H402 and Y402 Variants

The polymorphism of *CFH* at the nucleotide position 1277, corresponding to amino acid position 402, was analyzed by PCR. Venous blood (5 mL) was collected in EDTA-containing tubes. Genomic DNA was extracted from buffy coat by proteinase K/phenol/chloroform extraction and ethanol precipitation. A fragment of 458 bp containing exon 9 of the *CFH* gene was amplified from genomic DNA using specific primers derived from the 5′ and 3′ intronic sequences (forward, 5′-CCT TTG TTA GTA ACT TTA GTT CGT C-3′; reverse, 5′-GGT CCA TTG GTA AAA CAA GG-3′). PCR was performed with the use of a polymerase kit (Platinum Blue PCR SuperMix; Invitrogen) in a final volume of 25 μL The thermal profile consisted of an initial denaturation step at 94°C for 3 minutes; 35 cycles of denaturation at 94°C for 30 seconds, annealing at 57°C for 1 minute, and polymerization at 72°C for 30 seconds; and a terminal extension at 72°C for 10 minutes. Amplification was verified by electrophoresis of PCR products on 1.6% agarose gels. PCR products were purified using a PCR purification kit (QIAquick; Qiagen, Valencia, CA). Direct sequencing of PCR products was performed using an amplification primer (3130xl Genetic Analyser; ABI Prism; Applied Biosystems, Foster City, CA).

Purification of Full-Length fH from Human Plasma

fH was purified from the plasma of subjects homozygous for either the H402 or the Y402 variants by a sequential three-step FPLC method at 4°C on ÁKTAprime (GE Healthcare). First, filtered plasma (100 mL) was applied to a 5-mL column (HiTrap; GE Healthcare) to which 10 mg mouse anti-human fH mAb 35H9 (generated in house) was coupled. Bound protein was eluted at low pH, and fractions containing fH (identified by ELISA) were pooled, dialyzed against phosphate-buffered saline (PBS; 137 mM NaCl, 10 mM phosphate, 2.7 mM KCl, pH 7.4), and applied to a heparin column (HiTrap; GE Healthcare) equilibrated with PBS. Bound proteins were eluted with 1 M NaCl in PBS. Fractions containing fH were pooled and polished by gel filtration on preparative grade matrix (Superdex-200; GE Healthcare) in a XK16/70 column (GE Healthcare). Purity was confirmed by sodium dodecyl sulfate–polyacrylamide gel electrophoresis (SDS-PAGE); using plasma from identified homozygous donors, preparations of fH-H402 and fH-Y402 were obtained without any detectable contaminants or aggregates by this three-step method (Figs. 1A, B). Proteins were also free of fH-like-1 (FHL-1) and fH-related proteins. Yield was 25% to 50% and was similar for the two variants. Purified fH was used for testing established mAb and as a primary standard in the ELISA.

To obtain absolute protein concentrations for the fH assay standard, aliquots of pure fH-Y402 and fH-H402 (in 20 mM Tris buffer [pH 7.4], 150 mM NaCl) of known absorbance at 280 nm were lyophilized to dryness and hydrolyzed by incubation in 6 M HCl for 24 hours at 110°C. Standard (norleucine, 3 nM) was added, and the resultant amino acids were quantified on an amino acid analyzer (Biochrom 20; Pfizer, New York, NY). From these data, extinction coefficients (ε) at 280 nm for the fH-Y402 and fH-H402 proteins were calculated to be 2.0 and 1.9 $cm^{-1}(mg/mL)^{-1}$, respectively, reflecting the additional absorbing Y residue in the former. A mean value of 1.95 $cm^{-1}(mg/mL)^{-1}$ was used for subsequent fH preparations so that an absorbance at 280 nm of 1.0 corresponded to 513 mg/L.

Immunization and Generation of Monoclonal and Polyclonal Antibodies

Female BALB/c mice were immunized subcutaneously four times at 3-week intervals with 100 μg fH(6–8)-H402-Fc in Freund adjuvant, as described. Three weeks after the last injection, the mouse with the highest titer of anti-fH antibodies (tested in ELISA) was boosted intraperitoneally with 100 μg fH(6–8)-H402-Fc in PBS. Three days later, the spleen was harvested, and splenocytes were fused with a mouse myeloma cell line Sp2/0-Ag, as described.[20] Hybridoma clones were selected and screened in ELISA for reactivity toward purified fH from pooled plasma. Positive clones were further screened for reactivity by comparing their binding activity to purified fH-H402 and fH-Y402 in ELISA. Hybridomas producing mAbs that recognized only fH-H402 variant were identified, subcloned, and expanded. The mAbs were purified by protein G affinity chromatography (HiTrap Protein G; GE Healthcare). The isotype of the mAb was determined using an isotyping kit (IsoStrip Mouse Monoclonal Antibody Isotyping Kit; Roche Applied Science, Indianapolis, IN) according to the manufacturer's instructions. A similar strategy was adopted for obtaining fH-Y402—specific mAb by immunizing with fH(6–8)-Y402-Fc. No hybridomas producing mAb specific for the fH-Y402 variant were identified in any of three fusions.

Rabbit antiserum against fH was produced by repeated immunization with pure fH in adjuvant. Specific immunoglobulin was purified from antiserum by affinity chromatography using fH immobilized on a NHS column (Hi-Trap; GE Healthcare). Aliquots of mAb and affinity-purified rabbit polyclonal anti-fH antibody were labeled with horseradish peroxidase (EZ-Link Plus Activated Peroxidase Kit; Pierce Biotechnology, Inc., Rockford, IL). Animals were handled in accordance with

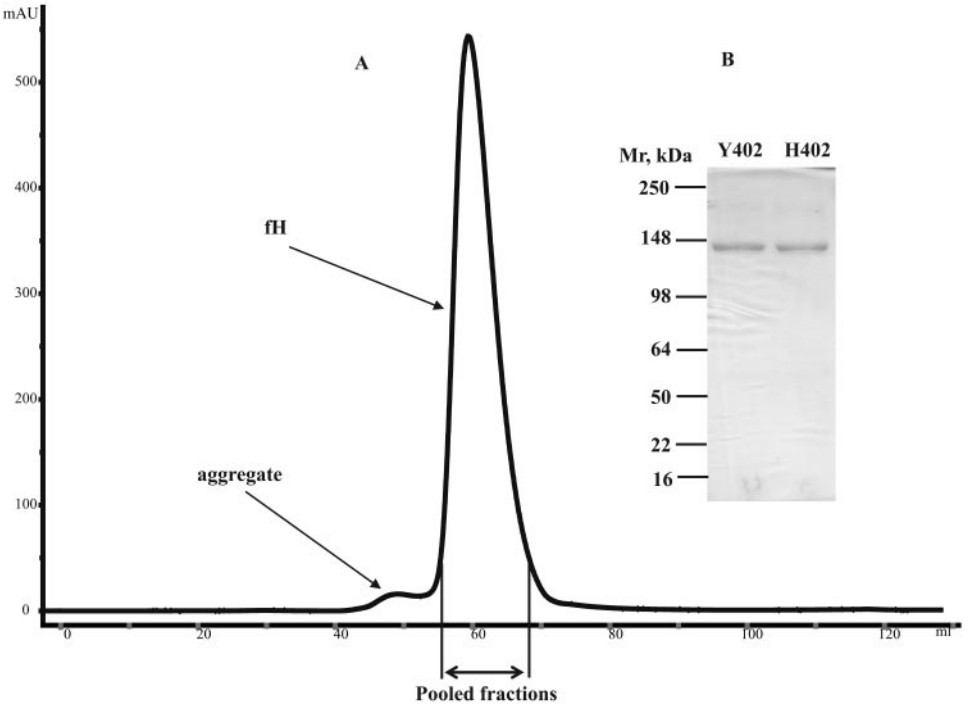

FIGURE 1. (**A**) Gel-filtration chromatogram from the final step of plasma fH purification after immunoaffinity and heparin affinity steps. The *y*-axis (milliabsorbance units [mAU]) plots absorbance at 280 nm, and the *x*-axis plots retention time in minutes. (**B**) Coomassie staining of final fH preparations.

the ARVO Statement for the Use of Animals in Ophthalmic and Vision Research.

Confirmation of Specificity of mAbs

Western Blotting. fH-H402 and fH-Y402 were subjected to SDS-PAGE and transferred to a nitrocellulose membrane. After blocking with 5% skimmed milk in PBS, the membrane was washed in PBS-Tween 20 (0.1% vol/vol) and incubated with the mAb (5 mg/L) in PBS-5% milk for 1 hour at room temperature. After extensive washing in PBS-Tween 20, bound mAb was detected using an HRP-conjugated goat anti-mouse IgG and visualized by enhanced chemiluminescence (ECL; GE Healthcare).

Dot Blotting. Serial dilutions of fH-H402 and -Y402 variants were spotted on a nitrocellulose membrane using a microfiltration apparatus (Bio-Dot SF; Bio-Rad, Hercules, CA). After blocking, immobilization of the proteins was confirmed by immunodetection, as described.

ELISA. fH-H402 and -Y402 variants (5 mg/L in bicarbonate coating buffer, pH 9.6) were immobilized on a microtiter plate for 1 hour at 37°C. After blocking in 1% PBS-BSA, serial dilutions of mAb in blocking buffer were added. The interaction was detected by an HRP-conjugated goat anti-mouse IgG in combination with orthophenylenediamine (OPD; AbD Serotec, Martinsreid, Germany).

Surface Plasmon Resonance Analysis. Binding of mAb to fH-H402 and -Y402 variants was analyzed by surface plasmon resonance using a biosensor (Biacore 3000; Biacore, Uppsala, Sweden). fH-H402 or -Y402 (300 RU) was immobilized on the CM-5 sensor chip using the amine-coupling kit (Biacore) according to the manufacturer's instructions. The reference flow cell was activated with ethyl-*N*-(3-diethylaminopropyl)carbodiimide and N-hydroxysuccinimide and was blocked with ethanolamine. Binding experiments were performed in HBS-P buffer (10 mM HEPES, pH 7.4, 150 mM NaCl, 0.005% P20 surfactant). mAb was injected in triplicate at concentrations of 0 (blank control), 6.25, 12.5, 25, 50, and 100 nM, at a flow rate of 20 μL/min for 1 minute and a dissociation time of 15 minutes. Reference curves were obtained by injection of mAb over the reference flow cell. Experimental data were corrected for the reference and blank control and were analyzed using Biacore software (BIAevaluation 4.1). The kinetic association, k_a, and dissociation, k_d, constants were estimated by global fitting analysis of the binding curves to the 1:1 Langmuir interaction model. The equilibrium dissociation constant (K_D) was calculated as $K_D = k_d/k_a$.

As a positive control in this series of experiments, mouse anti-human fH mAbs OX-24[21] and 35H9, which detect both variants of fH, were used.

Development of a Quantitative ELISA Distinguishing the fH-Y402H Variants

Affinity-purified rabbit anti-fH was diluted in coating buffer and dispensed into a 96-well microtiter plate at 0.5 μg/well. After 1 hour at 37°C, the plate was washed in PBS/0.1% Tween 20 (PBS/T) and then blocked with 1% BSA in PBS. After washing, standards or serum samples (100 μL, diluted 1:5000 in PBS) were added in triplicate or duplicate and incubated for 1 hour. Wells were washed and either HRP-labeled affinity-purified rabbit anti-fH (100 μL; 1 mg/L) or HRP-labeled H402-specific mAb (100 μL; 1 mg/L) added to measure total fH or fH-H402, respectively. After 1 hour, wells were washed three times, and bound antibody was detected using OPD substrate. Development was stopped by the addition of 10% sulfuric acid, and absorbance at 492 nm was measured. All incubation steps were performed for 1 hour at 37°C unless stated otherwise. Purified fH-H402 and an equimolar mixture of both variants were used as standards for estimation of plasma fH-H402 and total fH, respectively. Concentrations of total fH and fH-H402 in plasma were calculated by reference to the appropriate calibration curve prepared from the standards and expressed as milligram per liter of plasma. Standards were included on each plate, and the genotypes of subjects were not known before assay. Concentration of fH-Y402 was calculated by subtraction of fH-H402 from total fH concentration. The detection limit and working range in the ELISA were determined, as described.[22]

Measurement of fH Variants in Plasma Samples from Healthy Donors and AMD Patients

Samples were collected for studies approved by the Ethics Committee of the University of Navarra, and the study described adhered to the tenets of the Declaration of Helsinki. Written informed consent was obtained from all participants.

EDTA plasma was obtained from freshly drawn blood from 63 healthy young volunteers (Cardiff cohort; mean age, 35.0 years).

Plasma was separated within 1 hour of collection and was stored in aliquots at −80°C. fH variant concentrations in plasma samples were measured as described. Identical standards were used in each ELISA plate, and samples from control subjects and AMD patients were randomly assigned to plates to eliminate any possibility of bias in the assay.

fH concentration and the concentrations of the Y402 and H402 variants were also measured in plasma samples from 53 AMD patients (36 with the wet form and 17 with the dry form) and 75 age- and sex-matched control subjects (Spanish cohort). Most participants in the Spanish cohorts were current or recent smokers, making it impossible to independently assess effects of smoking behavior. All controls were examined by trained ophthalmologists to screen for any form of AMD.

Statistical Analysis

Data evaluation was performed with SPSS 13.0 (SPSS Inc., Chicago, IL). Obtained data were checked for normality with Komologrov-Smirnov test. The fH concentration in human plasma was expressed as the mean ± SD for each group. After a significant one-way ANOVA, differences between groups were evaluated using Student's *t*-test for independent samples. $P < 0.05$ was considered significant.

Results

Preparation and Characterization of Anti-fH-H402 mAb

From 20 positive wells cloned by limiting dilution, three stable anti-fH hybridomas were obtained that preferentially bound fH-H402 in screening ELISA; all were IgG_1 isotype. One of these, designated MBI-7, was confirmed in subsequent ELISA (Fig. 2A), dot blot, and Western blot (Fig. 2B) assays to react exclusively with fH-H402. Blotting of plasma samples from heterozygous donors or those homozygous for fH-H402 or fH-Y402 confirmed the specificity of MBI-7 for fH-H402 (Fig. 2C). The mAb was grown in bulk and purified. As a further test of specificity, plasma from homozygous or heterozygous donors was applied to a column of MBI-7-sepharose. This column failed to bind any fH from fH-Y402 homozygous donors, efficiently bound fH-H402 from fH-H402 homozygous donors, and selectively bound only fH-H402 from heterozygous donors (data not shown).

Comparison of the relative affinities of MBI-7 and OX-24 for fH-Y402 and fH-H402 was performed by surface plasmon resonance analysis (Biacore 3000; Biacore). The 1:1 Langmuir interaction data-fitting model was used to predict dissociation constants (K_D; Table 1). MBI-7 failed to bind fH-Y402 but bound fH-H402 with a K_D of 1.7 nM, whereas OX-24 bound both variants with a similar K_D (approximately 0.1 nM).

Establishment of a Sandwich ELISA for Quantification of Total fH and Its H402 Variant

Sandwich ELISA for quantification of the two forms of fH in plasma or serum samples was developed by using affinity-purified rabbit anti-fH as capture and either HRP-labeled affinity-purified rabbit anti-fH (to measure total fH) or HRP-labeled MBI-7 (to measure fH-H402) as detection. Calibration curves using different proportions of the fH variants as standard were identical for the total fH assay and precisely reflected the proportion of fH-H402 for the fH-H402-specific assay (not shown). Plasma and serum samples were diluted 1:5000 for assay; the calculated detection limit of the assay was 0.007 mg/L, and the working range was 0.01 to 0.2 mg/L. Assay performance was assessed by taking multiple measures from independently diluted aliquots of the same plasma samples, either within the same assay or in separate assays. The within-assay precision ranged from 4.1% to 7.0%, with an average of 5.5% for total fH measurement, and from 7.7% to 12.8%, with an average of 11.0% for fH-H402 measurement. Between-assay precision ranged from 4.9% to 10.1%, with an average of 8.0% for total fH measurement, and from 10.1% to 15.8%, with an average of 12.5% for fH-H402 measurement.

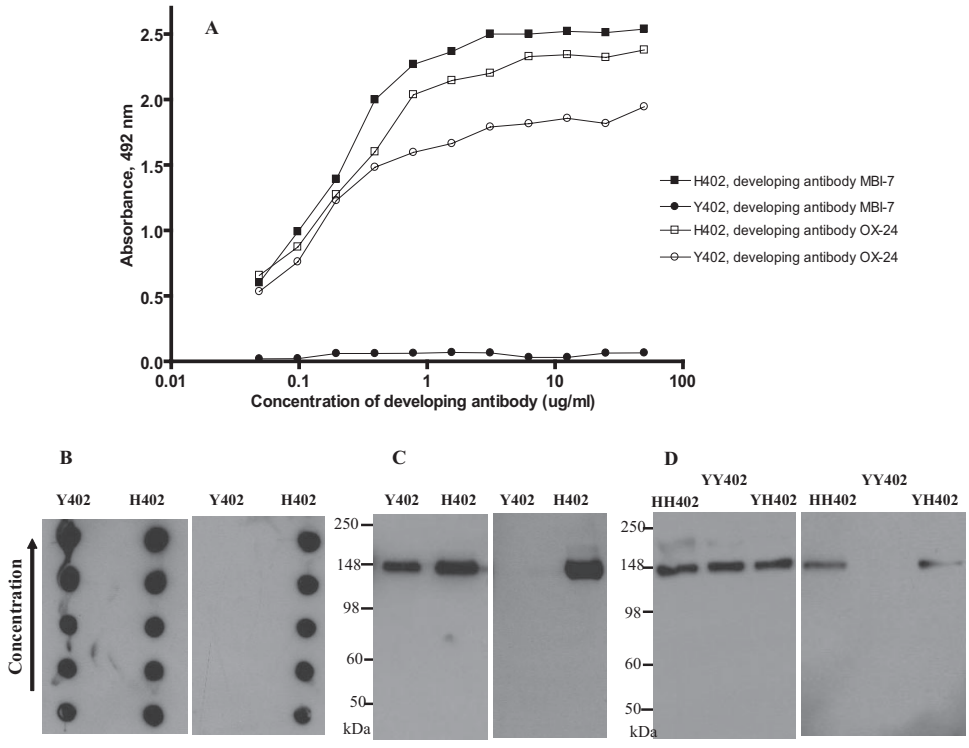

Figure 2. Specific detection of fH-H402 with MBI-7. (**A**) ELISA with each fH variant directly immobilized on plate. (**B**) Dot blot for detection of fH variants using nonselective (OX-24; *left*) and H402-specific (MBI-7; *right*) mAb. (**C**) Western blot detection of purified fH variants using mAb, as described. (**D**) Western blot detection of fH in plasma samples of H402 homozygous, Y402 homozygous, and YH402 heterozygous participants using mAb, as described.

TABLE 1. Kinetic Constants for the Interaction of OX-24 and MBI-7 Monoclonal Anti-fH Antibodies with Immobilized fH-H402 (300 RU) or fH-Y402 (300 RU) as Determined by Surface Plasmon Resonance

	k_a (1/Ms)	k_d (1/s)	K_D (M)	R_{max} (RU)
OX-24 with fH-H402	3.36×10^5	3.98×10^{-5}	1.19×10^{-10}	49.8
MBI-7 with fH-H402	4.01×10^5	6.8×10^{-4}	1.69×10^{-9}	49.3
OX-24 with fH-Y402	2.74×10^5	3.27×10^{-5}	1.19×10^{-10}	60.0
MBI-7 with fH-Y402	NB	NB	NB	NB

NB, no binding detected.

Measurement of Total fH and Its H402Y Variants in Healthy Donors and AMD Patients

Concentrations of total fH and fH-H402 were measured by ELISA in plasma from 63 healthy donors collected in the Cardiff laboratory (Table 2; Fig. 3A); concentration of fH-Y402 was calculated by subtraction. Y402H status of donors in this group, assigned by ELISA, was verified by subsequent genotyping of DNA of 30 of the donors; in every donor genotyped, the status assigned by ELISA was confirmed (data not shown). Of note, the concentrations of fH measured in the assay using, for the first time, absolute protein standards obtained with the extinction coefficient measured as described were less than half those quoted in the literature.[1,23] Previous studies have assumed an extinction coefficient close to 1.0 $cm^{-1}(mg/mL)^{-1}$ and so have systematically overestimated plasma concentrations. In young healthy donors, the mean total fH concentration was 233 mg/L and was not different in the three groups (YY402, YH402, and HH402). In the HH402 group, the fH-H402–specific ELISA yielded values almost identical with those obtained from the same samples in the total fH assay (mean, 260 mg/L vs. 249 mg/L). YY402 values were not above background in this assay, but YH402 donors had intermediate values, as expected (Fig. 3B).

Plasma samples from a cohort of Spanish patients with diagnoses of AMD ($n = 53$; 17 dry AMD, 36 wet AMD) and age- and sex-matched healthy controls ($n = 75$) were also analyzed (Table 3; Fig. 4). Y402H variant status was readily assigned from the ELISA and revealed an increased frequency of the H allele in the patients (Y/H ratios: 0.73:0.27 in controls and 0.59:0.41 in patients). Results were verified by genotyping of DNA of all donors; in every donor, the status assigned by ELISA was confirmed. Total fH concentration in the controls was not different among the three groups (YY402, HH402, YH402), whereas in AMD patients, total fH concentration was significantly higher in the YH402 group than in either the YY402 or the HH402 group (Fig. 4A). To further explore this observation, the concentrations of fH-H402 and fH-Y402 in heterozygous patients and controls was measured (Fig. 4B). Both variants were elevated to a similar degree in patients compared with controls.

DISCUSSION

A considerable body of evidence is accumulating to support the conjecture that AMD is a disease caused by dysregulation of the alternative complement pathway. The first clues came from the demonstration that complement components and regulators are abundant in drusen, the pathologic hallmark of AMD.[24–26] The discovery that a common polymorphism in fH, the principal fluid-phase regulator of the alternative pathway, is a major risk factor for AMD brought complement to the fore.[7–10] Recently, several other complement associations have been described, including a common fH haplotype that includes deletion of the fH-related proteins 1 and 3 (fHR-1 and fHR-3) and is protective against AMD.[27,28] The common F/S polymorphic variant in C3, the key player in the alternative pathway, has recently been reported to modulate risk for AMD,[29] and protective haplotypes in the linked C2/fB genes have been described.[30,31] A recent analysis of polymorphisms in the gene encoding fH described seven SNPs that modulated susceptibility to AMD; of these, only two (rs1061170, Y402H; rs800292, I62V) caused amino acid changes in the fH protein.[32] The other five were synonymous exonic substitutions or changes in noncoding regions, all of which are likely to mediate their effects by modulating expression levels of the gene to alter fH concentrations in plasma.

Identification of carriers of risk alleles for fH and other complement proteins would aid prediction of disease risk and

TABLE 2. Characteristics of fH Concentrations in the Cardiff Control Cohort

Characteristics	Values
No. of subjects	63
Females (%)	62
Age (years)*	35.03 ± 8.88 (21–56)
fH concentration (mg/L)*	233.24 ± 56.65 (135.54–349.27)
Y402 homozygous (%)	44.4
Y402 homozygous (fH; mg/L)*	220.63 ± 61.83 (102.28–359.35)
H402 homozygous (%)	15.9
H402 homozygous (fH; mg/L)*	248.89 ± 58.51 (172.06–348.65)
Y402H heterozygous (%)	39.7
Y402H heterozygous (fH; mg/L)*	230.21 ± 49.60 (132.28–339.81)
Y402H heterozygous (H402; mg/L)*	136.86 ± 41.64 (48.45–222.68)
Y402H heterozygous (Y402; mg/L)*	92.95 ± 37.84 (30.54–177.67)
Y402: H402 allele frequency	0.64 : 0.36

fH-Y402H polymorphic status was assigned from the ELISA and confirmed by sequencing. The total fH concentration and concentrations (in mg/L) of each variant were determined in each subgroup.

* Values are mean ± SD (range).

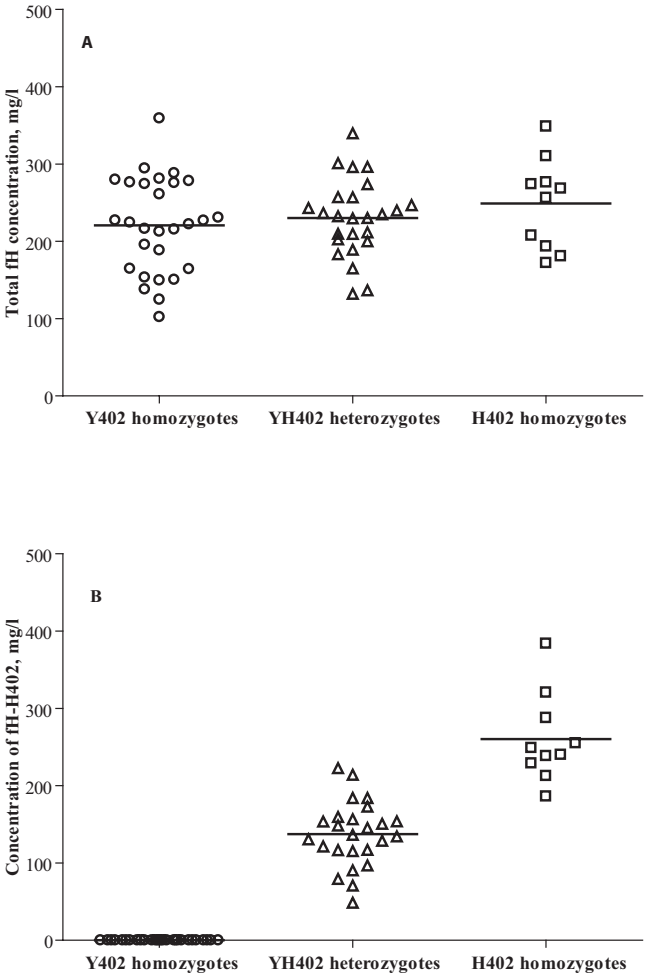

FIGURE 3. (**A**) Concentration of total fH in Y402 homozygous, Y402H heterozygous, and H402 homozygous subjects in the Cardiff control cohort. (**B**) Concentrations of fH-H402 variant in Y402 homozygous, Y402H heterozygous, and H402 homozygous subjects in Cardiff control cohort.

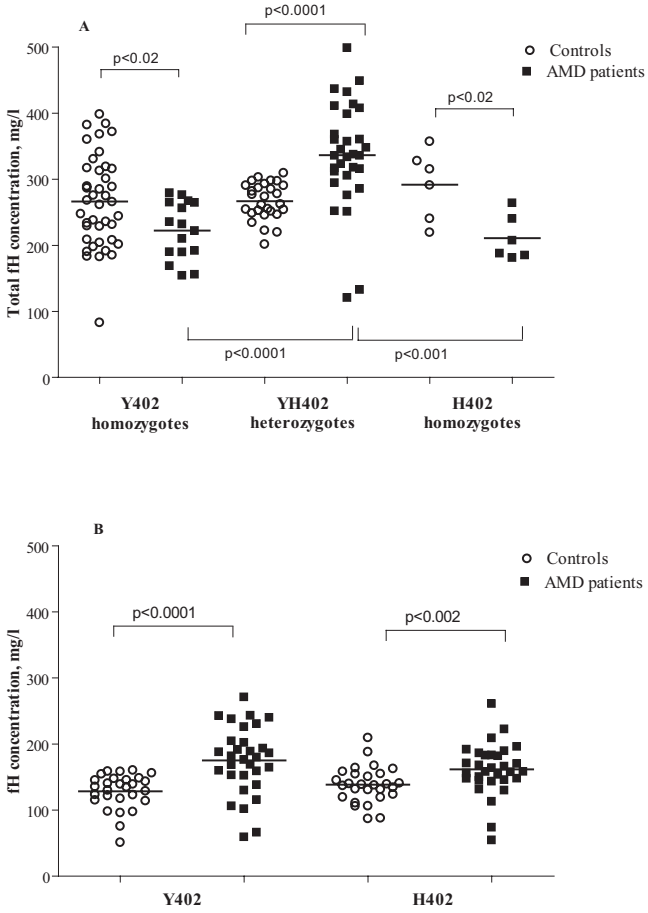

FIGURE 4. (**A**) Concentrations of total fH in Y402 homozygous, Y402H heterozygous, and H402 homozygous participants in the elderly control and AMD groups. (**B**) Concentrations of the fH variants in Y402H heterozygous participants in the elderly control and AMD groups.

guide attempts to reduce risk. For example, smoking is an important extrinsic risk factor for AMD, and it has recently been demonstrated that smoking is a much greater risk factor in those carrying the H402 allele.[33,34] Targeting smoking cessation therapies to this group would be of particular benefit. Interestingly, smoking has previously been associated with lower plasma levels of fH.[35] Current genotyping methods are not well suited for rapid screening in the clinic; a rapid, simple, and accurate serum test, amenable to near-patient use, is there-

TABLE 3. Characteristics of fH Concentrations in the Spanish Control and AMD Cohorts and Concentrations (in mg/L) of Each Variant Were Determined in Each Subgroup

	Controls	AMD
No. of subjects	75	53
Females (%)	40.0	43.4
Age (years)*	72.92 ± 6.40 (58–89)	75.98 ± 8.13 (56–93)
FH concentration (mg/L)*	268.69 ± 55.62 (83.05–398.38)	287.84 ± 88.44 (120.49–498.76)
Y402 homozygous (%)	54.7	30.2
Y402 homozygous (fH; mg/L)*	266.48 ± 69.03 (83.05–398.38)	222.37 ± 43.49 (150.41–279.41)
H402 homozygous (%)	8.0	11.3
H402 homozygous (fH; mg/L)*	291.87 ± 52.89 (219.47–357.16)	210.91 ± 34.03 (181.11–264.02)
Y402H heterozygous (%)	37.3	58.5
Y402H heterozygous (fH; mg/L)*	266.97 ± 27.73 (201.46–309.53)	336.52 ± 80.62 (120.49–498.76)
Y402H heterozygous (H402; mg/L)*	138.47 ± 27.14 (87.06–209.57)	161.53 ± 39.11 (54.37–260.90)
Y402H heterozygous (Y402; mg/L)*	128.50 ± 26.27 (50.84–160.15)	175.00 ± 51.34 (59.12–270.79)
Y402/H402 allele frequency	0.73/0.27	0.59/0.41

fH-Y402H polymorphic status was assigned from the ELISA and confirmed by sequencing. The total fH concentration and concentrations (in mg/L) of each variant were determined in each subgroup.

* Values are mean ± SD (range).

fore needed to identify the polymorphic status of the patient and also to give information on the plasma levels of fH protein. To this end, we first generated a panel of mAbs against SCR6–8 of fH and screened these for mAbs that specifically detected only one of theY402H polymorphic variants. One mAb, termed MBI-7, was strongly reactive against fH-H402 and showed no reactivity against fH-Y402 in multiple tests. This mAb specifically bound native fH-H402 in ELISA and immunoaffinity purification protocols and denatured fH-H402 after SDS-PAGE and Western blotting.

These findings demonstrate that this single, nonconservative amino acid change is sufficient to create a unique epitope in fH-H402. Indeed, a recent paper describes the production of polyclonal antipeptide antibodies that, after multiple adsorption and purification steps, differentiate the fH-Y402H variants in Western blot analysis.[36] However, no fluid-phase binding data were presented for these reagents, suggesting that, in common with many antipeptide reagents, they detect only the denatured molecule and are unsuitable for ELISA or other fluid-phase assays. There are numerous precedents in the literature in which single-residue substitutions have been shown to create or delete an epitope for a specific mAb in a large protein, such as mAbs that differentiate hemoglobins A and S[37] and placental and germ-line alkaline phosphatase.[38] Often, these changes are associated with conformational changes in the protein that amplify the differences between the two forms.[39,40] Several recent studies have investigated the structural consequences of the fH-Y402H polymorphism. Comparison by ultracentrifugation and x-ray scattering of fH SCR6–8 constructs containing either H or Y at the relevant position in SCR7 revealed no major differences other than a small increase in self-association for the former,[41] while comparison of nuclear magnetic resonance structures of SCR7 containing H or Y at the relevant position showed that they were almost identical.[42] These reports suggest that there are no major conformational changes associated with the polymorphism. Comparison of crystal structures, already solved for the SCR6–8 construct containing H at the relevant position in SCR7,[43] will provide a definitive answer to the degree of conformational change.

The mAb MBI-7 was used to develop a simple and robust assay for measurement of fH and the variants in plasma. The assay correctly identified the polymorphic status of all participants tested, confirmed by sequencing. ELISA and other antibody-based methods are the bedrock of the clinical immunology laboratory, and all necessary equipment and expertise are in place; in contrast, molecular detection of mutations requires access to patient DNA, specialist equipment, and expertise that is less widely available and more commonly found in the clinical genetics laboratory. The simplicity of the ELISA described here means that it could, subject to appropriate ethical constraints, be adopted by any clinical immunology laboratory, either in its current form or as a dip-stick test, to identify from a plasma sample the polymorphic status of those at risk for AMD. The association of noncoding and synonymous exonic polymorphisms in fH with AMD strongly suggests that altered expression,[32] hence measurement of plasma concentration of fH, will likely provide important additional information. Current clinical assays for quantification of fH use radial immunodiffusion or related methods and are compromised by the lack of international standards for fH measurement. The ELISA described here not only provides a measure of total fH but also a measure in those who are heterozygous of the amount of each form of fH in the plasma, a neglected parameter that may have major significance for understanding the roles of fH in health and disease. Analysis of plasma from healthy young volunteers showed that total fH levels varied widely, a finding previously attributed to genetic variation.[35] The fH-Y402H polymorphic status was easily assigned in this population and showed 100% agreement with genotyping. Plasma levels of fH were similar regardless of polymorphic status.

Plasma from a Spanish cohort of AMD patients and age- and sex-matched controls was then tested in the assay. Samples were assayed blind, and assignation of phenotype was made before knowledge of the genetic analyses; all patients and controls were correctly assigned in the ELISA. The elderly control group had significantly higher plasma levels of fH than the younger control group, in agreement with previous data.[35] Of note, these two control groups were not matched for other relevant factors such as smoking behavior, so no attempt was made here to directly compare the groups. Total fH levels of AMD patients were slightly higher than levels of the matched elderly controls. fH levels in the H402 homozygous, Y402 homozygous, and heterozygous subgroups were similar in elderly controls, but in AMD patients, fH levels were significantly higher in the heterozygous subgroup than in the other subgroups, and both variants were increased to a similar extent. We have no explanation for these differences and await confirmation in other cohorts.

The specificity of mAb MBI-7 for fH-H402 was retained, even after denaturation in Western blots. Our preliminary data show that this mAb also detects fH in immunohistochemical staining in tissues; we are confirming its specificity in this context before applying it to AMD tissue to further explore the roles of fH in pathology. The capacity to differentiate between the fH isoforms deposited in tissue may prove helpful in further elucidating mechanisms in AMD and other diseases in which fH is known to be deposited in the tissues.

The mechanism by which the fH-H402 variant increases risk for AMD has been the subject of intense interest in the past 2 years. It has been suggested that fH-H402 shows reduced binding to C-reactive protein, heparin, and cell surfaces, perhaps resulting in reduced capacity to protect cells, and that this deficit extends to fHL-1-H402.[36,44–46] However, others have found no difference in binding of the variants to relevant targets.[47] Further work is needed to elucidate the mechanism, and the reagents described here may facilitate these studies. Understanding of the mechanism and the precise roles of fH and complement activation will guide therapies targeted at fH itself or to inhibit complement activation locally or systemically.

References

1. Weiler JM, Daha MR, Austen KF, Fearon DT. Control of the amplification convertase of complement by the plasma protein βlH. *Proc Natl Acad Sci U S A*. 1976;73:3268–3272.
2. Rodriguez de Cordoba S, Esparza-Gordillo J, Goicoechea de Jorge E, Lopez-Trascasa M, Sanchez-Corral P. The human complement factor H: functional roles, genetic variations and disease associations. *Mol Immunol*. 2004;41:355–367.
3. Botto M, Walport MJ. Hereditary deficiency of C3 in animals and humans. *Int Rev Immunol*. 1993;10:37–50.
4. Reis E, Falcao DA, Isaac L. Clinical aspects and molecular basis of primary deficiencies of complement component C3 and its regulatory proteins factor I and factor H. *Scand J Immunol*. 2006;63:155–168.
5. Rodriguez de Cordoba S, Goicoechea de Jorge E. Translational mini-review series on complement factor H: genetics and disease associations of human complement factor H. *Clin Exp Immunol*. 2008;151:1–13.
6. Bird AC, Bressler NM, Bressler SB, et al. An international classification and grading system for age-related maculopathy and age-related macular degeneration: the International ARM Epidemiological Study Group. *Surv Ophthalmol*. 1995;39:367–374.
7. Edwards AO, Ritter R 3rd, Abel KJ, Manning A, Panhuysen C, Farrer LA. Complement factor H polymorphism and age-related macular degeneration. *Science*. 2005;308:421–424.

8. Hageman GS, Anderson DH, Johnson LV, et al. A common haplotype in the complement regulatory gene factor H (HF1/CFH) predisposes individuals to age-related macular degeneration. *Proc Natl Acad Sci U S A*. 2005;102:7227–7232.
9. Haines JL, Hauser MA, Schmidt S, et al. Complement factor H variant increases the risk of age-related macular degeneration. *Science*. 2005;308:419–421.
10. Klein RJ, Zeiss C, Chew EY, et al. Complement factor H polymorphism in age-related macular degeneration. *Science*. 2005;308:385–389.
11. Jakobsdottir J, Conley YP, Weeks DE, Mah TS, Ferrell RE, Gorin MB. Susceptibility genes for age-related maculopathy on chromosome 10q26. *Am J Hum Genet*. 2005;77:389–407.
12. Rivera A, Fisher SA, Fritsche LG, et al. Hypothetical LOC387715 is a second major susceptibility gene for age-related macular degeneration, contributing independently of complement factor H to disease risk. *Hum Mol Genet*. 2005;14:3227–3236.
13. Kaur I, Hussain A, Hussain N, et al. Analysis of CFH, TLR4, and APOE polymorphism in India suggests the Tyr402His variant of CFH to be a global marker for age-related macular degeneration. *Invest Ophthalmol Vis Sci*. 2006;47:3729–3735.
14. Lau LI, Chen SJ, Cheng CY, et al. Association of the Y402H polymorphism in complement factor H gene and neovascular age-related macular degeneration in Chinese patients. *Invest Ophthalmol Vis Sci*. 2006;47:3242–3246.
15. Gotoh N, Yamada R, Hiratani H, et al. No association between complement factor H gene polymorphism and exudative age-related macular degeneration in Japanese. *Hum Genet*. 2006;120:139–143.
16. Uka J, Tamura H, Kobayashi T, et al. No association of complement factor H gene polymorphism and age-related macular degeneration in the Japanese population. *Retina*. 2006;26:985–987.
17. Harris CL, Lublin DM, Morgan BP. Efficient generation of monoclonal antibodies for specific protein domains using recombinant immunoglobulin fusion proteins: pitfalls and solutions. *J Immunol Methods*. 2002a;268:245–258.
18. Harris CL, Williams AS, Linton SM, Morgan BP. Coupling complement regulators to immunoglobulin domains generates effective anti-complement reagents with extended half-life in vivo. *Clin Exp Immunol*. 2002b;129:198–207.
19. Harris CL, Hughes CE, Goodfellow I, Evans DJ, Caterson B, Morgan BP. Generation of anti-complement 'prodrugs': cleavable reagents for specific delivery to disease sites. *J Biol Chem*. 2003;278:36068–36076.
20. Kohler G, Milstein C. Continuous cultures of fused cells secreting antibody of predefined specificity. *Nature*. 1975;256:495–499.
21. Sim E, Palmer MS, Puklavec M, Sim RB. Monoclonal antibodies against the complement control protein factor H (beta 1 H). *Biosci Rep*. 1983;3:1119–1131.
22. Hayashi Y, Matsuda R, Maitani T, et al. An expression of within-plate uncertainty in sandwich ELISA. *J Pharm Biomed Anal*. 2004;36:225–229.
23. DiScipio RG. Factor H. In: Morley BJ, Walport MJ, eds. *The Complement Facts Book*. London: Academic Press; 2000:168–173.
24. Johnson LV, Ozaki S, Staples MK, Erickson PA, Anderson DH. A potential role for immune complex pathogenesis in drusen formation. *Exp Eye Res*. 2000;70:441–449.
25. Johnson LV, Leitner WP, Rivest AJ, Staples MK, Radeke MJ, Anderson DH. The Alzheimer's A beta -peptide is deposited at sites of complement activation in pathologic deposits associated with aging and age-related macular degeneration. *Proc Natl Acad Sci U S A*. 2002;99:11830–11835.
26. Nozaki M, Raisler BJ, Sakurai E, et al. Drusen complement components C3a and C5a promote choroidal neovascularization. *Proc Natl Acad Sci U S A*. 2006;103:2328–2333.
27. Hageman GS, Hancox LS, Taiber AJ, et al. Extended haplotypes in the complement factor H (CFH) and CFH-related (CFHR) family of genes protect against age-related macular degeneration: characterization, ethnic distribution and evolutionary implications. *Ann Med*. 2006;38:592–604.
28. Hughes AE, Orr N, Esfandiary H, Diaz-Torres M, Goodship T, Chakravarthy U. A common CFH haplotype, with deletion of CFHR1 and CFHR3, is associated with lower risk of age-related macular degeneration. *Nat Genet*. 2006;38:1173–1177.
29. Yates JR, Sepp T, Matharu BK, et al. Genetic factors in AMD study group: complement C3 variant and the risk of age-related macular degeneration. *N Engl J Med*. 2007;357:553–561.
30. Gold B, Merriam JE, Zernant J, et al. Variation in factor B (BF) and complement component 2 (C2) genes is associated with age-related macular degeneration. *Nat Genet*. 2006;38:458–462.
31. Spencer KL, Hauser MA, Olson LM, et al. Protective effect of complement factor B and complement component 2 variants in age-related macular degeneration. *Hum Mol Genet*. 2007;16:1986–1992.
32. Francis PJ, Schultz DW, Hamon S, Ott J, Weleber RG, Klein ML. Haplotypes in the complement factor H (CFH) gene: associations with drusen and advanced age-related macular degeneration. *PLoS ONE*. 2007;2:e1197.
33. Seddon JM, George S, Rosner B, Klein ML. CFH gene variant, Y402H, and smoking, body mass index, environmental associations with advanced age-related macular degeneration. *Hum Hered*. 2006;61:157–165.
34. Seddon JM, Francis PJ, George S, Schultz DW, Rosner B, Klein ML. Association of CFH Y402H and LOC387715 A69S with progression of age-related macular degeneration. *JAMA*. 2007;297:1793–1800.
35. Esparza-Gordillo J, Soria JM, Buil A, et al. Genetic and environmental factors influencing the human factor H plasma levels. *Immunogenetics*. 2004;56:77–82.
36. Yu J, Wiita P, Kawaguchi R, et al. Biochemical analysis of a common human polymorphism associated with age-related macular degeneration. *Biochemistry*. 2007;46:8451–8461.
37. Stanker LH, Branscomb E, Vanderlaan M, Jensen RH. Monoclonal antibodies recognizing single amino acid substitutions in hemoglobin. *J Immunol*. 1986;136:4174–4180.
38. Hoylaerts MF, Millán JL. Site-directed mutagenesis and epitope-mapped monoclonal antibodies define a catalytically important conformational difference between human placental and germ cell alkaline phosphatase. *Eur J Biochem*. 1991;202:605–616.
39. De Vito LD, Mason BP, Jankowska-Gan E, et al. Epitope fine specificity of human anti-HLA-A2 antibodies: identification of four epitopes including a haptenlike epitope on HLA-A2 at lysine 127. *Hum Immunol*. 1993;37:165–177.
40. Mani JC, Marchi V, Cucurou C. Effect of HIV-1 peptide presentation on the affinity constants of two monoclonal antibodies determined by Biacore technology. *Mol Immunol*. 1994;31:439–444.
41. Fernando AN, Furtado PB, Clark SJ, et al. Associative and structural properties of the region of complement factor H encompassing the Tyr402His disease-related polymorphism and its interactions with heparin. *J Mol Biol*. 2007;368:564–581.
42. Herbert AP, Uhrín D, Lyon M, Pangburn MK, Barlow PN. Disease-associated sequence variations congregate in a polyanion recognition patch on human factor H revealed in three-dimensional structure. *J Biol Chem*. 2006;281:16512–16520.
43. Prosser BE, Johnson S, Roversi P, et al. Expression, purification, cocrystallization and preliminary crystallographic analysis of sucrose octasulfate/human complement regulator factor H SCRs 6–8. *Acta Crystallograph Sect F Struct Biol Cryst Commun*. 2007;63:480–483.
44. Laine M, Jarva H, Seitsonen S, et al. Y402H polymorphism of complement factor H affects binding affinity to C-reactive protein. *J Immunol*. 2007;178:3831–3836.
45. Skerka C, Lauer N, Weinberger AA, et al. Defective complement control of factor H (Y402H) and FHL-1 in age-related macular degeneration. *Mol Immunol*. 2007;44:3398–3406.
46. Sjoberg AP, Trouw LA, Clark SJ, et al. The factor H variant associated with age-related macular degeneration (His-384) and the non-disease-associated form bind differentially to C-reactive protein, fibromodulin, DNA, and necrotic cells. *J Biol Chem*. 2007;282:10894–10900.
47. Biro A, Rovo Z, Papp D, et al. Studies on the interactions between C-reactive protein and complement proteins. *Immunology*. 2007;121:40–50.

http://www.kidney-international.org

see commentary on page 721

Variant-specific quantification of factor H in plasma identifies null alleles associated with atypical hemolytic uremic syndrome

Svetlana Hakobyan[1,3], Agustín Tortajada[2,3], Claire L. Harris[1], Santiago R. de Córdoba[2] and Bryan P. Morgan[1]

[1]*Department of Infection, Immunity and Biochemistry, School of Medicine, Cardiff University, Cardiff, UK and* [2]*Centro de Investigaciones Biológicas, CSIC, Ramiro de Maeztu 9, Madrid, Spain*

Atypical hemolytic uremic syndrome (aHUS) is associated with complement alternative pathway defects in over half the cases. Point mutations that affect complement surface regulation are common in factor H (CFH); however, sometimes individuals have null mutations in heterozygosis. The latter are difficult to identify, although a consistently low plasma factor H (fH) concentration is suggestive; definitive proof requires demonstration that the mutant sequence is not expressed *in vitro*. Here, novel reagents and assays that distinguish and individually quantify the common factor H-Y402H polymorphic variants were used to identify alleles of the *CFH* gene, resulting in low or null expression of full-length fH and also normal or increased expression of the alternative splice product factor H-like-1 (FHL-1). Our assay identified three Y402H heterozygotes with low or absent fH-H402 but normal or increased FHL-1-H402 levels in a cohort of affected patients. Novel mutations explained the null phenotype in two cases, which was confirmed by family studies in one. In the third case, family studies showed that a known mutation was present on the Y allele. The cause of reduced expression of the H allele was not found, although the data suggested altered splicing. In each family, inheritance of low expression or null alleles for fH strongly associated with aHUS. Thus, our assays provide a rapid means to identify fH expression defects without resorting to gene sequencing or expression analysis.

Kidney International (2010) **78,** 782–788; doi:10.1038/ki.2010.275; published online 11 August 2010

KEYWORDS: complement; family history; hemolytic uremic syndrome; polymorphisms

Correspondence: *Bryan P. Morgan, Department of Infection, Immunity and Biochemistry, School of Medicine, Cardiff University, Cardiff CF14 4XN, UK. E-mail: morganbp@cardiff.ac.uk*

[3]These authors contributed equally to this work.

Received 20 March 2010; revised 2 May 2010; accepted 1 June 2010; published online 11 August 2010

Hemolytic uremic syndrome (HUS), characterized by the triad of thrombocytopenia, microangiopathic hemolytic anemia, and acute renal failure, is one of the commonest causes of renal failure in children.[1] When not associated with diarrheal illness, or when recurrent, the disease is considered atypical HUS (aHUS), accounting for $<10\%$ of all HUS cases. aHUS has a poor prognosis; it is fatal in up to 25% in the acute phase and 50% of survivors require ongoing renal replacement therapy.[2] Numerous environmental precipitants of aHUS have been described, including infections,[3,4] tumors,[5] pregnancy,[6] drugs,[7] and metabolic syndromes.[8] In some families, both autosomal recessive and autosomal dominant inheritance modes were seen.[9,10] Research over the last decade has identified mutations in genes encoding complement regulators or components in 50% of aHUS cases; these include factor H (fH; reviewed in Rodriguez de Cordoba *et al.*[11]), membrane cofactor protein,[12] factor I,[13] C3,[14] and factor B,[15] provoking the suggestion that aHUS is a disease caused by dysregulation of the alternative pathway (AP) of complement.[15] Mutations in the gene encoding fH (*CFH*) are the most frequent association with aHUS, with over 100 different mutations identified.[16] The genetic basis of about half of aHUS cases in all cohorts remains undefined, provoking a search for other causative factors.

fH, a 150-kDa serum glycoprotein, regulates the AP of complement by acting as cofactor for factor I-mediated proteolytic inactivation of C3b, competing with factor B for C3b binding, and accelerating decay of the C3 convertase.[11] fH is the key fluid-phase regulator of the AP, but also regulates AP activation on host cells and exposed basement membranes by binding glycosaminoglycans through its C-terminal domain (short consensus repeats (SCRs) 19 and 20).[17] The complement regulatory domain (SCRs 1–4) then provides regulation on the surface. Mutations in *CFH* have been described in multiple cohorts (collated on http://www.fh-hus.org) and account for some 30% of aHUS cases.[16] The vast majority are heterozygous, either premature stop codons or single amino acid changes. Incomplete penetrance has been described in all series, suggesting that aHUS is multifactorial, resulting from a combination of environmental triggers that injure endothelial cells, activate complement, and

precipitate disease in genetically susceptible individuals.[18] Most fH mutations associated with aHUS are in the C-terminal SCRs and cause decreased binding of fH to glycosaminoglycans on endothelial cells and basement membranes.[19] This will cause impaired regulation of AP amplification at these sites, whereas fluid-phase regulation is unimpaired. In a minority of aHUS cases, null mutations are found, resulting in heterozygous or, rarely, homozygous deficiency of fH.[20] Although patients with null mutations in heterozygosity will usually have low plasma levels of fH,[20] the large variability in fH concentrations in normal individuals makes it difficult or impossible to identify cases simply by measuring fH levels in plasma. Definitive proof that a particular mutant is null has previously required gene sequencing and the demonstration that the mutant cDNA, transfected into an appropriate cell line, failed to make fH protein.[21,22] Methods for measuring expression from individual fH alleles would facilitate identification and assignation of null alleles without the need for laborious cloning and expression.

The Y402H polymorphism of fH is strongly linked to age-related macular degeneration.[23] In Caucasians, the allele frequency (Y:H) is approximately 2.5:1 in healthy individuals; hence, over 40% of Caucasians are Y402H heterozygous. This polymorphism therefore represents a useful 'marker' for individual *CFH* alleles. We have previously reported a monoclonal antibody (mAb) specific to fH-H402.[24] Here, we describe production of a mAb specific to fH-Y402 and the development of assays for independent quantification of the Y402H variants. Although the Y402H polymorphism has no apparent direct link to aHUS, application of the new assays to aHUS families enabled us to identify, characterize, and confirm new *CFH* alleles associated with low or no expression of full-length fH, but normal or increased expression of the alternative splice product of the *CFH* gene, factor H-like-1 (FHL-1). We show that these low or no expression alleles for fH conferred strong predisposition to aHUS. These novel tools will not only help in identification of the molecular basis of disease in patients with aHUS, but also aid in the prediction of risk in their relatives.

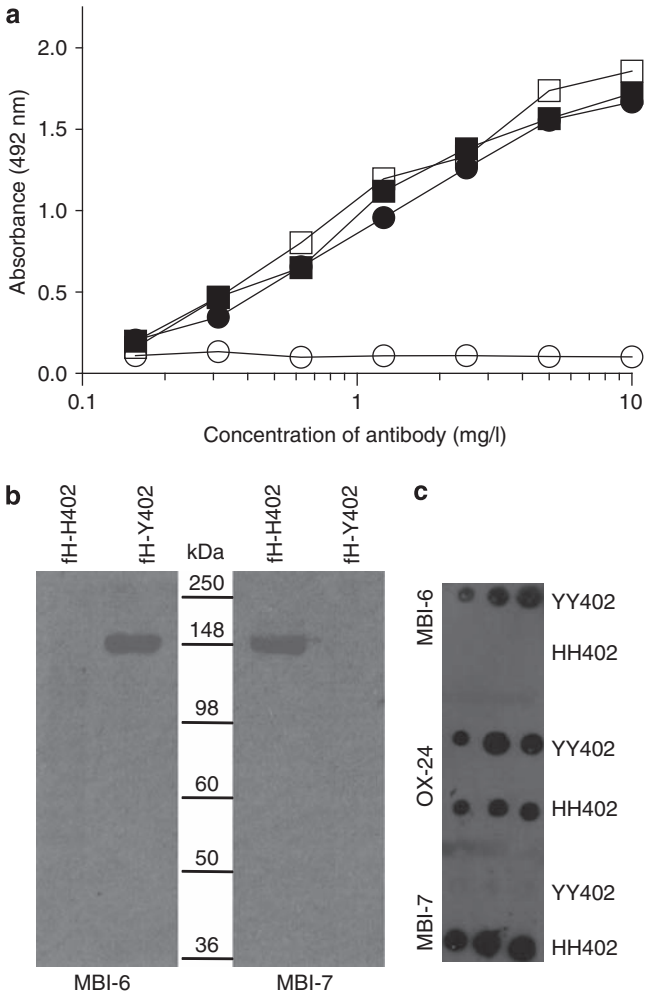

Figure 1 | Monoclonal antibody (mAb) MBI-6 specifically detects factor H (fH)-Y402. (**a**) Enzyme-linked immunosorbent assay with each fH variant directly immobilized on plate; OX-24 detected both Y402 (closed squares) and H402 (closed circles), whereas MBI-6 detected only Y402 (open squares) and failed to detect H402 (open circles). (**b**) Western blot showing the detection of fH variants using Y402-specific (MBI-6; left) and H402-specific (MBI-7; right) mAb. The same amount of each protein was loaded in each lane. MBI-6 detected only the Y402 variant and MBI-7 only the H402 variant. (**c**) Dot blot in which 5 μl, 10 μl, or 20 μl aliquots (from left to right) of 10-fold diluted plasma from YY402 and HH402 homozygous donors were spotted on the membrane and probed with either Y402-specific (MBI-6; top), non-selective (OX-24; middle), or H402-specific (MBI-7; bottom) mAb.

RESULTS

Variant-specific mAb permit independent measurement of *CFH* allele products

The fH-H402-specific mAb was described previously;[24] for this study a mAb specific for the Y402 variant was needed. From 10 fusions, two mAb were obtained that selectively bound fH-Y402; one immunoglobulin (Ig) G_1 isotype, the other IgM, designated as MBI-6 and MBI-8, respectively. The IgG_1 mAb MBI-6 was expanded and purified; specificity for fH-Y402 was confirmed using enzyme-linked immunosorbent assay (ELISA; Figure 1a) and western blot (Figure 1b), confirming that it reacted *exclusively* with fH-Y402. Dot blotting of plasma from donors of known Y402H polymorphic status confirmed specificity for fH-Y402 (Figure 1c). The fH-H402-specific mAb MBI-7 is included as an additional control and to demonstrate the utility of these mAb for independently identifying the presence of these two isoforms of fH. Affinities of MBI-6 for fH-Y402 and fH-H402 were assessed by surface plasmon resonance; the mAb failed to bind fH-H402, but bound fH-Y402 with a $K_D = 15.2$ nmol/l ($\chi^2 = 8.96$), confirming the high affinity and absolute specificity of the mAb.

ELISA for quantification of each variant in plasma was developed using the variant-specific antibodies. Both the variant-specific and total fH assays measure the combined

levels of fH and FHL-1, the latter an alternative splice product of the *CFH* gene comprising the first seven SCRs of fH and thus sharing the Y402H polymorphism (in SCR7), but neither assay detects any of the reported fH-related proteins (FHR-1, -2, -3, -4, -5). The plasma concentrations of fH and FHL-1 correlate in individual donors with FHL-1 concentrations 10–50 fold lower than fH in normal individuals.[11,25]

The calculated assay detection limit was 0.01 mg/l and the working range was 0.02–0.3 mg/l. Assay performance was assessed by taking multiple measures from independently diluted aliquots of the same samples. Within-assay precision was 1.3–15.5% across the working range with an average of 5.5% for fH-Y402 measurement, and 1.4–16.8% with an average of 5.6% for fH-H402 measurement. Between-assay precision was 6.7–17.6% with an average of 11.9% for fH-Y402 measurement, and 5.1–12.2% with an average of 9.7% for fH-H402 measurement.

Measurement of fH variants in healthy donors and aHUS patients

To confirm assay performance and establish normal range (nr), concentrations of fH variants were measured using ELISA in 46 healthy control donors (mean age 42.2 ± 13.8 years, range 25–66 years; 63% female; 21 YY402, 5 HH402, 20 YH402; Y402:H402 allele ratio 0.67:0.33). Total fH was calculated both by summing the amounts of each variant and by using a non-selective fH assay. Values obtained by summing variant concentrations closely matched fH values obtained in the non-selective assay, confirming the validity of the variant-specific assays (for the whole cohort, 257.5 ± 89.8 mg/l from sum of assays and 263.3 ± 69.4 mg/l from total fH assay). The nr (mean ± 2 s.d.) was 77.9–437.1 mg/l in the summed assay and 124.4–402 mg/l in the total fH assay, illustrating the broad range in plasma fH levels in this normal population. Values for plasma fH in our assays are lower than those quoted in past studies, a consequence of recalibration based on accurate extinction coefficients calculated as described.[24] Mean total fH was not different between the three groups (YY402, 267.2 ± 66.7 mg/l; YH402, 250.9 ± 56.9 mg/l; HH402, 214.7 ± 81.5 mg/l). In heterozygote controls, variant levels were not significantly different. Importantly, no heterozygote control had selective low or no expression of one allele.

From the Spanish aHUS cohort, 48 individuals heterozygous for the Y402H polymorphism were identified and tested in the Y402H variant-specific assays (Figure 2). Three unrelated individuals (Hus29, Hus90, and Hus169) were identified, in whom expression of the H402 allele was very low compared with the Y402 allele. fH level in index case Hus90 was 109 mg/l (Y402, 100 mg/l; H402, 9 mg/l), in case Hus169 was 73 mg/l (Y402, 60 mg/l; H402, 13 mg/l), and in case Hus29 was 148 mg/l (Y402, 130 mg/l; H402, 18 mg/l). Total fH level fell below the calculated nr (mean ± 2 s.d.) only for Hus169; in the others, total fH levels were in the lower quartile of the nr.

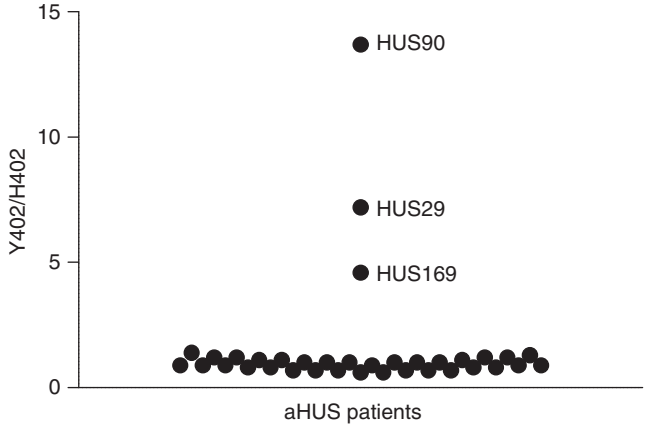

Figure 2 | Measurement of Y402 and H402 variants of factor H (fH) in atypical hemolytic uremic syndrome (aHUS) patients heterozygous for the Y402H polymorphism. Ratios of concentrations of fH-Y402 and fH-H402 were calculated for each individual and plotted on the graph. For the majority, the ratio was close to 1. For three unrelated individuals (Hus29, Hus90, and Hus169), the concentration of fH-H402 was very low compared with fH-Y402 in that individual, giving high ratios, apparent in the figure.

Index case Hus29 had been reported before as a carrier of the fH mutation R1210C, a known aHUS-associated mutation causing disulfide bonding of fH to albumin in plasma;[19,26] the albumin-bound protein is present in plasma in normal amounts, retains the capacity to inhibit fluid-phase complement activation, but has impaired binding to surfaces. All exons in *CFH* had been sequenced in Hus29 and no other mutations had been found. Eight family members, all healthy, were available, of whom five carried the R1210C mutation (Figure 3a). Father, aunt, and paternal great-grandfather were R1210C carriers, Y402 homozygous with normal plasma fH levels, demonstrating that R1210C was on the Y402 allele. Paternal grandfather, a R1210C carrier, was Y402H heterozygous with normal plasma fH levels and similar levels of fH-H402 and fH-Y402. Mother, a H402 homozygote, did not carry the R1210C mutation and had low plasma fH levels. Both the index case and her sister were Y402H heterozygous, and carried the R1210C mutation; however, whereas the sister had normal plasma fH levels with similar amounts of each variant, the index case had low total fH and very low fH-H402 levels in plasma. Western blot of plasma fH in the index case and her sister using the fH-H402-specific mAb demonstrated differential expression of the two maternal H402 alleles, 12% of control levels in the index case by densitometry, and normal expression (90% of control) in her sister (Figure 4). Because the R1210C mutation was on the Y402 allele, no high molecular weight albumin–fH complex was detected by this H402-specific mAb. Expression of the H402 allele of the alternative splice product of *CFH*, FHL-1, was increased fivefold (by densitometry) in the index case, but not increased compared with controls in her sister (Figure 4). Analysis of the promoter and intronic sequences

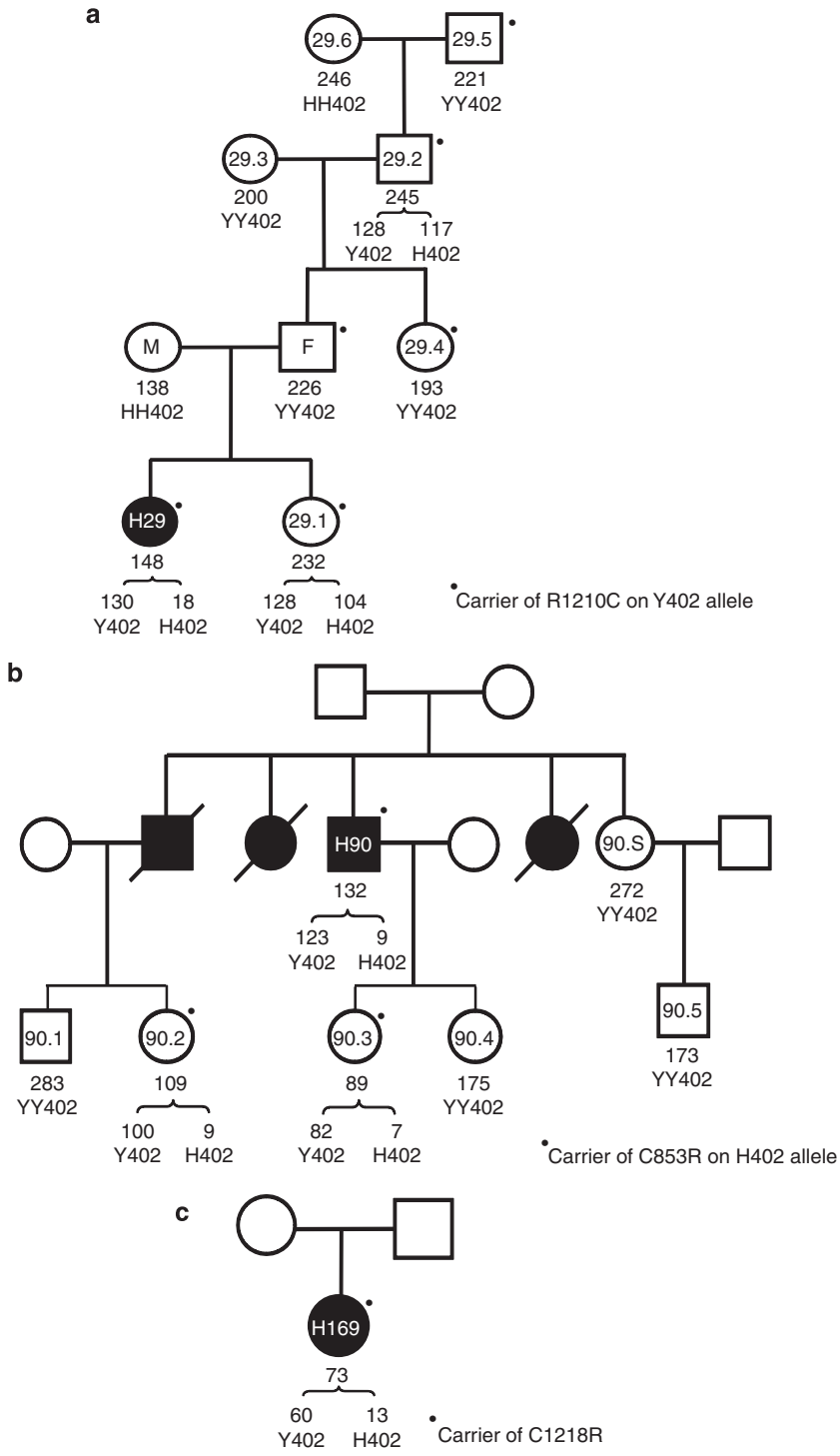

Figure 3 | Family studies in atypical hemolytic uremic syndrome (aHUS) pedigrees. Circles represent females, squares males; closed symbols are aHUS cases, open symbols healthy relatives, crossed-through symbols represent deceased relatives. Numbers within a symbol provide the case number. Total factor H (fH; mg/l) and Y402H status, where available, are shown below symbols; concentrations of Y402 and H402 variants in heterozygotes are shown below the brackets. Heavy dots indicate that the individual is a carrier for the stated mutation. (**a**) Pedigree Hus29; index case H29 is Y402H heterozygote expressing very low levels of the H402 allele, and a carrier of the R1210C mutation inherited from her father (F). Mother (M), a H402 homozygote, does not carry the R1210C mutation but had low plasma fH levels. The healthy sister, also Y402H heterozygote and R1210C carrier, expresses normal levels of the H402 allele. (**b**) Pedigree Hus90; index case H90 is Y402H heterozygote expressing very low levels of the H402 allele, and a carrier of the C853R mutation, shared with one daughter and a niece, both healthy. The same niece and his other daughter are Y402H heterozygotes expressing very low levels of the H402 allele. (**c**) Pedigree Hus169; index case H169, is Y402H heterozygote expressing very low levels of the H allele, and a carrier of the C1218R mutation. Levels of the Y402 allele were also low in this individual.

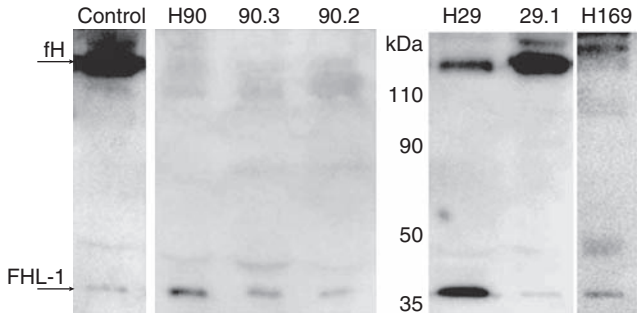

Figure 4 | Western blotting of plasma samples from hemolytic uremic syndrome (HUS) patients and their healthy relatives. Diluted plasma samples were separated on 10% SDS-polyacrylamide gel electrophoresis gels under non-reducing conditions, blotted to nitrocellulose, and probed with monoclonal antibody MBI-7 to detect factor H (fH)-H402. In the Hus90 pedigree, no fH-H402 was detectable in index case (H90), daughter (90.3), or niece (90.2); FHL-1-H402 was present in each case. In the Hus29 pedigree, fH-H402 was detectable in the index case (H29), but at only 12% (by densitometry) of that in the control sample or in her sister (H29.1); in contrast, FHL-1-H402 levels were increased fivefold (by densitometry) compared with control or sister samples. Index case H169 had no detectable fH-H402 but FHL-1-H402 was present at levels similar to controls.

within the gene has so far not revealed any genetic variation that could explain increased expression of FHL-1.

Index case Hus90 also had very low levels of fH-H402 in plasma (Figure 3b). Western blot with fH-H402-specific antibodies showed complete absence of fH-H402 but normal amounts of FHL-1-H402 (Figure 4), suggestive of a null mutation in the H402 allele downstream of SCR7. Subsequent *CFH* sequencing revealed the presence in heterozygosity of a novel mutation (C853R; SCR14). Hus90 had three deceased affected siblings; two died during infancy and their mutation status is unknown, whereas the third, though deceased, is an obligate carrier of the C853R mutation because one of his two children is a carrier. This niece of the index case and one of his two daughters, were the only carriers of the C853R mutation in the next generation; both were Y402H heterozygous and, like the index case, these individuals had very low plasma levels of the H402 allele by ELISA (Figure 3b). Western blotting confirmed complete absence of fH-H402 and normal expression of FHL-1-H402, as in the index case (Figure 4). The other daughter and two nephews of the index case were also tested and all were Y402 homozygous, non-carriers with normal plasma fH levels. Segregation analysis in this pedigree confirmed that the H402 allele carried the C853R mutation; likely a null mutation because the cysteine residue is essential for correct folding of SCR14.

Index case Hus169 was also selected for low plasma fH-H402 level. Subsequent *CFH* sequencing analysis revealed the presence in heterozygosity of a novel mutation (C1218R) in SCR20 (Figure 3c). Western blotting with the H402-specific mAb revealed the absence of fH-H402 but normal levels of FHL-1-H402, as in the Hus90 pedigree (Figure 4). The plasma concentration of fH-Y402 was low at 60 μg/ml; however, this concentration, from a single allele, is well within the broad nr for fH noted above (78–437 μg/ml from two alleles); these data further emphasize the importance of allele-specific quantification to detect occult null or low expression alleles of fH.

DISCUSSION

CFH mutations in aHUS are usually near the C-terminus (50% in SCRs 19/20), present in heterozygosity and cause impaired surface protection from complement activation.[16,27] In these cases, plasma fH levels are unaffected, and plasma fH is a mixture of mutant and normal protein. In a minority of reported aHUS cases, the *CFH* mutation causes very low or absent expression from that allele,[20] usually identified because of reduced fH levels in plasma. However, identification based on fH levels is unreliable not only because of the noted large variability in the normal population, but also because factors such as age and smoking behavior influence fH levels in plasma.[28]

We generated mAb specific for the Y402H polymorphic variants of fH and FHL-1 to identify and quantify expression in macular degeneration, where the H402 allele is a major risk factor.[21,22] This polymorphism has not been linked to aHUS; nevertheless, we reasoned that the mAb and assays would enable us to independently quantify expression from normal and mutant alleles in aHUS, facilitating rapid discovery of null mutations. We, here, describe the use of these mAb to identify in families with a HUS the presence of null or low expression alleles for full-length fH that are associated with disease. In each of the families described, disease was clearly associated with the inheritance of a previously unidentified *CFH* low or no expression allele revealed by the new assays.

In Hus90 and Hus169, the mutations responsible for low expression of fH-H402 were subsequently identified as novel loss of cysteine mutations in SCR14 (C853R) and SCR20 (C1218R), respectively. Accumulated data on fH mutations suggest that loss of cysteine mutations in fH are null because they disrupt SCR structure (http://www.fh-hus.org). Indeed, western blotting of plasma from Hus90 and Hus169, with fH-H402-specific mAb confirmed the complete absence of fH-H402, but normal expression of FHL-1 from this allele. Unhindered expression of FHL-1-H402 from the mutated gene explains the traces of fH-H402 reactivity detected in the H402-specific ELISA; all three ELISA used in the study utilize detection mAb that bind in SCR1–7, shared by fH and FHL-1, and thus detect both. Others have reported that null mutations distal to SCR7 permit normal expression of FHL-1,[21,22] whereas null mutations in the shared SCRs cause loss of both proteins.[29] Indeed, the differential effects on expression of fH and FHL-1 are useful predictors of the location of the mutation, proximal when both are absent and distal to SCR7 when only fH is affected. In this respect, the fact that the described assays detect both full-length fH

and the alternative splice product FHL-1 is a considerable advantage for the detection of occult mutations in fH.

In Hus29, the known point mutation R1210C was shown by western blot and segregation in the pedigree to be on the Y402 allele, and hence not responsible for the observed low expression of fH-H402 allele. The R1210C mutation is common, results in the formation of disulphide-bonded albumin–fH complexes that inhibit fluid-phase complement activation,[19] and in a large series has been shown to be associated with aHUS only in the presence of additional genetic predisposing factors.[26] In Hus29, we contend that the additional predisposing factor is the inheritance from the mother of a low expression H402 allele. The sister of the index case, also a Y402H heterozygote and carrier of the R1210C mutation, has not inherited the low expression allele and is therefore likely not at high risk of aHUS, a prediction only made possible by these novel assays. Critically, expression of FHL-1-H402 in the index case was increased fivefold compared with controls, suggesting that a mutation affecting the differential splicing of the *CFH* gene was responsible for the deficit. Although we have undertaken a thorough search for mutations in the large intronic regions flanking exons 9, 10, and 11 of the *CFH* gene, this putative mutation remains unidentified. Despite the fact that fH and FHL-1 are products of the same gene, independent regulation of their expression has been described previously,[30] and is confirmed in this study.

The families described above provide case histories that prove the value of the variant-specific mAbs and assays we describe here. Because we have targeted a common polymorphism, over 40% of Caucasians are Y402H heterozygous, these reagents will be useful in the large majority of families. Here, we showed their value in tracking the disease-associated allele through a family and, critically, in identifying previously unsuspected null or low expression alleles, themselves strong risk factors for the development of aHUS. The specificity of the mAbs permits unambiguous and rapid identification of occult low or no expression alleles, independent risk factors for aHUS that should now be sought in other cohorts.

MATERIALS AND METHODS

Generation and characterization of fH Y402H variant-specific mAb

Mice were immunized as described before using fusion proteins comprising fH-Y402 SCRs 6–8 linked to human IgG4 Fc (fH-Fc).[24,31] Hybridoma supernatants were screened for binding to native fH-H402 and fH-Y402 as described.[24] Two hybridomas producing mAb specific for fH-Y402 were identified, recloned, isotyped, expanded, and purified as described.[24] Specificity was confirmed by western and dot blotting on pure fH-H402 and fH-Y402 as described.[24] Affinities of the mAb for fH-H402 and fH-Y402 variants were determined by surface plasmon resonance on a Biacore T-100 (GE Healthcare, Chalfont, UK) as described.[24]

Development of fH variant-specific ELISA

Maxisorp (Nunc, Loughborough, UK) plates were coated with affinity-purified polyclonal rabbit anti-fH (100 µl, 5 mg/l) overnight at 4 °C and blocked with 1% bovine serum albumin in phosphate-buffered saline. Purified protein standards or serum samples (diluted 1:3000 in bovine serum albumin or phosphate-buffered saline, though lower dilutions (1:100) were used to confirm low fH levels) were added in triplicate and incubated. Wells were washed and incubated with horseradish peroxidase-labelled Y402-specific or H402-specific mAb (1 mg/l). All incubations were for 1 h, 37 °C Wells were washed and bound mAb was detected using ortho phenylene diamine substrate. Absorbance (492 nm) was measured. Standards were included on each plate and, samples from controls and patients were randomly assigned to eliminate assay bias. A nonlinear regression model was used to fit standard curves generated by ELISA. Total fH (mg/l) was calculated by summing results for fH-Y402 and fH-H402. Total fH was also measured in an ELISA, where horseradish peroxidase-labelled non-selective anti-fH mAb, OX-24, specific for an epitope in SCR5 of fH (Sim *et al.*[32]; RB Sim, personal communication) was used for detection. Detection limits, working ranges, nr, and assay performance were determined as described,[24] using plasma from 46 local healthy controls (Ethics approval from the Research and Ethics Committee for Wales. Ref 09/MRE09/35). Of note, because the capture antibody is polyclonal and the detecting mAbs identify epitopes in the shared SCRs 1–7, both the variant-specific and total fH assays will measure the combined levels of fH and FHL-1. However, none of the assays detect any of the fH-related proteins because none contain a SCR5-homologous SCR, and the SCR7-homologous SCR present in FHR-3 alone of these proteins is not conserved around the Y402H relevant region.

Western and dot-blot assays for fH variants

Western and dot-blot assays were performed as described.[24] To confirm the specificity of the mAbs, plasma from patients of known Y402H variant status was diluted 10-fold, 20-fold, or 40-fold, and dotted onto nitrocellulose. Separate sets were then probed with either Y402-specific (MBI-6), H402-specific (MBI-7), or non-selective (OX-24) mAb. Positive dots were developed using horseradish peroxidase-labelled anti-mouse IgG and chemiluminescent detection. As further proof of specificity, pure fH protein, Y402 and H402 in separate lanes, was run on 10% SDS-polyacrylamide gel electrophoresis under non-reducing conditions, and transferred to nitrocellulose. Separate strips were probed either with MBI-6 or MBI-7, and then developed using horseradish peroxidase-labelled anti-mouse IgG and chemiluminescent detection.

To test the presence of fH-H402 in patient samples, plasma (diluted 1:100; 20 µl) was separated on 10% SDS-polyacrylamide gel electrophoresis under non-reducing conditions, transferred to nitrocellulose (30 min transfer to retain FHL-1 on the membrane), and probed with MBI-7. Blots were developed as above. To quantify the relative amounts of fH and/or FHL-1 in and between samples, the specific bands were analyzed by densitometry.

Genomic analyses

The base change (T1277C) responsible for the Y402H polymorphism was analyzed by PCR amplification and sequencing of *CFH* exon 9 as described.[24] Patients and relatives were screened for other mutations and polymorphisms in *CFH* by automatic sequencing of each exon as described.[26]

Measurement of fH variants in plasma samples from aHUS patients and relatives

Patient samples were collected with the approval of the Ethics Committee of the Consejo Superior de Investigaciones Científicas

in accordance with the Declaration of Helsinki. All participants provided written informed consent. EDTA plasma was stored in aliquots at −80 °C. Study cases were selected for genetically determined heterozygosity at the locus encoding the fH-Y402H polymorphism. Concentrations of the Y402H variants were measured; index cases were identified with aberrant expression of either variant. Plasma and DNA were collected from all available family members of these index cases.

Statistical analysis

Data evaluation was performed using GraphPad Prism software (version 5.0 for Windows; GraphPad, La Jolla, CA, USA). The data were checked for normality using the D'Agostino–Pearson normality test.

DISCLOSURE

All the authors declared no competing interests.

ACKNOWLEDGMENTS

This work was supported by the UK Multiple Sclerosis Society no. 884/08 (to BPM), MRC Project Grant no. 84908 (to CLH and BPM), Ministerio de Ciencia e Innovación SAF 2005-00913, CIBER de Enfermedades Raras, and Fundación Renal Iñigo Alvarez de Toledo (to SRdeC).

REFERENCES

1. Richards A, Goodship J, Goodship T. The genetics and pathogenesis of haemolytic uraemic syndrome and thrombotic thrombocytopenic purpura. *Curr Opin Nephrol Hypertens* 2002; **11**: 431–436.
2. Noris M, Remuzzi G. Non-shiga toxin–associated hemolytic uremic syndrome. In: Zipfel P (ed). *Complement and Kidney Disease*. Birkhäuser: Basel, 2005, pp 65–83.
3. Becker S, Fusco G, Fusco J *et al.* Collaborations in HIV Outcomes Research/US Cohort. HIV-associated thrombotic microangiopathy in the era of highly active antiretroviral therapy: an observational study. *Clin Infect Dis* 2004; **39**: S267–S275.
4. Constantinescu AR, Bitzan M, Weiss LS *et al.* Non-enteropathic hemolytic uremic syndrome: causes and short-term course. *Am J Kidney Dis* 2004; **43**: 976–982.
5. Mungall S, Mathieson P. Hemolytic uremic syndrome in metastatic adenocarcinoma of the prostate. *Am J Kidney Dis* 2002; **40**: 1334–1336.
6. McMinn JR, George JN. Evaluation of women with clinically suspected thrombotic thrombocytopenic purpura-hemolytic uremic syndrome during pregnancy. *J Clin Apher* 2001; **16**: 202–209.
7. Dlott JS, Danielson CF, Blue-Hnidy DE *et al.* Drug-induced thrombotic thrombocytopenic purpura/hemolytic uremic syndrome: a concise review. *Ther Apher Dial* 2004; **8**: 102–111.
8. Kind T, Levy J, Lee M *et al.* Cobalamin C disease presenting as hemolytic-uremic syndrome in the neonatal period. *J Pediatr Hematol Oncol* 2002; **24**: 327–329.
9. Pirson Y, Lefebvre C, Arnout C *et al.* Hemolytic uremic syndrome in three adult siblings: a familial study and evolution. *Clin Nephrol* 1987; **28**: 250–255.
10. Kaplan BS, Papadimitriou M, Brezin JH *et al.* Renal transplantation in adults with autosomal recessive inheritance of hemolytic uremic syndrome. *Am J Kidney Dis* 1997; **30**: 760–765.
11. Rodriguez de Cordoba S, Esparza-Gordillo J, Goicoechea de Jorge E *et al.* The human complement factor H: functional roles, genetic variations and disease associations. *Mol Immunol* 2004; **41**: 355–367.
12. Fremeaux-Bacchi V, Moulton EA, Kavanagh D *et al.* Genetic and functional analyses of membrane cofactor protein (CD46) mutations in atypical hemolytic uremic syndrome. *J Am Soc Nephrol* 2006; **17**: 2017–2025.
13. Kavanagh D, Kemp E, Mayland E *et al.* Mutations in complement factor I (IF) predispose to the development of atypical HUS. *J Am Soc Nephrol* 2005; **16**: 2150–2155.
14. Frémeaux-Bacchi V, Miller EC, Liszewski MK *et al.* Mutations in complement C3 predispose to development of atypical hemolytic uremic syndrome. *Blood* 2008; **112**: 4948–4952.
15. Goicoechea de Jorge E, Harris CL, Esparza-Gordillo J *et al.* Gain-of-function mutations in complement factor B are associated with atypical hemolytic uremic syndrome. *Proc Natl Acad Sci USA* 2007; **104**: 240–245.
16. Saunders RE, Abarrategui-Garrido C, Frémeaux-Bacchi V *et al.* The interactive factor H-atypical hemolytic uremic syndrome mutation database and website: update and integration of membrane cofactor protein and factor I mutations with structural models. *Hum Mutat* 2007; **28**: 222–234.
17. Perkins SJ, Goodship TH. Molecular modelling of the C-terminal domains of factor H of human complement: a correlation between haemolytic uraemic syndrome and a predicted heparin binding site. *J Mol Biol* 2002; **316**: 217–224.
18. Esparza-Gordillo J, Jorge EG, Garrido CA *et al.* Insights into hemolytic uremic syndrome: segregation of three independent predisposition factors in a large, multiple affected pedigree. *Mol Immunol* 2006; **43**: 1769–1775.
19. Sánchez-Corral P, Perez-Cabalerro D, Huarte O *et al.* Structural and functional characterisation of factor H mutations associated with atypical hemolytic uremic syndrome. *Am J Hum Genet* 2002; **71**: 1285–1295.
20. Dragon-Durey MA, Fremeaux-Bacchi V, Loirat C *et al.* Heterozygous and homozygous factor H deficiencies associated with hemolytic uremic syndrome or membranoproliferative glomerulonephritis: report and genetic analysis of 16 cases. *J Am Soc Nephrol* 2004; **15**: 787–795.
21. Ault BH, Schmidt BZ, Fowler NL *et al.* Human factor H deficiency. Mutations in framework cysteine residues and block in H protein secretion and intracellular catabolism. *J Biol Chem* 1997; **272**: 25168–25175.
22. Schmidt BZ, Fowler NL, Hidvegi T *et al.* Disruption of disulfide bonds is responsible for impaired secretion in human complement factor H deficiency. *J Biol Chem* 1999; **274**: 11782–11788.
23. Edwards AO, Ritter III R, Abel KJ *et al.* Complement factor H polymorphism and age-related macular degeneration. *Science* 2005; **308**: 421–424.
24. Hakobyan S, Harris CL, Tortajada A *et al.* Measurement of factor H variants in plasma using variant-specific monoclonal antibodies: application to assessing risk of age-related macular degeneration. *Invest Ophthalmol Vis Sci* 2008; **49**: 1983–1990.
25. Zipfel PF, Skerka C. FHL-1/reconectin: a human complement and immune regulator with cell-adhesive function. *Immunol Today* 1999; **20**: 135–140.
26. Martinez-Barricarte R, Pianetti G, Gautard R *et al.* The complement factor H R1210C mutation is associated with atypical hemolytic uremic syndrome. *J Am Soc Nephrol* 2008; **19**: 639–646.
27. Pérez-Caballero D, González-Rubio C, Gallardo ME *et al.* Clustering of missense mutations in the C-terminal region of factor H in atypical hemolytic uremic syndrome. *Am J Hum Genet* 2001; **68**: 478–484.
28. Esparza-Gordillo J, Soria JM, Bui A *et al.* Genetic and environmental factors influencing the human factor H plasma levels. *Immunogenetics* 2004; **56**: 77–82.
29. Falcao DA, Reis ES, Paixao-Cavalcante D *et al.* Deficiency of the human complement regulatory protein factor H associated with low levels of component C9. *Scand J Immunol* 2008; **68**: 445–455.
30. Friese MA, Hellwage J, Jokiranta TS *et al.* FHL-1/reconectin and factor H: two human complement regulators which are encoded by the same gene are differentially expressed and regulated. *Mol Immunol* 1999; **36**: 809–818.
31. Harris CL, Lublin DM, Morgan BP. Efficient generation of monoclonal antibodies for specific protein domains using recombinant immunoglobulin fusion proteins: pitfalls and solutions. *J Immunol Methods* 2002; **268**: 245–258.
32. Sim E, Palmer MS, Puklavec M *et al.* Monoclonal antibodies against the complement control protein factor H (beta 1 H). *Biosci Rep* 1983; **3**: 1119–1131.

Functional basis of protection against age-related macular degeneration conferred by a common polymorphism in complement factor B

Tamara Montes[a], Agustín Tortajada[a], B. Paul Morgan[b], Santiago Rodríguez de Córdoba[a], and Claire L. Harris[b,1]

[a]Centro de Investigaciones Biológicas, Consejo Superior de Investigaciones Cientificas, Centro de Investigación Biomédica en Red de Enfermedades Raras and Fundación Renal Iñigo Alvarez de Toledo, Ramiro de Maeztu 9, 28040 Madrid, Spain; and [b]Department of Medical Biochemistry and Immunology, Henry Wellcome Building, School of Medicine, Cardiff University, Heath Park, Cardiff CF14 4XN, United Kingdom

Edited by Douglas T. Fearon, University of Cambridge, Cambridge, United Kingdom, and approved January 23, 2009 (received for review December 11, 2008)

Mutations and polymorphisms in complement genes have been linked with numerous rare and prevalent disorders, implicating dysregulation of complement in pathogenesis. The 3 common alleles of factor B (fB) encode Arg (*fB$_{32R}$*), Gln (*fB$_{32Q}$*), or Trp (*fB$_{32W}$*) at position 32 in the Ba domain. The *fB$_{32Q}$* allele is protective for age-related macular degeneration, the commonest cause of blindness in developed countries. Factor B variants were purified from plasma of homozygous individuals and were tested in hemolysis assays. The protective variant fB$_{32Q}$ had decreased activity compared with fB$_{32R}$. Biacore comparison revealed markedly different proenzyme formation; fB$_{32R}$ bound C3b with 4-fold higher affinity, and formation of activated convertase was enhanced. Binding and functional differences were confirmed with recombinant fB$_{32R}$ and fB$_{32Q}$; an intermediate affinity was revealed for fB$_{32W}$. To confirm contribution of Ba to binding, affinity of Ba for C3b was determined. Ba-fB$_{32R}$ had 3-fold higher affinity compared with Ba-fB$_{32Q}$. We demonstrate that the disease-protective effect of fB$_{32Q}$ is consequent on decreased potential to form convertase and amplify complement activation. Knowledge of the functional consequences of polymorphisms in complement activators and regulators will aid disease prediction and inform targeting of diagnostics and therapeutics.

alternative pathway | AMD

Dysregulation of the alternative pathway (AP) of complement is associated with numerous pathologies, including age-related macular degeneration (AMD), atypical hemolytic uremic syndrome (aHUS), rheumatoid arthritis, dense deposit disease (DDD), and lupus nephritis (1). The AP "ticks over" continuously in plasma, enabling rapid response to pathogen, and it also amplifies the other complement activation pathways (2). The critical AP activation step is cleavage of C3 to C3b. The C3-cleaving enzyme, or convertase, is formed through the Mg^{2+}-dependent binding of factor B (fB) to C3b, forming the proenzyme, C3bB. Factor B within the complex is then cleaved by a plasma serine protease, fD, releasing an amino terminal fragment, Ba (comprising 3 short consensus repeats; SCR). This fragment takes no further part in the complement cascade. Bb, comprising a serine protease domain and a von Willebrand factor Type A (vWF-A) domain, remains bound to C3b, and is an active serine protease capable of cleaving further C3. Convertase-generated C3b can itself form more C3bBb, providing amplification of activation. As the C3b clusters around the surface-bound convertases a C5-cleaving enzyme is formed (C3bBbC3b), C5b is generated and the lytic pathway proceeds, with formation of the membrane attack complex (MAC) (3).

To protect against the tendency of the AP to rapidly amplify, host cells express an armory of complement regulatory proteins (CReg), which inhibit convertases or prevent MAC formation on their surfaces (4, 5). These CReg are either membrane-associated (CD55, CD46, and CD59) or fluid phase (fH, C4b-binding protein) proteins. Dysregulation of the AP is brought about by loss-of-function/expression mutations in CReg or gain-of-function mutations in components, both scenarios result in uncontrolled complement activation on self-surfaces and subsequent tissue damage and/or inflammation. The best characterized disease of AP dysregulation is aHUS, where loss-of-function mutations in the CReg or gain-of-function mutations in components lead to increased complement activation at cell surfaces, resulting in renal damage (6, 7).

More remarkably, common polymorphisms in AP components and CReg have also been linked to disease. Of particular interest are 3 common polymorphic variants of fB that differ at position 32 in the Ba domain (amino acid 7 in the mature protein; *fB$_{32R}$*, *fB$_{32Q}$*, and *fB$_{32W}$*; rs12614 and rs641153) (8–10); *fB$_{32R}$* is the most frequent allele in Caucasians (allele frequency 0.79), and was originally described as fB-S ("slow," defined by electrophoretic mobility); the fB-F ("fast") allele was further defined as fB-FA (*fB$_{32Q}$*; allele frequency 0.05) and fB-FB (*fB$_{32W}$*; allele frequency 0.16) (11). Factor B-S and fB-F have long been associated with various pathologies, including susceptibility to pathogenic infection, for example, with *Trypanosoma cruzi*, where fB-S is protective in cardiomyopathy associated with Chagas disease (12). Factor B-S is reported to be overrepresented in multiple sclerosis (13), and weakly associated with Type I diabetes mellitus, where it is present in a HLA haplotype strongly linked to disease (14). However, the most striking example of linkage of common variants in fB to disease is in AMD, the commonest cause of irreversible blindness in the elderly in the Western world (15).

The hallmark lesion of AMD is the development of drusen, lipoproteinaceous deposits located between the retinal pigment epithelium (RPE) and Bruch's membrane (16). Deposition of drusen is followed by extensive atrophy of the RPE and overlaying photoreceptor cells (geographic atrophy, GA), or aberrant choroidal neovascularization (CNV). CNV under the macula is the primary cause of blindness. Although the pathogenesis of AMD is still unclear, inflammatory responses are implicated (17, 18). AMD is a multifactorial disease, influenced by age, ethnicity, and environmental and genetic risk factors (19). Two major AMD susceptibility loci (1q31, *CFH*, and 10q26, *LOC387715*/*HTRA1*) that independently contribute to disease risk have been recently identified by candidate region linkage and whole genome association analyses (20–23). Linkage to *CFH*, the gene

Author contributions: T.M., B.P.M., S.R.d.C., and C.L.H. designed research; T.M., A.T., S.R.d.C., and C.L.H. performed research; T.M., S.R.d.C., and C.L.H. analyzed data; and B.P.M., S.R.d.C., and C.L.H. wrote the paper.

The authors declare no conflict of interest.

This article is a PNAS Direct Submission.

[1]To whom correspondence should be addressed. E-mail: harriscl@cardiff.ac.uk.

This article contains supporting information online at www.pnas.org/cgi/content/full/0812584106/DCSupplemental.

encoding fH, was followed by reports describing association of AMD with polymorphic variations in other complement genes, *fB*, *C3*, and the fH-related genes *CFHR1* and *CFHR3* (24–28). Remarkably, although most AMD-associated polymorphisms are linked to increased disease risk, several replication studies have demonstrated that the *fB$_{32Q}$* variant confers significant protection from development of AMD (26, 27, 29).

The risk allele in *LOC387715* causes destabilization of the mRNA and subsequent reduced expression of the encoded protein, a mitochondrial protein normally expressed at high levels in the retinal photoreceptor cells (30). Thus, a functional consequence that increases risk of AMD is plausible. In contrast, no functional explanation of the association of any complement polymorphism with AMD has yet been provided. Here, we demonstrate the functional mechanism underlying the association of fB variants with pathology. Using purified and recombinant (r) fB variants, we demonstrate that the fB$_{32Q}$ variant, identified by genetic association studies to be protective in AMD, is less efficient at forming the amplifying AP convertase. This variant likely protects from development of pathology in AMD, and perhaps other chronic inflammatory diseases, by dampening complement activation, but may predispose to infection due to reduced amplification activity.

Results

Purification of fB Variants and Differential Activity in Hemolysis Assays. To investigate whether the R32Q polymorphism in fB influenced function, fB was purified from plasma of a donor identified by genotyping to be R32Q heterozygote. The 2 variants were separated by anion exchange chromatography at pH 6.0 [supporting information (SI) Fig. S1*A*], and individually gel filtered on Superdex 200 equilibrated in CFD. Fractions containing pure, monomeric fB were identified and used immediately for functional analyses. To compare functional activity of the 2 variants, fB was immunodepleted from human serum (NHSΔfB) and used as a source of all other complement components. Rabbit erythrocytes were incubated with NHSΔfB and different concentrations of fB variants, lysis was measured (Fig. S1*B*). The fB$_{32Q}$ variant was less hemolytically active than fB$_{32R}$, at least 2-fold more protein was required to achieve equivalent lysis.

To confirm and extend these data, fB was purified by affinity chromatography, and gel filtration from plasma of 6 individuals identified by genotyping to be homozygote for *fB$_{32R}$* (3 individuals), *fB$_{32Q}$* (2 individuals), and *fB$_{32W}$* (1 individual). The 3 variants showed consistent differences in hemolytic activities, with fB$_{32Q}$ the least lytic and fB$_{32R}$ the most lytic (Fig. 1). Calculated EC50s were 35.6 and 43.5 nM (for the fB$_{32Q}$ individuals); 15.4, 12.6, and 13.9 nM (for the fB$_{32R}$ individuals); and 17.9 nM (for the fB$_{32W}$ individual). The difference in means between fB$_{32R}$ and fB$_{32Q}$ was statistically significant (2-tailed unpaired T test; $P < 0.0038$).

Formation of AP Convertase by fB$_{32R}$, fB$_{32Q}$, and fB$_{32W}$ Variants. We previously used SPR (Biacore) to monitor proenzyme (C3bB) formation and convertase activation (C3bBb) in real-time. To dissect the mechanisms underlying differential hemolytic activities of fB$_{32R}$ and fB$_{32Q}$, fB, purified from homozygote donors (see inset in Fig. 2), was gel filtered into Biacore buffer, and analyzed immediately. Proenzyme formation was analyzed by SPR by flowing fB over the C3b-immobilized surface in the presence of Mg^{2+}, without fD. Factor B$_{32R}$ was more efficient in forming proenzyme, with higher levels of C3bB$_{32R}$ formed at identical fB concentrations. Decay was rapid for each variant. We have previously shown that several points of contact and conformational transitions are involved in the interaction between fB and C3b, which is best modeled by using a "2-state transition" model (31). Analysis of sensorgrams (Fig. 2), revealed a 4-fold higher affinity of binding for fB$_{32R}$ over fB$_{32Q}$; K_D calculated as a mean of 3 independent experiments by using "2-state reaction" model: fB$_{32R}$, 0.17 ± 0.03 μM; fB$_{32Q}$, 0.74 ± 0.25 μM.

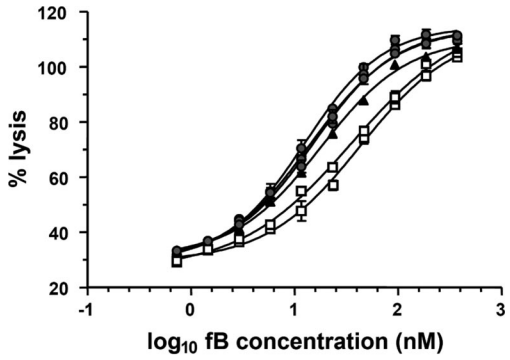

Fig. 1. Hemolytic activity of the fB variants. The variant fB proteins were purified from plasma of 6 donors known to be homozygous for fB$_{32R}$ (3 donors, circles), fB$_{32Q}$ (2 donors, squares), or fB$_{32W}$ (1 donor, triangles). Rabbit erythrocytes were incubated with fB-depleted serum and different concentrations of the purified fB variants. Lysis was developed for 45 min and hemoglobin release was used to calculate percentage lysis. Data points represent mean ± SD of 3 determinations. The log$_{10}$ of fB concentration was plotted against percentage lysis, and curves were fitted by using nonlinear regression analysis to calculate the EC$_{50}$.

To analyze formation of the convertase C3bBb, fD was included with the fB variants. Although the kinetics of convertase formation by fB$_{32R}$ and fB$_{32Q}$ were similar, because fB$_{32Q}$ bound with lower affinity, lower levels of convertase were formed (Fig. 3*A*).

To investigate the half-lives of the activated convertase, purified fB variants were flowed over a C3b surface in the presence of fD. Dissociation rates (kd) do not depend on concentration; therefore, decay curves were normalized in the y axis. There was an obvious gradation of enzyme formation (fB$_{32R}$ > fB$_{32W}$ > fB$_{32Q}$), whereas rates of decay of the 3 enzymes were identical (Fig. 3*B*), as expected, because Ba, containing the variant amino acid, is released from the convertase, and cannot influence decay of Bb from C3b.

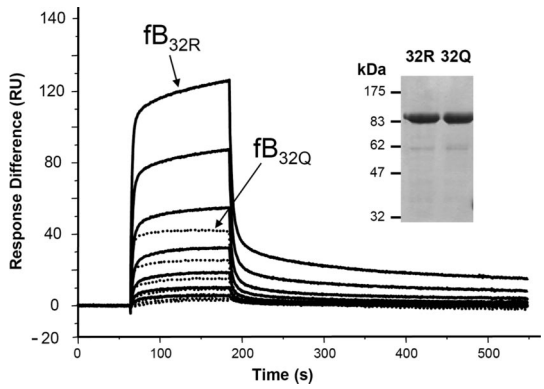

Fig. 2. SPR analysis of proenzyme formation by native fB. The variant fB proteins were purified from the plasma of donors known to be homozygous for fB$_{32R}$ or fB$_{32Q}$, representative preparation is indicated (reducing SDS/PAGE gel stained with Coomassie Blue R250). FB was flowed over the surface of the C3b-coated chip at concentrations between 460 and 7 nM in Biacore buffer (10 mM Hepes, pH 7.4/50 mM NaCl/1 mM $MgCl_2$/0.005% surfactant P20). Sensorgrams from fB$_{32R}$ are solid lines and fB$_{32Q}$ are dotted lines; identical concentrations are illustrated for the 2 proteins.

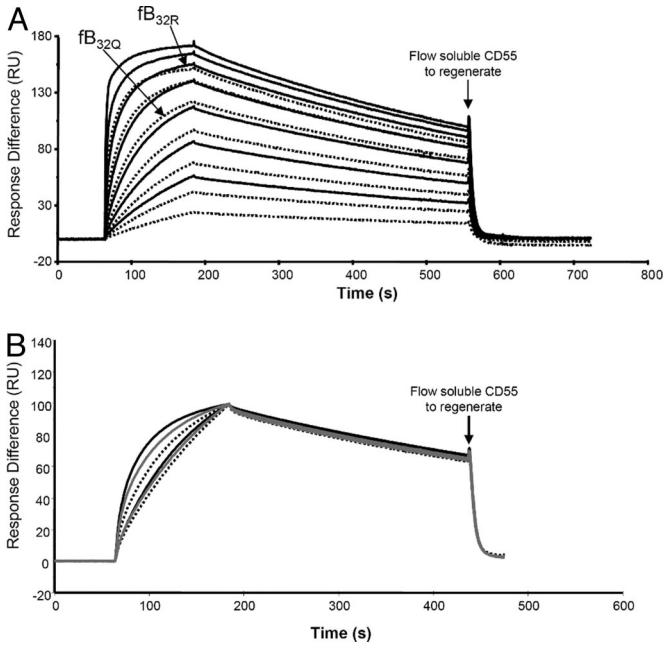

Fig. 3. SPR analysis of activated convertase formation by native fB. (*A*) The variant fB proteins were purified from the plasma of donors known to be homozygous for fB_{32R} or fB_{32Q}. FB was flowed over the surface of the C3b-coated chip in the presence of 1 μg/mL fD at concentrations between 460 and 7 nM in Biacore buffer (10 mM Hepes, pH 7.4/50 mM NaCl/1 mM $MgCl_2$/0.005% surfactant P20). Sensorgrams from fB_{32R} are solid lines and fB_{32Q} are dotted lines; identical concentrations are illustrated for the 2 variants. Arrows indicate sensorgram generated by either variant at 115 nM for comparison. Kinetic information from 2 independent experiments (different surface and preparation of fB each time) were analyzed by using 2-state reaction model, and data were identical for both experiments. K_D: fB_{32R}, 2.9 nM; and fB_{32Q}, 7.1 nM (χ^2 in replicate experiments was between 6 and 13). Data were also analyzed by using a 1:1 Langmuir model; although the fit was not as good, kinetic analysis revealed similar affinities (3.2 nM, fB_{32R}; 7.7 nM, fB_{32Q}) (χ^2 in replicates was between 7 and 32). (*B*) All 3 variants were purified from plasma of homozygous donors, and flowed over a C3b surface at 2 concentrations (156, 39 nM). Sensorgrams from fB_{32R} are solid lines, fB_{32Q} are dotted lines, and fB_{32W} are in gray. Data were normalized in the *y* axis, and sensorgrams overlaid.

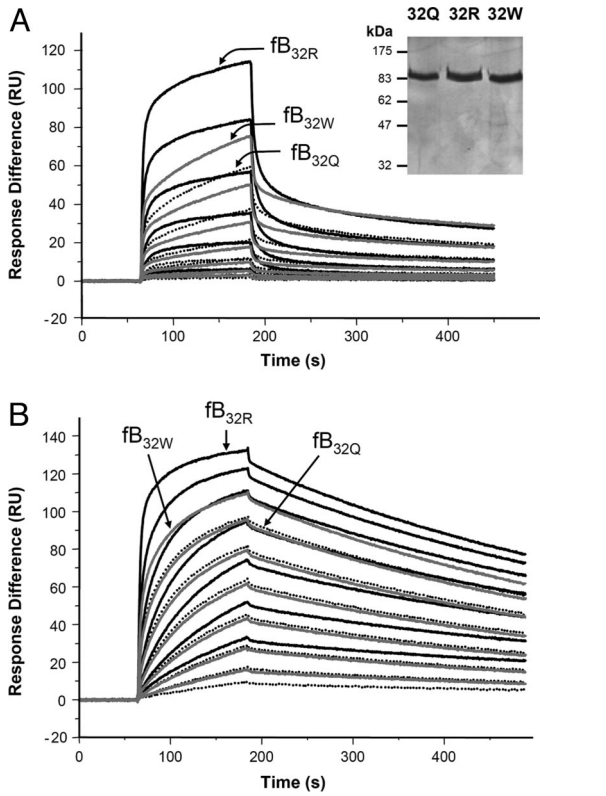

Fig. 4. SPR analysis of enzyme formation by rfB. The variant rfB proteins were purified from supernatant, representative preparation is indicated (reducing SDS/PAGE gel stained by silver). (*A*) Recombinant fB was flowed over the C3b-coated chip at concentrations between 233 and 4 nM in Biacore buffer (10 mM Hepes, pH 7.4/50 mM NaCl/1 mM $MgCl_2$/0.005% surfactant P20). Sensorgrams from rfB_{32R} are solid lines, rfB_{32Q} are dotted lines, and rfB_{32W} are in gray; identical concentrations are indicated for the 3 variants. Arrows indicate sensorgram generated by each variant at 233 nM for comparison. K_D calculated by using 2-state reaction model: rfB_{32R}, 0.06 μM; rfB_{32W}, 0.07 μM; and rfB_{32Q}, 0.12 μM. (*B*) Recombinant fB was flowed over the C3b-coated chip at concentrations between 233 and 4 nM in the presence of 1 μg/mL fD. Sensorgrams from rfB_{32R} are solid lines, rfB_{32Q} are dotted lines, and rfB_{32W} are in gray; identical concentrations are indicated for the 3 variants. K_D calculated by using 2-state reaction model: rfB_{32R}, 2.7 nM; rfB_{32W}, 6.0 nM; and rfB_{32Q}, 9.5 nM.

Formation of AP Convertase by Recombinant fB_{32R}, fB_{32Q}, and fB_{32W} Variants. To confirm these kinetic data, we expressed recombinant forms of fB differing only at position 32, rfB_{32R}, rfB_{32Q}, and rfB_{32W} in CHO cells, and purified from supernatant by affinity chromatography and gel filtration (see inset in Fig. 4*A*). Analysis of proenzyme formation by SPR revealed higher affinity binding of rfB_{32R} compared with rfB_{32Q}, confirming results obtained with the native proteins (Fig. 4*A*). The third variant, rfB_{32W}, revealed an intermediate efficiency of binding. Kinetic profiles differed slightly when compared with native protein, likely due to different glycosylation; however, measured affinities were similar for native and recombinant. Formation of activated convertase using rfB variants confirmed that rfB_{32R} generated most convertase and rfB_{32Q} the least, with rfB_{32W} intermediate (Fig. 4*B*); decay rates of Bb were identical for convertases generated by each recombinant protein.

Isolation of Ba and Binding to C3b. The above data imply that variation in Ba influences proenzyme formation and the amount of enzyme formed. FB binds C3b through a multipoint contact, involving Ba and the vWF-A domain. To confirm differential binding of the variant Ba domains to C3b, Ba fragments were generated from purified fB_{32R} and fB_{32Q} by incubating fB and fD with C3b immobilized on Sepharose. Bb was removed on an anti-Bb affinity column, Ba was "polished" by gel filtration, and used immediately in SPR binding studies with immobilized C3b (Fig. 5*A*). In contrast to fB, binding was very weak, necessitating high concentrations of Ba to determine binding affinity. Ba purified from fB_{32R} bound C3b with 3-fold higher affinity than Ba generated from fB_{32Q} (Fig. 5 *B* and *C*).

Effect of Ionic Strength on Convertase Formation. To dissect out the differences between the fB variants, enzyme formation and Ba binding were analyzed in low salt concentrations. To confirm that the differential binding occurred at physiological salt, proenzyme and convertase formation by fB_{32R} and fB_{32Q} were analyzed in Hepes-buffered saline (150 mM). The fB_{32R} variant again showed a 3- to 4-fold higher affinity in proenzyme formation compared with fB_{32Q}, with resultant enhanced convertase formation (Fig. S2).

Discussion

The common allotypes of fB affect risk of disease, the most striking example being AMD, where fB_{32Q} is protective (OR 0.32; 95% CI: 0.21–0.48; see refs. 26, 27). The variant amino acid in fB is just 7 aa from the amino terminus (25-aa leader sequence

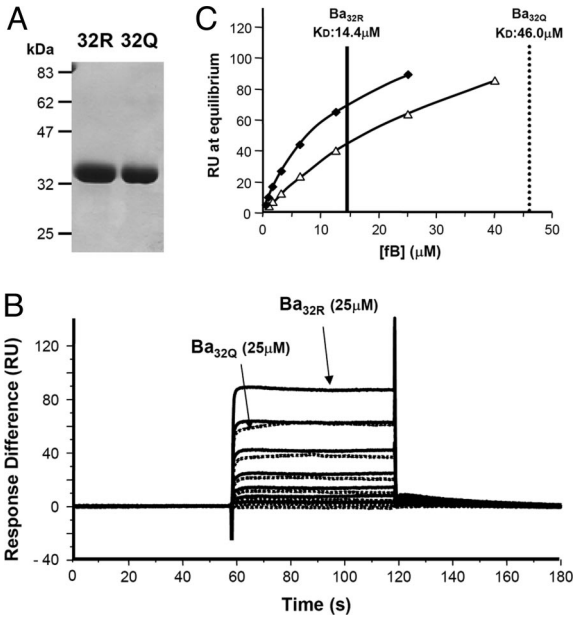

Fig. 5. SPR analysis of Ba binding to C3b. (*A*) The variant fB proteins were purified from plasma of donors known to be homozygous for fB_{32R} or fB_{32Q}, and Ba was isolated. (*B*) Ba was flowed over the surface of the C3b-coated chip at concentrations between 25 and 0.4 μM in Biacore buffer (10 mM Hepes, pH 7.4/50 mM NaCl/1 mM $MgCl_2$/0.005% surfactant P20). Sensorgrams from Ba_{32R} are solid lines and Ba_{32Q} are dotted lines; identical concentrations are indicated for the 2 variants. (*C*) Steady state analysis of the data indicate the affinities for C3b in these buffer conditions are: K_D Ba_{32R}, 14.4 μM; and K_D Ba_{32Q}, 46.0 μM. For Ba_{32Q}, a sample at 40 μM was included, because the affinity was markedly lower than Ba_{32R}.

removed) within the Ba domain; a location that is paradoxical in that Ba is not part of the activated convertase. Therefore, it cannot affect enzyme activity (Fig. 6). The crystal structure of fB demonstrated that Ba was folded back onto the Bb domain, with SCR2 and SCR3 of Ba packed tightly into an antiparallel dimer capped by SCR1, this amino-terminal SCR likely hindering access of C3b to the vWF-A domain in Bb (32). It was suggested that initial binding of the 3 SCRs to C3b displaced them from the vWF-A and serine protease domains, allowing access of C3b, and triggering structural rearrangements that enabled proteolytic cleavage of fB by fD. The amino terminus of fB is unstructured, and the crystal structure commences at Q_{34} (amino acid 9 in the mature protein; see ref. 32); Q_{34} (and, by inference, the variant amino acid R_{32}/Q_{32}) is in close proximity to 2 residues in the vWF-A domain (D_{279} and F_{286}), known to affect proenzyme formation (Fig. 6; see ref. 7). The location of the variant amino acid in fB, and data indicating a binding interaction between Ba and C3b (33), led us to hypothesize that the polymorphism would affect proenzyme formation.

To test the hypothesis, fB variants were isolated from plasma. In hemolysis assays using rabbit erythrocytes as target, they showed differential activities, with fB_{32Q} being the least lytic (Fig. 1). The underlying mechanism was dissected by using SPR. When proenzyme formation was analyzed, fB_{32Q} bound C3b with a 4-fold lower affinity compared with fB_{32R}; the fB_{32W} variant had an intermediate affinity (Fig. 2). These data were confirmed by using rfB variants (Fig. 4). The influence of the polymorphism in the Ba domain on C3b binding was confirmed by isolating the variant Ba, and directly comparing binding to C3b (Fig. 5). Although the affinity of Ba for C3b is weak, avidity effects from simultaneous multisite binding in the Ba and Bb domains likely explains the striking effect of variation in Ba on apparent affinity of fB. When effects of fB variants on formation of the activated convertase, C3bBb were studied, fB_{32R} generated 2.5-fold more enzyme than fB_{32Q} under the experimental conditions (Fig. 3). These data show that fB_{32Q} is less efficient at maintaining amplification in the AP, and provide a mechanism for the observation that fB_{32Q} protects from pathology in AMD.

Previous investigations into functional differences between the fB variants have produced variable results. Early studies using hemolytic overlay assays indicated that fB_{32Q} had either decreased or equivalent functional activity compared with fB_{32R} (34–36). These data were complicated by variable plasma concentrations of fB and differences in expression levels of the allele products, making quantitative comparisons difficult. A later study by Horiuchi et al. (37) analyzed the functional activity of recombinant forms of fB_{32R} and fB_{32Q}, and concluded that there was no functional difference. In this study, convertase was assembled on the surface of C3b-coated sheep erythrocytes by using native properdin and fD, and rfB (quantified by ELISA in cell culture supernatant). We have shown that the R32Q polymorphism influences the efficiency of proenzyme formation, rather than the activity of the convertase itself; therefore, the functional difference would only be revealed if

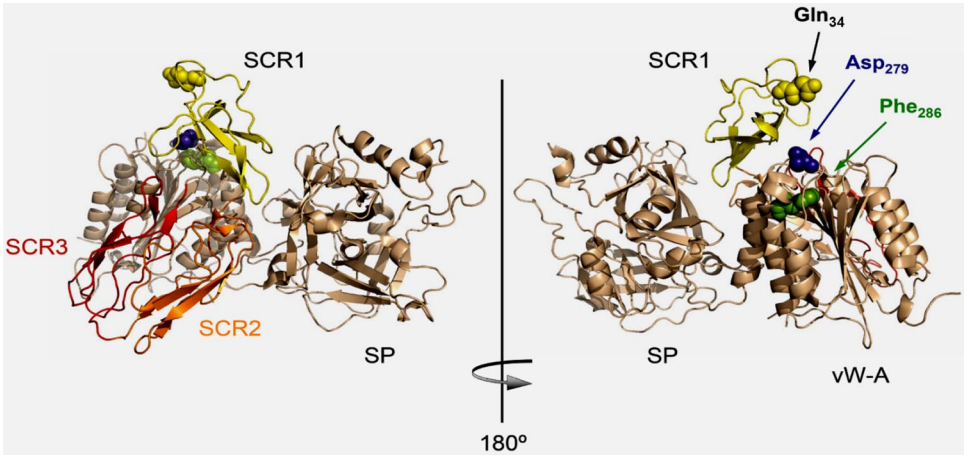

Fig. 6. Structural analysis of the fB R32Q amino acid substitution. (*Left*) The crystal structure of human fB shows the SCRs of Ba folded back across the VWF-A domain [Milder et al. (32), Protein Data Bank accession number 2OK5]. (*Right*) Amino acid Q_{34} is illustrated in the structure, this amino acid is 2 residues downstream of Q_{32}, and lies in close proximity to D_{279} and F_{286}, alterations in which are known to affect proenzyme formation (C3bB). The molecular graphic was generated by using PyMOL Molecular Graphics System (DeLano, 2002, available at www.pymol.org).

the assay reported by Horiuchi et al. (37) was developed at a point where formation of activated convertase was incomplete, and not all of the fB was cleaved to Bb and stabilized by properdin. In our studies, all proteins were highly purified and polished by gel filtration into assay buffer immediately before each assay, the resultant sensitive assays have enabled us to establish beyond doubt functional differences between the variants.

The fB_{32Q} variant is apparently only protective in AMD and not in other diseases of complement dysregulation (e.g., DDD and aHUS). The reasons for disease specificity are unclear. Several studies have demonstrated elevated plasma levels of complement activation products (including C3a, C3d, Ba, and SC5b-9) in AMD compared with controls, indicating systemic dysregulation of complement, and implying that AMD is a systemic disease with local manifestation in the retina (38, 39). This systemic component may amplify the effects of the fB polymorphism, explaining the disease specificity. Comparative expression levels from the fB alleles in controls and AMD are not yet available; early studies using crossed immunoelectrophoresis and radial immunodiffusion assays demonstrated a trend for higher expression from the fB_{32Q} allele in normal individuals (38, 39) although, as with many complement components, the range around the mean was large. Decreased plasma levels of the fB_{32R} allele product may indicate decreased expression, or increased catabolism due to AP tickover or chronic inflammatory processes.

The triggers for drusen accumulation and retinal pathology in AMD are unknown; however, autoimmune mechanisms have been suggested. Lipid moieties in the rod photoreceptor membranes become photo-oxidized over time, forming omega-(2-carboxyethyl)pyrrole (CEP) adducts that may elicit an immune response, generating autoantibodies that trigger local inflammatory processes, including complement activation (40, 41). Damaged tissue and accumulation of extracellular insoluble debris is in itself inflammatory, likely driving complement activation and immune responses in AMD, as in other chronic pathologies such as Alzheimer's disease, where damaged neurons and deposits of amyloid β peptide drive complement activation (42).

We here explain the mechanism by which a common polymorphism in a complement component protects an individual from AMD. The R32Q polymorphism in fB (rs12614 and rs641153) affects risk of AMD by altering AP activity. Variations in *C3* (R102G) and *CFH* (V62I and Y402H) are also linked to altered risk of AMD, although the functional consequences of these changes have not been characterized; early reports that fH_{402H} bound less well to CRP in drusen have not been substantiated (43). Because fB_{32Q} is less efficient at amplifying the AP, it protects from AMD and perhaps other chronic inflammatory pathologies; however, it may have the opposite effect in infection, where fB_{32Q} may predispose to disease due to suboptimal AP activation on pathogens. Indeed, the association of variants of multiple complement components or CReg with disease (e.g., C3, fB, and fH in AMD; fH, fI, fB, C3, and CD46 in aHUS) suggest that particular combinations of variants, or "complotypes," may combine to influence systemic complement activity in an individual; thus, affecting risk of chronic inflammatory damage and susceptibility to infection. The multilocus risk model of AMD suggests that the effects of common variants are additive, and the model can identify individuals whose lifetime risk of AMD ranges from <1 to $>50\%$ (20–28). Thus, specific variant sets of complement components and CReg can dramatically influence outcome, an observation that is increasingly important as the population ages, likely impacting not only in AMD, but also in other chronic inflammatory diseases such as Alzheimer's disease and atheroma. Understanding of the mechanisms underlying these associations is an essential prerequisite to the design of therapies that target complement activation in these diseases. For example, our data suggest that anti-Ba antibodies may have potential in the clinic, particularly for those individuals who carry high risk combinations of complement components and CReg.

Materials and Methods

Genotyping. Healthy volunteers were screened for mutations/polymorphisms in the CFB gene by DNA sequencing of PCR amplified fragments. Genomic DNA was prepared from peripheral blood cells according to standard procedures. Each exon of the CFB gene was amplified from genomic DNA by using specific primers derived from the 5′ and 3′ intronic sequences as described (7). Sequencing was performed in an ABI 3730 sequencer by using a dye terminator cycle sequencing kit (Applied Biosystems).

Preparation of Complement Components and Activation Fragments. C3 and factor B were purified from normal human serum by classical chromatography (C3) or affinity chromatography (fB); details are given in *SI Methods*. Ba was purified as a by-product of AP activation as detailed in *SI Methods*. All proteins used for Biacore studies were gel-filtered into the appropriate Biacore buffer before experimentation.

Production of Recombinant fB. A cDNA encoding full-length fB_{32R} was introduced in the eukaryote expression vector pCI-Neo (Promega), and R32Q-aa and R32W-aa substitutions introduced by using QuikChange site-directed mutagenesis kit (Stratagen) and appropriate primers. All fB cDNA clones were fully sequenced to confirm fidelity. CHO cells, maintained in Ham-F12 medium (GIBCO-BRL) supplemented with 10% FCS, L-glutamine (2 mM final concentration), penicillin, and streptomycin (10 U/mL and 100 μg/mL), were plated in p60 plates at 5×10^5 cells per well. Transfections were carried out 1 day later with 10 μg of the pCI-Neo constructs and 24 μL of Lipofectine (Invitrogen) in a total volume of 1 mL of medium per well. Transfected cells were selected in G418 sulfate (Geneticin; GIBCO-BRL) at 500 μg/mL, cloned by limiting dilution, and clones producing the highest levels of rfB as assessed by ELISA (7) were expanded for production; rfB was purified from tissue culture supernatant by affinity chromatography on anti-Bb as described above. Eluate was concentrated, and rfB was polished by gel filtration on Superdex200 in Biacore buffer.

Hemolysis Assays. NHS was depleted of fB by flowing over the JC1 anti-Bb affinity column in CFD. Run-through was collected, and undiluted fractions pooled and stored at −80 °C. Use of this standard fB-depleted serum eliminated any variation in hemolysis due to polymorphisms or concentration differences in other complement components and regulators. Rabbit erythrocytes (Erb), washed in CFD (Complement Fixation Diluent, Oxoid) and resuspended to 2% (vol/vol), were mixed with fB depleted NHS (NHSΔfB; 1/38 final dilution; 50 μL of cells, 25 μL of diluted NHSΔfB) and 50 μL of a dilution of purified, gel-filtered fB. CFD permits activation of all pathways of complement activation; therefore, lysis resulted from direct activation of the AP on the surface of Erb or from AP-mediated amplification of the other pathways. After 45 min, cells were pelleted by centrifugation, and hemoglobin release was measured by absorbance at 415 nm. Control incubations included 0% lysis (buffer only) and 100% lysis (0.1% Nonidet-P40). Percentage lysis = 100*(A415 test sample-A415 0% control)/(A415 100% control-A415 0% control). The $\log_{10}$ of fB concentration (final concentration in the incubation) was plotted on the *x* axis, and percentage lysis on the *y* axis. Nonlinear regression was used to fit the curves (GraphPad Prism), and EC_{50} was calculated as the concentration of fB giving a response half way between background (no fB) and maximum.

Biosensor Analysis. All analyses were carried out on a Biacore T100 (GE Healthcare). C3b was amine coupled to the sensor chip as instructed by the manufacturers (NHS/EDC coupling kit). In the example illustrated in Figs. 2 and 3, 880RU C3b are immobilized, although replicate experiments used differing amounts. In Fig. 4, 458RU C3b are immobilized. For kinetic analyses a CM5 (carboxymethylated dextran) chip was used, and data collected at 25 °C at a flow rate of 30 μL/min; data from a reference cell was subtracted to control for bulk refractive index changes. Samples were injected by using the KINJECT command to ensure accurate association kinetics. To analyze proenzyme formation, fB variants were flowed across the C3b surface at different concentrations; the surface was regenerated with EDTA containing buffer as previously described (31). To analyze formation of the activated convertase, fD was included at 1 μg/mL, and the surface was regenerated by using soluble rCD55 (gift of Susan Lea, Oxford, United Kingdom; see ref. 31). In the case of Ba, no regeneration step was required. Due to the low affinity of the Ba interaction, high levels of C3b (4058RU) were immobilized, and steady state analysis was used to quantitate affinity. Data were evaluated by using Biaevaluation T100 evaluation software (Version 1.1), global fitting was used to determine kinetic parameters that fitted all curves (differing concentrations of fB) within an experiment. Concentration of analytes was assessed by using absorbance at A_{280}, molarities were calculated by using the following extinction coefficients (molecular masses and coefficients obtained by using Protean software, DNAStar): fB, 1.43; and Ba, 1.74.

ACKNOWLEDGMENTS. We thank the blood donors for their invaluable contribution to the project. This work was supported by Wellcome Trust University Award 068823 (to C.L.H.), Medical Research Council Project Grant 84908 (to C.L.H. and B.P.M.), Ministerio de Ciencia e Innovación Grant SAF 2008-00226 (to S.R.d.C.), and the Centro de Investigación Biomédica en Red de Enfermedades Raras and Fundación Renal Iñigo Álvarez de Toledo (to S.R.d.C.). B.P.M. was funded by a Wellcome Trust Program Grant (06850).

1. Holers VM (2008) The spectrum of complement alternative pathway-mediated diseases. *Immunol Rev* 223:300–316.
2. Lachmann PJ, Hughes-Jones NC (1984) Initiation of complement activation. *Springer Semin Immun* 7:143–162.
3. Morgan BP (2000) The complement system: An overview. *Methods Mol Biol* 150:1–13.
4. Morgan BP, Meri S (1994) Membrane proteins that protect against complement lysis. *Springer Semin Immun* 15:369–396.
5. Morgan BP, Harris CL (1999) *Complement Regulatory Proteins* (Academic, London).
6. Atkinson JP, Liszewski MK, Richards A, Kavanagh D, Moulton EA (2005) Hemolytic uremic syndrome: An example of insufficient complement regulation on self-tissue. *Ann N Y Acad Sci* 1056:144–152.
7. Goicoechea de Jorge E, et al. (2007) Gain-of-function mutations in complement factor B are associated with atypical hemolytic uremic syndrome. *Proc Natl Acad Sci USA* 104:240–245.
8. Alper CA, Boenisch T, Watson L (1972) Genetic polymorphism in human glycine-rich beta-glycoprotein. *J Exp Med* 135:68–80.
9. Jahn I, et al. (1994) Genomic analysis of the F subtypes of human complement factor B. *Eur J Immunogenet* 21:415–423.
10. Abbal M, et al. (1985) Two subtypes of BfF by isoelectrofocusing: Differential linkage to other HLA markers. *Hum Genet* 69:181–183.
11. Davrinche C, Abbal M, Clerc A (1990) Molecular characterization of human complement factor B subtypes. *Immunogenetics* 32:309–312.
12. Messias-Reason IJ, Urbanetz L, Pereira da Cunha C (2003) Complement C3 F and BF S allotypes are risk factors for Chagas disease cardiomyopathy. *Tissue Antigens* 62:308–312.
13. Papiha SS, Duggan-Keen M, Roberts DF (1991) Factor B (BF) allotypes and multiple sclerosis in north-east England. *Hum Hered* 41:397–402.
14. Hagglof B, et al. (1986) Studies of HLA, factor B (Bf), complement C2 and C4 haplotypes in type 1 diabetic and control families from northern Sweden. *Hum Hered* 36:201–212.
15. Gehrs KM, Anderson DH, Johnson LV, Hageman GS (2006) Age-related macular degeneration–emerging pathogenetic and therapeutic concepts. *Ann Med* 38:450–471.
16. Abdelsalam A, Del Priore L, Zarbin MA (1999) Drusen in age-related macular degeneration: Pathogenesis, natural course, and laser photocoagulation-induced regression. *Surv Ophthalmol* 44:1–29.
17. Anderson DH, Mullins RF, Hageman GS, Johnson LV (2002) A role for local inflammation in the formation of drusen in the aging eye. *Am J Ophthalmol* 134:411–431.
18. Donoso LA, Kim D, Frost A, Callahan A, Hageman GS (2006) The role of inflammation in the pathogenesis of age-related macular degeneration. *Surv Ophthalmol* 51:137–152.
19. Klein R, Peto T, Bird A, Vannewkirk MR (2004) The epidemiology of age-related macular degeneration. *Am J Ophthalmol* 137:486–495.
20. Edwards AO, et al. (2005) Complement factor H polymorphism and age-related macular degeneration. *Science* 308:421–424..
21. Klein RJ, et al. (2005) Complement factor H polymorphism in age-related macular degeneration. *Science* 308:385–389.
22. Haines JL, et al. (2005) Complement factor H variant increases the risk of age-related macular degeneration. *Science* 308:419–421.
23. Hageman GS, et al. (2005) A common haplotype in the complement regulatory gene factor H (HF1/CFH) predisposes individuals to age-related macular degeneration. *Proc Natl Acad Sci USA* 102:7227–7232.
24. Maller J, et al. (2006) Common variation in three genes, including a noncoding variant in CFH, strongly influences risk of age-related macular degeneration. *Nat Genet* 38:1055–1059.
25. Yates JR, et al. (2007) Complement C3 variant and the risk of age-related macular degeneration. *N Engl J Med* 357:553–561.
26. Gold B, et al. (2006) Variation in factor B (BF) and complement component 2 (C2) genes is associated with age-related macular degeneration. *Nat Genet* 38:458–462.
27. Spencer KL, et al. (2007) Protective effect of complement factor B and complement component 2 variants in age-related macular degeneration. *Hum Mol Genet* 16:1986–1992.
28. Spencer KL, et al. (2008) Deletion of CFHR3 and CFHR1 genes in age-related macular degeneration. *Hum Mol Genet* 17:971–977.
29. Jakobsdottir J, Conley YP, Weeks DE, Ferrell RE, Gorin MB (2008) C2 and CFB genes in age-related maculopathy and joint action with CFH and LOC387715 genes. *PLoS ONE* 3:e2199.
30. Fritsche LG, et al. (2008) Age-related macular degeneration is associated with an unstable ARMS2 (LOC387715) mRNA. *Nat Genet* 40:892–896.
31. Harris CL, Abbott RJ, Smith RA, Morgan BP, Lea SM (2005) Molecular dissection of interactions between components of the alternative pathway of complement and decay accelerating factor (CD55). *J Biol Chem* 280:2569–2578.
32. Milder FJ, et al. (2007) Factor B structure provides insights into activation of the central protease of the complement system. *Nat Struct Mol Biol* 14:224–228.
33. Pryzdial EL, Isenman DE (1987) Alternative complement pathway activation fragment Ba binds to C3b. Evidence that formation of the factor B-C3b complex involves two discrete points of contact. *J Biol Chem* 262:1519–1525.
34. Mauff G, Adam R, Wachauf B, Hitzeroth HW, Hiller C (1980) Serum concentration and functional efficiency of factor B alleles. *Immunobiology* 158:86–90.
35. Mortensen JP, Lamm LU (1981) Quantitative differences between complement factor-B phenotypes. *Immunology* 42:505–511.
36. Lokki ML, Koskimies SA (1991) Allelic differences in hemolytic activity and protein concentration of BF molecules are found in association with particular HLA haplotypes. *Immunogenetics* 34:242–246.
37. Horiuchi T, et al. (1993) Human complement factor B: cDNA cloning, nucleotide sequencing, phenotypic conversion by site-directed mutagenesis and expression. *Mol Immunol* 30:1587–1592.
38. Sivaprasad S, et al. (2007) Estimation of systemic complement C3 activity in age-related macular degeneration. *Arch Ophthalmol* 125:515–519.
39. Scholl HP, et al. (2008) Systemic complement activation in age-related macular degeneration. *PLoS ONE* 3:e2593.
40. Gu X, et al. (2003) Carboxyethylpyrrole protein adducts and autoantibodies, biomarkers for age-related macular degeneration. *J Biol Chem* 278:42027–42035.
41. Hollyfield JG, et al. (2008) Oxidative damage-induced inflammation initiates age-related macular degeneration. *Nat Med* 14:194–198.
42. McGeer PL, McGeer EG (2004) Inflammation and the degenerative diseases of aging. *Ann N Y Acad Sci* 1035:104–116.
43. Hakobyan S, et al. (2008) Complement factor H binds to denatured rather than to native pentameric C-reactive protein. *J Biol Chem* 45:30451–30460.

Human Molecular Genetics, 2009, Vol. 18, No. 18 **3452–3461**
doi:10.1093/hmg/ddp289
Advance Access published on June 23, 2009

The disease-protective complement factor H allotypic variant Ile62 shows increased binding affinity for C3b and enhanced cofactor activity

Agustín Tortajada[1], Tamara Montes[1], Rubén Martínez-Barricarte[1], B. Paul Morgan[2], Claire L. Harris[2,*,†] and Santiago Rodríguez de Córdoba[1*,†]

[1]Centro de Investigaciones Biológicas, Consejo Superior de Investigaciones Científicas, Centro de Investigación Biomédica en Enfermedades Raras, Instituto Reina Sofía de Investigaciones Nefrológicas, Ramiro de Maeztu 9 28040 Madrid, Spain and [2]Department of Medical Biochemistry and Immunology, School of Medicine, Cardiff University, Cardiff CF14 4XN, UK

Received May 4, 2009; Revised May 28, 2009; Accepted June 16, 2009

Mutations and polymorphisms in the gene encoding factor H (*CFH*) have been associated with atypical haemolytic uraemic syndrome, dense deposit disease and age-related macular degeneration. The disease-predisposing *CFH* variants show a differential association with pathology that has been very useful to unravel critical events in the pathogenesis of one or other disease. In contrast, the factor H (fH)-Ile$_{62}$ polymorphism confers strong protection to all three diseases. Using ELISA-based methods and surface plasmon resonance analyses, we show here that the protective fH-Ile$_{62}$ variant binds more efficiently to C3b than fH-Val$_{62}$ and competes better with factor B in proconvertase formation. Functional analyses demonstrate an increased cofactor activity for fH-Ile$_{62}$ in the factor I-mediated cleavage of fluid phase and surface-bound C3b; however, the two fH variants show no differences in decay accelerating activity. From these data, we conclude that the protective effect of the fH-Ile$_{62}$ variant is due to its better capacity to bind C3b, inhibit proconvertase formation and catalyze inactivation of fluid-phase and surface-bound C3b. This demonstration of the functional consequences of the fH-Ile$_{62}$ polymorphism provides relevant insights into the complement regulatory activities of fH that will be useful in disease prediction and future development of effective therapeutics for disorders caused by complement dysregulation.

INTRODUCTION

Complement is a major component of innate immunity with crucial roles in microbial killing, apoptotic cell clearance and immune complex handling. Activation of complement by foreign surfaces (alternative pathway, AP), antibody (classical pathway, CP) or mannan (lectin pathway; LP) causes target opsonization, leucocyte recruitment, and cell lysis. The critical steps in complement activation are the formation of unstable protease complexes, named C3-convertases (AP, C3bBb; CP/LP, C4b2a) and the cleavage of C3 to generate C3b. Convertase-generated C3b can form more AP C3 convertase, providing exponential amplification to the initial activation. Binding of C3b to the C3-convertases generates the C5-convertases with the capacity to bind and cleave C5, initiating formation of the lytic membrane attack complex (MAC).

Nascent C3b binds indiscriminately to pathogens and adjacent host cells. To prevent damage to self and to avoid wasteful consumption of components, complement is under the control of multiple regulatory proteins that limit complement activation by inactivating C3b or C4b, dissociating the multimolecular C3/C5 convertases or inhibiting MAC formation.

*To whom correspondence should be addressed at: Complement Genetics and Molecular Pathology Unit, Department of Cellular and Molecular Medicine, Centro de Investigaciones Biologicas, Ramiro de Maeztu 9, Madrid 28040, Spain (S.R.C.) and Complement Biology Group, Department of Medical Biochemistry and Immunology, School of Medicine, Cardiff University, Henry Wellcome Building, Heath Park, Cardiff CF14 4XN, UK (C.L.H.). Tel: +34 917373112 x4432; Fax: +34 915360432; Email: srdecordoba@cib.csic.es (S.R.C.) and Tel: +44 2920687012; Fax: +44 2920687079; Email: harriscl@cardiff.ac.uk (C.L.H.)
†The authors wish it to be known that, in their opinion, the last two authors should be regarded as joint Last Authors.

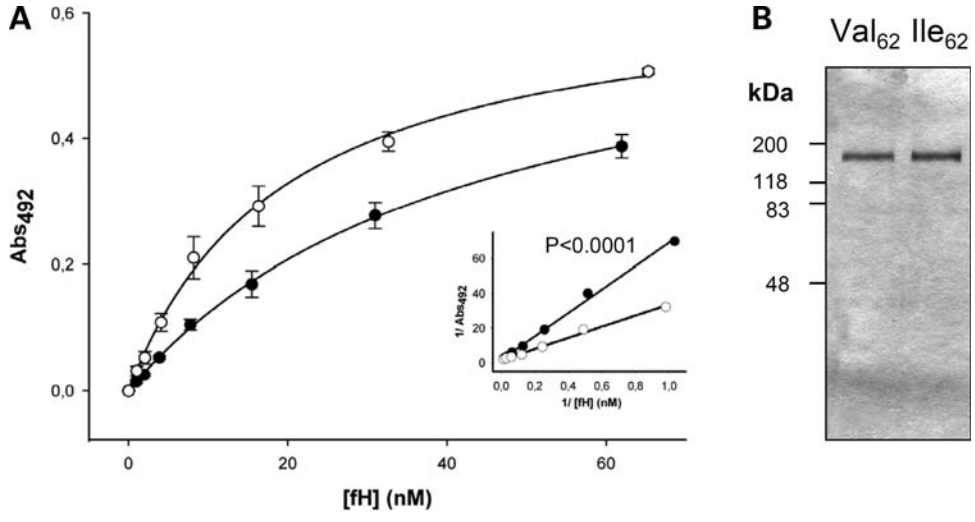

Figure 1. ELISA of fH-Ile$_{62}$ and fH-Val$_{62}$ binding to C3b. (**A**) Interaction between serial dilutions of purified fH-Ile$_{62}$ (open circles) or fH-Val$_{62}$ (filled circles) with C3b deposited in 96-well plates is expressed as Abs$_{492}$. Mean ± SD of three independent experiments are shown. Inset panel shows the double reciprocal plot of the fH-Ile$_{62}$ (open circles) and fH-Val$_{62}$ (filled circles) C3b binding curves. Multiple linear regression analysis revealed significant differences between Val$_{62}$ and Ile$_{62}$ binding to C3b ($P < 0.0001$). (**B**) SDS–PAGE illustrating the fH-Ile$_{62}$ and fH-Val$_{62}$ purified from the plasma of homozygote carriers as described in Materials and Methods and then gel filtered to remove aggregates.

In health, activation of C3 in the blood is kept at a low level and deposition of C3b and further activation of complement is limited to the surface of pathogens (1).

Factor H (fH) is a relatively abundant plasma protein that is essential to maintain complement homeostasis and to restrict the action of complement to activating surfaces. fH binds to C3b, accelerates the decay of the AP C3 convertase (C3bBb) and acts as a cofactor for the factor I (fI)-mediated proteolytic inactivation of C3b (2–4). fH regulates complement both in fluid phase and on cellular surfaces (5–7). The fH molecule is a single polypeptide chain glycoprotein of 155 kDa composed of 20 repetitive units of ∼60 amino acids (8), named short consensus repeats (SCR), arranged end-to-end like 'beads on a string'. fH presents different interaction sites for C3b and polyanions which delineate distinct functional domains at the N- and C-termini. The C3b binding site in SCR1-4 is the only site essential for the C3 convertase decay accelerating and fI cofactor activities of fH. Similarly, the C3b/polyanion binding site located within SCR19–20 is the most important site for preventing AP activation through binding to host cell membranes (9).

Several reports in the last few years have established that membranoproliferative glomerulonephritis type II or dense deposit disease (MPGN2/DDD) (10–13), atypical haemolytic uraemic syndrome (aHUS) (14–17) and age-related macular degeneration (AMD) (18–21) are each associated with mutations or polymorphisms in the *CFH* gene. The available data support the hypothesis that AP dysregulation is a unifying pathogenetic feature of these diverse conditions. They also illustrate a remarkable genotype–phenotype correlation in which distinct genetic variations at *CFH* specifically predispose to aHUS, AMD or MPGN2. In addition to these *CFH* variants conferring increased risk to disease, one common extended haplotype in the *CFH* gene has been described associated with lower risk to aHUS, AMD and MPGN2/DDD (18,22). This *CFH* haplotype carries the Ile$_{62}$ variant within the SCR1 domain in the N-terminal region that is essential for fH regulatory activities. It is, therefore, possible that the substitution of Val for Ile at position 62 may increase the fH regulatory activity and thus confer lower risk to AMD, MPGN2/DDD and aHUS by reducing AP activation.

To test this hypothesis, we have purified the two fH variants from the plasma of fH-Val$_{62}$ and fH-Ile$_{62}$ homozygote donors and performed a series of binding and functional analyses. Our data show that the fH-Ile$_{62}$ variant exhibits increased binding to C3b compared with fH-Val$_{62}$ and is also a more efficient cofactor for fI in the proteolytic inactivation of C3b. Together these data provide an explanation for why fH-Ile62 protects from diseases associated with AP dysregulation.

RESULTS

Interaction of fH-Ile$_{62}$ and fH-Val$_{62}$ with surface-bound C3b

Purified C3b was immobilized on microtiter plates and serial dilutions of fH-Ile$_{62}$ or fH-Val$_{62}$ variants, 'polished' free from potential aggregates by gel filtration, were allowed to interact with C3b for 2 h at 37°C. The fH bound to C3b was detected using an anti-fH mAb (35H9) that recognises equally both variants as described in Materials and Methods section. Binding of the protective fH-Ile$_{62}$ variant to surface-bound C3b was significantly higher than that of the fH-Val$_{62}$ variant ($P < 0.0001$) (Fig. 1A). These data suggest that the Val62Ile polymorphism influences the interaction between fH and C3b. To confirm these findings in a different assay, we performed surface plasmon resonance (SPR) studies using chips coated with identical amounts of fH-Ile$_{62}$ or fH-Val$_{62}$ variants and flowed increasing concentrations of C3b. These SPR assays replicated and extended the findings from ELISA experiments, showing that fH-Ile$_{62}$ binds C3b with a higher affinity than fH-Val$_{62}$ (Fig. 2A). Steady-state

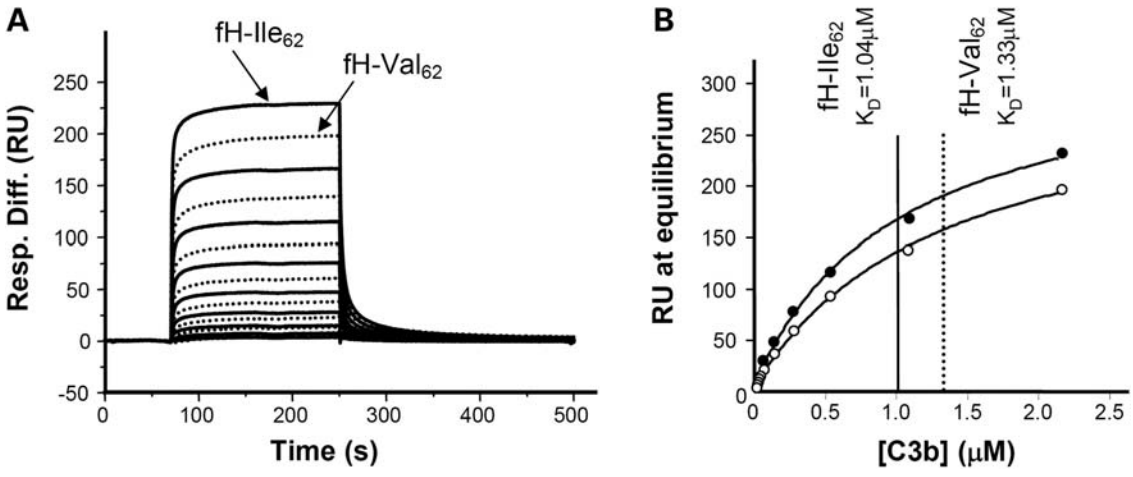

Figure 2. surface plasmon resonance (SPR) analysis of fH-Ile$_{62}$ and fH-Val$_{62}$ binding to C3b. (**A**) Identical amounts of fH were immobilized onto a CM5 chip (fH-Ile$_{62}$ 1004RU immobilized; fH-Val$_{62}$ 1003RU immobilized). C3b (2.2 μM–8.6 nM; 1/2 serial dilution) was flowed across the fH-Ile$_{62}$ or fH-Val$_{62}$ surfaces in 10 mM HEPES pH 7.4, 100 mM NaCl, 0.005% surfactant P20. Data from a reference cell was subtracted to control for any bulk changes in refractive index. Sensorgrams resulting from fH-Ile$_{62}$ are solid lines and fH-Val$_{62}$ are dotted lines; identical concentrations are illustrated for the two variants. (**B**) Steady-state analysis of the data in these buffer conditions indicate the affinities for C3b are: K_D fH-Ile$_{62}$: 1.04 μM, K_D fH-Val$_{62}$: 1.33 μM. The standard errors (SE) in the fits are 0.14 μM for fH-Val$_{62}$ and 0.12 μM for fH-Ile$_{62}$.

analysis under defined buffer conditions gave a K_D of 1.04 μM for fH-Ile$_{62}$ and 1.33 μM for fH-Val$_{62}$ (Fig. 2B).

Cofactor activity for fI-mediated proteolysis of fluid phase C3b

In order to study the fI cofactor activity of the fH-Ile$_{62}$ and fH-Val$_{62}$ variants, we first performed a fluid phase cofactor activity assay. Identical amounts of purified fH-Ile$_{62}$ and fH-Val$_{62}$ variants were added to purified C3b in the presence of fI and incubated for 2.5, 5, 7.5 and 10 min at 37°C. Under the conditions of these experiments, 100% of C3b cleavage was reached after 20 min of incubation. Controls for 0% cleavage were obtained in the absence of fI. The ratio between α′-chain and β-chain of C3b, determined by densitometry, was used to determine the percentage of C3b cleavage. Figure 3A illustrates one experiment representative of several, showing that the fH-Ile$_{62}$ variant is more efficient as a cofactor for fI in the cleavage of C3b in the fluid phase. Figure 3B shows a significant difference ($P = 0.0012$) in the % C3b cleavage catalyzed by identical amounts of purified fH-Ile$_{62}$ and fH-Val$_{62}$ variants at different incubation times. Figure 3C shows the densitometry analysis for the differences in cofactor activities between the fH-Ile$_{62}$ and fH-Val$_{62}$ variants at 6 min incubation time in an independent set of assays. From these experiments, it was calculated that fH-Ile$_{62}$ is ∼20% more active than fH-Val$_{62}$ as a cofactor for the fI-mediated cleavage of fluid phase C3b.

Cofactor activity of fI-mediated inactivation of surface-bound C3b

To determine whether the fH-Ile$_{62}$ variant is also more active than fH-Val$_{62}$ as cofactor for the fI-mediated inactivation of surface-bound C3b, we used a haemolytic assay. C3b deposited onto sheep erythrocytes (EA) was subjected to degradation by fI in the presence of increasing amounts of purified fH-Ile$_{62}$ or fH-Val$_{62}$. For each fH concentration, the residual surface-bound C3b was determined by measuring sheep EA lysis after lytic pathway reconstitution (see Materials and Methods).

Three different experiments, each in triplicate, were performed with identical results (Fig. 4). Calculated EC50 was 14 and 22.6 nM for fH-Ile$_{62}$ and fH-Val$_{62}$, respectively. These experiments consistently show that fH-Ile$_{62}$ is significantly more active than fH-Val$_{62}$ as a cofactor for the fI-mediated proteolysis of surface-bound C3b ($P = 0.0025$; two-tailed unpaired *t*-test). From these experiments, it was estimated that the dose of fH-Val$_{62}$ needed to achieve 50% fI-mediated inactivation of C3b is 1.6–1.8-fold that required when fH-Ile$_{62}$ is used.

Decay accelerating activity of the AP C3 convertase

To measure AP convertase decay accelerating activity of the fH-Ile$_{62}$ and fH-Val$_{62}$ variants, sheep EA were coated with AP convertase (C3bBb) and incubated with increasing amounts of purified fH-Ile$_{62}$ or fH-Val$_{62}$ in the absence of fI. Residual AP convertase on the sheep EA was determined by measuring EA lysis after lytic pathway reconstitution (see Materials and Methods). In three independent experiments, these haemolytic assays showed that fH-Ile$_{62}$ and fH-Val$_{62}$ have equivalent decay accelerating activity (Fig. 5A). Independent confirmation of this finding was sought using Biacore (Fig. 5B). AP C3 convertase was assembled on a C3b-coated chip and allowed to decay naturally for 160 s; fH-Ile$_{62}$ or fH-Val$_{62}$ at a concentration of 73 nM was then flowed over the chip. Binding of fH and accelerated convertase decay occurred simultaneously. Following dissociation of fH from the surface, remaining convertase was measured; this was identical for each fH variant. Note the increased binding of fH-Ile$_{62}$ to the surface in agreement with Figure 2A.

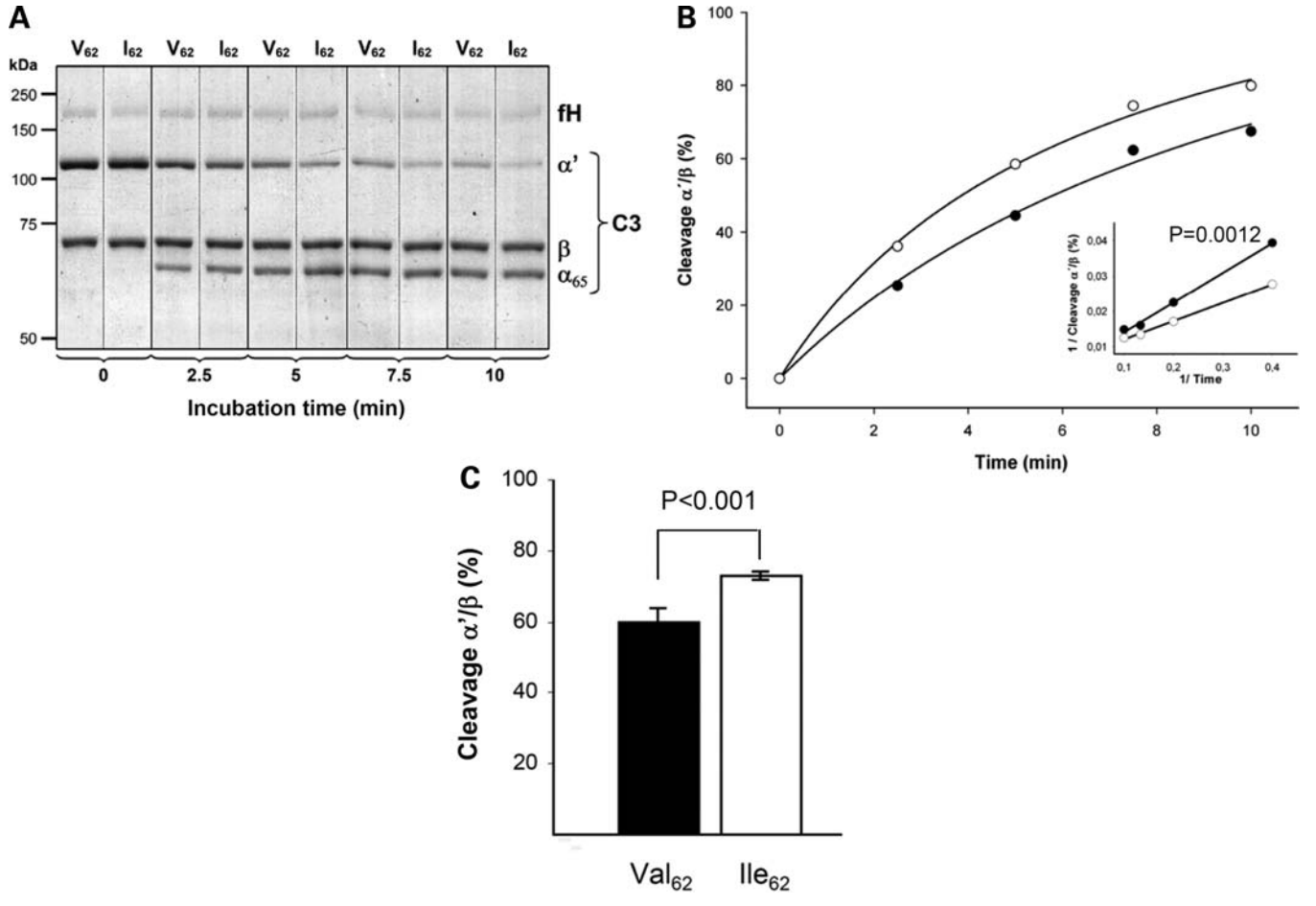

Figure 3. Cofactor activity of fH-Ile$_{62}$ and fH-Val$_{62}$ variants in the proteolysis of fluid phase C3b. (**A**) SDS–PAGE of C3b proteolysis. C3b, fH and fI were incubated for the times indicated, the reaction was stopped by the addition of SDS sample buffer. Samples were analyzed by SDS–PAGE under reducing conditions and gels were Coomassie stained. (**B**) Densitometric analysis of C3b proteolysis. Fluid phase cofactor activity was measured be examining C3b cleavage at 2.5, 5, 7.5 and 10 min reaction for both fH-Ile$_{62}$ (open circles) and fH-Val$_{62}$ (filled circles) variants. Percentage of cofactor activity was determined by the ratio of cleaved α′-chain:β-chain, normalized to 0% proteolysis of control samples. Inset panel shows the double reciprocal plot of the fH-Ile$_{62}$ (open circles) and fH-Val$_{62}$ (filled circles) of the cofactor activity curves. Multiple linear regression analysis revealed significant differences between the slopes for fH-Val$_{62}$ and fH-Ile$_{62}$ cofactor activities ($P = 0.0012$). (**C**) Densitometric analysis of C3b proteolysis from an independent set of assays at 6 min incubation time. Difference in percentage of cofactor activity between fH-Val$_{62}$ and fH-Ile$_{62}$ was significant ($P < 0.001$).

Competition between fH and fB for binding to C3b

From the experiments presented above, it is clear that the differences in binding affinity for C3b of the fH-Ile$_{62}$ and fH-Val$_{62}$ variants affect their capacity to function as cofactor for fI in the proteolysis of C3b. To explore whether these differences in affinity also influence the ability of fH to prevent formation of the C3 proconvertase by competing with factor B (fB) for binding to C3b competition assays were performed on Biacore. We first showed, in keeping with previous reports, that fH does not accelerate decay of the pre-formed proconvertase C3bB (Fig. 6A). When fB together with increasing amounts of fH was flowed over a C3b surface, competition between fB and fH for binding to C3b was apparent from the fH-dependent decrease in the formation of proconvertase measured following dissociation of fH (Fig. 6B). Next, fB was flowed over C3b and binding competed using identical amounts of the fH-Ile$_{62}$ and fH-Val$_{62}$ variants. As expected, fH-Ile$_{62}$, shown to bind better to C3b, was a more efficient competitor and caused a small but consistent decreased formation of the proconvertase (Fig. 6C). These data illustrate that the increased C3b binding affinity of the fH-Ile$_{62}$ variant makes it not only a better cofactor for the fI-dependent inactivation of C3b, but also a more efficient inhibitor of the formation of the C3 proconvertase.

Combined effects of the fH Val62Ile and fB Arg32Gln polymorphisms in the formation of the AP C3 convertase

Previously, we have characterized the common fB polymorphism, fB-Arg$_{32}$/fB-Gln$_{32}$/fB-Trp$_{32}$, and found that the AMD-protective allele fB-Gln$_{32}$ had decreased affinity for C3b compared with the fB-Arg$_{32}$ and fB-Trp$_{32}$ alleles. SPR comparison revealed markedly different proenzyme formation activities; fB-Arg$_{32}$ bound C3b with 4-fold higher affinity than fB-Gln$_{32}$, and formation of activated convertase was enhanced (23). Here we tested combinations of these two variants of fB with the two variants of fH characterized above in order to explore the consequences of different combinations of variant components

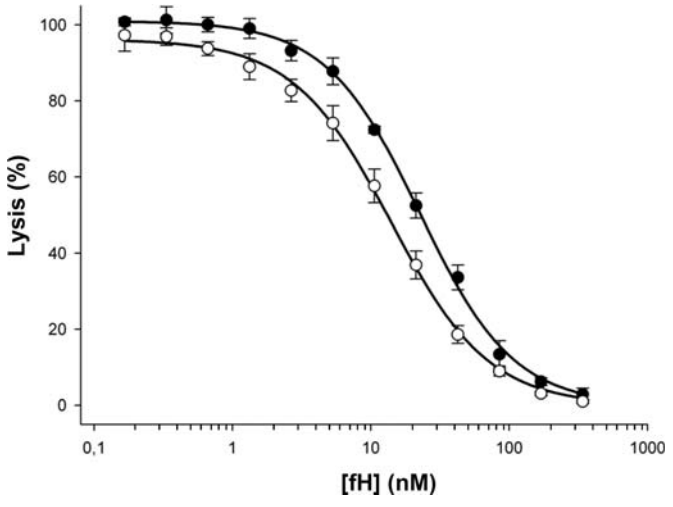

Figure 4. Cofactor activity of fH-Ile$_{62}$ and fH-Val$_{62}$ variants in the proteolysis of surface-bound C3b. The ability of the fH variants to mediate fI-catalyzed inactivation of surface-bound C3b was assessed using a haemolysis assay. C3b was deposited on the surface of sheep E using the classical pathway as described in Materials and Methods. E-C3b cells were incubated in AP buffer with different concentrations of fH-Ile$_{62}$ (open circles) or fH-Val$_{62}$ (filled circles) and constant fI for 7 min at 22°C. Cells were washed and AP convertase was formed using purified fB and fD. Lysis was developed in EDTA-containing buffer using serum depleted of fB and fH. Percent lysis was calculated for each concentration of fH. The log 10 of fB concentration (final concentration in the incubation) was plotted on the *x*-axis, and percentage lysis on the *y*-axis. Data points represent mean ± SD of three determinations. The curves were fitted by using non-linear regression analysis to calculate the EC50. There are significant differences ($P = 0.0025$) between the EC50 values corresponding to the fH-Ile$_{62}$ (14 nM) and fH-Val$_{62}$ (22.6 nM) variants.

and regulators. In haemolytic assays, we found that the combinations complemented each other as predicted from their individual activities (Fig. 7). The fH-Ile$_{62}$–fB-Gln$_{32}$ combination was the least lytic and the fH-Val$_{62}$–fB-Arg$_{32}$ combination the most lytic (Fig. 7). Calculated EC50s were 4.3 and 3.5 nM (for the fH-Ile$_{62}$–fB-Gln$_{32}$ and fH-Val$_{62}$–fB-Gln$_{32}$ combinations, respectively) and 3 and 2.1 nM (for the fH-Ile$_{62}$–fB-Arg$_{32}$ and fH-Val$_{62}$–fB-Arg$_{32}$ combinations, respectively). Differences in the EC50 were statistically significant between the combinations fH-Val$_{62}$–fB-Arg$_{32}$ and fH-Ile$_{62}$–fB-Gln$_{32}$ ($P < 0.001$); fH-Val$_{62}$–fB-Arg$_{32}$ and fH-Ile$_{62}$–fB-Arg$_{32}$ ($P = 0.004$) and fH-Val$_{62}$–fB-Gln$_{32}$ and fH-Ile$_{62}$–fB-Gln$_{32}$ ($P = 0.034$). *P*-values were calculated using a two-tailed unpaired *t*-test. No significant differences were observed between the combinations fH-Val$_{62}$–fB-Gln$_{32}$ and fH-Ile$_{62}$–fB-Arg$_{32}$.

DISCUSSION

fH plays a key role in regulating the AP by acting as a cofactor for fI-mediated cleavage of C3b to iC3b, by accelerating the dissociation of the AP C3 convertases and by competing with fB for binding to C3b in proconvertase formation (9). All these activities are mediated by the interaction between fH and C3b. Functional studies using truncated molecules have demonstrated that fH possesses binding sites for C3b located at the N terminus (SCR1–4), the C terminus (SCR19–20) and in the middle of the molecule (SCR7) (24,25). The C3b binding sites at the C-terminal and N-terminal ends are well characterized, whereas that in SCR7 is a very weak binding site of unknown function. The C3b binding site in SCR19–20 shows the highest affinity for C3b and plays a critical role in the recognition of foreign surfaces by fH. At the other end of the molecule, the C3b binding site in SCR1–4 is essential for the regulatory activities of fH as it carries the fI-mediated cofactor and decay-accelerating activities of fH. Deletion mutagenesis studies have demonstrated that the N-terminal four SCRs are necessary and sufficient for these activities of fH, suggesting that multiple interactions occur between C3b and the N-terminal region of fH (26,27).

Here we report that the Val62Ile substitution in SCR1 of fH increases its affinity for C3b; as a consequence, when compared with fH-Val$_{62}$, fH-Ile$_{62}$ competes more efficiently with fB for C3b binding in proconvertase formation and acquires enhanced cofactor activity for the factor-I mediated cleavage of C3b proteolysis; however, its decay accelerating activity is not altered. These findings show that fH-Ile$_{62}$ is a better AP convertase inhibitor and provide an explanation for the association of the fH-Ile$_{62}$ variant with protection in three distinct disorders linked by AP dysregulation. The fact that the Val62Ile substitution affects binding to C3b but not decay accelerating activity suggests that different regions in fH may be involved in binding C3b/cofactor activity and in decay accelerating activity.

SCR1 is necessary for both cofactor and decay accelerating activities (26,27). Our findings imply that the C3b binding site in SCR1 is not directly involved in decay accelerating activity and that SCR1 may contain distinct, although perhaps overlapping, sites for cofactor and decay accelerating activities. This scenario dictates that the interactions of fH with C3b and with C3bBb are structurally distinct. Previously, we showed that the aHUS-associated fB mutation, K323E, located remote from the C3b-fB interaction site, makes the C3bBb convertase resistant to decay by decay accelerating factor (DAF) and fH (28,29). The mutation apparently affects a complement regulator binding site in the von Willebrand factor type A domain of fB (28). We have also previously showed that DAF–SCR2 interacts with Bb, whereas DAF–SCR4 interacts with C3b in the C3bBb complex (30). From comparison with DAF, it is likely that decay accelerating activity of fH also requires binding to both Bb and C3b. We suggest that there are two distinct binding sites in SCR1, one including the Val62Ile fH polymorphism that is necessary for cofactor activity, and a second that binds fB at, or close to, K323 in fB that is essential for decay accelerating activity. We also postulate that fH has a C3b binding site in SCR3/SCR4 that contributes to both cofactor and decay accelerating activities.

Overwhelming evidence has associated MPGN2/DDD, aHUS and AMD with mutations or polymorphisms in the *CFH* gene and provided conclusive data that AP dysregulation is a unifying pathogenetic feature of these diverse conditions (31). However, only MPGN2/DDD and AMD have pathological similarities. Indeed, occasionally, they occur in the same patient (32). The hallmark of AMD is drusen, a complex, complement-containing material that accumulates beneath the retinal pigmented epithelium; in MPGN2/DDD, accumulation of a drusen-like C3 and electron-dense material occurs along the glomerular basement membrane. In contrast to

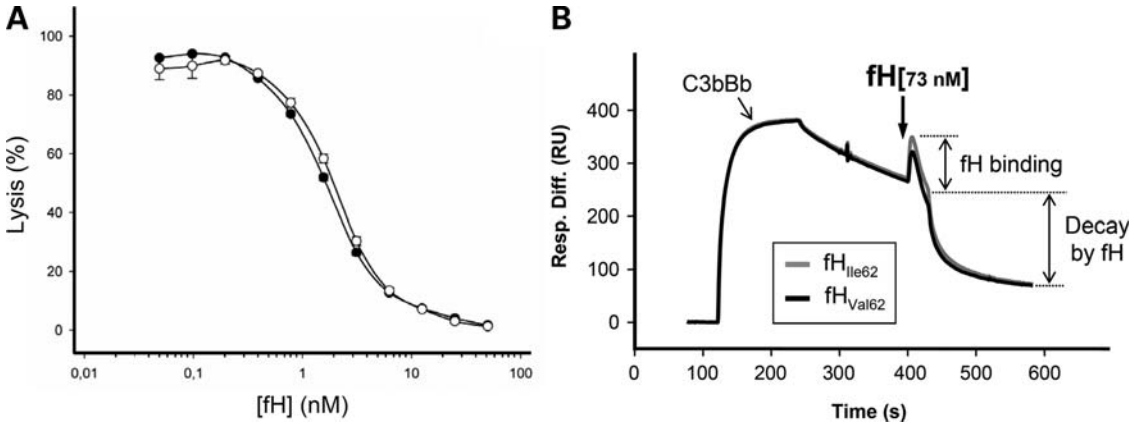

Figure 5. Decay accelerating activity of fH-Ile$_{62}$ and fH-Val$_{62}$ variants on surface-bound AP convertase. The ability of the fH variants to accelerate decay of the AP convertase, C3bBb, was assessed using haemolysis assays with convertase coated sheep E as target (**A**) and in real-time using SPR (**B**). (A) C3b was deposited on the surface of sheep E using the classical pathway as described in Materials and Methods. AP convertase was formed on the cell surface using purified fB and fD, convertase formation was stopped after 15 min using EDTA. E-C3bBb were incubated in EDTA with different concentrations of fH-Ile$_{62}$ (open circles) or fH-Val$_{62}$ (filled circles) for 12 min to allow decay of the convertase and lysis was developed using serum depleted of fB and fH. Percent lysis was calculated for each concentration of fH. (B) AP convertase was formed on the surface of a C3b-coated Biacore chip by flowing fB and fD over the surface. Convertase decayed naturally for 160 s prior to injection of either fH variant (73 nM). Change in RU (*y*-axis) during the fH injection represents the combined effect of fH binding to the surface and to C3bBb, and loss of Bb from the convertase due to fH-mediated accelerated decay. Despite enhanced binding of fH-Ile$_{62}$ to the surface (grey line), an identical amount of Bb was decayed from the surface as measured following complete dissociation of fH from the chip surface.

these 'debris-associated' conditions, aHUS is characterized by renal endothelial cell injury and thrombosis (thrombotic microangiopathy), resulting in haemolytic anaemia, thrombocytopenia and renal failure. Consistent with these differences, distinct functional alterations in fH associate with pathogenesis in these disorders. Mutations or polymorphisms altering the C3b/polyanions binding site located at the C-terminal region of fH are strongly associated with aHUS, because they impair the capacity of fH to protect host cells but have no effect on fluid-phase fH activities. On the other hand, mutations that disrupt the capacity of fH to inhibit complement activation in plasma result in massive activation of C3 that causes MPGN2/DDD. This clear genotype–phenotype correlation contrasts with the association of the fH Val62Ile polymorphism, associated with lower risk for the three diseases (18,22).

To understand why the fH-Ile$_{62}$ variant confers protection from aHUS, MPGN2/DDD and AMD, we purified to homogeneity both fH-Val$_{62}$ and fH-Ile$_{62}$ variants and compared in a series of functional assays for potential effects on proenzyme formation and cofactor and decay accelerating activities in fluid phase and on cell surfaces. Using four different experimental approaches, we showed that fH-Ile$_{62}$ binds better to C3b, competes better with fB to reduce proenzyme formation and performs more efficiently as a cofactor of fI in the proteolysis of fluid phase and surface-bound C3b. These enhanced activities explain the protective role of fH-Ile$_{62}$ both in diseases associated with fluid phase complement dysregulation, like MPGN2/DDD, and membrane-restricted dysregulation as is the case in aHUS.

One important conclusion from this report is that the protective effect of the fH-Ile$_{62}$ variant is subtle, with alterations in activities of between 20 and 50% depending on the assay used. This is consistent with the recent observation (33) that the Val62Ile polymorphism causes a very minor perturbation in the structure of SCR1, this contrasts with the larger structural disturbance caused by an aHUS-associated mutation (Arg53His) which has detrimental consequences on the functional activities of fH. Nevertheless, the very nature of the complement system will amplify these small effects. Further, as we show here by combining known functional variants in fB with fH-Ile$_{62}$ and fH-Val$_{62}$, particular combinations of variants in components and regulators will result in very different AP characteristics, markedly affecting formation and regulation of the AP C3 convertase in plasma and on cell surfaces. Identification of individuals carrying 'high risk' or 'low risk' combinations ('complotypes') of the polymorphic complement component and regulator variants will be of great importance for prediction of disease risk and may also help in diagnosis and choice of treatment for diseases involving complement dysregulation.

MATERIALS AND METHODS

Purification of complement components and activation fragments

Normal healthy volunteers were screened for mutations/polymorphisms in the *CFH* gene by automatic DNA sequencing of PCR amplified fragments. Genomic DNA was prepared from peripheral blood cells according to standard procedures (34). Each exon of the *CFH* gene was amplified from genomic DNA by using specific primers derived from the 5′ and 3′ intronic sequences as described (14). Automatic sequencing was performed in an ABI 3730 sequencer using a dye terminator cycle sequencing kit (Applied Biosystems, Foster City, CA, USA).

Factor H was purified from individuals homozygous for either the fH-Ile$_{62}$ and fH-Val$_{62}$ variants who were identical at all other amino acid residues. Fresh EDTA plasma (100 ml) was precipitated with 7% polyethylene glycol 8000 overnight at 4°C. The precipitate was re-dissolved in PBS,

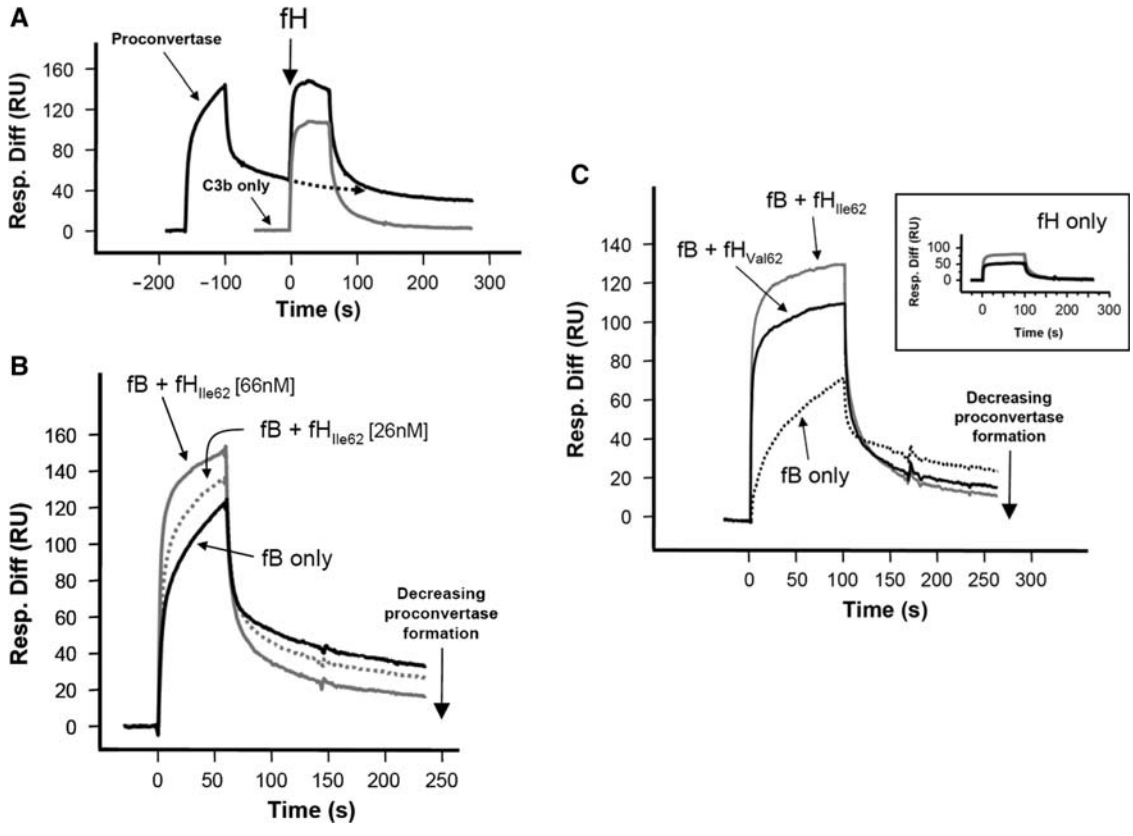

Figure 6. Competition between fH and fB for binding to C3b. (**A**) Proconvertase was formed on the surface of a C3b-coated Biacore chip by flowing fB, this was allowed to decay naturally for a short time before injection of fH as indicated. As expected, fH did not accelerate decay of the proenzyme. The binding profile of fH on the C3b surface only (no fB injected) is illustrated in grey for comparison. (**B**) In order to demonstrate competition between fB and fH for binding to the C3b-coated surface, fB (662 nM) was flowed across the C3b-coated surface alone (black line) or was premixed with 26 or 66 nM fH (dotted grey and solid grey lines, respectively) before injection. Note that the change in RU (*y*-axis) represents the sum of both fB and fH binding to the surface. Decreased proconvertase formation is evident with increasing fH. (**C**) In order to analyse differential effects of fH-Ile$_{62}$ and fH-Val$_{62}$ on proconvertase formation, 132 nM of either variant was premixed with fB (338 nM) and injected over the surface. Comparison of binding curves (following dissociation of fH from the surface) with fB binding in the absence of any fH demonstrates that both fH variants prevent proconvertase formation and that the fH-Ile$_{62}$ variant is more effective.

dialysed extensively against 20 mM Tris–HCl (pH 7.4), 50 mM NaCl, 5 mM EDTA and applied to a heparin-Sepharose column (Heparin 6B Fast Flow, Amersham) equilibrated in the same buffer. The proteins bound to the column were eluted with a 100–200 mM NaCl gradient in 20 mM Tris–HCl, pH 7.4, 5 mM EDTA. Fractions containing fH were identified by sodium dodecyl sulphate–polyacrylamide gel electrophoresis (SDS–PAGE), pooled, dialysed against 20 mM Tris–HCl, pH 7.6, 20 mM NaCl and 10 mM EDTA and applied to a DEAE-Sephacel column. Bound proteins were eluted with a 20–300 mM NaCl gradient. Fractions containing fH were identified by SDS–PAGE, pooled and further purified by gel filtration on a Superose^{TM} 6 10/300 column (GE Healthcare). The fH peak fractions were pooled and stored frozen at −70°C. The fH used in haemolysis assays and Biacore studies was purified by affinity chromatography using immobilized anti-fH (35H9; in house). Protein was eluted with 0.1 M Glycine/HCl pH 2.5 and gel filtered into assay buffer using a Superdex 200 10/300 column (GE Healthcare) immediately prior to analysis. The purity of the final preparations was confirmed by SDS–PAGE. Preparations of fH-Ile$_{62}$ and fH-Val$_{62}$ were obtained without any detectable contaminants or aggregates (Fig. 1B).

C3 and fB were purified by affinity chromatography and gel filtration as described previously (28). Concentration of proteins was assessed using absorbance at A280, molarities were calculated using an extinction coefficient for fH of 1.95 (35), for fB of 1.43 and for C3 of 0.98 (coefficients were obtained by using Protean Software, DNAStar). C3b was generated by limited digestion with trypsin or convertase as previously described (28,36) and re-purified by ion exchange and/or gel filtration as described above (GE Healthcare). C3b was obtained without any detectable contaminants or aggregates. Factor I, factor D and properdin were purchased from Comptech (Tyler, TX, USA).

ELISA C3b binding assay

The binding of fH variants to surface-bound C3b was determined by ELISA. In a 96-well polystyrene microtiter plate, C3b (5 μg/ml) in coupling buffer (0.1 M $NaHCO_3$ pH 9.5) was coated overnight at 4°C. The plate was blocked with washing buffer (20 mM Tris, 150 mM NaCl and 0.1% Tween 20) with 1% bovine serum albumin for 1 h at room temperature (RT). After washing, serial dilutions of fH variants (10 μg/ml) in blocking buffer containing 150 mM NaCl,

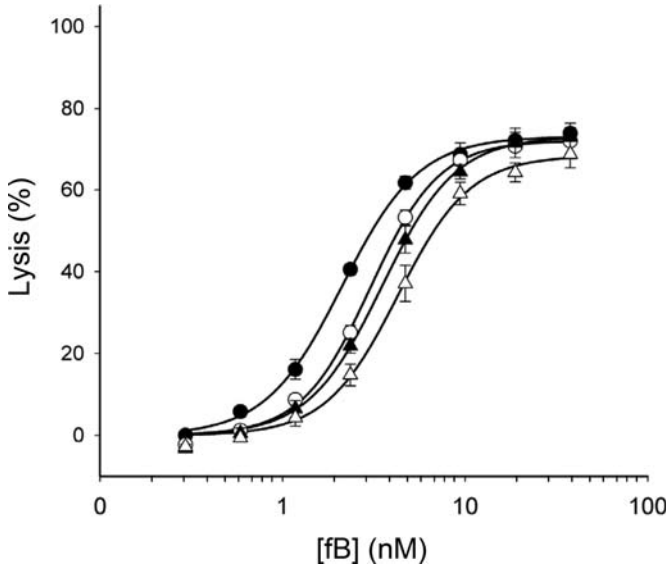

Figure 7. Haemolytic activity of different fH and fB variant combinations. To test the combined effect of the fH-Ile$_{62}$, fH-Val$_{62}$ and the fB-Arg$_{32}$, fB-Gln$_{32}$ variants, C3b was deposited on the surface of sheep E using the classical pathway as described in Materials and Methods. E-C3b cells were incubated in AP buffer with 1 nM of fH-Ile$_{62}$ or fH-Val$_{62}$ (final concentration) and constant fI for 7 min at 22°C. Cells were washed and AP convertase was formed using different concentrations of purified fB-Arg$_{32}$ or fB-Gln$_{32}$, and constant fD and properdin. Lysis was developed in EDTA-containing buffer using serum depleted of fB and fH. Percent lysis was calculated for each concentration of fH. The log 10 of fB concentration (final concentration in the incubation) was plotted on the *x*-axis, and percentage lysis on the *y*-axis. Data points represent mean ± SD of three determinations. The curves were fitted by using non-linear regression analysis to calculate the EC50. Two-tailed unpaired *t*-test showed significant differences in the EC50 between the combinations fH-Val$_{62}$–fB-Arg$_{32}$ (filled circles) and fH-Ile$_{62}$–fB-Gln$_{32}$ (open triangles) ($P < 0.001$); fH-Val$_{62}$–fB-Arg$_{32}$ (filled circles) and fH-Ile$_{62}$–fB-Arg$_{32}$ (open circles) ($P = 0.004$); and fH-Val$_{62}$–fB-Gln$_{32}$ (filled triangles) and fH-Ile$_{62}$–fB-Gln$_{32}$ (open triangles) ($P = 0.034$).

5 mM EDTA were added and incubated with surface-bound C3b for 2 h at 37°C. After washing, the plate was incubated with anti-fH monoclonal antibody (mAb) 35H9 (in house) in blocking buffer, for 1 h at RT, and then with a secondary antibody coupled with horseradish peroxidase (DAKO). Colour reaction was developed with *o*-phenylene-diamine (DAKO) and absorbance measured at 492 nm. fH preparations used in the ligand assay were quantified in duplicate in the same ELISA plate using immobilized polyclonal anti-fH antibody to capture fH and the same anti-fH mAb, 35H9, and secondary antibodies to measure the amount of protein. Concentrations of fH were calculated from curves obtained using purified standard samples.

Biosensor analysis

Kinetic analyses (Fig. 2) were carried out on a Biacore T100, all other analyses were carried out using a Biacore 3000 (GE Healthcare). To measure affinity, fH was amine coupled to a CM5 (carboxymethylated dextran) chip as instructed by the manufacturer (NHS/EDC coupling kit). Number of RUs loaded for both variants were 1004RU (fH-Ile$_{62}$) and 1003RU (fH-Val$_{62}$). C3b was flowed across the surface at different concentrations and bound protein was allowed to decay naturally, the buffer was 10 mM HEPES pH 7.4, 100 mM NaCl, 0.005% Surfactant P20. Data were collected at 25°C at a flow rate of 30 μl/min and were double-referenced (data from reference cell and blank inject were subtracted) to control for bulk refractive index changes. To calculate K_D-values (Fig. 2), we repeated this experiment on three different surfaces: twice with C3b flowing and once with hydrolysed C3 flowing. Pooling the data from different runs is difficult. However, the ratio of the derived K_D-values was the same for each run as follows: fH-Ile$_{62}$ was 0.77, 0.78 or 0.8-fold lower than the fH-Val$_{62}$ form. We flowed C3b over the surface (rather than fH over C3b) in order to minimize the avidity effects seen when flowing fH over the surface. In order to obtain the best quality data, the C3b was gel-filtered prior to use to remove any aggregates and then used in the experiment without further concentration. The C3b needed to be at a very high concentration pre-filtration in order to achieve 1 mg/ml post-filtration, this was the maximum concentration that we could use without precipitating the protein pre-filtration. Although we did not achieve saturation in these experiments, in each case the concentration of C3b used exceeded the K_D-value (2.2-fold for fH-Ile$_{62}$ and 1.7-fold for fH-Val$_{62}$).

In the following experiments, the buffer was 10 mM HEPES pH 7.4, 150 mM NaCl, 1 mM Mg^{2+}. To test the decay activity of fH (Fig. 5), fB at 100 μg/ml (1.1 μM) and fD (2 μg/ml) were flowed across the C3b surface to form the AP C3 convertase as previously described (30). The fH variants were subsequently flowed across the C3b surface at 11.3 μg/ml (73 nM) and decay was monitored. To examine competition between fH and fB for binding to C3b (Fig. 6), both proteins were mixed at the indicated concentrations and flowed at 30 μl/min across the C3b surface in the absence of fD. To determine whether fH accelerated decay of the proenzyme, fH was flowed over the surface subsequent to the fB injection rather than being premixed.

Cofactor activity for fI-mediated proteolysis of fluid phase C3b

The fluid-phase cofactor activity of fH was determined in a C3b proteolysis assay using purified proteins. In brief, C3b, fH and fI were mixed in 10 mM HEPES pH 7.5, 150 mM NaCl, 0.02% Tween 20 at final concentrations of 50 μg/ml (263 nM), 4 μg/ml (25.8 nM) and 10 μg/ml (114 nM), respectively. Mixtures were incubated at 37°C in a water bath and 20 μl aliquots were collected at 2.5, 5, 7.5 and 10 min. The reaction was stopped by the addition of 3 μl of SDS sample buffer (2% SDS, 62.5 mM Tris, 10% Glycerol, 0.75% Bromophenol Blue). Samples were analyzed in 10% SDS–PAGE under reducing conditions. Gels were stained with Coomassie brilliant blue R-250 (BioRad) and proteolysis of C3b determined by measuring the cleavage of the α′-chain using a GS-800 calibrated densitometer (BioRad) and the MultiGauge software package (FUJIFILM). The C3b β-chain was used as an internal control to normalize the % of cleavage between samples. Percentage of cleavage was determined by the ratio between α′-chain/β-chain of C3b and setting as 0% the amount of α′-chain at time 0.

fH-dependent haemolysis assays

Normal human serum (NHS) was sequentially depleted of fB and fH (NHSΔBΔH) by flowing over immobilized anti-Bb (JC1 mAb; in house) and immobilized anti-fH (35H9; in house) affinity columns in complement fixation diluent (CFD; Oxoid), undiluted depleted serum was pooled and used in haemolysis assays as described below. Antibody-coated sheep EA were prepared by incubating sheep E (2% v/v) with Amboceptor (1/1000 dilution; Behring Diagnostics) in CFD (Oxoid) for 30 min at 37°C, EA were washed and resuspended at 2% (v/v) in CFD. To deposit C3b on the E surface (E-C3b), equal volumes of EA and NHSΔBΔH (8% v/v) were incubated at 37°C for 10 min, the C5 inhibitor (OmCI; 6 μg/ml; gifted from Varleigh Ltd, Jersey (37) was added to block the terminal pathway).

To test fH-dependent decay accelerating activity, washed E-C3b cells were resuspended to 2% (v/v) in AP buffer (5 mM sodium barbitone pH 7.4, 150 mM NaCl, 7 mM $MgCl_2$, 10 mM EGTA) and AP convertase was formed on the cell surface by incubating with fB 42 μg/ml (0.46 μM) and fD (0.4 μg/ml) at 37°C for 15 min. PBS/0.25 M EDTA (4% v/v) was added to prevent further enzyme formation and cells (50 μl) were mixed and incubated with 50 μl of fH [serial dilution from 15.4 μg/ml (99 nM)] in PBS/10 mM EDTA for 12 min. Lysis was developed by adding 50 μl NHSΔBΔH (4%, v/v) in PBS/EDTA and incubating at 37°C for 20 min. To calculate lysis, cells were pelleted by centrifugation, and haemoglobin release was measured by absorbance at 415 nm. Control incubations included 0% lysis (buffer only) and 100% lysis (0.1% Nonidet-P40). Percentage lysis 100 × (A415 test sample − A415 0% control)/(A415 100% control − A415 0% control).

To test fH cofactor activity, washed EA-C3b cells were resuspended to 2% in AP buffer and incubated with an equal volume of different concentrations of fH as indicated and constant fI (2.5 μg/ml) for 7 min at 22°C. After three washes in AP buffer, 50 μl cells (2%) were mixed with 50 μl of 70 μg/ml fB (0.75 μM; fB_{32R} or fB_{32Q}) and fD (0.4 μg/ml) and incubated for 10 min at 22°C to form convertase on residual C3b (EA-C3bBb). Lysis was developed by adding 50 μl NHSΔBΔH (4%, v/v) in PBS/EDTA and incubating at 37°C for 20 min. Percentage lysis was calculated as described above.

To assess the effect on lysis by combining different polymorphic variants of fB and fH, the above two assays were combined and modified as follows. EA-C3b cells were incubated with 80 ng/ml (0.5 nM) fH-Ile_{62} or fH-Val_{62} variant and 2.5 μg/ml fI for 7 min at 22°C. Washed cells were incubated as described above with different concentrations of $fBArg_{32}$ or $fBGln_{32}$, fD and properdin (1 μg/ml) and lysis was developed using NHSΔBΔH.

ACKNOWLEDGEMENTS

C.L.H., B.P.M. and S.R.deC. designed research, analysed the data and wrote the paper. C.L.H. and S.R.deC. contribute equally to this work. A.T., T.M. and R.M.B. prepared the proteins. A.T. and C.L.H. performed the binding and functional assays.

Conflicts of Interest statement. None declared.

FUNDING

This work was supported by MRC Project Grant Ref 84908 (to C.L.H. and B.P.M.), Ministerio de Ciencia e Innovación Ref SAF 2005-00913 (to S.R.deC.) the CIBER de Enfermedades Raras and Fundación Renal Iñigo Alvarez de Toledo (to S.R.deC.). We thank the blood donors for their invaluable contribution to the project.

REFERENCES

1. Law, S. and Reid, K. (1995) *Complement*, 2nd edn. IRL Press, Oxford, UK.
2. Pangburn, M.K., Schreiber, R.D. and Müller-Eberhard, H.J. (1977) Human complement C3b inactivator: isolation, characterization, and demonstration of an absolute requirement for the serum protein beta1H for cleavage of C3b and C4b in solution. *J. Exp. Med.*, **146**, 257–270.
3. Weiler, J.M., Daha, M.R., Austen, K.F. and Fearon, D.T. (1976) Control of the amplification convertase of complement by the plasma protein beta1H. *Proc. Natl Acad. Sci. USA*, **73**, 3268–3272.
4. Whaley, K. and Ruddy, S. (1976) Modulation of the alternative complement pathway by beta1H globulin. *J. Exp. Med.*, **144**, 1147–1163.
5. Fearon, D.T. (1978) Regulation by membrane sialic acid of beta1H-dependent decay-dissociation of amplification C3 convertase of the alternative complement pathway. *Proc. Natl Acad. Sci. USA*, **75**, 1971–1975.
6. Kazatchkine, M.D., Fearon, D.T. and Austen, K.F. (1979) Human alternative complement pathway: membrane-associated sialic acid regulates the competition between B and beta1H for cell-bound C3b. *J. Immunol.*, **122**, 75–81.
7. Pangburn, M.K., Schreiber, R.D. and Muller Eberhard, H.J. (1983) C3b deposition during activation of the alternative complement pathway and the effect of deposition on the activating surface. *J. Immunol.*, **131**, 1930–1935.
8. Ripoche, J., Day, A.J., Harris, T.J.R. and Sim, R.B. (1988) The complete amino acid sequence of human complement factor H. *Biochem. J.*, **249**, 593–602.
9. Rodriguez de Cordoba, S., Esparza-Gordillo, J., Goicoechea de Jorge, E., Lopez-Trascasa, M. and Sanchez-Corral, P. (2004) The human complement factor H: functional roles, genetic variations and disease associations. *Mol. Immunol.*, **41**, 355–367.
10. Dragon-Durey, M.-A., Fremeaux-Bacchi, V., Loirat, C., Blouin, J., Niaudet, P., Deschenes, G., Coppo, P., Herman Fridman, W. and Weiss, L. (2004) Heterozygous and homozygous factor H deficiencies associated with hemolytic uremic syndrome or membranoproliferative glomerulonephritis: report and genetic analysis of 16 cases. *J. Am. Soc. Nephrol.*, **15**, 787–795.
11. Levy, M., Halbwachs-Mecarelli, L. and Gubler, M.C. (1986) H deficiency in two brothers with atypical dense intramembranous deposit disease. *Kidney Int.*, **30**, 949–956.
12. Licht, C., Heinen, S., Józsi, M., Löschmann, I., Saunders, R.E., Perkins, S.J., Waldherr, R., Skerka, C., Kirschfink, M., Hoppe, B. *et al.* (2006) Deletion of Lys224 in regulatory domain 4 of factor H reveals a novel pathomechanism for dense deposit disease (MPGN II). *Kidney Int.*, **70**, 42–50.
13. López-Larrea, C., Dieguez, M.A., Enguix, A., Dominguez, O., Marin, B. and Gómez, E. (1987) A familial deficiency of complement factor H. *Biochem. Soc. T.*, **15**, 648–649.
14. Perez-Caballero, D., Gonzalez-Rubio, C., Esther Gallardo, M., Vera, M., Lopez-Trascasa, M., Rodriguez de Cordoba, S. and Sanchez-Corral, P. (2001) Clustering of missense mutations in the C-terminal region of factor H in atypical hemolytic uremic syndrome. *Am. J. Hum. Genet.*, **68**, 478–484.
15. Caprioli, J., Castelletti, F., Bucchioni, S., Bettinaglio, P., Bresin, E., Pianetti, G., Gamba, S., Brioschi, S., Daina, E., Remuzzi, G. *et al.* (2003) Complement factor H mutations and gene polymorphisms in haemolytic uraemic syndrome: the C-257T, the A2089G and the G2881T

polymorphisms are strongly associated with the disease. *Hum. Mol. Genet.*, **12**, 3385–3395.
16. Richards, A., Buddles, M.R., Donne, R.L., Kaplan, B.S., Kirk, E., Venning, M.C., Tielemans, C.L., Goodship, J.A. and Goodship, T.H.J. (2001) Factor H mutations in hemolytic uremic syndrome cluster in exons 18–20, a domain important for host cell recognition. *Am. J. Hum. Genet.*, **68**, 485–490.
17. Warwicker, P., Goodship, T.H.J., Donne, R.L., Pirson, Y., Nicholls, A., Ward, R.M., Turnpenny, P. and Goodship, J.A. (1998) Genetic studies into inherited and sporadic hemolytic uremic syndrome. *Kidney Int.*, **53**, 836–844.
18. Hageman, G.S., Anderson, D.H., Johnson, L.V., Hancox, L.S., Taiber, A.J., Hardisty, L.I., Hageman, J.L., Stockman, H.A., Borchardt, J.D., Gehrs, K.M. *et al.* (2005) A common haplotype in the complement regulatory gene factor H (HF1/CFH) predisposes individuals to age-related macular degeneration. *Proc. Natl Acad. Sci. USA*, **102**, 7227–7232.
19. Edwards, A.O., Ritter, R., Abel, K.J., Manning, A., Panhuysen, C. and Farrer, L.A. (2005) Complement factor H polymorphism and age-related macular degeneration. *Science*, **308**, 421–424.
20. Haines, J.L., Hauser, M.A., Schmidt, S., Scott, W.K., Olson, L.M., Gallins, P., Spencer, K.L., Kwan, S.Y., Noureddine, M., Gilbert, J.R. *et al.* (2005) Complement factor H variant increases the risk of age-related macular degeneration. *Science*, **308**, 419–421.
21. Klein, R.J., Zeiss, C., Chew, E.Y., Tsai, J.-Y., Sackler, R.S., Haynes, C., Henning, A.K., SanGiovanni, J.P., Mane, S.M., Mayne, S.T. *et al.* (2005) Complement factor H polymorphism in age-related macular degeneration. *Science*, **308**, 385–389.
22. Pickering, M.C., Goicoechea de Jorge, E., Martinez-Barricarte, R., Recalde, S., Garcia-Layana, A., Rose, K.L., Moss, J., Walport, M.J., Cook, H.T., Rodriguez de Cordoba, S. *et al.* (2007) Spontaneous hemolytic uremic syndrome triggered by complement factor H lacking surface recognition domains. *J. Exp. Med.*, **204**, 1249–1256.
23. Montes, T., Tortajada, A., Morgan, B.P., Rodriguez de Cordoba, S. and Harris, C.L. (2009) Functional basis of protection against age-related macular degeneration conferred by a common polymorphism in complement factor B. *Proc. Natl Acad. Sci. USA*, **106**, 4366–4371.
24. Sharma, A.K. and Pangburn, M.K. (1996) Identification of three physically and functionally distinct binding sites for C3b in human complement factor H by deletion mutagenesis. *Proc. Natl Acad. Sci. USA*, **93**, 10996–11001.
25. Schmidt, C.Q., Herbert, A.P., Kavanagh, D., Gandy, C., Fenton, C.J., Blaum, B.S., Lyon, M., Uhrin, D. and Barlow, P.N. (2008) A new map of glycosaminoglycan and C3b binding sites on factor H. *J. Immunol.*, **181**, 2610–2619.
26. Kuhn, S., Skerka, C. and Zipfel, P.F. (1995) Mapping of the complement regulatory domains in the human factor H-like protein I and in factor H. *J. Immunol.*, **155**, 5663–5670.
27. Gordon, D.L., Kaufman, R.M., Blackmore, T.K., Kwong, J. and Lublin, D.M. (1995) Identification of complement regulatory domains in human factor H. *J. Immunol.*, **155**, 348–356.
28. Goicoechea De Jorge, E., Harris, C.L., Esparza-Gordillo, J., Carreras, L., Aller Arranz, E., Abarrategui Garrido, C., Lopez-Trascasa, M., Sanchez-Corral, P., Morgan, B.P. and Rodriguez De Cordoba, S. (2007) Gain-of-function mutations in complement factor B are associated with atypical hemolytic uremic syndrome. *Proc. Natl Acad. Sci. USA*, **104**, 240–245.
29. Torreira, E., Tortajada, A., Montes, T., Rodriguez de Cordoba, S. and Llorca, O. (2009) 3D structure of the C3bB complex provides insights into the activation and regulation of the complement alternative pathway convertase. *Proc. Natl Acad. Sci. USA*, **106**, 882–887.
30. Harris, C.L., Abbott, R.J.M., Smith, R.A., Morgan, B.P. and Lea, S.M. (2005) Molecular dissection of interactions between components of the alternative pathway of complement and decay accelerating factor (CD55). *J. Biol. Chem.*, **280**, 2569–2578.
31. Rodriguez de Cordoba, S. and Goicoechea de Jorge, E. (2008) Translational mini-review series on complement factor H: genetics and disease associations of human complement factor H. *Clin. Exp. Immunol.*, **151**, 1–13.
32. Montes, T., Goicoechea de Jorge, E., Ramos, R., Goma, M., Pujol, O., Sanchez-Corral, P. and Rodriguez de Cordoba, S. (2008) Genetic deficiency of complement factor H in a patient with age-related macular degeneration and membranoproliferative glomerulonephritis. *Mol. Immunol.*, **45**, 2897–2904.
33. Hocking, H.G., Herbert, A.P., Kavanagh, D., Soares, D.C., Ferreira, V.P., Pangburn, M.K., Uhrin, D. and Barlow, P.N. (2008) Structure of the N-terminal region of complement factor H and conformational implications of disease-linked sequence variations. *J. Biol. Chem.*, **283**, 9475–9487.
34. Miller, S.A., Dykes, D.D. and Polesky, H.F. (1988) A simple salting out procedure for extracting DNA from human nucleated cells. *Nucleic Acids Res.*, **16**, 1215.
35. Hakobyan, S., Harris, C.L., Tortajada, A., Goicochea de Jorge, E., Garcia-Layana, A., Fernandez-Robredo, P., Rodriguez de Cordoba, S. and Morgan, B.P. (2008) Measurement of factor H variants in plasma using variant-specific monoclonal antibodies: application to assessing risk of age-related macular degeneration. *Invest. Ophthalmol. Vis. Sci.*, **49**, 1983–1990.
36. Sanchez-Corral, P., Anton, L.C., Alcolea, J.M., Marques, G., Sanchez, A. and Vivanco, F. (1989) Separation of active and inactive forms of the third component of human complement C3, by fast protein liquid chromatography (FPLC). *J. Immunol.*, **122**, 105–113.
37. Hepburn, N.J., Williams, A.S., Nunn, M.A., Chamberlain-Banoub, J.C., Hamer, J., Morgan, B.P. and Harris, C.L. (2007) *In vivo* characterization and therapeutic efficacy of a C5-specific inhibitor from the soft tick ornithodoros moubata. *J. Biol. Chem.*, **282**, 8292–8299.

http://www.kidney-international.org

see commentary on page 11

Complement factor H variants I890 and L1007 while commonly associated with atypical hemolytic uremic syndrome are polymorphisms with no functional significance

Agustín Tortajada[1,2], Sheila Pinto[1,2], Jorge Martínez-Ara[3], Margarita López-Trascasa[2,4], Pilar Sánchez-Corral[2,4] and Santiago Rodríguez de Córdoba[1,2]

[1]Departamento de Medicina Celular y Molecular, Centro de Investigaciones Biológicas (CSIC), Ramiro de Maeztu 9, Madrid, Spain; [2]Ciber de Enfermedades Raras, Madrid, Spain; [3]Servicio de Nefrologia. Hospital Universitario de La Paz, idiPaz. Paseo de la Castellana 261, Madrid, Spain and [4]Unidades de Investigación e Inmunología, Hospital Universitario de La Paz, idiPaz. Paseo de la Castellana 261, Madrid, Spain

Mutations and polymorphisms in the gene-encoding factor H (*CFH*) are associated with atypical hemolytic uremic syndrome, dense deposit disease, and age-related macular degeneration. Many of these *CFH* genetic variations disrupt the regulatory role of factor H, supporting the concept that dysregulation of complement is a unifying pathogenic feature of these disorders. Evidence of a causal relationship with the disease is, however, not available for all *CFH* genetic variations found in patients, which is a potential cause of misinterpretations with important consequences for the patients and their relatives. CFH I890 and L1007 are two genetic variations repeatedly associated with atypical hemolytic uremic syndrome and also found in patients with dense deposit disease and age-related macular degeneration. Here we report an extensive genetic and functional analysis of these *CFH* variants. Our results indicate that I890 and L1007 segregate together as part of a distinct and relatively infrequent *CFH* haplotype in Caucasians. Extensive analysis of the S890/V1007 (control) and I890/L1007 (disease-associated) factor H protein variants failed to provide evidence that these amino acid changes have functional implications. Thus, the presence of the I890 and L1007 variants in healthy individuals and their high frequency in sub-Saharan African and African-American populations strongly suggest that I890 and L1007 are rare factor H polymorphisms unrelated to disease.

Kidney International (2012) **81,** 56–63; doi:10.1038/ki.2011.291; published online 31 August 2011

KEYWORDS: complement factor H; hemolytic uremic syndrome; disease-associated mutations

Correspondence: *Santiago Rodríguez de Córdoba, Departamento de Medicina Celular y Molecular, Centro de Investigaciones Biológicas (CSIC), Ramiro de Maeztu 9, 28040 Madrid, Spain.*
E-mail: SRdeCordoba@cib.csic.es

Received 14 April 2011; revised 1 June 2011; accepted 21 June 2011; published online 31 August 2011

Complement factor H (FH) is the main regulator of the alternative pathway (AP) of the complement system. FH exerts this regulatory activity in three different ways: it binds to C3b, competing with factor B in the assembly of the AP C3-proconvertase complex; it accelerates the decay of the AP C3-convertase; and functions as a cofactor of factor I (FI) in the proteolytic inactivation of C3b.[1–3] FH regulates complement activation both in fluid phase and on cellular surfaces,[4–6] preserving complement homeostasis and preventing uncontrolled C3b deposition and host tissue damage.

FH is a relative abundant plasma protein that is secreted as a single-chain glycoprotein of 155 kDa composed of 20 homologous domains of 60 amino acids,[7] named short consensus repeats (SCRs). FH concentration in plasma is highly variable, ranging from 116 to 562 μg/ml.[8] Different interaction sites for C3b and polyanions have been identified along the 20 SCRs of FH. The SCR 1–4 region is the unique C3b-binding site capable to function as a cofactor for FI in the cleavage of C3b and to accelerate the decay of AP C3-convertase.[9] Similarly, the C3b- and polyanion-binding site at SCRs 19–20 determines the ability of FH to bind C3b deposited on the cell surface, with this region of FH being essential for self-pathogen discrimination.[10,11]

Mutations and polymorphisms in the *CFH* gene are associated with atypical hemolytic uremic syndrome (aHUS), dense deposit disease (DDD), and age-related macular degeneration (AMD; reviewed in ref. 12). The available data support the hypothesis that AP dysregulation is a unifying pathogenic feature of these diverse conditions. They also illustrate a remarkable genotype–phenotype correlation in which distinct genetic variations at *CFH* specifically predispose to aHUS, AMD, or DDD. In fact, the functional characterization of these disease-specific *CFH* genetic variations is instrumental to understand the molecular basis underlying each of these pathologies.

In aHUS, a thrombotic microangiopathy characterized by thrombocytopenia, hemolytic anemia, and acute renal

failure, and where endothelial cell injury appears to be the primary pathogenic event, the most prevalent genetic alterations in the *CFH* gene are missense mutations that alter the C3b- and polyanion-binding site at the C terminus of FH. These mutations rarely result in hypocomplementemia or decreased FH plasma levels.[13–16] Functional studies have demonstrated that these aHUS-associated FH molecules present normal regulatory activity in plasma but a limited capacity to protect cells from complement lysis.[17–21] This functional alteration is clearly distinct from the lack of complement regulation in plasma, leading to complete C3 consumption and severe hypocomplementemia that characterizes DDD patients.

DDD is a very rare form of glomerulonephritis with isolated C3 deposits characterized by the presence of dense deposits within the glomerular basement membrane.[22] DDD is associated with complement abnormalities that lead to persistent reduction of C3 serum levels and intense deposition of degradation products of C3 in the glomerular basement membrane. Among the different factors associated with these complement abnormalities are mutations in the *CFH* gene. These *CFH* mutations result in truncations or amino acid substitutions that impair secretion of FH into circulation or that eliminate the complement regulatory activities located at the N terminus of FH.[23–26] Thus, *CFH* mutations that decrease FH in plasma, or eliminate its complement regulatory activity, lead to unrestricted activation of complement in plasma, causing damage to glomerular cells and deposition of complement products in the glomerular basement membrane.

Age-related macular degeneration, the most common cause of blindness in the elderly in developed countries, is characterized by drusen, lipoproteinaceous deposits localized between the retinal pigment epithelium and Bruch's membrane, which leads to an extensive atrophy of the retinal pigment epithelium and overlaying photoreceptor cells (geographic atrophy) or aberrant choroidal neovascularization under the macular area. AMD and DDD share pathological similarities with accumulation of complement-containing debris within the eye and kidney, respectively. Indeed, AMD-like pathology is well recognized in patients with DDD.[27] The identification of *CFH* as a major susceptibility locus for AMD and the characterization of multiple genetic variants in the *CFH* genomic regions conferring risk or protection to AMD indicate that the complement system has a significant role in AMD pathogenesis.[28–32] However, *CFH* association data showed no overlapping between *CFH* at-risk polymorphisms for aHUS and AMD.[20]

The peculiar genotype–phenotype correlation between specific *CFH* genetic variations and a particular disease contrast with the situation of the *CFH* I890 and L1007 variations (in SCR 15 and SCR 17, respectively) that have been repeatedly reported to be associated with aHUS and are also found in DDD and AMD patients.[31,33–35] To characterize the functional consequences of these *CFH* genetic variations, we have purified the different FH protein variants to homogeneity from the plasma of appropriate carriers and tested their capacity to bind to surface-bound C3b, analyzed their cofactor activity in the FI-mediated inactivation of fluid-phase C3b, and performed FH-dependent hemolytic assays. None of these assays showed functional alterations in the regulatory activity of the FH, which strongly suggest that they are rare FH polymorphisms without functional consequences.

RESULTS

Sequencing analyses of the *CFH* gene in the aHUS ($n = 259$) and DDD ($n = 19$) Spanish cohorts identified four aHUS patients (H54, H97, H142, and H244) and one DDD patient (GN3) carrying two nucleotide changes (c.2669 G>T; S890I and c.3019 G>T; V1007L) in heterozygosis. The same c.2669 G>T and c.3019 G>T nucleotide changes were also detected in heterozygosis in 2 out of 173 controls, an occurrence that is not significantly different from that found in patients. Complement profiles and clinical data of the aHUS and DDD patients carrying the S890I and V1007L amino acid changes, as well as additional genetic alterations in other complement genes found in these patients, are summarized in Table 1.

Two aHUS pedigrees were available for segregation analysis. In both cases it was demonstrated that the patients inherited both nucleotide changes (c.2669 G>T and c.3019 G>T) from the same progenitor, illustrating that they were carried by the same *CFH* allele. Further analyses of several single-nucleotide polymorphisms within the *CFH* gene demonstrated that, in all carriers, these I890 and L1007 amino acid changes associated with the same *CFH* haplotype, suggesting a single evolutionary origin for the I890/L1007 *CFH* haplotypes identified in the aHUS, DDD, and control individuals (Table 2). Interestingly, the I890/L1007 *CFH* haplotype carries the AMD and DDD risk polymorphism His402, which may have implications for its association with AMD and DDD. The I890/L1007 *CFH* haplotype is probably old. This is supported by the existence of I890/L1007 *CFH* 'recombinant' haplotypes, such as that of H97, affecting the 5′ end region of *CFH*, or the genomic rearrangement that resulted in the generation of the *CFH*::*CFHR1* hybrid gene in H142.

As indicated, the I890/L1007 *CFH* haplotype in H142 is remarkable because, in addition, it encodes a *CFH*::*CFHR1* hybrid gene that resulted from a nonhomologous recombination between the *CFH* and *CFHR1* genes. Thus, the FH protein encoded by this *CFH* allele carries a total of four amino acid changes compared with a normal *CFH* allele: I890 and L1007 and another two (L1191 and A1197) characteristic of the exon 6 of *CFHR1*, which replaces the exon 23 of *CFH* in the *CFH*::*CFHR1* hybrid gene (Table 2).[36]

To purify the I890/L1007 FH variant from nonmutated FH in heterozygote carriers, we used affinity chromatography with the MBI-7 anti-human FH monoclonal antibody.[37,38] This antibody specifically recognizes the H402 variant of FH, and was used to capture the FH allele carrying the I890 L1007

Table 1 | Clinical and complement data of patients carrying the *CFH* I890 and L1007 genetic variants

	aHUS				DDD
	H54[a]	H97	H142[b]	H244[c]	GN3[d]
Age at onset (years)	51	41	3.5	1	5.5
C3 (70–140 mg/dl)	59	123	94.3	135	135
C4 (14–47 mg/dl)	7	24.5	24.2	31.5	31.5
Total FH (116–562 μg/ml)	127.4	256.8	150	316	161.8
% $FH_{I890-L1007}$[e]	46	47	56	—	—
FI (75–115%)[f]	99	52	104	80	103
Additional mutations	None	CFI C86Y	*CFH*::*CFHR1* hybrid gene	None	None
Del CFHR1–CFHR3	None	None	Het	None	None
Autoantibodies	None	None	None	None	C3Nef
Renal status (outcomes)	Deceased	ESRD	ESRD	MRI	MRI
Transplantation (recurrences)	None	Yes (no)	Yes (no)	None	None

Abbreviations: aHUS, atypical hemolytic uremic syndrome; AMD, age-related macular degeneration; C3Nef, C3 nephritic factor; DDD, dense deposit disease; ESRD, end-stage renal disease; FH, complement factor H; FI, factor I; GBM, glomerular basement membrane; Het, heterozygous; MRI, moderate renal insufficiency.

[a]Male patient who was diagnosed of post-transplant HUS (microangiopathic hemolytic anemia with schistocytes, and renal failure) associated with tacrolimus and cyclosporin treatment. He died 1 month later from pneumonia caused by acinetobacter and aspergillus.

[b]After almost 4 years of hemodialysis, this male patient received a cadaver kidney transplantion on September 2010. He was treated with eculizumab (Soliris) before transplantation and every 15 days afterward, following the protocol recommended by Alexion Pharmaceuticals, Cheshire, CT. He is actually in good condition.

[c]This is a male child from Nigeria. He developed HUS after diarrhea and a respiratory infection. He was under peritoneal dialysis and recovered partial renal function. No recurrences. Actually present moderate renal insufficiency.

[d]Diagnosis of DDD in this patient was established on the basis of renal biopsy (light microscopy, immunofluorescence, and electron microscopy (EM)) performed at presentation of the disease. Moderate mesangial hypercellularity and increased mesangial matrix without double contour in the capillary walls was observed. Immunofluorescence showed intense isolated granular C3 staining in the capillary walls and in the mesangium in the form of nodular rings, negative for immunoglobulins or other complement proteins. EM revealed abundant electron-dense ribbon-like deposits within the GBM and local electron-dense deposits in the mesangium. The presentation was a nephritic syndrome with microhematuria and without proteinuria. He showed persistence hypocomplementemia C3 (8 mg/dl) and 4 months after was C3NeF-positive. This situation was maintained for 12 years. In 1992, at the age of 20 years, he presented proteinuria 5.75 g/day; serum creatinine: 1.0 mg/dl; creatinine clearance: 147 ml/min, and remained C3Nef-positive. He was treated with prednisone. By 2007, after 33 years of evolution, the C3Nef titers were only detected as traces, with normalization of C3 levels and with an almost complete remission of the proteinuria after combined angiotensin converting enzyme inhibitor (ACEi) and angiotensin receptor blocker (ARB) therapy. He presented ocular manifestations of AMD (drusen) at the age of 33 years. The patient actually presented a moderate renal insufficiency (creatinine: 1.9 mg/dl; creatinine clearance: 65 ml/min) and proteinuria 1.2 g/day.

[e]In FH His402Tyr heterozygotes, levels of expression of the $FH_{I890-L1007}$ allele were determined by enzyme-linked immunosorbent assay using anti-FH 402His-specific antibodies.[37]

[f]Factor I levels are referred to a reference pool of sera.

Table 2 | *CFH* haplotypes carrying the FH I890 and L1007 amino acid substitutions

	Promoter -332 C>T	V62I c.184 G>A	Y402H c.1204 T>C	Q672Q c.2016 A>G	E936D c.2808 G>T	S890I c.2669 G>T	V1007L c.3019 G>T	S1191 c.3645 C	V1197 c.3663 T
N1	C	G	C	A	G	T	T	C	T
N2	C	G	C	A	G	T	T	C	T
H54	C	G	C	A	G	T	T	C	T
H244	C	G	C	A	G	T	T	C	T
GN3	C	G	C	A	G	T	T	C	T
H97	C	A	C	A	G	T	T	C	T
H142	C	G	C	A	G	T	T	T	C

amino acid changes from the plasma of patients H54 and H142, who are FH Y402H heterozygotes. The eluted protein was further purified by gel filtration and concentrated, free of contaminants. We followed the same protocol to purify the S890/V1007 FH allele from control FH Y402H heterozygote donors (Figure 1). After quantification by enzyme-linked immunosorbent assay (ELISA), the purified proteins, S890/V1007, I890/L1007, and I890/L1007/L1191/A1197, were tested functionally in a number of different assays.

To test whether the I890/L1007 amino acid changes affect the cofactor activity for the FI-mediated proteolysis of C3b, S890/V1007 and I890/L1007 FH variants were mixed with C3b and incubated in the presence of FI at 37 °C. After densitometric analysis of Coomassie-stained gels, the ratio between α′-chain and β-chain of C3b was used to calculate the percentage of C3b cleavage. As illustrated, no differences in the cofactor activities between FH variants S890/V1007 and I890/L1007 (Figure 2a and b) or between S890/V1007 and I890/L1007/L1191/A1197 (Figure 2a–c) were appreciated, indicating that these amino acid substitutions do not have a significant effect on the cofactor activity of FH. As a control that our assays have appropriate sensitivity to detect small functional alterations we have included in these experiments the V62 and I62 FH polymorphic variants, which we previously showed that present slightly differences in their FI cofactor activities.[39]

To explore the effect of the I890/L1007 amino acid changes in the interaction with C3b, we performed a C3b-binding plate assay. Purified C3b was immobilized on microtiter plates and identical quantities of the I890/L1007 and

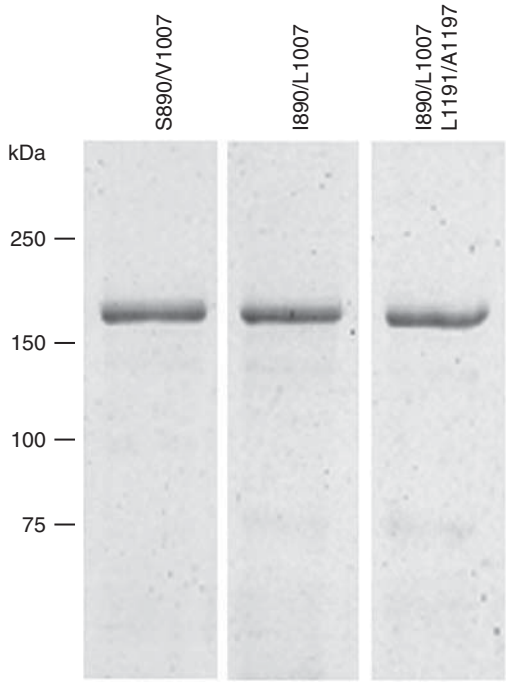

Figure 1 | SDS-PAGE Coomassie-stained gel of the purified FH variants. The S890/V1007, I890/L1007, or I890/L1007/L1191/A1197 factor H (FH) variants were purified from the plasma of a healthy individual and the atypical hemolytic uremic syndrome (aHUS) patients H54 and H142, as described in Materials and Methods.

S890/V1007 FH variants were added and allowed to interact for 2 h at 37 °C. FH bound to C3b was detected using the Ox24 monoclonal antibody. FH was quantified in parallel in the same ELISA experiment. Our results show that the binding to C3b of the purified FH protein I890/L1007 was undistinguishable from that of the control FH S890/V1007 (Figure 3). These results indicate that the amino acid changes in the SCRs 15 and 17 do not alter the capacity of FH to bind C3b. We also used in these experiments the V62 and I62 FH polymorphic variants, as it has also been shown previously that they present slight differences in their C3b-binding capacity[39] (Figure 3).

To investigate the potential effect of the I890 and L1007 amino acid changes in the regulatory activity of FH on cell surfaces, the S890/V1007 and I890/L1007 FH variants were tested in an FH-dependent hemolytic assay developed in our laboratory. In these assays, a human serum sample carrying a well-characterized *CFH* mutation, which alters the C terminus of FH,[18] was reconstituted with identical amounts of the S890/V1007, I890/L1007, or I890/L1007/L1191/A1197 FH variants and incubated with sheep erythrocytes in the presence of 7 mmol/l Mg^{2+} and ethylene glycol tetraacetic acid. Lysis of erythrocytes in this assay inversely correlates with the capacity of FH to regulate the AP on the cellular surface. Our results indicate that the I890/L1007/L1191/A1197 FH variant presents decreased inhibition of the erythrocyte lysis compared with the native nonmutated variant of FH (Figure 4b). This reduced capacity to regulate the AP on the cellular surface was expected because this FH variant is also the product of a *CFH*::*CFHR1* hybrid gene.[36] In contrast, the FH variant from H54 showed no difference with the FH control and demonstrated to function efficiently in the protection against erythrocyte lysis (Figure 4a). These data, again, indicate that the S890I and V1007L amino acid substitutions are not altering the capacity of FH to regulate the complement AP on the cellular surface.

DISCUSSION

Mutation screening of complement genes in aHUS, DDD, and AMD has become a laboratory routine. Identification of mutations helps diagnosis and provides useful information to anticipate the evolution of the disease in the patients and their response to treatments, conditioning clinical decisions. For example, among aHUS patients, those carrying *CFH* mutations have the worse prognosis and poorest renal transplantation outcomes, although they associate with good responses to plasma treatment. In addition, identification of mutations and polymorphisms associated with increased risk to these pathologies also influence the genetic counseling provided to patients and their relatives. It is therefore critical to obtain evidence supporting the fact that the disease-associated mutations identified in these screenings have a causal relationship with the pathology. Here we have studied two FH amino acid substitutions, I890 and L1007, lacking this functional information that has repeatedly been found among Spanish aHUS and DDD patients and that has also been reported to be associated with aHUS in other Caucasian cohorts.[33–35] In addition, S890I and V1007L were described as rare polymorphisms associated with AMD.[31,35]

The peculiar concurrence of both S890I and V1007L amino acid substitutions in all these cases is explained by the segregation analysis performed here in two aHUS pedigrees that revealed that these two amino acid changes segregate together with a unique *CFH* haplotype characterized by a specific combination of single nucleotide polymorphisms (Table 2). The high allelic frequency of the S890I and V1007L polymorphisms in sub-Saharan African (0.267; 0.317) and African-American (0.455; 0.591) populations (rs515299 and rs534399, respectively) suggest that this *CFH* haplotype has an African origin and was introduced in Caucasians some time ago. In support of this conclusion, one of the patients in our cohort carrying this haplotype (H244) is of sub-Saharan African origin.

Carriers of the I890/L1007 *CFH* haplotype present normal FH levels in plasma with a contribution of the I890/L1007 FH allele of approximately 50% (Table 1). These data illustrate that these amino acid substitutions do not influence the expression/secretion of FH. To characterize the potential consequences of the S890I and V1007L substitutions in the functional activities of FH, we performed three different functional assays using purified FH proteins. We tested the capacity of the I890/L1007 FH variant to bind to surface-bound C3b, analyzed its cofactor activity in the FI-mediated

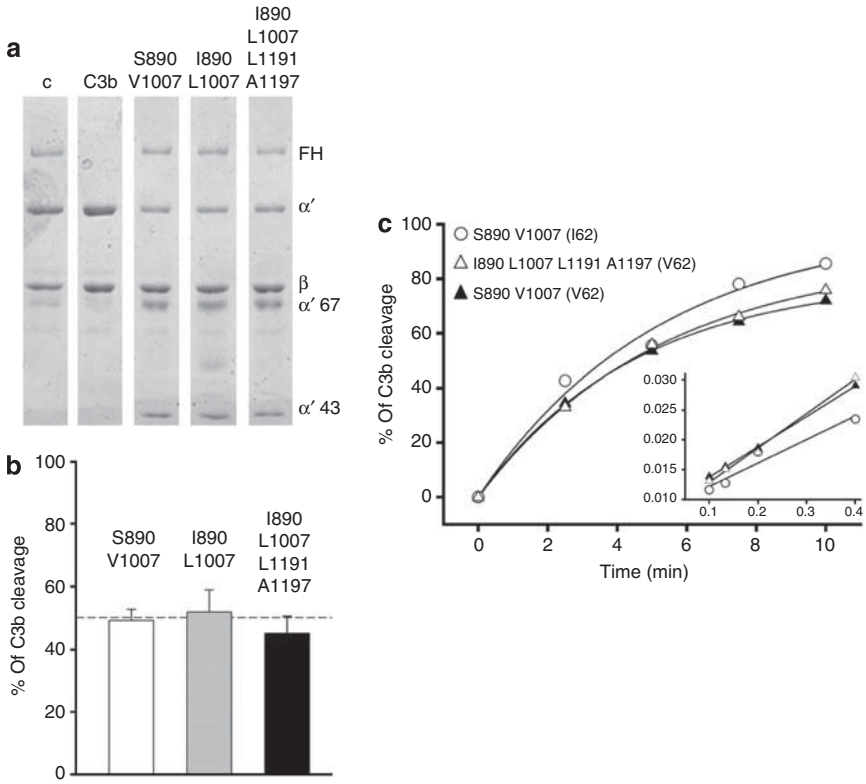

Figure 2 | Cofactor activity of FH variants in the proteolysis of fluid-phase C3b. C3b and factor I (FI) were incubated with equal amounts of S890/V1007, I890/L1007, or I890/L1007/L1191/A1197 factor H (FH) variants for 10 min at 37 °C and the reaction was stopped by the addition of SDS sample buffer. Samples were analyzed by SDS-PAGE under reducing conditions, and gels were stained with Coomassie (**a**). A densitometric analysis of C3b proteolysis from triplicates of these experiments is shown in (**b**). A time-course analysis of C3b proteolysis is shown in (**c**). Fluid-phase cofactor activity was measured by examining C3b cleavage at 2.5, 5, 7.5, and 10 min of reaction for both control S890/V1007 (filled triangles) and I890/L1007/L1191/A1197 (open triangles) FH variants. Percentage of cofactor activity was determined by the ratio of C3b-cleaved, α′-chain/β-chain, and normalized to 0% proteolysis of control samples. Inset panel shows the double reciprocal plot of the S890/V1007 and I890/L1007/L1191/A1197 of the cofactor activity curves. Multiple linear regression analysis showed no significant differences between the slopes for S890/V1007 and I890/L1007/L1191/A1197 cofactor activities. The sensitivity of our assay was demonstrated by including in the experiment a S890/V1007 FH carrying the I62 polymorphism (open circles).

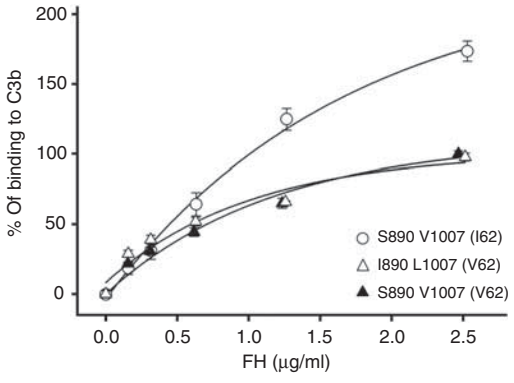

Figure 3 | Capacity of the FH variants to bind to C3b. The interaction between serial dilutions of purified factor H (FH) and C3b deposited in 96-well plates is expressed as percentage of the amount of S890/V1007 FH variant bound to C3b at a concentration of 2.5 μg/ml. Means ± s.d. of three independent experiments are shown for S890/V1007 (filled triangles), I890/L1007 (open triangles) FH variants, and for a S890/V1007 FH variant carrying the I62 polymorphism (open circles). The last sample illustrates the sensitivity of our assay.

inactivation of fluid-phase C3b, and performed an FH-dependent hemolytic assay to determine its capacity to regulate the AP on cellular surfaces. None of these assays showed functional alterations in the regulatory activity of FH. This failure to detect functional alterations caused by the S890I and V1007L substitutions is not a consequence of a lack of sensitivity of our assays. They clearly revealed the subtle functional differences caused by the FH Val62Ile polymorphism or by the modification of the C-terminal region of FH that occurs in the *CFH*::*CFHR1* hybrid gene.[36,39] We therefore concluded that the FH S890I and V1007L variants are most likely *CFH* polymorphisms without functional consequences. Furthermore, recent structural data have shown that SCR15 and SCR17, including these variations, are not implicated in the interaction between FH and C3b.[40]

Carriers of the I890/L1007 *CFH* haplotype in the Spanish aHUS cohort present other well-characterized mutations and/or polymorphisms in complement genes that may help to explain the development of the disease in these

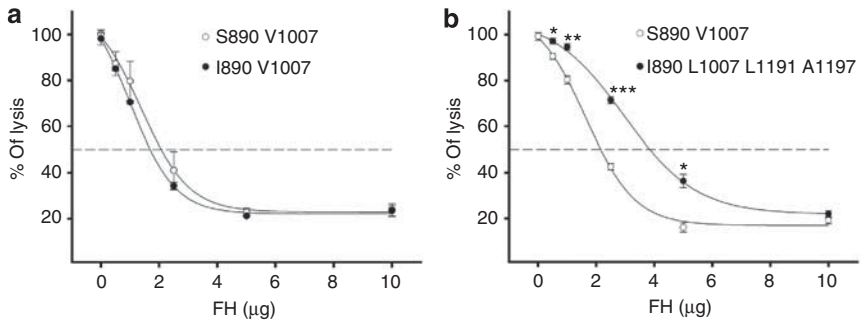

Figure 4 | Inhibition of the lysis of sheep erythrocytes by the FH variants. A volume of serum from a control patient carrying a well-characterized mutation in *CFH* giving 100% lysis when added to sheep erythrocytes was mixed with different amounts of the purified factor H (FH) variants. The lysis observed is shown as percentage of the lysis in the absence of added FH and was plotted against added FH. Means ± s.d. of three independent experiments are shown for S890/V1007 (open circles) and I890/L1007 (filled circles) (**a**), and for S890/V1007 (open circles) and I890/L1007/L1191/A1197 (filled circles) FH variants (**b**). Statistical differences are as follows: $*P<0.05$; $**P<0.01$; $***P<0.001$.

individuals. Thus, patient H54 carries in homozygosis the aHUS-conferring risk allele MCP_{ggaac};[41] patient H97 also carries in homozygosis the MCP_{ggaac} allele and, in addition, the mutation C86Y in the *CFI* gene, which produces a partial deficiency of FI in plasma (Table 1); and in patient H142, the I890/L1007 *CFH* haplotype also carries a *CFH*::*CFHR1* hybrid gene, which produces a FH protein with reduced capacity to regulate the AP on cellular surfaces (Figure 4b).[36] Similarly, patient GN3 is positive for C3 nephritic factor. Finally, an increased frequency of the I890/L1007 *CFH* haplotype in DDD and AMD should be expected because this *CFH* haplotype also carries the *CFH* H402 allele (rs1061170), a very strong risk factor for both AMD and DDD.[20,28]

In conclusion, we failed to provide evidence supporting a causal relationship of I890/L1007 with aHUS. The lack of functional consequences of the *CFH* S890I and V1007L amino acid substitutions, their presence in healthy individuals, and their very high frequency in sub-Saharan African and African-American populations strongly suggest that S890I and V1007L are rare FH polymorphisms unrelated with the disease.

MATERIALS AND METHODS

Complement analysis, mutation screening, and genotyping

C3 and C4 concentrations were determined by nephelometry (Immage, Beckman Coulter, Brea, CA) and FH plasma concentration was quantified by a specific sandwich ELISA method using polyclonal and monoclonal antibodies developed in-house, which do not cross-react with the CFHRs proteins. C3 nephritic factor was measured in serum plasma by standard procedures.[42] Patients and healthy volunteers were screened for mutations and polymorphisms in the *CFH*, *MCP*, *CFI*, *CFB*, *C3*, and *THBD* genes by automatic DNA sequencing of PCR-amplified fragments. Genomic DNA was prepared from peripheral blood cells according to standard procedures. Each exon was amplified from genomic DNA by using specific primers derived from the 5′ and 3′ intronic sequences as described.[15,43–45] Automatic sequencing was performed in an ABI 3730 sequencer using a dye terminator cycle sequencing kit (Applied Biosystems, Foster City, CA). Copy number variations in the *CFHR1-R3* genes were analyzed by multiplex ligation-dependent probe amplification as described.[46]

The studies described herein received IRB approval (Comision de Bioetica, Consejo Superior de Investigaciones Científicas and CEIC, Hospital Universitario La Paz, Madrid, Spain). Patients and their relatives gave their informed consent.

Proteins

FH allele carrying the mutations I890 and L1007 was isolated from fresh plasma of aHUS patient H54 and a relative of the aHUS patient H142. We used a CNBr-activated sepharose 4B (GE Healthcare, Little Chalfont, UK) column coupled with the monoclonal antibody MBI-7 that exclusively recognizes the FH H402 protein variant.[37,38] Fractions containing FH were collected, concentrated, and applied to a gel-filtration column (Superose 6, GE Healthcare). Fractions containing the FH were pooled and the purity of final preparations was confirmed in SDS-PAGE Coomassie-stained gels (Figure 1). C3 was purified by affinity chromatography and gel filtration as described previously.[47] C3b was generated by limited digestion with trypsin and re-purified by gel filtration as described above. C3b was obtained without any detectable contaminants or aggregates. Factor I was purchased from Comptech (Tyler, TX). Concentration of sample proteins was assessed using absorbance at 280 nm, and molarities were calculated using an extinction coefficient for *CFH* of 1.95 (ref. 37) and for C3 of 0.98 (Protean Software, DNAStar, Madison, WI).

Cofactor activity for FI-mediated proteolysis of fluid-phase C3b

The fluid-phase cofactor activity of FH was determined in a C3b proteolysis assay using purified proteins. In brief, C3b, FH, and FI were mixed in 10 mmol/l Hepes, pH 7.5, 150 mmol/l NaCl, and 0.02% Tween 20 at final concentrations of 50, 4, and 2.5 μg/ml, respectively. Mixtures were incubated at 37 °C for 10 min. In another set of assays, samples were collected at 2.5, 5, 7.5, and 10 min of incubation. The reactions were stopped by the addition of 3 μl of SDS sample buffer (2% SDS, 62.5 mmol/l Tris, 10% glycerol, and 0.75% bromophenol blue). Samples were analyzed in 10% SDS-PAGE under reducing conditions. Gels were stained with Coomassie brilliant blue R-250 (BioRad, Berkeley, CA) and proteolysis of C3b determined by measuring the cleavage of the α′-chain using a GS-800 calibrated densitometer (BioRad) and the MultiGauge software package (Fujifilm, Fujifilm Europe GmbH, Barcelona, Spain). The C3b β-chain was used as an internal control

to normalize the amount of protein added between samples. Percentage of cleavage was determined by the ratio between α′-chain and β-chain of C3b and setting as 0% of proteolysis by using a control FH in the absence of FI.

ELISA C3b-binding assay

The binding of FH variants to surface-bound C3b was determined by ELISA method. Polystyrene microtiter plates (96 well) were coated with C3b (2.5 μg/ml) in coupling buffer (0.1 M $NaHCO_3$, pH 9.5) overnight at 4 °C. The plate was blocked with washing buffer (20 mmol/l Tris, 150 mmol/l NaCl, and 0.1% Tween 20) with 1% bovine serum albumin for 1 h at room temperature. After washing, serial dilutions of FH variants (starting dilution was 2.5 μg/ml) were added and incubated with surface-bound C3b for 2 h at 37 °C. After washing, the plate was incubated with anti-FH monoclonal antibody Ox24 for 1 h at room temperature, and then with a secondary antibody coupled with horseradish peroxidase (DAKO, Glostrup, Denmark). Color reaction was developed with *O*-phenylenediamine (DAKO) and absorbance measured at 492 nm. FH preparations used in the ligand assay were quantified in duplicate in the same ELISA plate using immobilized polyclonal anti-FH antibody to capture FH, followed by the Ox24 and secondary antibodies to measure the amount of FH. Concentrations of FH were calculated from curves obtained using purified standard samples.

Factor H-dependent hemolytic assay

The capacity of FH to regulate the activity of the AP on cellular surfaces was assessed with a hemolytic assay using sheep erythrocytes and a serum carrying a well-characterized *CFH* mutation, FH-W1183L.[18] In brief, 1×10^7 sheep erythrocytes in AP buffer: veronal buffer saline (2.5 mmol/l barbital, 1.5 mmol/l sodium barbital, 144 mmol/l NaCl, pH 7.4) with 7 mmol/l $MgCl_2$ and 10 mmol/l ethylene glycol tetraacetic acid, were incubated with 10% FH-W1183L serum in AP buffer and increasing amounts of the different FH variants for 30 min at 37 °C. The reaction was stopped by adding veronal buffer saline containing 20 mmol/l EDTA. After centrifugation, supernatants were read at 414 nm. FH variants I890/L1007 and I890/L1007/L1191/A1197 were compared with the same control FH variant, S890/V1007, in two independent assays. FH-W1183L serum without added FH was taken as 100% of lysis and serum diluted in AP buffer plus 20 mmol/l EDTA was used as blank for spontaneous lysis.

DISCLOSURE

All the authors declared no competing interests.

ACKNOWLEDGMENTS

We are grateful to the patients and their relatives for their participation in this study, as well as to the physicians: Dr Jiménez (Nephrology, Hospital Universitario La Paz, Madrid), Dr Carreras, (Nephrology, Hospital de Bellvitge, Barcelona), Dr Zamora (Paediatric Nephrology, Hospital la Fé, Valencia), and Dr Serrano (Intensive Care Unit, Hospital Niño Jesús, Madrid). We thank the members of Secugen SL and the DNA sequencing laboratory at the CIB for invaluable technical assistance with patient sequencing and genotyping. This work was funded by the Spanish Ministerio de Ciencia e Innovacion (SAF2008-00226 to SRdeC, PS09/00268 to PS-C and PS09/00122 to ML-T), the Ciber de Enfermedades Raras, and the Fundación Renal Iñigo Alvarez de Toledo.

REFERENCES

1. Weiler JM, Daha MR, Austen KF *et al.* Control of the amplification convertase of complement by the plasma protein beta1H. *Proc Natl Acad Sci USA* 1976; **73**: 3268–3272.
2. Whaley K, Ruddy S. Modulation of C3b hemolytic activity by a plasma protein distinct from C3b inactivator. *Science* 1976; **193**: 1011–1013.
3. Pangburn MK, Schreiber RD, Muller-Eberhard HJ. Human complement C3b inactivator: isolation, characterization, and demonstration of an absolute requirement for the serum protein beta1H for cleavage of C3b and C4b in solution. *J Exp Med* 1977; **146**: 257–270.
4. Fearon DT. Regulation by membrane sialic acid of beta1H-dependent decay-dissociation of amplification C3 convertase of the alternative complement pathway. *Proc Natl Acad Sci U S A* 1978; **75**: 1971–1975.
5. Kazatchkine MD, Fearon DT, Austen KF. Human alternative complement pathway: membrane-associated sialic acid regulates the competition between B and beta1 H for cell-bound C3b. *J Immunol* 1979; **122**: 75–81.
6. Pangburn MK, Schreiber RD, Muller-Eberhard HJ. C3b deposition during activation of the alternative complement pathway and the effect of deposition on the activating surface. *J Immunol* 1983; **131**: 1930–1935.
7. Ripoche J, Day AJ, Harris TJ *et al.* The complete amino acid sequence of human complement factor H. *Biochem J* 1988; **249**: 593–602.
8. Esparza-Gordillo J, Soria JM, Buil A *et al.* Genetic and environmental factors influencing the human factor H plasma levels. *Immunogenetics* 2004; **56**: 77–82.
9. Sharma AK, Pangburn MK. Identification of three physically and functionally distinct binding sites for C3b in human complement factor H by deletion mutagenesis. *Proc Natl Acad Sci U S A* 1996; **93**: 10996–11001.
10. Meri S, Pangburn MK. Discrimination between activators and nonactivators of the alternative pathway of complement: regulation via a sialic acid/polyanion binding site on factor H. *Proc Natl Acad Sci U S A* 1990; **87**: 3982–3986.
11. Pangburn MK, Pangburn KL, Koistinen V *et al.* Molecular mechanisms of target recognition in an innate immune system: interactions among factor H, C3b, and target in the alternative pathway of human complement. *J Immunol* 2000; **164**: 4742–4751.
12. de Cordoba SR, de Jorge EG. Translational mini-review series on complement factor H: genetics and disease associations of human complement factor H. *Clin Exp Immunol* 2008; **151**: 1–13.
13. Warwicker P, Goodship TH, Donne RL *et al.* Genetic studies into inherited and sporadic hemolytic uremic syndrome. *Kidney Int* 1998; **53**: 836–844.
14. Richards A, Buddles MR, Donne RL *et al.* Factor H mutations in hemolytic uremic syndrome cluster in exons 18–20, a domain important for host cell recognition. *Am J Hum Genet* 2001; **68**: 485–490.
15. Perez-Caballero D, Gonzalez-Rubio C, Gallardo ME *et al.* Clustering of missense mutations in the C-terminal region of factor H in atypical hemolytic uremic syndrome. *Am J Hum Genet* 2001; **68**: 478–484.
16. Neumann HP, Salzmann M, Bohnert-Iwan B *et al.* Haemolytic uraemic syndrome and mutations of the factor H gene: a registry-based study of German speaking countries. *J Med Genet* 2003; **40**: 676–681.
17. Sanchez-Corral P, Perez-Caballero D, Huarte O *et al.* Structural and functional characterization of factor H mutations associated with atypical hemolytic uremic syndrome. *Am J Hum Genet* 2002; **71**: 1285–1295.
18. Sanchez-Corral P, Gonzalez-Rubio C, Rodriguez de Cordoba S *et al.* Functional analysis in serum from atypical hemolytic uremic syndrome patients reveals impaired protection of host cells associated with mutations in factor H. *Mol Immunol* 2004; **41**: 81–84.
19. Manuelian T, Hellwage J, Meri S *et al.* Mutations in factor H reduce binding affinity to C3b and heparin and surface attachment to endothelial cells in hemolytic uremic syndrome. *J Clin Invest* 2003; **111**: 1181–1190.
20. Pickering MC, de Jorge EG, Martinez-Barricarte R *et al.* Spontaneous hemolytic uremic syndrome triggered by complement factor H lacking surface recognition domains. *J Exp Med* 2007; **204**: 1249–1256.
21. Heinen S, Jozsi M, Hartmann A *et al.* Hemolytic uremic syndrome: a factor H mutation (E1172Stop) causes defective complement control at the surface of endothelial cells. *J Am Soc Nephrol* 2007; **18**: 506–514.
22. Fakhouri F, Fremeaux-Bacchi V, Noel LH *et al.* C3 glomerulopathy: a new classification. *Nat Rev Nephrol* 2010; **6**: 494–499.
23. Ault BH, Schmidt BZ, Fowler NL *et al.* Human factor H deficiency. Mutations in framework cysteine residues and block in H protein secretion and intracellular catabolism. *J Biol Chem* 1997; **272**: 25168–25175.
24. Dragon-Durey MA, Fremeaux-Bacchi V, Loirat C *et al.* Heterozygous and homozygous factor h deficiencies associated with hemolytic uremic syndrome or membranoproliferative glomerulonephritis: report and genetic analysis of 16 cases. *J Am Soc Nephrol* 2004; **15**: 787–795.
25. Zipfel PF, Heinen S, Jozsi M *et al.* Complement and diseases: defective alternative pathway control results in kidney and eye diseases. *Mol Immunol* 2006; **43**: 97–106.

26. Licht C, Heinen S, Jozsi M *et al.* Deletion of Lys224 in regulatory domain 4 of Factor H reveals a novel pathomechanism for dense deposit disease (MPGN II). *Kidney Int* 2006; **70**: 42–50.
27. Mullins RF, Aptsiauri N, Hageman GS. Structure and composition of drusen associated with glomerulonephritis: implications for the role of complement activation in drusen biogenesis. *Eye (Lond)* 2001; **15**: 390–395.
28. Hageman GS, Anderson DH, Johnson LV *et al.* A common haplotype in the complement regulatory gene factor H (HF1/CFH) predisposes individuals to age-related macular degeneration. *Proc Natl Acad Sci U S A* 2005; **102**: 7227–7232.
29. Edwards AO, Ritter III R, Abel KJ *et al.* Complement factor H polymorphism and age-related macular degeneration. *Science* 2005; **308**: 421–424.
30. Haines JL, Hauser MA, Schmidt S *et al.* Complement factor H variant increases the risk of age-related macular degeneration. *Science* 2005; **308**: 419–421.
31. Klein RJ, Zeiss C, Chew EY *et al.* Complement factor H polymorphism in age-related macular degeneration. *Science* 2005; **308**: 385–389.
32. Rivera A, Fisher SA, Fritsche LG *et al.* Hypothetical LOC387715 is a second major susceptibility gene for age-related macular degeneration, contributing independently of complement factor H to disease risk. *Hum Mol Genet* 2005; **14**: 3227–3236.
33. Noris M, Bucchioni S, Galbusera M *et al.* Complement factor H mutation in familial thrombotic thrombocytopenic purpura with ADAMTS13 deficiency and renal involvement. *J Am Soc Nephrol* 2005; **16**: 1177–1183.
34. Caprioli J, Noris M, Brioschi S *et al.* Genetics of HUS: the impact of MCP, CFH, and IF mutations on clinical presentation, response to treatment, and outcome. *Blood* 2006; **108**: 1267–1279.
35. Maga TK, Nishimura CJ, Weaver AE *et al.* Mutations in alternative pathway complement proteins in American patients with atypical hemolytic uremic syndrome. *Hum Mutat* 2010; **31**: E1445–E1460.
36. Heinen S, Sanchez-Corral P, Jackson MS *et al. De novo* gene conversion in the RCA gene cluster (1q32) causes mutations in complement factor H associated with atypical hemolytic uremic syndrome. *Hum Mutat* 2006; **27**: 292–293.
37. Hakobyan S, Harris CL, Tortajada A *et al.* Measurement of factor H variants in plasma using variant-specific monoclonal antibodies: application to assessing risk of age-related macular degeneration. *Invest Ophthalmol Vis Sci* 2008; **49**: 1983–1990.
38. Hakobyan S, Tortajada A, Harris CL *et al.* Variant-specific quantification of factor H in plasma identifies null alleles associated with atypical hemolytic uremic syndrome. *Kidney Int* 2010; **78**: 782–788.
39. Tortajada A, Montes T, Martinez-Barricarte R *et al.* The disease-protective complement factor H allotypic variant Ile62 shows increased binding affinity for C3b and enhanced cofactor activity. *Hum Mol Genet* 2009; **18**: 3452–3461.
40. Morgan HP, Schmidt CQ, Guariento M *et al.* Structural basis for engagement by complement factor H of C3b on a self surface. *Nat Struct Mol Biol* 2011; **18**: 463–470.
41. Esparza-Gordillo J, Goicoechea de Jorge E, Buil A *et al.* Predisposition to atypical hemolytic uremic syndrome involves the concurrence of different susceptibility alleles in the regulators of complement activation gene cluster in 1q32. *Hum Mol Genet* 2005; **14**: 703–712.
42. Rother U. A new screening test for C3 nephritis factor based on a stable cell bound convertase on sheep erythrocytes. *J Immunol Methods* 1982; **51**: 101–107.
43. Richards A, Kemp EJ, Liszewski MK *et al.* Mutations in human complement regulator, membrane cofactor protein (CD46), predispose to development of familial hemolytic uremic syndrome. *Proc Natl Acad Sci U S A* 2003; **100**: 12966–12971.
44. Fremeaux-Bacchi V, Dragon-Durey MA, Blouin J *et al.* Complement factor I: a susceptibility gene for atypical haemolytic uraemic syndrome. *J Med Genet* 2004; **41**: e84.
45. Martinez-Barricarte R, Heurich M, Valdes-Canedo F *et al.* Human C3 mutation reveals a mechanism of dense deposit disease pathogenesis and provides insights into complement activation and regulation. *J Clin Invest* 2010; **120**: 3702–3712.
46. Zipfel PF, Edey M, Heinen S *et al.* Deletion of complement factor H-related genes CFHR1 and CFHR3 is associated with atypical hemolytic uremic syndrome. *PLoS Genet* 2007; **3**: e41.
47. Goicoechea de Jorge E, Harris CL, Esparza-Gordillo J *et al.* Gain-of-function mutations in complement factor B are associated with atypical hemolytic uremic syndrome. *Proc Natl Acad Sci U S A* 2007; **104**: 240–245.